NASA/CP–2006–214146

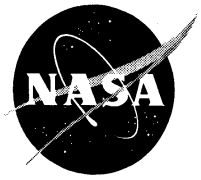

NASA GSFC Science Symposium on Atomic and Molecular Physics

Anand K. Bhatia, Editor

NASA Goddard Space Flight Center, Greenbelt, Maryland

In Honor of Aaron Temkin's and Richard Drachman's Retirement

National Aeronautics and
Space Administration

Goddard Space Flight Center
Greenbelt, Maryland 20771

January 2007

FOREWORD

Dr. Aaron Temkin and Dr. Richard J. Drachman retired on April 3, 2005 after long service to NASA/Goddard Space Flight Center and to the atomic physics community. Needless to say, they have been very active in the field of atomic physics for many years and have made important contributions. A symposium in their honor was held on November 18, 2005 at Goddard Space Flight Center. The presentations were on topics, which have been of interest to Aaron and Richard in the course of their work spanning a century together.

The symposium was attended by scientists from all over the world and was highly successful. It was opened by Chief Scientist of GSFC, Dr. J. Garvin and Chief of the Division, Dr. J. Slavin.

I have been associated with Dr. Temkin since July, 1963 and with Dr. Drachman since September, 1963. It has been very educational for me to have the privilege to be asssociated with them and to work with them closely throughout these years. It was a great pleasure to organize the Symposium to celebrate their achievements.

I wish to thank Dr. Douglas M. Rabin, Head of Solar Physics Branch, for the support in arranging the symposium and providing funds for refreshments throughout the day. I thank Kristine D. Glass, secretary of our branch, for help in sending e-mails to the participants to arrange the badges for admission to the campus.

I thank Chriss Guss of the Infonetic Team of Goddard Space Flight Center for taking photographs of the participants at the symposium.

I thank Dr. Julie Saba for designing the pages of program and biographies with the background images of the astrophysical plasmas.

I thank Dr. Barbara Thompson for bringing two cakes, one for Dr. Temkin and the other for Dr. Drachman, suitably colored which happened to be their choice too.

The banquet was arranged by the wives of the honorees Gladys Temkin and Elizabeth Drachman at the Conference Center of the University of Maryland and was also financially supported by them for all the participants. Next day, Temkins had an open house for all the participants and accompanying persons. I wish to thank Gladys and Elizabeth for making the event very pleasant and enjoyable.

I wish Aaron and Richard good health and all the best in their retirement.

Finally, I wish to thank all the participants, speakers, and chairpersons for making this a successful symposium.

Anand Bhatia

Goddard Space Flight Center

TABLE OF CONTENTS

Dr. Ray and Dr. Ward could not attend the Symposium.

Program of the NASA GSFC Science Symposium

In Honor of Aaron Temkin's and Dick Drachman's Retirement

8.30–8.45: Welcome
Dr. J. B. Garvin: Chief Scientist, GSFC
Dr. J. Slavin: Lab Chief, Solar & Space Physics

Session I

Chairman: Prof. E. Gerjuoy, University of Pittsburgh

8.50–9.15: Introduction
A.K. Bhatia, GSFC

9.20–9.50: Converged Close-Coupling Approach to Electron-Atom Collisions
I. Bray, Flinders University, Australia

9.55–10.25: Electron-Molecule Collisions using the R-Matrix, Linear-Algebra and Kohn-Variational Methods
B. I. Schneider, NSF

10.30–10.50: Coffee Break

Session II:

Chairman: Prof. A. Dalgarno, Harvard Smithsonian CFA

10.55 – 11.25: Double Photoionization Near Threshold
R. Wehlitz, University of Wisconsin

11.30 – 12.00: Applications of the Finite Element Method in Atomic and Molecular Physics
J. Shertzer, College of Holy Cross, Worcester, MA

Session III:

Chairperson: Prof. G. Peach, University College, London, UK

12.05–12.20: States of Dipositronium
D. Shrader, Marquette University, Milwaukee

12.25–12.40: Resonances in Positronium Negative Ions
Y.K. Ho, Institute of Atomic and Molecular Sciences, Academia Sinica, Taiwan

12.45–2.25: Lunch and Tours

1.15–2.25: Tour of Buildings 3 and 14

Session IV:

Chairman: Prof. J. W. Humberston, University College London, UK

2.30–3.00 Asymptotic QED Shifts for Rydberg States
G. W. F. Drake, University of Windsor, Canada

3.05–3.35: Physics with a Trap-Based Beam: Resonances and Bound States in Positron-Molecule Interactions
C. M. Surko, UCSD

3.40–4.00: Coffee Break

Session V:

Chairman Prof. Stephen Lundeen, Colorado State University

4.05–4.35: Calculations of Positron and Positronium Collisions
Dr. H.R J. Walters, The Queen's University, Belfast, UK

4.40–5.20: Muon Catalyzed Fusion Dr. Edward Armour, University of Nottingham, UK

5.20–Closure: Open Session
Remarks by R. J. (Dick) Drachman
Remarks by Aaron Temkin
Additional Remarks by
A. Dasgupta, C. Y. Hu, A. Stauffer, others.

6.30 Reception & Dinner at University of Maryland Conference Center
After Dinner Speaker: Prof. J. Sucher

Short Biographies of Dr. Drachman and Dr. Temkin

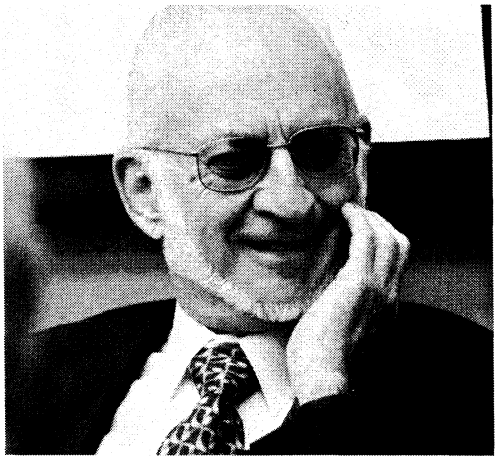

Richard (Dick) Drachman was born in New York City on June 2, 1930. All his formal education took place in New York: beginning in 1936 at the "Chicken Coop," then public school 225, Brooklyn Technical High School, and, finally, Columbia University, where he received three degrees. His Ph.D. research was in quantum field theory under T.D. Lee. His education continued while he worked at the U.S. Naval Research Laboratory on the quantum many-body problem. During part of this period he was an NAS-NRC Associate, and he learned about nuclear weapons effects both theoretically and in the field. He learned some more from his students during a four-year stint as Assistant Professor of Physics at Brandeis University, where his lifelong interest in positron physics began. He returned to the Government at Goddard and worked here for over 40 years. He says he is still learning.

Aaron Temkin was born on August 15, 1929, in New Jersey. He went to elementary and high school in Jersey City, graduated Phi Beta Kappa, summa cum laude, from Rutgers University in 1951 with a B.S. in physics, and obtained his Ph.D. in physics from MIT in 1956. He won a Fulbright fellowship to the University of Heidelberg, and was subsequently awarded a National Academy of Sciences-National Research Council research associateship at the Naval Research Laboratory. From NRL he went to the National Bureau of Standards (now NIST) as a civil servant (physicist), where he worked under Ugo Fano, before coming to NASA/Goddard in 1960. He has worked at Goddard ever since (45 years) as a theorist in atomic physics, specializing in low energy electron-atom collisions (elastic and inelastic scattering, impact ionization, and autoionization) and electron-molecule scattering (elastic, vibrational/rotational excitation). Dr. Temkin retired in 2005, but continues his research in an emeritus status.

Some Astrophysical Motivations for the Calculations

Julia L.R. Saba and K.T. Strong
Lockheed Martin Advanced Technology Center

Astrophysical plasmas make up 99% of the visible matter in the universe. The atomic, molecular, and nuclear physics discussed in the meeting provide some of the calculations needed both to devise and to interpret observations of astrophysical objects. In turn, those objects help to motivate and guide the calculations, as scientists try to reconcile theory and observation. For example, the calculations are a sine qua non in simulating model spectra by tuning the input of physical parameters to match observed spectra, and in determining diagnostic ratios of spectral lines that are temperature and density sensitive (to measure physical conditions) or insensitive (e.g., to calibrate the spectrometer), and in deriving elemental abundances from spectra. On the other hand, odd or unexpected observational "results" sometimes indicate where the calculations have gone astray or need to be worked out in more detail.

The Sun, our nearest star, is a plasma "laboratory" in which many calculations can be tested and refined. As we come to understand the Sun better, it becomes a kind of Rosetta Stone for helping decode more distant and exotic cosmic objects. Figure 1 shows an image of the Sun taken by the Soft X-ray Telescope (SXT) on the Japanese spacecraft Yohkoh (meaning "sunbeam") on 1992 May 08 near the peak of the (nominal 11-year) sunspot cycle. Much of the coronal emission in the broadband SXT filter comes from highly ionized iron at a few million Kelvin. Although the corona is predominantly composed of hydrogen, most of the information we have about its physical conditions comes from spectroscopic diagnosis of the forest of spectral lines emitted by trace elements.

The coronal image in Figure 1 shows a high degree of structure, reflecting the influence of the highly structured magnetic field that channels the plasma (and produces solar activity and, incidentally, makes the Sun as interesting as it is). Information about the strength of the magnetic field comes from Zeeman splitting of the energy levels of magneto-sensitive spectral lines at visible wavelengths in the photosphere (the visible solar surface) or at infrared wavelengths from the overlying layer, the chromosphere. At low latitudes, bright knots of emission come from plasma confined to closed loops in so-called "active regions," the source of copious electromagnetic radiation during flares. Analysis of flare spectra, from the radio to gamma-ray regimes, also both requires and challenges the theoretical calculations.

The bright dots that occur at all latitudes in the image are "X-ray bright points," now understood to be smaller scale bipolar loops. Even the extended, apparently diffuse emission may show magnetic structure at sufficiently high resolution. The dark area at the North Pole corresponds to the lower density plasma streaming out on open field lines in a high-speed solar wind that reaches far out into the solar system, bathing the planets. Measuring the "frozen-in" temperatures of the collisionless particles in the solar wind requires an understanding of the ionization balance in the denser source plasma where the temperature is established.

An example of a "more distant and exotic object" is given in Figure 2. This figure shows a composite image of the archetypal starburst galaxy Messier 82 (M82), viewed in ionized hydrogen, nitrogen, and sulfur by the WIYN[a] 3.5-m telescope on Kitt Peak and by the Wide Field and Planetary Camera 2 (WFPC2) on the Hubble Space Telescope. In the cigar-shaped galactic disk, the birth and death of massive stars occur at 10 times the rate in our Milky Way. At right angles to the disk, an outflowing supergalactic wind is powered by winds from massive stars and supernova explosions. An irregular galaxy 12 million light years distant in the direction of the constellation Ursa Major, M82 is the brightest infrared galaxy in the sky, much brighter in the infrared than in the visible. Its turbulent, explosive wind is a strong radio source. Cataclysmic interaction with its large neighboring galaxy, M81, about 100 million years ago is thought to have triggered the burst of star formation. Even choosing the most appropriate spectral bands for capturing the information on the physical conditions in such an object is based on theoretical calculations, and,

a. The WIYN telescope is so-named because it is operated jointly by University of Wisconsin, University of Indiana, Yale University, and the National Optical Astronomy Observatory (NOAO).

of course, our understanding of star formation, stellar evolution, and supernova explosions is at once a stringent test and a vindication of the nuclear physics calculations underpinning it.

Objects in the heavens have been a source of wonder for both lay and scientific observers for millennia. Our growing physics-based understanding of the wealth of new observations of cosmic phenomena adds depth to our appreciation of their beauty and inspires us to probe even further into their origin and meaning, with ever-improving theoretical calculations continuing to hone our vision.

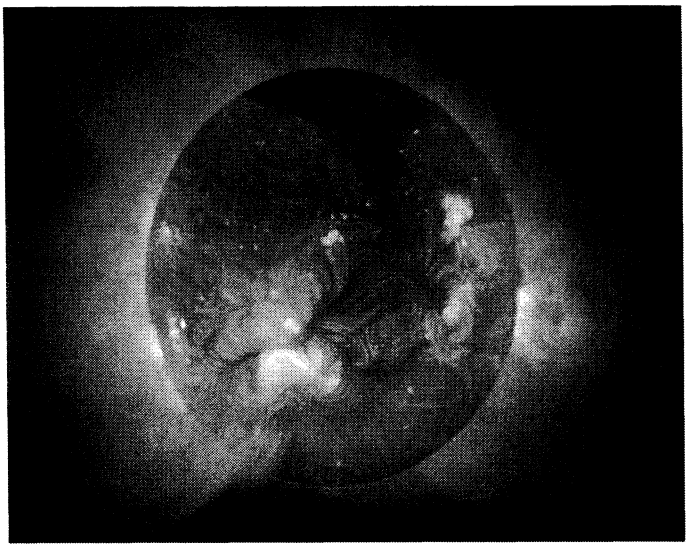

Fig.1: This soft X-ray image of the Sun was provided by the SXT team. The Yohkoh mission was supported by the Japanese Institute of Space and Astronautical Science (ISAS) and by NASA. SXT was built by the Lockheed Martin Advanced Technology Center under NASA contract.

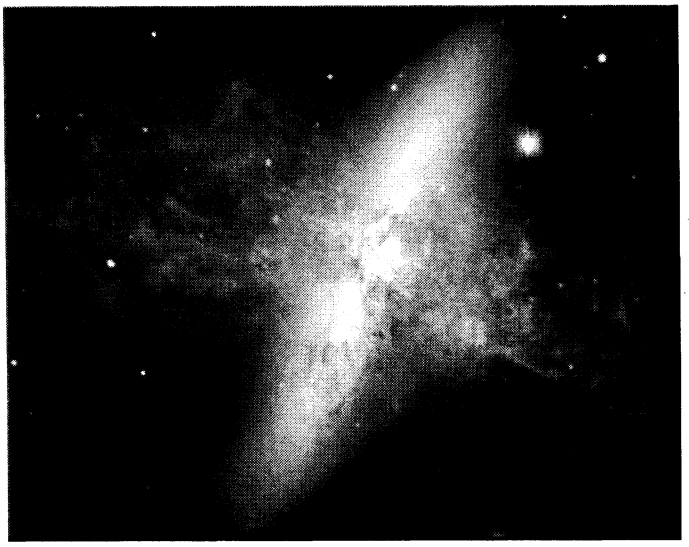

Fig. 2: This image composite of M82 was provided by Mark Westmoquette (University College London), Jay Gallagher (University of Wisconsin-Madison), and Linda Smith (University College London), and made possible by the WIYN consortium, the National Science Foundation, NASA, and the European Space Agency.

Introduction to the contributions of A. Temkin and R. J. Drachman to atomic physics

A. K. Bhatia
NASA/Goddard Space Flight Center, Greenbelt, Maryland 20771

Dr. Aaron Temkin and Dr. Richard J. Drachman have made significant contributions in the field of atomic physics during nearly the last fifty years. It is not possible to enumerate all of their contributions but I will describe a few, first those of Temkin and then of Drachman. Some of the topics of their research are discussed in the articles that follow this one.

Method of Polarized Orbitals

Their work, as is the work of most atomic theorists, is concerned with solving the Schrödinger equation accurately for wave function in cases where there is no exact analytical solution. In particular, Temkin is associated with electron scattering from atoms (and ions). When he started there already were a number of methods to study the scattering of electrons from atoms. The simplest approximation for a hydrogenic target is the static approximation

$$\Psi(\mathbf{r}_1, \mathbf{r}_2) = u(\mathbf{r}_1)\Phi_{\text{target}}(\mathbf{r}_2), \tag{1}$$

where $u(\mathbf{r}_1)$ is the scattering function. This gives rise, in a partial wave expansion, to differential equations which can be solved easily. An important improvement on this approximation is the exchange approximation of Morse and Allis [1] in which the target is assumed to remain in its original state in the presence of the incident electron but the ansatz for the wave function is explicitly (anti)symmetrized

$$\Psi(\mathbf{r}_1, \mathbf{r}_2) = u(\mathbf{r}_1)\Phi_{\text{target}}(\mathbf{r}_2) \pm u(\mathbf{r}_2)\Phi_{\text{target}}(\mathbf{r}_1), \tag{2}$$

where the upper sign refers to singlet scattering and the lower sign to the triplet scattering. This gives rise to an integro-differential equation which will be given later.

But in reality, the target does not stay in its original state and various forms of polarization potentials have been added to the equation for $u(r)$ to take into account this distortion. The method of polarized orbitals proposed by Temkin [2] was the first method to include the effect of polarization in the ansatz for the total wave function. It has been used for scattering of slowly moving electrons from various targets so that the target is distorted adiabatically. This means the target is assumed to follow the instantaneous motion of the scattered electron. The basic problem is how to take into account this distortion mathematically. I will discuss it for a simple target like the hydrogen atom in its ground state (1s), following Temkin [3]. The Hamiltonian H (in Ry units) for two electrons in the field of the nucleus of charge Z is given by

$$H = -\nabla_1^2 - \nabla_2^2 - \frac{2Z}{r_1} - \frac{2Z}{r_2} + \frac{2}{r_{12}}, \tag{3}$$

which for an incoming electron 1 can be written as

$$H = H_0 + V(\mathbf{r}_1, \mathbf{r}_2), \tag{4}$$

where H_0 also contains ∇_1^2

$$H_0 = -\nabla_1^2 - \nabla_2^2 - \frac{2Z}{r_2} - \frac{2(Z-1)}{r_1}, \tag{5}$$

$$V(\mathbf{r}_1, \mathbf{r}_2) = -\frac{2}{r_1} + \frac{2}{r_{12}}, \tag{6}$$

and $r_{12} = |\mathbf{r}_1 - \mathbf{r}_2|$. The first order perturbed wave function of the electron 2 due to the potential V can be written as

$$\Psi_{\rm pol}(\mathbf{r}_1, \mathbf{r}_2) = \Phi_{100}(\mathbf{r_2}) - \sum_{n,l}{}' \frac{< nl0|V(\mathbf{r}_1, \mathbf{r}_2'|100 >}{\epsilon_n - \epsilon_1} \Phi_{nl0}(\mathbf{r}_2), \tag{7}$$

where integration over continuum states is implied and $\epsilon_n = -Z^2 n^{-2}$ is the energy of the nth hydrogenic state Φ_{nlm} which is given by

$$\Phi_{nlm}(\mathbf{r}_2) = \frac{u_{nl}(r_2)}{r_2} Y_{lm}(\Omega_2). \tag{8}$$

The perturbing potential V for $r_1 > r_2$ is given by

$$V(\mathbf{r}_1, \mathbf{r}_2) = 2 \sum_{l=1} \frac{r_2^l}{r_1^{l+1}} P_l(\cos\theta_2), \tag{9}$$

where we have fixed the z-axis in the direction of $\mathbf{r}_1$ and have used the well-known expansion of $1/r_{12}$. Noting that the $l = 0$ term drops out of $V(\mathbf{r}_1, \mathbf{r}_2)$, we can write the matrix in Eq. (7) as

$$\begin{aligned} < nl0|V(\mathbf{r}_1, \mathbf{r}_2')|100 > Y_{l0}(\Omega_2) \quad = \quad & [\frac{1}{r_1^{l+1}} \int_0^{r_1} u_{nl}(r_2') r_2'^l u_{10}(r_2') dr_2' \\ & + r_1^l \int_{r_1}^{\infty} u_{nl}(r_2') \frac{1}{r_2'^{l+1}} u_{10}(r_2') dr_2'] \frac{2}{(4\pi)^{\frac{1}{2}}} P_l(\cos\theta_2). \end{aligned} \tag{10}$$

The second integral vanishes in the limit $r_1 \to \infty$ and the above matrix for large r_1 can be approximated by

$$< nl0|V(\mathbf{r}_1, \mathbf{r}_2')|100 > Y_{l0}(\Omega_2) \cong \left[\frac{1}{r_1^{l+1}} \int_0^{\infty} u_{nl}(r_2') r_2'^l u_{10}(r_2') dr_2'\right] \frac{2}{(4\pi)^{\frac{1}{2}}} P_l(\cos\theta_2), \tag{11}$$

which can be written as

$$< nl0|V(\mathbf{r}_1, \mathbf{r}_2')|100 > Y_{l0}(\Omega_2) \cong \left[\frac{1}{r_1^{l+1}} < nl|r_2'^l|10 >\right] \frac{2}{(4\pi)^{\frac{1}{2}}} P_l(\cos\theta_2). \tag{12}$$

Now Eq. (7) can be written as

$$\Psi_{\rm pol}(\mathbf{r}_1,\mathbf{r}_2) \cong \Phi(\mathbf{r}_1,\mathbf{r}_2) = \Phi_{100} - \sum_{l=1}^{\infty} \frac{2}{r_1^{l+1}} \frac{P_l(\cos\theta_2)}{(4\pi)^{\frac{1}{2}}} \sum_{n=l+1}^{\infty} \frac{< nl|r_2'^l|10 >}{\epsilon_n - \epsilon_1} \frac{u_{nl}(r_2)}{r_2}. \tag{13}$$

To sum this series, use the fact that the bound states satisfy

$$\left[-\nabla_2^2 - \frac{2Z}{r_2}\right] u_{nl}(\mathbf{r}_2) = \epsilon_n \frac{u_{nl}(r_2)}{r_2} P_l(\cos\theta_2), \tag{14}$$

and therefore

$$\left[-\nabla_2^2 - \frac{2Z}{r_2} - \epsilon_1\right] u_{nl}(\mathbf{r}_2) = (\epsilon_n - \epsilon_1) \frac{u_{nl}(r_2)}{r_2} P_l(\cos\theta_2), \tag{15}$$

which implies (letting $\Delta\Phi \equiv \Phi_{100} - \Phi(r_1,\mathbf{r}_2)$)

$$\begin{aligned}\left[-\nabla_2^2 - \frac{2Z}{r_2} - \epsilon_1\right] \Delta\Phi &= \sum_{l=1}^{\infty} \frac{2}{r_1^{l+1}} \sum_{n=l+1}^{\infty} < nl|r_2'^l|10 > \frac{u_{nl}(r_2)}{r_2} \frac{P_l(\cos\theta_2)}{(4\pi)^{\frac{1}{2}}} \\ &= \sum_{l=1}^{\infty} \frac{2}{r_1^{l+1}} \sum_{n=l+1}^{\infty} |u_{nl}(r_2) >< nl|r_2'^l|10 > \frac{P_l(\cos\theta_2)}{r_2(4\pi)^{\frac{1}{2}}}. \end{aligned} \tag{16}$$

Use now completeness

$$\sum_{n=l+1}^{\infty} |u_{nl}(r_2) >< u_{nl}(r_2')| = \delta(r_2 - r_2'), \tag{17}$$

for any l, so that $\Delta\Phi$ satisfies the differential equation

$$\left[-\nabla_2^2 - \frac{2Z}{r_2} - \epsilon_1\right] \Delta\Phi = 2 \sum_{l=1}^{\infty} \frac{r_2^l}{r_1^{l+1}} \Phi_{100}(r_2) P_l(\cos\theta_2), \tag{18}$$

where we have used Eq. (8) for Φ_{100}. Expanding

$$\Delta\Phi = \sum_{l=1}^{\infty} \frac{u_{1s\to l}(r_2)/r_2}{r_1^{l+1}} \frac{P_l(\cos\theta_2)}{(4Z\pi)^{\frac{1}{2}}}. \tag{19}$$

reduces Eq. (18) to the set of uncoupled equations for each l

$$\left[-\frac{d^2}{dr_2^2} - \frac{2Z}{r_2} + \frac{l(l+1)}{r_2^2} - \epsilon_1\right] u_{1s\to l}(r_2) = 2\sqrt{Z} r_2^l u_{1s}(r_2), \tag{20}$$

where $u_{1s}(r) = 2\sqrt{Z^3} r e^{-Zr}$. Eq. (20) can be solved analytically

$$u_{1s\to l}(r_2) = 2e^{-Zr_2} \left(Z \frac{r_2^{l+2}}{l+1} + \frac{r_2^{l+1}}{l}\right). \tag{21}$$

The method of polarized orbitals uses only the dipole part ($l = 1$) of $\Delta\Phi$ [4] so that the polarized part of the target is

$$\Phi_1^{\rm pol} = \Phi_{100} - \frac{\epsilon(r_1, r_2)}{r_1^2} \frac{u_{1s\to p}(r_2)}{r_2} \frac{P_1(\cos\theta_{12})}{(4Z\pi)^{\frac{1}{2}}}, \tag{22}$$

where θ_{12} is the angle between r_1 and r_2 and Temkin has introduced the step function

$$\begin{aligned} \epsilon(r_1, r_2) &= 1, \quad r_1 > r_2 \\ &= 0, \quad r_1 < r_2. \end{aligned} \tag{23}$$

which ensures that polarization takes place only when the scattered electron is outside the orbital electron. The second term in Eq. (22) is called $\Phi_1^{\rm pol}(\mathbf{r}_1, \mathbf{r}_2)$ and gives the distortion of the orbit of hydrogen atom in its ground state (1s). This then solves the problem of the inclusion of polarization in the wave function, for substituting Eq. (22) into Eq. (13) one gets the explicit form of the polarized orbital wave function

$$\Psi(\mathbf{r}_1, \mathbf{r}_2) = u_l(\mathbf{r}_1) \left[\Phi_{100}(\mathbf{r}_2) + \Phi_1^{\rm pol}(\mathbf{r}_1, \mathbf{r}_2)\right] \pm u_l(\mathbf{r}_2) \left[\Phi_{100}(\mathbf{r}_1) + \Phi_1^{\rm pol}(\mathbf{r}_2, \mathbf{r}_1)\right], \tag{24}$$

where

$$u_l(\mathbf{r}) = \frac{u_l(r)}{r} Y_{l0}(\Omega) \tag{25}$$

The scattering equation is obtained from

$$\int Y_{10}^*(\Omega_1) \Phi_0^*(\mathbf{r}_2)(H - E)\Psi(\mathbf{r}_1, \mathbf{r}_2) d\Omega_1 d\mathbf{r}_2 = 0, \tag{26}$$

$$E = -Z^2 + k^2, \tag{27}$$

where H is the Hamiltonian, E is the total energy, k^2 is the energy of the incident electron and $\Phi_{100} \equiv \Phi_0$. We will derive the scattering equation for any Z, the charge of the nucleus. If the variational principle were used it would require that we operate on the left by $(\Phi_0 + \Phi_1^{\rm pol})$. This would give us higher order terms which are not in accord with the first-order perturbation theory. (It would also give quadratic terms involving $\Phi_1^{\rm pol}$ which would be singular if the step function $\epsilon(r_1, r_2)$ were retained in its definition.) Therefore, Temkin has multiplied on the left by Φ_0 only in Eq. (26). (In retrospect, the main disadvantage of this ansatz is the loss of any bound on the calculated phase shifts from this equation.) The resulting integro-differential equation for $u_l(r)$ [5], including the p-wave (l=1) correction of Sloan [6] is, letting r_1=r,

$$\begin{aligned} [\frac{d^2}{dr^2} + \quad k^2 \quad + v_{st}(r) - \frac{l(l+1)}{r^2}] u_l(r) \pm 4Z^3 e^{-Zr} [(k^2 + Z^2) r \delta_{l0} \int_0^\infty dr_2 e^{-Zr_2} r_2 u_l(r_2) \\ - \quad \frac{2}{2l+1} (r^{-l} \int_0^r dr_2 e^{-Zr_2} r_2^{l+1} u_l(r_2) + r^{l+1} \int_r^\infty dr_2 \frac{e^{-Zr_2}}{r_2^l} u_l(r_2))] \end{aligned}$$

$$
\begin{aligned}
&= -\frac{\beta(Zr)}{(Zr)^4}u_l(r) \\
&\mp 4Ze^{-Zr}[\frac{1}{3}\delta_{l1}(-\frac{1}{2}Z(Z^2+k^2)r^3+(Z^2-k^2)r^2)\int_r^\infty dr_2\frac{e^{-Zr_2}}{r_2^l}u_l(r_2) \\
&+ 2(\frac{Zr^3}{2}+r^2)(\frac{l}{(2l-1)(2l+1)}r^{l-1}\int_r^\infty dr_2\frac{e^{-Zr_2}}{r_2^{l+1}}u_l(r_2) \\
&+ \frac{l+1}{(2l+1)(2l+3)}r^{l+1}\int_r^\infty dr_2\frac{e^{-Zr_2}}{r_2^{l+3}}u_l(r_2))] \\
&\pm \frac{4}{3}Ze^{-2Zr}\delta_{l1}[(\frac{3}{2}Z^2r^2+\frac{1}{2}Zr-3)u_l(r)-(\frac{Zr^2}{2}+r)\frac{du_l}{dr}],
\end{aligned}
\tag{28}
$$

where the static potential is given by

$$
v_{st}(r) = 2\frac{(Z-1)}{r} + 2(Z+\frac{1}{r})e^{-2Zr}, \tag{29}
$$

and the direct polarization potential is given by

$$
\beta(Zr)/(Zr)^4 \to \alpha/r^4 \quad \text{for r} \to \infty, \tag{30}
$$

where

$$
\beta(x) = \frac{9}{2} - \frac{2}{3}e^{-2x}(x^5+\frac{9}{2}x^4+9x^3+\frac{27}{2}x^2+\frac{27}{2}x+\frac{27}{4}). \tag{31}
$$

Note that the polarized orbital ansatz Eq. (24) provides a natural cut off for the polarization potential $\beta(Zr)/r^4 \to 0$ as $r \to 0$ and gives the correct polarizability as $r \to \infty$, where $\alpha = 9/2Z^4$ is the dipole polarizability of the target with nuclear charge Z. We get the equation for the exchange approximation [1] by putting the right hand side equal to 0 and we get exchange adiabatic approximation by retaining the first term on the right hand side which is the direct polarization potential.

Eq. (28) can be solved for the function $u_l(r)$ with the phase shifts η_l being obtained from the values of the function at large distance:

$$
\lim_{\text{r}\to\infty}\text{u}_\text{l}(\text{r}) \propto \sin(\text{kr} - \text{l}\frac{\pi}{2} + \eta_\text{l}) \tag{32}
$$

The phase shifts for electron-hydrogen scattering for S-wave and P-wave are given in Table I for various k in three different methods: exchange approximation, polarized orbital method and Kohn variation principle [7,8]. The effect of the polarization is dominated by the direct -α/r^4 potential and always has the effect of increasing the phase shifts relative to the exchange approximation. The effect of exchange polarization terms is smaller and can be either positive or negative depending on the spin. The ^1S and ^3S results decrease with increasing k while ^3P results increase with increasing k. The effect of the exchange polarization terms in the ^1P case leads to three changes in sign of phase shift as k increases, indicating that the method does include the essential physics. This is the first method to give three changes of sign of the ^1P phase shifts correctly (cf. Fig. 6-1-5 in [9]). We will return to the question of bounds in another section.

TABLE I. e-H phase shifts of ^1S, ^3S, ^1P, and ^3P for various k in different approximations.

Partial Wave	k	Exch.	PO[a]	KVP[b]	Exch.	PO[a]	KVP[b]
		Singlet			Triplet		
	0[c]	8.10	5.9	5.965	2.35	1.9	1.7686
	0.1	2.396	2.583	2.553	2.907	2.945	2.939
	0.2	1.870	2.144	2.0673	2.679	2.732	2.7171
	0.3	1.508	1.750	1.6964	2.461	2.519	2.4996
S	0.4	1.239	1.469	1.4146	2.257	2.320	2.2938
	0.5	1.031	1.251	1.202	2.070	2.133	2.1046
	0.7[d]	0.7415	0.947	0.930	1.748	1.815	1.7797
	0.8[d]	0.6513	0.854	0.886	1.617	1.682	1.643
	0.1	-0.0012	0.0067	0.007	0.00220	0.0109	0.0114
	0.2	-0.0084	0.0171	0.0147	0.01666	0.0486	0.0450
	0.3	-0.0240	0.0210	0.0170	0.05192	0.1151	0.1063
P	0.4	-0.0461	0.0163	0.0100	0.10497	0.2005	0.1872
	0.5	-0.0703	0.0064	-0.0007	0.16935	0.2867	0.2705
	0.6	-0.0919	-0.0039	-0.009	0.23183	0.3574	0.3412
	0.7	-0.1077	-0.0100	-0.013	0.28329	0.4063	0.3927
	0.8	-0.1154	-0.0095	-0.004[e]	0.32044	0.4351	0.427
	0.9	-0.1146	-0.0015		0.34436	0.4487	
	1.0	-0.1058	0.0135		0.35791	0.4520	

[a] S-wave phase shifts obtained by Temkin and Lamkin [5] using the method of polarized orbital. The P-wave results are from Sloan [6].

[b] Kohn variational results for S-wave are from Schwartz [7] and P-wave results are from Armstead [8].

[c] The k=0 entries are scattering lengths [5].

[d] The polarized orbital results are from [9].

[e] Beyond k=0.8 the phase shift becomes positive and in fact goes through a (^1P) resonance at k=0.846

On the other hand, scattering length a, which is defined as

$$\lim_{k\to 0} k\cot\eta = -1/a, \tag{33}$$

does have an upper bound, in the variational calculation [7] $a_{\text{exact}} \leq a_{\text{calculated}}$. The scattering lengths in various approximations are given in Table I. For the triplet state, Rosenberg *et al.* [10] had obtained $a_t \leq 1.91$ for the electron-hydrogen scattering. They used an s-wave function having a correct asymptotic form at infinity but did not have a slowly vanishing part ($\frac{1}{r^2}$), as subsequently pointed out by Temkin [11]. Furthermore, Temkin [11] showed that the expression for the scattering length calculated at a finite distance R should be corrected

$$a = a(R) - \alpha\left(\frac{1}{R} - \frac{a}{R^2} + \frac{1}{3}\frac{a^2}{R^3}\right), \tag{34}$$

where a is the true scattering length, and α the polarizabilty of the target. With this modification Temkin obtained an improved value

$$a_t = 1.74, \tag{35}$$

compared to the previous value of 1.91 [5] given in the Table I. After the publication of Temkin's formula (34) and his numerical result in Eq. (35), Schwartz [7] did use such a slowly vanishing part $1/r^2$ in his trial wave function, obtaining precision results:

$$a_s = 5.965 \pm 0.0003 \quad \text{and} \quad a_t = 1.7686 \pm 0.0002, \tag{36}$$

for the singlet (s) and triplet (t) scattering lengths.

Symmetric Euler-Angle Decomposition

In most of the scattering and eigenvalue problems, it is necessary to write the required wave function in terms of a product of two components: radial and angular. Only then the Hamiltonian operating on such a wave function gives equations which depend on the internal coordinates only, with terms arising from the operation of the angular part contained in the Hamiltonian. For one particle scattering from a fixed center, (or the relative motion of two particles) the Laplacian operator is of the form

$$\nabla^2 = \frac{1}{r^2}\frac{\partial}{\partial r}(r^2\frac{\partial}{\partial r}) + \frac{1}{r^2}(\frac{1}{\sin\theta}\frac{\partial}{\partial\theta}\sin\theta\frac{\partial}{\partial\theta} + \frac{1}{\sin^2\theta}\frac{\partial^2}{\partial\phi^2}), \tag{37}$$

where the radial and angular parts can be separated and the second term is propotional to the square of the angular momentum operator. When acting on a wave function which is an eigenfunction of angular momentum l, the Laplacian simplifies to

$$\nabla^2 = \frac{1}{r^2}\frac{\partial}{\partial r}(r^2\frac{\partial}{\partial r}) - \frac{l(l+1)}{r^2}, \tag{38}$$

thus converting a 3-dimensional partial differential equation into an ordinary differential equation.

In the case of two particles in an external force field, e.g., the field of the fixed nucleus (i.e., of infinite mass), the decomposition of the Laplacians is not as simple as in the case of relative motion of two particles. The wave function describing these particles is a function of the internal (i.e., meaning coordinates depending on the position of the nucleus and on two electrons in a plane) coordinates (r_1, r_2, θ_{12}) or (r_1, r_2, r_{12}) and the angular component which is a function of three Euler angles which describe the orientation of the instantaneous plane formed by the two particles and the nucleus in space. The Euler angles are not unique. Breit [12] used the Euler angles which Hylleraas [13] introduced. These are two spherical angles of one the particles and the angle between the $r_1 - z$ plane and $r_1 - r_2$ plane, the internal coordinates being (r_1, r_2, θ_{12}). Breit introduced these angles for P-wave functions and - because they are not symmetrically defined with respect to the two electrons - it is not easy to generalize this decomposition for all angular momenta. Temkin introduced a different set of symmetric Euler angles which allowed the separation of the radial part and angular part for any angular momentum l. The analysis of this problem was carried out by Bhatia and Temkin [14]. Fig. 1 contains a perspective drawing of the Euler angles which define the particle plane with respect to the space fixed x, y, and z axes.

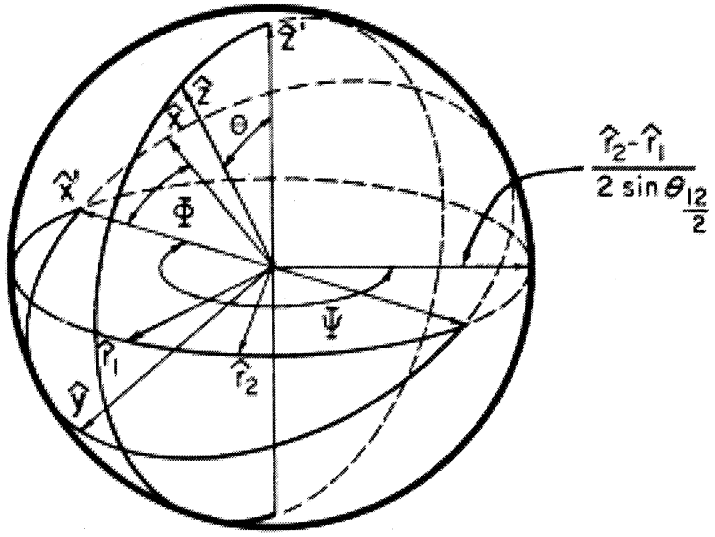

Figure 1: Perspective drawing of the Euler angles the unit vector of the problem.

The rotated axes x', y', z' with respect to the space fixed axes x, y, z are defined by

$$\hat{z}' = \frac{\hat{r}_1 \times \hat{r}_2}{|\hat{r}_1 \times \hat{r}_2|}. \tag{39}$$

Having defined $\hat{z}'$, define $\hat{x}'$

$$\hat{x}' = \frac{\hat{z} \times \hat{z}'}{|\hat{z} \times \hat{z}'|}. \tag{40}$$

Having defined $\hat{z}'$ and $\hat{x}'$, define $\hat{y}'$

$$\hat{y}' = \hat{z}' \times \hat{x}'. \tag{41}$$

The Euler angles are then

$$\Theta \equiv \text{angle between } \hat{z} \text{ and } \hat{z}', \tag{42}$$

$$\Phi \equiv \text{angle between } \hat{x}' \text{ and } \hat{x}, \tag{43}$$

$$\Psi \equiv \text{angle between } \hat{x}' \text{ and } (\hat{r}_2 - \hat{r}_1). \tag{44}$$

The operation of parity ($\mathbf{r}_1 \to -\mathbf{r}_1$ and $\mathbf{r}_2 \to -\mathbf{r}_2$) only involves the Euler angles

$$\begin{aligned} \Theta &\to \Theta, \\ \Phi &\to \Phi, \\ \Psi &\to \pi + \Psi. \end{aligned} \tag{45}$$

Exchange corresponds to the transformation $\mathbf{r}_1 \Leftrightarrow \mathbf{r}_2$ and is given by $r_1 \Leftrightarrow r_2$ plus the following transformation of the Euler angles

$$\begin{aligned} \Theta &\to \pi - \Theta, \\ \Phi &\to \pi + \Phi, \\ \Psi &\to 2\pi - \Psi. \end{aligned} \tag{46}$$

The eigenfunctions of total angular momentum are purely functions of the Euler angles. Temkin has coined the name "rotational harmonics" for these eigenfunctions (they are usually called $\mathcal{D}$ functions). The angular momentum properties of these functions are

$$\mathbf{M}^2 \mathcal{D}_l^{m,k} = \hbar l(l+1)\mathcal{D}_l^{m,k}, \tag{47}$$

and

$$M_z \mathcal{D}_l^{m,k} = \hbar m \mathcal{D}_l^{m,k}. \tag{48}$$

They transform under parity as

$$\mathcal{P}\mathcal{D}_l^{m,k}(\Theta,\Phi,\Psi) \equiv \mathcal{D}_l^{m,k}(\Theta,\Phi,\pi+\Psi) = (-1)^k \mathcal{D}_l^{m,k}(\Theta,\Phi,\Psi), \tag{49}$$

and exchange as

$$\mathcal{E}_{12}\mathcal{D}_l^{m,k}(\Theta,\Phi,\Psi) \equiv \mathcal{D}_l^{m,k}(\pi-\Theta,\pi+\Phi,2\pi-\Psi) = (-1)^l \mathcal{D}_l^{m,-k}(\Theta,\Phi,\Psi). \tag{50}$$

We see that whereas the $\mathcal{D}$ functions are eigenfunctions of parity, that they actually change indices under $\mathcal{E}_{12}$. But operation of exchange commutes with the total Hamiltonian, therefore it must be possible to construct eigenfunctions of exchange: they are linear combinations of the above $\mathcal{D}$ functions. For m=0 they are

$$\mathcal{D}_l^{\kappa+} = \frac{\mathcal{D}_l^{0,\kappa} + (-1)^\kappa \mathcal{D}_l^{0,-\kappa}}{\sqrt{2}[1+\delta_{0\kappa}(\sqrt{2}-1)]}, \tag{51}$$

and

$$\mathcal{D}_l^{\kappa-} = \frac{\mathcal{D}_l^{0,\kappa} - (-1)^\kappa \mathcal{D}_l^{0,-\kappa}}{i\sqrt{2}}. \tag{52}$$

Under exchange these linear combinations have the property

$$\mathcal{E}_{12}\mathcal{D}_l^{\kappa\pm} = \pm(-1)^{l+\kappa}\mathcal{D}_l^{\kappa\pm}. \tag{53}$$

Thus they are indeed eigenfunctions of exchange. Having constructed eigenfunctions (of the angular part) of exchange, one can construct a total wave function which has the correct properties under operations of parity and full exchange

$$\Psi_{l0}(\mathbf{r}_1,\mathbf{r}_2)=\sum_{\kappa}''[f_l^{\kappa+}(r_1,r_2,\theta_{12})\mathcal{D}_l^{\kappa+}(\Theta,\Phi,\Psi)+f_l^{\kappa-}(r_1,r_2,\theta_{12})\mathcal{D}_l^{\kappa-}(\Theta,\Phi,\Psi)], \tag{54}$$

where the double prime on the summation indicates that the sum goes over every second value of κ. The operation under exchange on Eq. (54) gives,

$$\begin{aligned}\mathcal{E}_{12}\Psi_{l0}(\mathbf{r}_1,\mathbf{r}_2)=\Psi_{l0}(\mathbf{r}_2,\mathbf{r}_1) &= \sum_{\kappa}''[f_l^{\kappa+}(r_2,r_1,\theta_{12})(-1)^{l+\kappa}\mathcal{D}_l^{\kappa+}(\Theta,\Phi,\Psi)\\ &+ f_l^{\kappa-}(r_2,r_1,\theta_{12})(-1)^{l+\kappa+1}\mathcal{D}_l^{\kappa-}(\Theta,\Phi,\Psi)].\end{aligned} \tag{55}$$

If therefore

$$f_l^{\kappa+}(r_2,r_1,\theta_{12})=\pm(-1)^{l+\kappa}f_l^{\kappa+}(r_1,r_2,\theta_{12}), \tag{56}$$

and

$$f_l^{\kappa-}(r_2,r_1,\theta_{12})=\pm(-1)^{l+\kappa+1}f_l^{\kappa-}(r_1,r_2,\theta_{12}), \tag{57}$$

then under complete exchange

$$\mathcal{E}_{12}\Psi_{l0}(\mathbf{r}_1,\mathbf{r}_2)\equiv\Psi_{l0}(\mathbf{r}_2,\mathbf{r}_1)=\pm\Psi_{l0}(\mathbf{r}_1,\mathbf{r}_2), \tag{58}$$

i.e., the total wave function will be symmetric (singlet) or antisymmetric (triplet). Under parity we see from Eq. (54) that

$$\mathcal{P}\Psi_{l0}(\mathbf{r}_1,\mathbf{r}_2)=\Psi_{l0}(-\mathbf{r}_1,-\mathbf{r}_2)=(-1)^{\kappa}\Psi_{l0}(\mathbf{r}_1,\mathbf{r}_2), \tag{59}$$

so that parity is determined by evenness or oddness of κ in Eq. (54).

The kinetic energy part is given by

$$\begin{aligned}\nabla_1^2+\nabla_2^2=\frac{1}{r_1}\frac{\partial^2}{\partial r_1^2}r_1+\frac{1}{r_2}\frac{\partial^2}{\partial r_2^2}r_2 &+ \frac{1}{r_1^2}\left(\frac{1}{\sin\theta_1}\frac{\partial}{\partial\theta_1}\sin\theta_1\frac{\partial}{\partial\theta_1}+\frac{1}{\sin^2\theta_1}\frac{\partial^2}{\partial\phi_1^2}\right)\\ &+\frac{1}{r_2^2}\left(\frac{1}{\sin\theta_2}\frac{\partial}{\partial\theta_2}\sin\theta_2\frac{\partial}{\partial\theta_2}+\frac{1}{\sin^2\theta_2}\frac{\partial^2}{\partial\phi_2^2}\right).\end{aligned} \tag{60}$$

Historically, this was the extent of the development when I came to work with Dr. Temkin in 1963. I worked for almost a year to convert the kinetic energy into Euler angles (plus internal coordinates) form. The following is the result

$$\nabla_1^2+\nabla_2^2=\frac{1}{r_1}\frac{\partial^2}{\partial r_1^2}r_1+\frac{1}{r_2}\frac{\partial^2}{\partial r_2^2}r_2+\left(\frac{1}{r_1^2}+\frac{1}{r_2^2}\right)\left(\frac{1}{\sin\theta_{12}}\frac{\partial}{\partial\theta_{12}}\sin\theta_{12}\frac{\partial}{\partial\theta_{12}}\right)+\frac{\mathrm{F}_1}{\mathrm{r}_1^2}+\frac{\mathrm{F}_2}{\mathrm{r}_2^2} \tag{61}$$

$$
\begin{aligned}
F_1 \;=\; & \frac{1}{\sin^2\theta_{12}}[\sin^2(\Psi+\frac{1}{2}\theta_{12})\frac{\partial^2}{\partial\Theta^2}+\cos^2(\Psi+\frac{1}{2}\theta_{12})\cot\Theta\frac{\partial}{\partial\Theta} \\
& +\cos^2(\Psi+\frac{1}{2}\theta_{12})\frac{1}{\sin^2\Theta}\frac{\partial^2}{\partial\Phi^2}+\sin(2\Psi+\theta_{12})\frac{\cot\Theta}{\sin\Theta}\frac{\partial}{\partial\Phi} \\
& -\sin(2\Psi+\theta_{12})\frac{1}{\sin\Theta}\frac{\partial^2}{\partial\Theta\partial\Phi}+\sin(2\Psi+\theta_{12})\cot\Theta\frac{\partial^2}{\partial\Psi\partial\Theta} \\
& -2\cos^2(\Psi+\frac{1}{2}\theta_{12})\frac{\cot\Theta}{\sin\Theta}\frac{\partial^2}{\partial\Psi\partial\Phi}]-\frac{\partial^2}{\partial\Psi\partial\theta_{12}}+\mathrm{A}_1\frac{\partial^2}{\partial\Psi^2}+\mathrm{B}_1\frac{\partial}{\partial\Psi} \qquad (62)
\end{aligned}
$$

$$
A_1=\frac{1}{4}+(\cot^2\Theta/\sin^2\theta_{12})\cos^2(\Psi+\frac{1}{2}\theta_{12}) \qquad (63)
$$

$$
B_1=(\cos\Psi/\sin^2\theta_{12})\sin(\Psi+\theta_{12})-[\sin(2\Psi+\theta_{12})/\sin^2\theta_{12}\sin^2\Theta]-\frac{1}{2}\cot(\frac{1}{2}\theta_{12}). \qquad (64)
$$

The expressions for F_2, A_2, and B_2 can be obtained by replacing θ_{12} by -θ_{12} in the above expressions for F_1, A_1, and B_1.

With these results the Schrödinger equation

$$
H\Psi_{lm}=E\Psi_{lm} \qquad (65)
$$

for any m, can be reduced to radial equations which are independent of m:

$$
\begin{aligned}
[L_{\theta_{12}} \;+\; & \frac{2m_e}{\hbar^2}(E-V)]f_l^{\kappa+}-(\frac{1}{r_1^2}+\frac{1}{r_2^2})[\{\frac{l(l+1)-\kappa^2}{2\sin^2\theta_{12}}+\frac{\kappa^2}{4}-\frac{\cot\theta_{12}}{4\sin\theta_{12}}l(l+1)\delta_{1\kappa}\}f_l^{\kappa+} \\
+\; & \frac{\cot\theta_{12}}{4\sin\theta_{12}}B_l^{\kappa+2}f_l^{(\kappa+2)+}+\frac{\cot\theta_{12}}{4\sin\theta_{12}}(1-\delta_{0\kappa}-\delta_{1\kappa}+\delta_{2\kappa})B_{l\kappa}f_l^{(\kappa-2)+}] \\
+\; & (\frac{1}{r_1^2}-\frac{1}{r_2^2})[-\kappa(\frac{1}{2}\cot\theta_{12}+\frac{\partial}{\partial\theta_{12}})\mathrm{f}_1^{\kappa-}-\frac{\mathrm{l(l+1)}}{4\sin\theta_{12}}\delta_{1\kappa}\mathrm{f}_1^{\kappa-} \\
+\; & \frac{B_l^{\kappa+2}}{4\sin\theta_{12}}f_l^{(\kappa+2)-}-\frac{1}{4\sin\theta_{12}}(1-\delta_{0\kappa}-\delta_{1\kappa}-\delta_{2\kappa})B_{l\kappa}f_l^{(\kappa-2)-}]=0 \qquad (66)
\end{aligned}
$$

and

$$
\begin{aligned}
[L_{\theta_{12}} \;+\; & \frac{2m_e}{\hbar^2}(E-V)]f_l^{\kappa-}-(\frac{1}{r_1^2}+\frac{1}{r_2^2})[\{\frac{l(l+1)-\kappa^2}{2\sin^2\theta_{12}}+\frac{\kappa^2}{4}+\frac{\cot\theta_{12}}{4\sin\theta_{12}}l(l+1)\delta_{1\kappa}\}f_l^{\kappa-} \\
& +\frac{\cot\theta_{12}}{4\sin\theta_{12}}(1-\delta_{0\kappa})B_l^{\kappa+2}f_l^{(\kappa+2)-}+\frac{\cot\theta_{12}}{4\sin\theta_{12}}(1-\delta_{0\kappa}-\delta_{1\kappa}-\delta_{2\kappa})B_{l\kappa}f_l^{(\kappa-2)-}] \\
& +(\frac{1}{r_1^2}-\frac{1}{r_2^2})[\kappa(\frac{1}{2}\cot\theta_{12}+\frac{\partial}{\partial\theta_{12}})\mathrm{f}_1^{\kappa+}-\frac{\mathrm{l(l+1)}}{4\sin\theta_{12}}\delta_{1\kappa}\mathrm{f}_1^{\kappa+} \\
& -\frac{(1-\delta_{0\kappa})}{4\sin\theta_{12}}B_l^{\kappa+2}f_l^{(\kappa+2)+}+\frac{1}{4\sin\theta_{12}}(1-\delta_{0\kappa}-\delta_{1\kappa}+\delta_{2\kappa}B_{l\kappa}f_l^{(\kappa-2)+}]=0 \qquad (67)
\end{aligned}
$$

where $L_{\theta_{12}}$ is the S-wave part of the kinetic energy, and is the only term which survives in the description of S-waves

$$L_{\theta_{12}} = \frac{1}{r_1}\frac{\partial^2}{\partial r_1^2}r_1 + \frac{1}{r_2}\frac{\partial^2}{\partial r_2^2}r_2 + (\frac{1}{r_1^2} + \frac{1}{r_2^2})\frac{1}{\sin\theta_{12}}\frac{\partial}{\partial\theta_{12}}(\sin\theta_{12}\frac{\partial}{\partial\theta_{12}}), \tag{68}$$

and

$$B_{l\kappa} = \frac{[(l-\kappa+1)(l-\kappa+2)(l+\kappa)(l+\kappa-1)]^{\frac{1}{2}}}{[1+\delta_{2\kappa}(\sqrt{2}-1)]} \tag{69}$$

$$B_l^\kappa = B_{l\kappa}[1+\delta_{2\kappa}(\sqrt{2}-1)]^2. \tag{70}$$

The above equations can be written in terms of (r_1, r_2, r_{12}) [14]. These equations have been generalized to the case when the nucleus is of finite mass [15], and also to the case when all the particles are of unequal masses [15].

The equation given by Breit [12] for P-wave can be obtained from our equations by noting the relation between his angles and our Euler angles (cf. Appendix of our paper [14]).

I believe this analysis is one of the major mathematical achievements of Dr. Temkin and I am happy to have been a part of it. And this laid the mathematical foundation of much of our future research, also with Dr. Drachman.

Optical Potential Approach for Scattering

We follow here the Feshbach projection operator formalism [16] to obtain equations for the scattering function giving phase shifts in the elastic region. The phase shifts obtained have property of having a rigorous lower bounds.

In this formalism, in order to project out the ground state we use symmetric projection operators P and Q, which for the hydrogenic (i.e., one-electron) target can be written expicitly [17]

$$P = P_1 + P_2 - P_1P_2, \tag{71}$$

and

$$Q = 1 - P, \tag{72}$$

which implies that $P+Q=1$ and where the spatial projectors are such that for any arbitrary function $\Phi_L(\mathbf{r}_1, \mathbf{r}_2)$

$$P_1\Phi_L(\mathbf{r_1}, \mathbf{r_2}) = \phi_0(\mathbf{r_1}) \int \phi_0(\mathbf{r_1'})\Phi_L(\mathbf{r_1'}, \mathbf{r_2})d\mathbf{r_1'}. \tag{73}$$

Note, P_1 and P_2 commute with each other and are each idempotent, hence the complete P and Q operators are idempotent ($P^2=P$; $Q^2=Q$) and orthogonal ($PQ=0$). In the lim $r \to \infty$,

$$P\Psi_L \rightarrow \sin(\mathrm{kr} - \mathrm{L}\frac{\pi}{2} + \eta_\mathrm{L}), \tag{74}$$

therefore $P\Psi_L$ represents a scattering function, and

$$Q\Psi_L \rightarrow 0. \tag{75}$$

Effectively $Q\Psi_L$ describes the short range part of the total wave function of the system Ψ_L. The Schrödinger equation is reduced, via an analysis which by now is well known [16], to an equation for $P\Psi_L$.

$$[PHP + \frac{PHQ >< QHP}{E - QHQ} - E]P\Psi_L = 0 \tag{76}$$

The middle term in Eq. (76) is the formal, but well defined expression for the optical potential $\mathcal{V}_{op}$.

The total spatial function for the e-H and e-He^+ for the Lth partial wave is written as

$$\Psi_L(\mathbf{r_1}, \mathbf{r_2}) = \frac{u_L(r_1)}{r_1} Y_{L0}(\hat{r_1})\phi_0(\mathbf{r_2}) \pm (1 \leftrightarrow 2) + \Phi_L(\mathbf{r_1}, \mathbf{r_2}), \tag{77}$$

and

$$P\Psi_L = \Psi_L - \Phi_L, \tag{78}$$

where the target function is given by

$$\phi_0(\mathbf{r_2}) = \sqrt{\frac{Z^3}{\pi}} \exp(-Zr_2). \tag{79}$$

The upper and lower signs correspond to singlet and triplet states, respectively. The first two terms containing u_L explicitly give rise to the exchange approximation [1] and the function Φ_L is the correlation function. For arbitrary L this function is most efficiently written in terms of the symmetric Euler angles [14]: Φ_L has exactly the form of Ψ_L in Eq. (54), whereas here the open channel part is added explicitly in Eq. (77).

The f's we here take as functions of r_1, r_2, and r_{12}. The $u_L(r_1)$ of the scattered electron in Eq. (77) is determined by projecting on $< Y_{L0}(\Omega_1)\phi_0(\mathbf{r_2})$:

$$\int \left[Y_{L0}(\Omega_1)\phi_0(\mathbf{r_2})(PHP + \frac{PHQ >< QHP}{E - QHQ} - E)P\Psi_L \right] d\Omega_1 d\mathbf{r_2} = 0, \tag{80}$$

Carrying out the integration leads to an integro-differential equation for the scattering function $u_L(r_1)$ and letting r_1=r,

$$\left[\frac{d^2}{dr^2} - \frac{L(L+1)}{r^2} + v_{st}(r) \pm V_{ex} - \mathcal{V}_{op} + k^2 \right] u_L = 0, \tag{81}$$

where $v_{st}(r)$ is the direct potential [Eq. (29)] and V_{ex} is the non-local exchange potential of the "exchange approximation" [1] (cf. Eq. (28)). It should be noted that the many-body problem has

been reduced to one-body problem and the Eq. (81) can be solved for u_L easily. The integral of the optical potential acting on u_L(r) is:

$$\mathcal{V}_{op}u_L = r\left\langle Y_{L0}\phi_0 PHQ\frac{1}{E-QHQ}QHP\Psi_L\right\rangle. \tag{82}$$

The optical potental is expanded in terms of the eigenspectrum of the QHQ problem:

$$\delta\left[\frac{<\Phi_L^* QHQ\Phi_L>}{<\Phi_L^* Q\Phi_L>}\right] = 0. \tag{83}$$

This leads to eigenfunctions $\Phi_L^{(s)}$ and eigenvalues $\mathcal{E}_s$. By inserting a complete set of the functions obtained from the above equation into Eq. (82), $\mathcal{V}_{op}u_L$ can be written as

$$\mathcal{V}_{op}u_L(r_1) = r_1\sum_s^{N\omega}\frac{<Y_{L0}(\hat{r}_1)\phi_0(r_2)\frac{2}{r_{12}}Q\Phi_L^{(s)}><Q\Phi_L^{(s)}\frac{2}{r_{12}}P\Psi_L>}{E-\mathcal{E}_s}. \tag{84}$$

TABLE II. e-H phase shifts of ^1S, ^3S, ^1P, and ^3P states for various k obtained from the method of polarized orbitals and from the optical potenial approach.

Partial Wave	k	PO[a]	OP[b]	PO[a]	OP[b]
		Singlet		Triplet	
	0.1	2.583	2.55358	2.945	2.93853
	0.2	2.144	2.06678	2.732	2.71741
	0.3	1.750	1.69816	2.519	2.49975
S	0.4	1.469	1.41540	2.320	2.29408
	0.5	1.251	1.20094	2.133	2.10454
	0.6		1.04083		1.93272
	0.7[c]	0.947	0.93111	1.815	1.77950
	0.8[c]	0.854	0.88718	1.682	1.64379
	0.1	0.0067	0.0063083	0.0109	0.010382
	0.2	0.0171	0.014988	0.0486	0.045345
	0.3	0.0210	0.016613	0.1151	0.10679
P	0.4	0.0163	0.099980	0.2005	0.18730
	0.5	0.0064	-0.00084017	0.2867	0.27058
	0.6	-0.0039	-0.010359	0.3574	0.34128
	0.7	-0.0100	-0.013483	0.4063	0.39257
	0.8	-0.0095	-0.0048524	0.4351	0.42730

[a] S-wave phase shifts obtained by Temkin and Lamkin [5] using the method of polarized orbital. The P-wave results are from Sloan [6].
[b] Phase shifts obtained from the optical potential approach. S-wave results are from Ref. [19] and P-wave results are from Ref. [20].
[c]The polarized orbital results are from [9].

For S-wave (i.e., L=0), $\mathcal{D}_L$=constant and the correlation function is only a function of the radial coordinates. The formalism up to this point had already been developed. The innovation which Dr. Temkin and I introduced was the use of a correlated function of Hylleraas form

$$\Phi_{L=0} = \mathrm{e}^{-\gamma r_1 - \delta r_2} \sum_{lmn}^{N_\omega} C_{lmn} r_1^l r_2^m r_{12}^n \pm (1 \rightleftharpoons 2). \tag{85}$$

In particular the projection of P_1 on Φ_{L0} requires a nontrivial analytical integration [18]. Here the sum includes all triples such that $l+m+n=\omega$ and ω= 0, 1, 2, ..., 7,8,9. The number of terms for each ω depends on spin and whether $\gamma=\delta$ or not. For P-wave (i.e., L=1) the correlation functions $f_L^{\kappa\pm}$ are also taken of the Hylleraas form.

To summarize the calculations, the QHQ problem is solved (for a given L, γ and δ and N_ω). The result is a set of eigenvalues $\mathcal{E}_s$ (s=1,2,.....N_ω) and associated eigenfunctions $\Phi^{(s)}$. From them the optical potential, Eq. (82) is constructed, and the integro-differential Eq. (81) is solved noniteratively. The solution is unique (up to an arbitrary normalization) with asymptotic form

$$\lim_{r\to\infty} u_L(r) \propto \sin(\mathrm{kr} - \mathrm{L}\frac{\pi}{2} + \frac{\mathrm{Z}-1}{\mathrm{k}}\ln(2\mathrm{kr}) + \arg[\Gamma(1 - \frac{\mathrm{i}(\mathrm{Z}-1)}{\mathrm{k}})] + \eta_\mathrm{L}). \tag{86}$$

Electron-hydrogen phase shifts (i.e., Z=1) are given in Table II. For ^1S-wave scattering, the optical potential (OP) phase shifts converged to the accuracy shown when the maximum number of terms in the wave function was 95 and in ^3S-wave the convergence was obtained when the number of terms was 84. The P-wave phase shifts converge slowly compared to the S-wave results. Therefore, the computation was carried up to 220 terms. The convergence [19, 20] of results suggest that they are accurate up to five significant figures after the decimal and to that accuracy they are rigorous lower bounds, provided the total energy of the system is less than those of all the resonance positions [21] . Phase shifts are compared in Table II to the polarized orbital results of Temkin and Lamkin [5] for S-wave, for P-wave with those of Sloan [6], including the exchange polarization terms. The polarized orbital method does not provide any bound on the phase shifts but they are seen to contain the dominant part of the correlation enhancement over the exchange approximation. In particular the polarized orbital ^1P results show the correct undulations (as a function of k) as the precision results.

A similar calculation has been carried out for the scattering of electrons from helium ions [22,23]. The non-Coulomb part of the phase shifts as a function of k are given in Tables III for ^1S, ^3S, ^1P and ^3P. In this case because the Coulomb field extends very far, Eq. (81) has to be integrated to large distance especially for small values of k.

In the singlet P case, the exchange approximation results are negative and there is a lot of cancellation with the contributions to the phase shifts from the optical potential, unlike in the triplet case where the exchange approximation results are always positive.

TABLE III. e-He$^+$ phase shifts of ^1S, ^3S, ^1P, and ^3P states for various k obtained from the method of polarized orbitals and from the optical potenial approach.

Partial Wave	k	Exch	PO[a]	OP[b]	Exch.	PO[a]	OP[b]
		Singlet			Triplet		
	0.4		0.4301	0.42601		0.9235	0.91300
	0.5			0.41964			0.90275
	0.6		0.4153	0.41278		0.9015	0.89050
S	0.7	0.34871		0.40561			0.87640
	0.8	0.33949	0.3986	0.39857	0.85195	0.8723	0.86069
	0.9	0.33100		0.39202	0.83444		0.84356
	1.0	0.32302	0.3823	0.38634	0.81645	0.8371	0.82531
	1.1	0.31577		0.38187	0.79764		0.80625
	1.2	0.30940	0.3685	0.37899	0.77821	0.7984	0.78666
	1.3	0.30400		0.37832	0.75851		0.76684
	1.4	0.29957	0.3579	0.38560	0.73872	0.7591	0.74697
	0.1	-0.070322		-0.038311	0.17705		0.21516
	0.2	-0.074161	-0.0404	-0.038958	0.17913	0.2232	0.21681
	0.3	-0.075219		-0.039911	0.18238		0.21944
P	0.4	-0.076473	-0.0428	-0.040971	0.18653	0.2290	0.22283
	0.5	-0.077742		-0.041951	0.19123		0.22661
	0.6	-0.078820	-0.0450	-0.042633	0.19615	0.2364	0.23048
	0.7	-0.079501		-0.042834	0.20096		0.23415
	0.8	-0.079626	-0.0457	-0.042383	0.20540	0.2429	0.23744
	0.9	-0.079078		-0.041158	0.20927		0.24008
	1.0	-0.077762	-0.0436	-0.039036	0.21245	0.2469	0.24202
	1.1	-0.075639		-0.035948	0.21489		0.24322
	1.2	-0.072707	-0.0384	-0.031838	0.21659	0.2479	0.24378
	1.3	-0.068996		-0.026592	0.21757		0.24370
	1.4	-0.064574	-0.0301	-0.019982	0.21790	0.2317	0.24320

[a] S-wave and P-wave phase shifts obtained by Sloan [6] using the method of polarized orbital.
[b] Phase shifts obtained from the optical potential approach: S-wave results are from Ref. [22] and P-wave results are from Ref. [23].

Resonances in Two-Electron Systems

In the above section, projection operators P and Q for one-electron targets were given. These have been used to calculate resonance parameters for a number of $^{1,3}S$, $^{1,3}P$, and $^{1,3}D$ states in H^- and He. Unlike other methods where one has to hunt for resonance positions, they are obtained by optimizing the functional $< \Phi QHQ\Phi > / < \Phi Q\Phi >$ by using the Rayleigh-Ritz variation principle. The positions obtained do not include the shift due to their being embedded in the continuum [17] and this shift is calculated separately using various approximations for the continuum functions. For illustration, only two sets of results (positions and widths) are given in Table IV for ^1S in H^-

Table IV. Some results for resonance states in H^- and He

State	Position(eV)	Width(eV)	Position(eV)	Width(eV)
$^1S(H^-)$	9.55735±0.00005[a]	0.0004717±0.00002	9.558±0.010[b]	
^1P(He)	60.133±0.015[c]	0.038±0.004	60.151±0.010[d]	0.038±0.002[d]

[a]Resonance position is with respect to the ground state of H atom [24]
[b]Experimental result are from Sanche and Burrow [27].
[c]Resonance position is with respect to the ground state of He atom [25].
[d]Experimental results are from Morgan and Ederer [28].

[24] and ^1P states in He [25]. This odd-parity resonance is the lowest one in the series of resonances observed in vacuum ultraviolet absorption by Madden and Codling [26].

We see that results have been calculated with high precision and they agree with the experimental results. The line shape parameter q=-2.80±0.025 which we have precisely defined and calculated by further manipulation of the Feshbach theory [25] also agrees very well with the experimental result -2.55±0.16 [28].

Projection Operators for More Than Two-electron Systems

For targets with more than one electron, it is difficult to construct projection operators which are idempotent, i.e., P^2=P and Q^2=Q. One of the difficulties is that target wave functions for more than one-electron targets cannot be written down exactly. But we can construct them in such a way that the matrix elements $< \Phi_m Q^2 \Phi_n > = < \Phi_m Q \Phi_n >$ for any arbitrary antisymmetric wave functions Φ_m and Φ_n. One of our motivations was to study ^2S resonance below the ^3S (elastic region) of the helium atom.

In order to include all coordinates explicitly, we assume LS (i.e, Russel-Saunders) coupling and introduce channel functions in such a way that the ground state ϕ_0 is coupled to the angular momentum l_i and spin $\frac{1}{2}$ of partial wave of the incoming electron

$$\psi_0(r^{(i)}) = \sum (L_0 l_i M_0 m_i | LM)(S_0 \frac{1}{2} M_{S_0} m_s | S M_S) \phi_0(x^{(i)}) Y_{l_i m_i}(\Omega_i) \chi_{\frac{1}{2} m_s}(i). \tag{87}$$

In Eq. (87) $x^{(i)}$ (both space and spin) indicates the *absence* of the ith coordinates from the total $(N+1)$ coordinates in the electron-target system. The $x^{(i)}$ signifies

$$x^{(i)} = (x_{i+1}, x_{i+2}, ...x_{N+1}, x_1, x_2, ...x_{i-1}). \tag{88}$$

Eq. (88) implies that the target has N electrons and $r^{(i)}$ in Eq. (87) implies the absence of r_i

$$r^{(i)} = (\Omega_i, s_i; x^{(i)}). \tag{89}$$

Let p_i represent a cyclic permutation, so that

$$(-1)^{p_i} = \text{parity of the permutation which carries } [1, 2, ..N+1] \text{ into } [i, i+1, ..i-1]. \tag{90}$$

Specifically $(-1)^{p_i}$=1 for $(N+1)$=odd, $(-1)^{p_i}=(-1)^{i-1}$ for $(N+1)$=even, and $(-1)^{p_1}$=1 for all N.

Following Feshbach [16], we can define the $P\Psi_l$ part of the total wave function as

$$P\Psi_l = \sum_{i=1}^{N+1} (-1)^{p_i} u_l(r_i)\psi_0(r^{(i)}). \tag{91}$$

Here $u_l(r_i)$ are scattering functions which have not been specified but have the asymptotic property for $r_i \to \infty$

$$\lim_{r_i\to\infty} u_l(r_i) = \frac{\sin(kr_i - l\pi/2 + \eta_l)}{kr_i}, \tag{92}$$

which implies that both $P\Psi$ and Ψ have the same asymptotic form

$$\lim_{r_i\to\infty} P\Psi = \lim_{r_i\to\infty} \Psi = (-1)^{p_i} \frac{\sin(kr_i - l\pi/2 + \eta_l)}{kr_i} \psi_0(r^{(i)}). \tag{93}$$

To derive a specific form of P (and Q) we also require that $Q\Psi$ have no ground state in it for any coordinate of the scattered r_i (not only as $r_i \to \infty$)

$$< \psi_0(r^{(i)})(1-P)\Psi >= 0, \tag{94}$$

which for the purpose of the derivation can be written

$$< \psi_0(r^{(i)})\Psi >=< \psi_0(r^{(i)})P\Psi > . \tag{95}$$

Define the left hand side as

$$w(r_i) \equiv (-1)^{p_i} < \psi_0(r^{(i)})\Psi >_{r^{(i)}} . \tag{96}$$

Substituting Eq. (91) into Eq. (95), we can express Eq. (96) as

$$w(r_i) = u(r_i) - \int_0^\infty K(r_i|r_j)u(r_j)r_j^2 dr_j \tag{97}$$

where the kernel K is given by

$$K(r_i|r_j) = (-1)^{p_i+p_j+1} N < \psi_0(r^{(i)})\psi_0(r^{(j)}) >_{r^{(ij)}} . \tag{98}$$

Here the integration is over $r^{(ij)}$, which denotes all coordinates except r_i and r_j $(i \neq j)$. The kernel K can be expressed in terms of discrete and orthonormal set of eigenfunctions v_α

$$v_\alpha(r_1) = \lambda_\alpha \int_0^\infty K(r_1|r_2)v_\alpha(r_2)r_2^2 dr_2. \tag{99}$$

Some reflection will show that $K(r_1|r_2)$ can be written as

$$K(r_1|r_2) = \sum_{\beta=1}^{n_\lambda} \frac{v_\beta(r_1)v_\beta(r_2)}{\lambda_\beta}. \tag{100}$$

then substituting Eq. (100) in Eq. (99) the latter will be an identity. Using Eq. (100) in Eq. (97) allows $u(r_i)$ to be written

$$u(r_i) = \sum_{\lambda_\alpha=1} v_\alpha(r_i) < v_\alpha u > + w(r_i) + \sum_{\lambda_\beta \neq 1} \frac{v_\beta(r_i) < v_\beta w >}{\lambda_\beta - 1}. \tag{101}$$

Here v_β is the eigenfunction associated with λ_β and v_α with λ_α=1. It can be verified that the first term in Eq. (101) does not contribute to the projection $< \Psi_0 P\Psi >$ (cf. Refs. [29,30]). Thus we can write

$$< \Psi_0(r^{(1)})P\Psi > = < \psi_0^{(1)} \sum_{i=1}^{N+1} (-1)^{p_i}[w(r_i) + \sum_{\lambda_\beta}{}' \frac{v_\beta(r_i) < v_\beta w >}{\lambda_\beta - 1}]\psi_0(r^{(i)}) >_{r^{(1)}} . \tag{102}$$

Substituting for $w(r_i)$ from Eq. (97) and rearranging, we get

$$< \Psi_0(r^{(1)})P\Psi > = < \psi_0^{(1)}| \sum_{i=1}^{N+1} [\psi_0(r^{(i)} >< \psi_0(r^{(i)}) + \sum_{\lambda_\alpha}{}' \frac{v_\beta(r_i) < v_\beta w >}{\lambda_\alpha - 1}]\Psi > . \tag{103}$$

By comparing the left- and right-sides of Eq. (103), The expression for P can be extracted

$$P = \sum_{i=1}^{N+1} [\psi_0(r^{(i)} >< \psi_0(r^{(i)}) + \sum_{\lambda_\alpha}{}' \frac{v_\alpha(r_i)\psi_0(r^{(i)}) >< v_\alpha\psi_0(r^{(i)})}{\lambda_\alpha - 1}]. \tag{104}$$

which implies

$$Q = 1 - \sum_{i=1}^{N+1} [\psi_0 >< \psi_0 + \sum_{\lambda_\alpha}{}' \frac{v_\alpha\psi_0 >< v_\alpha\psi_0}{\lambda_\alpha - 1}]. \tag{105}$$

These operators are symmetric in all $(N+1)$-particle coordinates and they contain the dependence on space and spin of all coordinates explicitly. The main advantage of these expressions for P and Q, as compared to the heuristic form given by Feshbach, are they are complete and explicit. In addition they have been extended to scattering (including resonances) occuring in the inelastic domain (cf. Appendix B of Ref. [29]).

It has been shown in Ref. [30] that even though the above operators are not idempotent ($P^2 \neq P$ and $Q^2 \neq Q$) as operator identities that the matrix elements are equivalent $< \Phi_i P^2 \Phi_j > = < \Phi_i P \Phi_j >$ and $< \Phi_i Q^2 \Phi_j > = < \Phi_i Q \Phi_j >$ for any arbitrary antisymmetric functions Φ_i and Φ_j.

When the second term in Eq. (104) and the third term in Eq. (105) are dropped, we get the quasi-projection operators $\hat{P}$ and $\hat{Q}$. These operators were employed by Temkin *et al.* [31] to calculate the resonance parameters of the He^- $[1s(2s)^2]$ ^2S resonance (first observed by Schulz

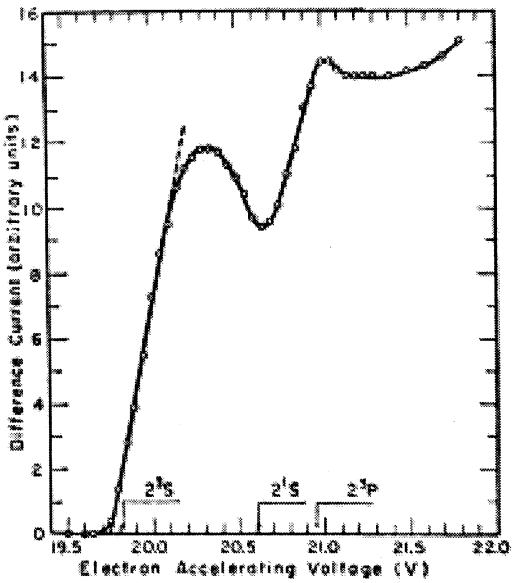

Figure 2: Metastable helium excitation from Schultz and Fox [35].

[32]), using open shell and closed shell target wave functions ϕ_0 and an angle-independent trial wave function as well as a configuration-interaction wave function containing up to 40 configurations. They obtained $E_{res}(^2S)$=19.363 eV plus a width Γ=0.014 eV. The difference between the results obtained by using the two different wave functions ϕ_0 is of the order of 0.02 eV. The resonance position agrees with the experimental result 19.31±0.03 eV of Kuyatt *et al.* [33]. Calculations have also been carried out by Berk *et al.* [34] using target wave functions going up to a 10 term Hylleraas type wave functions and the full projection operators P and Q given in Eqs. (104) and (105). Again configuration interaction type wave functions containing up to 40 terms were employed obtaining resonance position of $(1s2s^2)^2S$ He^- which is ~0.013 eV above the experimental position at 19.37 eV given by Schulz and Fox [35]. (That difference is presumably due to the uncalculated shift, which also occurs in the Feshbach theory.)

Now we come to ^2P wide resonance in He^- above the 2^3S threshold but below the 2^1S threshold of He, which has been first observed by Schulz and Fox [35](cf. Fig. 2).

Initially, it was thought to be a shape resonance because of its being above the ^3S threshold. Bhatia and Temkin [36] used the same program which was used to calculate the ^2S resonance below the ^3S threshold and where quasi-projection operators were employed. Only those configurations in the trial wave functions were included which were orthogonal to the ^3S state of He, thus avoiding the need to project out the ^3S state. The calculations were carried out by using closed shell as well as open shell functions in the projection operators, giving the resonance position at 20.52489 and 20.56029 eV, repectively, for a trial wave function consisting of 40 terms. The position agrees with the result 20.536 eV obtained by Chung using his hole-projection technique [37]. The partial widths to ^1S and ^3S thresholds were found to be 0.0024 and 0.437 eV, and the calculation also showed that the total width is dominated by the decay to the (excited) 2^3S state of He. These results also indicated that the resonance was a Feshbach resonance associated with the closed 2^1S state of the target He rather than a shape resonance caused by the open 2^3S state. An accurate calculation carried out by Junker [38] using the complex rotation method gave 20.33 and 0.575 eV for the position and width, respectively. These results agree with average experimental results

20.3±0.3 and total width 0.5 eV of Schultz and Fox [35], and Brunt *et al.* [39].

I shall not discuss here Dr. Temkin's (and collaborators') work on dispersion relations [40, 41] and in particular his work on threshold laws for electron-impact ionization of atoms and ions [which also apply to photon double (detachment/ionization) of (negative ions/atoms)]. The latter is discussed by Dr. R. Wehlitz in these Proceedings. A dispersion relation (DR) relates the real part of the scattering amplitude to an integral over the imaginary part, which in turn is proportional to total cross section. Such relations are important in judging the consistencies and accuracy of both theoretical calculations and experimental measurements. The problem in electron-atom scattering has been to correctly include the effects of exchange. Dr. Temkin has proposed using partial wave dispersion relations to solve this problem. At this point the correct partial wave DR have been constructed both approximately [42] and exactly [43] in the static-exchange approximation.

Up to now, I have described some of Dr. Temkin's important contributions in electron-atom scattering and associated problems in atomic physics mentioned above . He has also made important contributions in the field of electron-molecule scattering: Briefly stated, Dr. Temkin (with various coworkers) introduced the "fixed nuclei" approximation (as well as the name) in electron-(diatomic) molecule scattering [44,45]. They showed that the (partial wave) scattering amplitude could be expressed as the product of the two factors; one of which depends on scattering parameters resulting from the dynamical interaction of the electron with the molecule, which is most conveniently calculated in the body-frame of the molecule, and a second factor, depending on geometrical functions representing the rotation of the scattering angles from the body to the lab frame. The cross sections, averaged over orientations of the internuclear axis could then be expressed as a sum of scattering parameters multiplied by spherical harmonics together with vector coupling coefficients. A second contribution concerns the "adiabatic nuclei" approximation, originally introduced by Chase [46] in the context of nuclear physics. Chase showed that in a cogent approximation that the amplitude for rotational excitation can be expressed as a matrix element of the fixed-nuclei amplitude between initial and final rotational states. Because the dependence on the orientation is analytic (actually $\mathcal{D}$ function), these integrals can also be done analytically, again - first - by Temkin and coworkers [46,47]. (The name adiabatic-nuclei was also coined by Temkin [48].) Temkin was also involved in other developments, most notably the hybrid theory [49], which will further be discussed by Dr. B. I. Schneider in his contribution to these Proceedings.

Having described some of Dr. Temkin's work, I now will describe some of the work carried out by Dr. Drachman. Perhaps, after Sir Harrie Massey, Dr. Drachman has not only made important contributions to positron physics but has also made it a popular subject of research.

Scattering of Positrons from Hydrogen Atoms

Calculation of positron-hydrogen scattering at low energies can be carried out by the method of polarized orbitals as in the case of e-H scattering. Instead, Drachman [50], employing a variation of the method, chose the wave function of the form

$$\Psi(\mathbf{r}_1, \mathbf{r}_2) = u(\mathbf{r}_1)[1 + G(\mathbf{r}_1, \mathbf{r}_2)]\phi_0(\mathbf{r}_2). \tag{106}$$

The function $G(\mathbf{r}_1, \mathbf{r}_2)$, correct to first order in the potential

$$V(\mathbf{r}_1, \mathbf{r}_2) = \frac{2}{r_1} - \frac{2}{|\mathbf{r}_1 - \mathbf{r}_2|}, \tag{107}$$

has been determined by Dalgarno and Lynn [51] as a solution of the differential equation

$$[G, H(2)]\phi_0(\mathbf{r}_2) = (V - < V >)\phi_0(\mathbf{r}_2) \tag{108}$$

where

$$H(2)\phi_0(\mathbf{r}_2) = [-\nabla_2^2 - \frac{2}{r_2}]\phi_0(\mathbf{r}_2) = -\phi_0(\mathbf{r}_2), \tag{109}$$

and

$$< V >= \int d\mathbf{r}_2 \phi_0(\mathbf{r}_2) V(\mathbf{r}_1, \mathbf{r}_2) \phi_0(\mathbf{r}_2). \tag{110}$$

The function G includes all multipoles $\geq$0. The adiabatic equation, correct to second order in V, is given by

$$[-\nabla_1^2 - k^2 + v_{st} + V_2]u(\mathbf{r}_1) = 0. \tag{111}$$

In the derivation of the above equation, we have taken $< G >$=0. Here

$$v_{st} = 2e^{-2r_1}(1 + \frac{1}{r_1}), \tag{112}$$

and

$$\begin{aligned} V_2 \quad &= r_1^{-2}[5 - (4r_1^2 + 8r_1 + 10)e^{-2r_1} + (4r_1^3 + 7r_1^2 + 8r_1 + 5)e^{-4r_1} \\ &-2(r_1 + 1)^2(e^{-2r_1} + e^{-4r_1})(\mathrm{Ei}[2\mathrm{r}_1] - 2\ln[2\gamma \mathrm{r}_1]) \\ &-2\mathrm{Ei}[-2\mathrm{r}_1]([\mathrm{r}_1 - 1]^2\mathrm{e}^{2\mathrm{r}_1} + [\mathrm{r}_1^2 + 2\mathrm{r}_1 - 3] + 4[\mathrm{r}_1 + 1]\mathrm{e}^{-2\mathrm{r}_1})], \end{aligned} \tag{113}$$

where lnγ=0.57721 is the Euler's constant and

$$\mathrm{Ei}[-\mathrm{z}] = -\int_{\mathrm{z}}^{\infty} \frac{\mathrm{e}^{-\mathrm{y}}}{\mathrm{y}} \mathrm{dy}. \tag{114}$$

For small value of r_1, $v_{st} \rightarrow 2r_1^{-1}$-2 and $V_2 \rightarrow$ -1, while for $r_1 \rightarrow \infty$ V_2= -4.5r^{-4}. Eq. (111) can be solved for various values of k to determine the phase shifts and the results are given in Fig. 3. For k=0, the scattering length requires a correction due to the long-range potential [11], as indicated in Eq. (34), and its value is -2.54 versus Schwartz's -2.10 [7], which is the upper bound on the scattering length. This shows that the potential in Eq. (113) is too attractive. Drachman [50] modified the potential to

$$v_{st} + V_2 + (\alpha - 1)V_{20}, \tag{115}$$

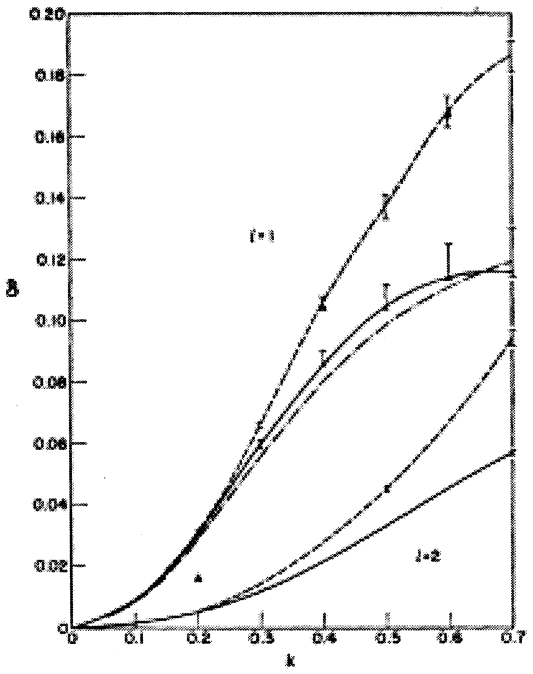

Figure 3: Phase shifts in radians for p- and d-wave scattering. The solid curves are for α=0.1, and the vertical bars indicate α=1.0 and α=0 limits. The triangles are Brandsden's p-wave values (Ref. [52]).

where V_{20} is the monopole part of V_2. The complete suppression of monopole or short-range part of the potential, i.e., α=0 gives scattering length -2.07, in good agreement with Schwartz's value. Drachman calculated P-wave and D-wave phase shift for various values of k and found reasonable agreement with those of Brandsen [52] (cf. Fig. 3).

In the same calculation, Drachman concluded, from the change of sign of the scattering length with increasing mass of the positron, that there is no bound state of the system e^+-e^--P unless the mass of the positron is $3.6m_e$ for α=0.1, while for α=1 it is about $3.1m_e$.

Houston and Drachman [53] using a more flexible wave function than that of Schwartz [7] in the Kohn variational method, obtained an upper-bound scattering length $a \leq$ -2.10278. They obtained an extrapolated estimate a= - 2.1036±0.0004. These results are in good agreement with Schwartz's result $a \leq$ -2.10. They applied the Harris method [54] to obtain S-wave phase shifts at nonzero energies which are in good agreement with those obtained by the Feshbach formalism [16] described below.

One of my first calculations with Drachman [55] was the S-wave elastic scattering of positrons (e^+) from hydrogen atoms below the positronium pickup threshold. As mentioned above for electron-hydrogen scattering, rigorous lower bounds have been obtained using the Feshbach projection formalism [16]. Similarly, the results for e^+-H have rigorous lower bounds. Since there is no exchange between a positron (labeled 1) and an electron (labeled 2) in the hydrogen atom in this process, the projection operators P and Q are defined as

$$P = |\phi_0(r_2) >< \phi_0(r_2)|, \tag{116}$$

$$Q = 1 - P, \tag{117}$$

such that P operating on the wave function does not change its asymptotic form in the limit $r_1 \to \infty$

$$P\Psi = \Psi. \tag{118}$$

TABLE V. e^+-H phase shifts for S-wave scattering for various k.

	S-wave				P-wave	
k	Schwartz [7]	η_{extrap}	$\Delta\eta$	η_{final}	Armstead[a] [8]	η_{final}
0.1	0.151	0.148085	0.000223	0.1483	0.008,0.009(1)	0.0094
0.2	0.188	0.187496	0.000200	0.1877	0.032,0.033(1)	0.0338
0.3	0.168	0.167407	0.000306	0.1677	0.064,0.065(1)	0.0665
0.4	0.120	0.119724	0.000420	0.1201	0.099,0.102(1)	0.1016
0.5	0.062	0.061934	0.000429	0.0624	0.130,0.132(1)	0.1309
0.6	0.007	0.003191	0.000689	0.0039	0.153,0.156(2)	0.1547
0.7	-0.054	-0.052183	0.000980	-0.0512	0.175,0.178(3)	0.1799

[a] Armstead [8] has given two sets of results. The first entry gives his converged results while the second entry his estimate of most probable results with uncertainty in the last figure given in perenthesis.

Here Ψ is given by

$$\Psi_L(\mathbf{r}_1, \mathbf{r}_2) = u_L(\mathbf{r}_1)\phi_0(\mathbf{r}_2) + \Phi(\mathbf{r}_1, \mathbf{r}_2), \tag{119}$$

where the generalized Hylleraas function is

$$\Phi = e^{-(\delta r_1 + \gamma r_2 + \alpha r_{12})} \sum_{lmn}^{N} C_{lmn} r_1^l r_2^m r_{12}^n. \tag{120}$$

In the absence of exchange, the e^+-H problem should be easy to solve but not so due to the virtual positronium formation. Therefore, we have included $e^{-\alpha r_{12}}$ in Φ, where r_{12} is the distance between the positron and the electron. An integro-differential equation of the form Eq. (81) (V_{ex}=0 here) is solved for the scattering functions $u_L(r_1)$ and phase shifts η_L are obtained in the limit $r_1 \to \infty$ from

$$u_L(r_1) = \sin(\mathrm{kr_1} - \mathrm{L}\pi/2 + \eta_{\mathrm{L}}). \tag{121}$$

It should be pointed out that the phase shifts are negative in the absence of the optical potential. The inclusion of the optical potential, which is attractive as in the e-H scattering, increases the phase shifts from the values obtained in the presence of only the repulsive static potential v_{st} in Eq. (81). The phase shifts were calculated for up to N=84 and extrapolated for $N \to \infty$. These phase shifts plus a correction $\Delta\eta$ for the long-range polarization potential are compared in Table V with those obtained by Schwartz [7] using the Kohn variational principle. The long-range effects

are not well included in a Hylleraas type correlation functions and therefore have to be calculated separately. Our final results ($\eta_{\text{final}} = \eta_{\text{extrapolated}} + \Delta\eta$), which, we believe, are accurate within ± 0.0002 radians, differ at k=0.6 and 0.7 from those obtained by Schwartz [7].

A similar calculation [56] has been carried out for P-wave scattering. Here the closed channel function is given by

$$\Phi = f_1 \cos(\frac{1}{2}\theta_{12})\mathcal{D}_1^{1+} + f_2 \sin(\frac{1}{2}\theta_{12})\mathcal{D}_1^{1-}. \tag{122}$$

The f_i are taken of the Hylleraas type with two non-linear parameters:

$$f_1 = e^{-(\delta_1 r_1 + \gamma_1 r_2)} \sum_{l\geq 1} \sum_{m\geq 0} \sum_{\geq 0} C_{lmn}^{(1)} r_1^l r_2^m r_{12}^n, \tag{123}$$

and

$$f_2 = e^{-(\delta_2 r_1 + \gamma_2 r_2)} \sum_{l\geq 1} \sum_{m\geq 0} \sum_{\geq 0} C_{lmn}^{(2)} r_2^l r_1^m r_{12}^n. \tag{124}$$

The f_i are linearly independent functions because the positron and the electron are distinguishable. Now there are four nonlinear paremeters to be veried to get the best results. The maximum number of terms for each f is 84, giving a total of 168 terms in Φ. Here we have added the dipole adiabatic and the quadrupole plus nonadiabatic corrections to the extrapolated phase shifts. Our final results are compared to those of Armstead [8] in Table V. The rigorous lower bound is lost due to the addition of corrections for the long-range potential. Nevertheless, the results still are accurate.

Needless to say, these results have stood the test of the time and are still considered to be the benchmark results.

Annihilation of Positrons with Electrons, Z_{eff}

An important process is the annihilation in flight of positrons by atomic hydrogen resulting in the 511 KeV line which has been observed in solar flares [57] and from the galactic center [58]. This line can be used to infer properties of flares and the solar plasmas. Having calculated the wave functions for the scattering of positrons from hydrogen atoms, the partial cross sections for annihilation can be calculated from the expression given below [59]

$$\sigma_a = Z_{\text{eff}} \frac{\alpha^3}{k} (\pi a_0^2), \tag{125}$$

where α is the fine-structure constant, a_0 is the Bohr radius, and k is the incident positron momentum in units of a_0^{-1}. The quantity Z_{eff}, whch is the measure of the probability that the positron and electron are at the same point, depends on specific properties of the positron-atom system. Z_{eff} is equal to Z, the number of electrons in the atom, when the positron can be represented as a free particle. For the hydrogen atom

$$Z_{\text{eff}} = \int\int d\mathbf{r}_1 d\mathbf{r}_2 |\Psi(\mathbf{r}_1, \mathbf{r}_2)|^2 \delta(\mathbf{r}_1 - \mathbf{r}_2), \tag{126}$$

where $\Psi(\mathbf{r}_1, \mathbf{r}_2)$ is the positron-hydrogen wave function. It should be noted that for the calculation of Z_{eff}, $u_L(\mathbf{r})$ should have a plane wave normalization, i.e.,

$$u_L(\mathbf{r}) = (2L+1)\frac{\sin(\mathrm{kr} - \frac{1}{2}\mathrm{L}\pi + \eta_\mathrm{L})}{kr} P_L(\cos(\theta)) \tag{127}$$

We present Z_{eff} for L=0 and 1 [60,61] in Table VI and compare them with those obtained by Humberston and Wallace [62] and Humberston [63]. For $L > 1$, we use the plane wave expansion for the incident positron

$$Z_{\mathrm{eff}}(L > 1) \cong \sum_{L=2}^{\infty}(2L+1)\int_0^\infty drr^2\phi_0^2(r)j_L^2(kr). \tag{128}$$

Using the identity

$$\sum_{L=0}^{\infty}(2L+1)j_L^2 = 1 \tag{129}$$

we get [with $\phi_0(r) = 2e^{-r}$]

$$\begin{aligned} Z_{\mathrm{eff}}(L > 1) &= 4\int_0^\infty drr^2e^{-2r}(1 - j_0^2 - 3j_1^2) \\ &= \frac{k^2}{k^2+1} + \frac{6}{k^2}\left(\frac{1}{k^2}\ln(1+\mathrm{k}^2) - \frac{1+\mathrm{k}^2/2}{1+\mathrm{k}^2}\right). \end{aligned} \tag{130}$$

We give the total Z_{eff} in Table VI.

Table VI. Z_{eff} for e^+-H annihilation. k=0 results are from Ref. [64,65].

	L=0		L=1		Z_{eff}(Total)
k	$Z_{\mathrm{eff}}(L=0)$	Ref. [62]	$Z_{\mathrm{eff}}(L=1)$	Ref. [63]	
0					8.868
0.1	7.363	7.5	0.13008	0.1335	7.493
0.2	5.538	5.7	0.53994	0.5366	6.079
0.3	4.184	4.3	1.12441	1.114	5.312
0.4	3.327	3.3	1.76292	1.719	5.100
0.5	2.730	2.7	2.33910	2.353	5.091
0.6	2.279	2.3	2.84988	2.823	5.168
0.7	1.950		3.67030	3.637	5.683

We can calculate the thermally averaged annihilation parameter

$$\bar{Z}(T) = \int_0^\infty dk f_T(k) Z_{\mathrm{eff}}(k), \tag{131}$$

where $f_T(k)$ is the Maxwell-Boltzman distribution function. We can fit the calculated $Z_{\mathrm{eff}}(k)$ to a sixth-degree polynomial of the form

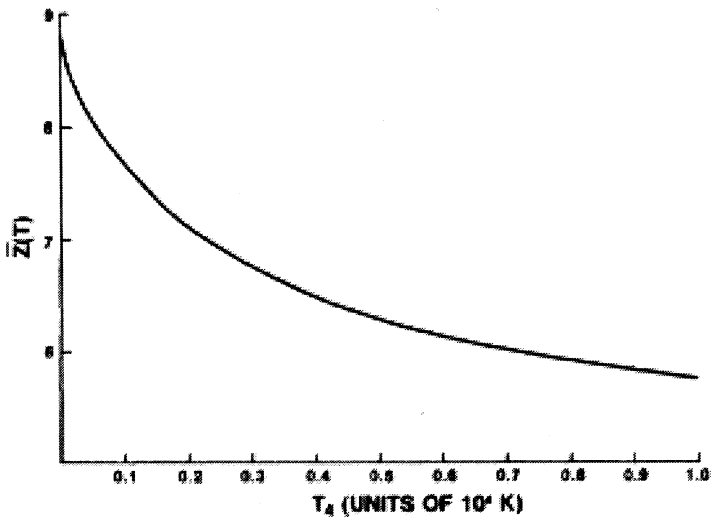

Figure 4: Thermally averaged annihilation parameter $\bar{Z}$(T) obtained from the polynomial fit $Z_{eff}(k)$.

$$Z_{\rm eff}(k) = \sum_{0}^{6} Z_n k^n. \tag{132}$$

Using this expansion, the integration in Eq. (131) can be carried out analytically and we have

$$\bar{Z}(T) = \sum_{n=0}^{6} \bar{Z}_n (T_4)^{n/2}, \tag{133}$$

where T_4 is the temperature in units of 10^4 K and

$$\bar{Z}_n = \alpha_n Z_n A_0^{-n/2}. \tag{134}$$

Here A_0=15.789 and Z_n, $\bar{Z}_n$, and α_n are given in Table VII.

Table VII. Coeffients of the polynomial, Z_n, $\bar{Z}_n$, and α_n.

n	Z_n	$\bar{Z}_n$	α_n
0	8.868	8.868	1
1	-7.38	-2.226	$2\pi^{-1/2}$
2	-102.77	-9.763	$\frac{3}{2}$
3	527.38	18.971	$4\pi^{-1/2}$
4	-978.68	-14.722	$\frac{16}{4}$
5	773.15	5.284	$12\pi^{-1/2}$
6	-197.17	-0.658	$\frac{105}{4}$

Now $\bar{Z}(T)$ can be calculated at any temperature (cf. Fig. 4).

e^+-He Scattering

Although accurate calculations for e^+-H can be carried out because wave functions of hydrogen atoms are known exactly it is difficult to perform experiments on this system. On the other hand, e^+-He experiments can be performed relatively easily but the calculations are rather tedious because elaborate He functions are difficult to employ. However, Houston and Drachman [53] used those simple wave functions which gave a reasonable value of the polarizabilty of the He atom. They used the Harris method [54] to calculate phase shifts at low energies and their results agreed with the results of the variational calculation of Drachman [65]. They added a term to the wave function to represent the long-range dipole potential and obtained scattering length a=-0.524 and Z_{eff}=4.3 at k^2=0, using the Kohn variational method.

Properties of Ps^- and Photodetachment

The positronium negative ion (Ps^-), consisting of two electrons and a positron, is particle stable and decays only by e^+-e^- annihilation into gamma rays. Mills [66,67] has produced and detected this ion and measured its lifetime. Drachman and I [68] calculated its ground state (^1S) energy by using a trial function of the Hylleraas form, calculated expectation values of delta functions, and cusp conditions given by

$$\nu_i = \left\langle \delta(\mathbf{r}_i) \frac{\partial}{\partial r_i} \right\rangle < \delta(\mathbf{r}_i) >^{-1}, \tag{135}$$

$$\nu_{12} = \left\langle \delta(\mathbf{r}_{12}) \frac{\partial}{\partial r_{12}} \right\rangle < \delta(\mathbf{r}_{12}) >^{-1} . \tag{136}$$

Table VIII. Binding energy (Ry) of ^1S state of Ps^-, expectation values of δ functions, cusp conditions, and decay rate $\Gamma((\text{nsec})^{-1})$. [The notation $A(-B)$ stands for $A \times 10^{-B}$.]

N	γ	δ	Binding energy	$\delta(\mathbf{r}_i)$	$\delta(\mathbf{r}_{12})$	ν_i	ν_{12}	Γ
125	0.2585	0.3585	0.024009788	0.020722	1.7151(-4)	-0.49910	0.49711	2.0850
161	0.3700	0.3700	0.024010026	0.020732	1.7136(-4)	-0.49986	0.49695	2.0860
202	0.380	0.380	0.024010089	0.0200730	1.7129(-4)	-0.49740	0.49740	2.0858
120	0.604	0.296	0.024009966	0.020733	1.7190(-4)	-0.50000	0.49347	2.0861
165	0.604	0.314	0.024010079	0.020773	1.7164(-4)	-0.49999	0.49441	2.0861
220	0.604	0.313	0.024010113	0.020733	1.7150(-4)	-0.50000	0.49508	2.0861

Here r_1 and r_2 are the relative distances of electrons 1 and 2 with respect to the positron, and $r_{12} = |\mathbf{r}_1 - \mathbf{r}_2|$. Results are in given in Table VIII for the Hylleraas wave functions (see Eq. (141) below) with up to N=203 with $\gamma = \delta$, and up to 220 terms with $\gamma \neq \delta$, respectively. These functions have been used to calculate other properties. The cusp conditions test the accuracy of the wave functions near points of coalescence, since $\nu_1 = \nu_2 = -\frac{1}{2}$ and $\nu_{12} = +\frac{1}{2}$ for exact solutions of the Schrödinger equation. The convergence of results, given in Table VIII, shows that our wave functions should be fairly accurate. To a sufficient accuracy the Ps^- decay rate is given by

$$\begin{aligned}\Gamma &= 2\pi\alpha^4(c/a_0)[1-\alpha(17/\pi-19\pi/12)] < \delta(\mathbf{r}_1) > \\ &= 100.6174 < \delta(\mathbf{r}_1) > \ (\text{nsec})^{-1}, \end{aligned} \tag{137}$$

where the correction term proportional to α is due to the triplet lifetime [69] and the leading radiative correction to the singlet lifetime [70]. Our calculated value is in agreement with the measured [67] value $\Gamma = 2.09 \pm 0.09(\text{nsec})^{-1}$.

Mills [71] recognized that the existence of $^3P^e$ state of positronium, as in H^- [72], would have interesting experimental consequences: The state would be metastable against breakup because $Ps^-(^3P^e) \rightarrow Ps(^1S) + e^-$ is nonrelativistically forbidden. Using 70-term Hylleraas wave function, Mills [71] did not find such a state . We [68] too failed to find this state even when we used larger expansions and also included long-range terms of several types [73].

Photodetachment of Ps^-

Mills [66] suggested that Ps^- ion could be used to generate positronium (Ps) beams of controlled energy; this would involve acceleration of Ps^- ions and photodetachment of one electron. Drachman and I [74] calculated the dipole transition matrix elements by two simplifications: the intial Ps^- wave function is represented by an asymptotic form whose normalization comes from our most accurate wave function [68], and the final state is a plane wave.

The Hamiltonian of the system consisting of two electrons (ρ_1, ρ_2) and one positron ($\mathbf{x}$) is

$$H = -\nabla_{\rho_1}^2 - \nabla_{\rho_2}^2 + \nabla_{\mathbf{x}}^2 - \frac{1}{|\rho_1 - \mathbf{x}|} - \frac{1}{|\rho_2 - \mathbf{x}|} + \frac{1}{|\rho_1 - \rho_2|}. \tag{138}$$

The center-of-mass system is

$$\mathbf{R} = \frac{1}{3}(\rho_1 + \rho_2 + \mathbf{x}), \quad \mathbf{r}_1 = \rho_1 - \mathbf{x}, \quad \mathbf{r}_2 = \rho_2 - \mathbf{x}, \tag{139}$$

where $\mathbf{R}$ is the coordinate of the center of mass of the entire system, $\mathbf{r}_1$ and $\mathbf{r}_2$ are the distances of electrons 1 and 2 from the positron, respectively. The Hamiltonian is given by

$$H = -\frac{1}{3}\nabla_{\mathbf{R}}^2 - 2\left[\nabla_{\mathbf{r}_1}^2 + \nabla_{\mathbf{r}_2}^2 + \nabla_{\mathbf{r}_1}\cdot\nabla_{\mathbf{r}_2} + \frac{1}{r_1} + \frac{1}{r_2} - \frac{1}{r_{12}}\right]. \tag{140}$$

Omitting the center of mass coordinate $\mathbf{R}$, which describes uniform motion of the center of mass, we write a wave function for the Ps^- ground state in the Hylleraas form

$$\Psi_i(\mathbf{r}_1, \mathbf{r}_2) = \Psi_i(r_1, r_2, r_{12}) = \frac{1}{\sqrt{8\pi^2}} \sum_{lmn} [r_1^l r_2^m e^{-\gamma r_1 - \delta r_2} + r_2^l r_1^m e^{-\gamma r_2 - \delta r_1}] r_{12}^n. \tag{141}$$

The final state consists of an electron in a p state moving away relative to the center-of-mass of the Ps atom. We use the coordinate $\mathbf{R}_2 = \mathbf{r}_2 - \mathbf{r}_1/2$ in place of $\mathbf{r}_2$, while retaining $\mathbf{r}_1$ as the distance between the positron and electron. The Hamiltonian for these asymmetric coordinates is

$$H = -2\left[\nabla^2_{\mathbf{r}_1} + \frac{3}{4}\nabla^2_{\mathbf{R}_2} + \frac{1}{r_1} + \frac{1}{|\mathbf{R}_2 + \frac{1}{2}\mathbf{r}_1|} - \frac{1}{|\mathbf{R}_2 - \frac{1}{2}\mathbf{r}_1|}\right]. \tag{142}$$

The final state is given by the p-wave part of the symmetrized product of a plane wave in relative coordinates:

$$\Psi_f = \frac{1}{\sqrt{2}}[\phi(\mathbf{r}_1)e^{i\mathbf{k}\cdot\mathbf{R}_2} + \phi(\mathbf{r}_2)e^{i\mathbf{k}\cdot\mathbf{R}_1}], \tag{143}$$

where $E = \frac{3}{2}k^2$. The photodetachment cross section in the velocity form can be written as [75]

$$\sigma_v = \frac{2k\alpha a_0^2}{9\omega}| < \Psi_f|Q_V|\Psi_i > |^2, \tag{144}$$

where the dipole transition operator in the velocity form is

$$Q_V = 2\hat{\mathbf{k}} \cdot (\nabla_{\rho_1} + \nabla_{\rho_2} - \nabla_{\mathbf{x}}), \tag{145}$$

and ω is energy of the incident wave. The finite mass of the positron gives a factor of $\frac{2}{3}$ when compared with the photodetachment expression for an infinitely massive atomic ion. The cross section in the length form can be written as [75]

$$\sigma_L = \frac{2k\omega\alpha a_0^2}{9}| < \Psi_f|Q_L|\Psi_i > |^2, \tag{146}$$

where the dipole operator in the length form is

$$Q_L = \hat{\mathbf{k}} \cdot (\rho_1 + \rho_2 - \mathbf{x}). \tag{147}$$

These transition operators can be written in terms of the unsymmetric coordinates:

$$Q_V = \hat{\mathbf{k}} \cdot (\frac{2}{3}\nabla_{\mathbf{R}} + 4\nabla_{\mathbf{r}_1} + 2\nabla_{\mathbf{R}_2}). \tag{148}$$

and

$$Q_L = \hat{\mathbf{k}} \cdot (\mathbf{R} + \mathbf{r_1} + \frac{2}{3}\mathbf{R_2}). \tag{149}$$

Now we represent the initial loosely bound state function in the following form [76,77]:

$$\Psi_i = C\frac{e^{-\gamma R_j}}{R_j}\phi(r_k), \quad \text{for } \mathrm{R_j} >> \mathrm{r_k}, \tag{150}$$

where γ=0.12651775 from our best variational value [68] of the Ps^- binding energy 0.024010113 Ry.

$$C(r) \equiv \sqrt{8\pi}re^{\gamma r}\Psi_i(0, r, r). \tag{151}$$

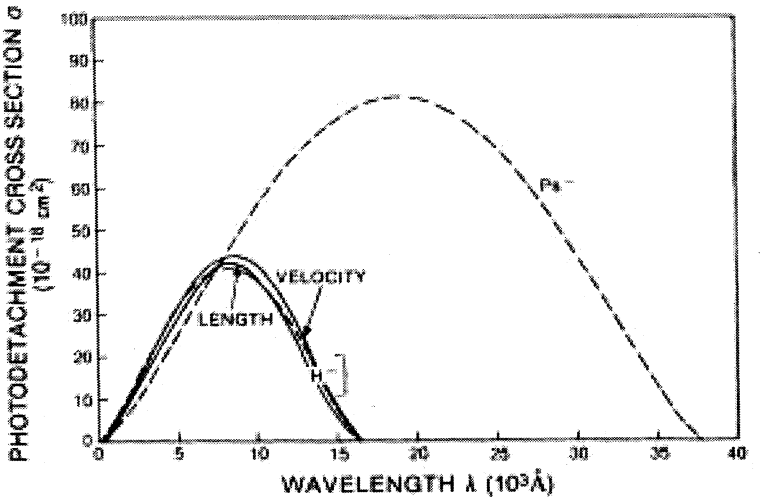

Figure 5: Photodetachment cross sections (dashed lines) in the asymptotic approximation for Ps^- and H^- as functions of wavelengths of the incident light. The length and velocity forms of the H^- cross sections are from more elaborate theory of K. L. Bell and A. E. Kingston [78] (solid lines).

We find C=0.1856(2) (cf. Ref. [74] for details). We find

$$\sigma_V = \sigma_L = (3.8245 \times 10^{-17}\mathrm{cm}^2)\frac{\mathrm{k}^3\mathrm{C}^2}{(\mathrm{k}^2+\gamma^2)^3}, \tag{152}$$

which can be written as

$$\sigma = (1.32 \times 10^{-18}\mathrm{cm}^2)\frac{\mathrm{k}^3}{(\mathrm{k}^2+\gamma^2)^3}. \tag{153}$$

We can write the cross section in terms of the wave length of the incident light,

$$\sigma = (650 \times 10^{-18}\mathrm{cm}^2)(\frac{\lambda}{\lambda_0})^{3/2}(1-\frac{\lambda}{\lambda_0})^{3/2}, \quad \mathrm{for}\lambda \leq \lambda_0, \tag{154}$$

where λ_0=37953.46 Å . In Fig. 5 we have plotted the present results [Eq. (154)], compared with the corresponding results [77] for H^-. In the latter case the asymptotic approximation is seen to compare fairly well with the more elaborate calculations of Bell and Kingston [78], and we expect the present results to be similarly reliable.

A scattering calculation for the final state has been carried out by Ward, Humberston and McDowell [79] to calculate the photodetachment cross section of Ps^-. See the article by Dr. S. J. Ward in these Proceedings.

Muonic Molecules

There have been speculations of the possibility of realizing useful muonic catalyzed fusion. The Born-Oppenheimer approximation has been used traditionally to calculate energy levels of muonic

systems. Drachman and I [80], for the first time, using Hylleraas type wave functions for such systems, carried out straightforward Rayleigh-Ritz variational calculations and showed that the binding energy of even the weekly bound $td\mu$ molecular state of the angular momentum equal to 1 and vibrational state 1 ($J = 1, v = 1$) can be obtained fairly accuarately. We [81] further studied the deexcitation of $td\mu$ muonic molecule by internal conversion and also calculated the $J = 2$ binding energy. We wrote an easy-to-read review article [82] on this subject. I will not discuss further our work because Prof. E. A. G. Armour has carried out extensive work on muonic systems and has written an article on muonic physics which appears in these Proceedings.

Polarizabilities of Two-Electron Systems

We will see in the subsequent section that in order to calculate the Rydberg levels of three-electron systems, the interaction between valence electron and core should be known. This interaction can be represented by the potential

$$U(x) = -\frac{\alpha_1}{x^4} + \frac{6\beta_1 - \alpha_2}{x^6} + \text{ higher} - \text{order terms}, \tag{155}$$

where x is the relative distance between the valence electron and the core, and α_1 and α_2 are dipole and quadrupole polarizabilities, respectively, and β_1 is the first nonadiabatic coefficient. These polarizabilities, in the second-order perturbation calculations, are given by the general expression

$$S_{k,i} = \sum_N \frac{< 0|v_i|N >< N|v_i|0 >}{(E_N - E_0)^k}, \tag{156}$$

where $|0>$ represents the ground state of the core and $|N>$ intermediate states, determined by diagonalizing the appropriate Hamiltonian. We can write

$$S_{1,i} \equiv \alpha_i = \sum_N \frac{< 0|v_i|N >< N|v_i|0 >}{(E_N - E_0)}, \tag{157}$$

$$S_{2,i} \equiv \beta_i = \sum_N \frac{< 0|v_i|N >< N|v_i|0 >}{(E_N - E_0)^2}, \tag{158}$$

and

$$S_{3,i} \equiv \gamma_i = \sum_N \frac{< 0|v_i|N >< N|v_i|0 >}{(E_N - E_0)^3}. \tag{159}$$

The potential between the valence electron at a distance x from the nucleus and the core can be expanded in the form

$$V \simeq \frac{v_1}{x^2} + \frac{v_2}{x^3} + ... \tag{160}$$

where

$$v_1 = 2\left[1 + \frac{K(Z-2)}{2}\right](\mathbf{w}\cdot\hat{\mathbf{x}}), \tag{161}$$

and

$$v_2 = 2\left[r_1^2 P_2(\hat{\mathbf{r}}_1\cdot\hat{\mathbf{x}}) + r_2^2 P_2(\hat{\mathbf{r}}_2\cdot\hat{\mathbf{x}}) - Kw^2 P_2(\hat{\mathbf{w}}\cdot\hat{\mathbf{x}})\right]. \tag{162}$$

Here $\mathbf{w} = \mathbf{r}_1 + \mathbf{r}_2$, $K = 2/(1+M)$, M is the nuclear mass, and Z is the nuclear charge. Drachman and I [83] calculated various quantities in Eq. (156) using the pseudostate summation method. We used Hylleraas type wave functions for the ground state and intermediate states. The nonlinear parameters in intermediate states are optimized by maximizing α_1, which according to the variational principle, has a lower bound to the exact α_1. In Table IX, we give our results for various ions.

Table IX. Adiabatic and nonadiabatic polarizabilities for three isoelectronic systems. A(-B)implies A$\times 10^{-B}$

System	Li^+	Be^{+2}	B^{+3}
α_1	0.192485	0.052282	0.019651
β_1	0.03529	4.919(-3)	1.125(-3)
γ_1	6.806(-3)	4.847(-4)	6.723(-5)
α_2	0.11389	0.01532	3.427(-3)
β_2	0.01668	1.132(-3)	1.524(-4)
γ_2	2.584(-3)	8.819(-5)	7.136(-6)

Polarizabilities of He and H^-

We now turn to calculations of such quantities for He and H^-, where the convergence is rather slow for He and even slower for H^-. For He, we [84] used up to 525 terms for the ground state, 364 terms for the P-wave intermediate states. For D-wave intermediate states, both *sd* and *pp* terms are required, and therefore we used up to 165 *sd* terms and up to 56 *pp* terms in our wave function. In Table X, we show our final results for He.

Table X. Adiabatic and nonadiabatic polarizabilities for ^{4}He. We also give the estimated errors.

k	i=1(Dipole)	i=2(Quadrupole)
1	α_1=1.383 241 013 80±10	α_2=2.443 372 616 06±20
2	β_1=0.707 521 492 749±55	β_2=1.035 440 519 03±20
3	γ_1=0.375 538 368 413±21	γ_2=0.467 345 191 67±23

Since we include the mass polarization term in the Hamiltonian, it is interesting to see how large an effect this has on various polarizabilities. Therefore, we carried out our calculations, using the largest expansion lengths, for K=0 and for finite K, both for ^{4}He and ^{3}He. We present the results in Table XI.

Table XI. Effect of the finite nuclear mass on the polarizabilities of both isotopes of helium. Δ is the difference between the results for finite and infinite mass.

Quantity	$\Delta(^3\mathrm{He})$	$\Delta(^4\mathrm{He})$
α_1	6.4798(-5)	4.88345(-5)
β_1	1.5044(-5)	1.1341(-5)
γ_1	4.5918(-6)	3.4638(-6)
α_2	-2.270054(-3)	-1.7107096(-3)
β_2	-8,70263(-4)	-6.55793(-6)
γ_2	-3.64039(-4)	-2.74316(-4)

We carried out a similar calculation for H^- for finite K, except that in this case we used 615 terms in the ground state wave function. The quantities are much larger than in the case of He and the results are given in Table XII.

Table XII. Adiabatic and nonadiabatic polarizabilities for H^-. We also give the estimated errors.

k	i=1(Dipole)	i=2(Quadrupole)
1	α_1=206.148 7618±37	α_2=7766.79 374±48
2	β_1=1886.699 325±34	β_2=70 155.536 09±25
3	γ_1=20 046.0671±30	γ_2=711 88.8802±96

To ckeck the accuracy of our results, we consider two special cases, related to $S_{0,1}$ and $S_{1,-1}$. The first one tests the completeness of pseudostates that we are using without considering the ground-state accuracy:

$$\sum_N < 0|\mathbf{w}\cdot\hat{\mathbf{x}}|N >< N|\mathbf{w}\cdot\hat{\mathbf{x}}|0 >=< 0|(\mathbf{w}\cdot\hat{\mathbf{x}})^2|0 > \tag{163}$$

Comparison between the left and right sides of Eq. (163) gives a measure of completeness of the set N. We give results in Table XIII, along with the difference of the ratio from unity.

Table XIII. Comparison between left and right side of Eq. (163). Δ=difference of the ratio from unity.

System	left hand side	right hand side	Δ
He	0.752 552 891 661	0.752 552 891 770	1.0(-9)
H^-	7.488 423 814 28	7.488 424 910 34	1.5(-7)

The second test is the Thomas-Reiche-Kuhn sum rule, which for the finite-nuclear mass takes the form

$$\sum_N < 0|\mathbf{w}\cdot\hat{\mathbf{x}}|N >< N|\mathbf{w}\cdot\hat{\mathbf{x}}|0 > (E_N - E_0) = 2 + K \tag{164}$$

Now the extent of the agreement between the left and right sides of Eq. (164) measures both the accuracy of the ground state $|0>$ and the completeness of intermediate states $|N>$. We find

the ratio of the left side to the right side is 0.999 999 87 for He, and the corresponding ratio for H^- is 0.999 9787, respectively. All these tests show that H^- is a more sensitive system than He. Nevertheless, our results are accurate to the accuracy given.

Polarizabilities of H_2^+ and D_2^+

Having calculated polarizabilities of two-electron sytems, it must appear that there should be no difficulty in calculating polarizabilities of molecular ions H_2^+ and D_2^+, the only difference being that two light particles have been replaced by two heavy particles and the mass-polarization term becomes as important as other kinetic energy terms in the Hamiltonian. Since, with a hammer in hand the whole world looks like a nail, I just went ahead with the calculations for H_2^+ and D_2^+ systems using Hylleraas type wave functions, with the appropriate change of masses in the Hamiltonian. But I found no expansion length in these functions was adequate enough for approaching the known results obtained using the Born-Oppenheimer approximation, leaving aside to surpass them. The problem remained dormant till Drachman heard from Steve Lundeen about his experimental results on high Rydberg states of H_2. It is possible to extract accurate properties like quadrupole moment and the parallel and perpendicular polarizabilities of the molecular ion H_2^+ from these results [85,86]. The Born-Oppenheimer results [87] disagreed with the experimental results. We tried to resurrect our old work and tried various extrapolations, but had no success. Drachman came up with an excellent idea: simply raise r_{12} (the interparticle distance between similar particles) to a power close to 30 or so and choose the nonlinear parameter α in $e^{-\alpha r_{12}}$ equal to half of that power of r_{12} in the Hylleraas functions being used. This was a miracle in the sense that nearly six terms in the Hylleraas expansion now were equivalent to hundreds of terms in the earlier expansion! It is easy to understand, after the fact, that now two protons stayed clamped at their respective positions whereas they enjoyed the same freedom as electrons with the usual generalized Hylleraas functions. This was just what was needed to get excellent results without making Born-Oppenheimer like approximations. The expression for polarizability [88] is given by

$$\alpha_1 = \frac{4}{\mu^3(1+\mu)^2} \sum_N \frac{|<0|z_A + z_B|N>|^2}{E_N - E_0} a_0^3, \tag{165}$$

where $z_A = r_A \cdot \hat{\epsilon}$ and $z_B = r_B \cdot \hat{\epsilon}$, ϵ being the direction of the external electric field which can be considered to be in the z direction, r_A and r_B are the distances of the electron from protons A and B, respectively. The reduced mass $\mu = M/(M+1)$. It should be pointed out that we are treating all the particles on an equal footing and we do not refer to any special "molecular" quantum numbers. Thus we are not interested here in the "axial" or "transverse" polarizabilities that appear in the Born-Oppenheimer approximation.

With these modified Hylleraas functions, we obtained ground state energy $E(H_2^+)$=-1.194 277 909 Ry, differing by only about 2.2×10^{-7} Ry from the accurate value [89]. We calculate the intermediate P states also using high powers of r_{12} (cf. [88] for details). Our final results for H_2^+ and D_2^+ are given in Table XIV.

Table XIV. Polarizabilities of H_2^+ and D_2^+ obtained in different ways, both theoretically and experimentally. Quantities in perentheses are errors in the last decimal place given.

Method	$\alpha_1(H_2^+)$	$\alpha_1(D_2^+)$
Experiment[a]	3.1681(7)	3.0712(7)
Born-Oppenheimer [b]	3.1713	3.0731
Modified generalized Hylleraas functions	3.1680	3.0671
Finite element[c]	3.1682(4)	3.0714(4)

[a]Jacobson *et al.* [86]. [b]Bishop and Lam [87]. [c]Shertzer and Greene [90].

It is obvious that the results for D_2^+ are not as close to the experimental results as in the case of H_2^+, showing that even the modified wave functions have limitations: as the nuclei get heavier it becomes more difficult to generate a well-enough localized two-nucleus part of the trial wave function. Clearly, the method fails as the nuclei become infinity heavy.

Dr. J. Shertzer discusses in these Proceedings the results obtained by the finite-element method.

Polarizabilities of HD^+

After we had studied the polarizability of the homonuclear molecular ions it should have been simple to extend our methods to the heteronuclear ion HD^+. Janine Shertzer reminded Drachman that in this case there would be dipole coupling between rotational levels with J=0 and J=1, which was not possible in the earlier cases because of symmetry. In addition she pointed out that the lowest-lying J=1 level is so close to the ground state that one would expect a very high value of polarizability, since the denominator of the second-order perturbation sum would be so small. Drachman and I [91] carried out calculations to see if this prediction was borne out.

The dipole polarizability α_1 is given by the second-order perturbation theory:

$$\alpha_1 = \sum_N \frac{< 0|d|N >< N|d|0 >}{E_N - E_0} a_0^3. \tag{166}$$

The dipole operator d depends on masses of the nuclei and is given by

$$d = 2\left[\frac{M_D + 1}{M_T}\mathbf{r}_1 + \frac{M_P + 1}{M_T}\mathbf{r}_2\right] \cdot \hat{\epsilon}, \tag{167}$$

where the unit vector $\hat{\epsilon}$ is in the direction of the applied electric field, M_P and M_D are the masses of the proton and deuteron nuclei and

$$M_T = M_P + M_D + 1. \tag{168}$$

The calculation of the dipole polarizability of HD^+ is similar to that of H_2^+ and D_2^+: we treat all three particles on an equal footing and do not refer to any special "molecular" quantum numbers. We use the modified generalized Hylleraas type wave functions, i.e., we use very high powers of n in $r_{12}^n e^{-\alpha r_{12}}$ and α is of the order of $n/2$. The energy eigenvalues using the Rayleigh-Ritz variational

principle are E_0=-1.195 795 889, using 560 terms, and E_p=-1.195 372 602 Ry, using 728 terms, for the ground S state and the lowest P state, respectively. These compare well with E_0=-1.195 795 931 and E_p=-1.195 396 2560 Ry obtained by Moss [92]. The energies of these two states are so close to each other that they are almost degenerate states of opposite parity. This is the important difference between the homonuclei H_2^+ and D_2^+, and heteronuclei HD^+ molecules.

The polarizability due to the lowest P term alone in Eq. (166) is $392.0814a_0^3$ and the sum over the remaining intermediate states contributes $\bar{\alpha_s}$=$3.2076a_0^3$. The total polarizability, α_1=$395.289a_0^3$, is very much larger than might be expected from the results [88] in H_2^+ and D_2^+. This can be traced to the fact, as indicated above, that there is a coupling between the two lowest S and P states due to their closeness in energy. If we exclude the ground state, we can calculate the polarizability of the lowest P state by summing over all the intermediate S states. We find this result to be $\bar{\alpha_p}$=$2.03008a_0^3$.

But second-order perturbation theory can only be legitimately carried out if the perturbation is small compared to the spacing of the unperturbed energies, and this condition is hard to satisfy in the present case. If the perturbation is due to a unit charge it must lie further from the ion than about $32a_0$ for the perturbation theory to be valid. What happens for larger fields or smaller distances? Clearly, for these larger fields the opposite parity levels act essentially as degenerate levels, so the techniques of degenerate perturbation theory must be applied. This leads to an energy shift that is linear in the electric field, falling like R^{-2} rather than R^{-4} as we expect for ordinary polarizability. This is usually described as the effect of a permanent dipole moment. We then went on to diagonalize the perturbation matrix in various approximations and were able to give a good description of the energy shift as a function of R.

In observing the Rydberg states of HD, the effective polarizability should be $\bar{\alpha_s}$=$3.2076a_0^3$, which is close to the polarizabilities of H_2^+ and D_2^+ [88]. With this value, we have calculated energy shifts

$$\Delta_{NL} \equiv -\bar{\alpha_s} \int \Psi_{NL}(\mathbf{R}) \frac{1}{R^4} \Psi_{NL}(\mathbf{R}) d\mathbf{R}, \tag{169}$$

using hydrogenic wave functions. We give these energy shifts Δ_{NL} of a series of Rydberg levels due to the polarizability of the HD^+ ionic core omitting the lowest rotationally excited level in the summation over intermediate states.

Table XV. Energy shifts Δ_{NL} of a series of Rydberg levels.

N	L	-Δ_{NL}(MHz)
9	4	11501
	5	3943.6
	6	1594.9
	7	720.08
	8	350.41
10	4	8527.4
	5	2951.8
	6	1208.8
	7	554.8
	8	275.89
	9	145.2

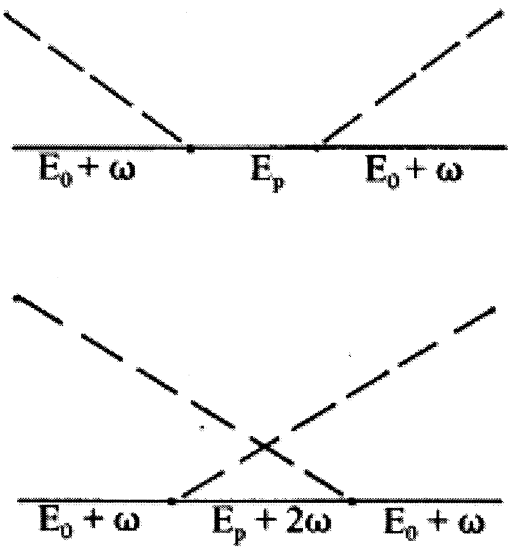

Figure 6: Diagrams symbolizing the nonrelativistic calculation of $\alpha(\omega)$, with energies of each state indicated.

Optical Properties of He Including Relativistic Corrections

An interesting application of polarizabilities is the calculation, which Drachman and I [93] carried out, of the index of refraction n of He from which the Verdet constant V, which measures the rotation of the plane of polarization in the Faraday effect, can be obtained. The rotation θ, measured in degrees, is given by

$$\theta = VBL, \tag{170}$$

where B is the magnetic field and L is the length traversed by light. If the static field is replaced by an oscillating field (an electromagnetic wave), it is possible to define a frequency-dependent polarizability $\alpha(\omega)$ from which the index of refraction can be obtained (cf. Fig 6). The expression for the polarizability is given by

$$\begin{aligned} \alpha(\omega) &= \frac{1}{2}\sum_N < 0|Z|N >< 0|Z|N > \left[\frac{1}{E_N - (E_0+\omega)} + \frac{1}{(E_N+2\omega) - (E_0+\omega)}\right] \\ &= \sum_N \frac{< 0|Z|N >< N|Z|0 > (E_N - E_0)}{(E_N - E_0)^2 - \omega^2}, \end{aligned} \tag{171}$$

where $N \equiv p$ and the dipole operator Z is given by

$$Z = 2(z_1 + z_2). \tag{172}$$

We can define a set of "generalized dipole polarizabilities" as follows

$$[\alpha_1, \beta_1, \gamma_1, \delta_1, \epsilon_1, \xi_1, \eta_1] = \sum_N \frac{< 0|Z|N >< N|Z|0 >}{(E_N - E_0)^{(1,2,3,4,5,6,7)}}. \tag{173}$$

As indicated earlier, we use Hylleraas basis sets for the ground state as well as for pseudostates N and the results for various quantities are given in Table XVI.

Table XVI. Various quantities for ^{4}He.

α_1	1.383 241 01
β_1	0.707 521 493
γ_1	0.385 538 368
δ_1	0.218 735 026
ϵ_1	0.127 538 649
ξ_1	0.075 827 657
η_1	0.045 731 135

The denominator in Eq. (171) can be expanded in powers of $\omega/(E_N - E_0) \leq 0.2$ for wavelengths of visible light:

$$\alpha(\omega) = \alpha_1 + \gamma_1\omega^2 + \epsilon_1\omega^4 + \eta_1\omega^6 + ... \tag{174}$$

The relativistic corrections are calculated by using the Breit-Pauli relativistic Hamiltonian which has the following form:

$$B = \alpha^2 \left\{ -\frac{1}{4}[\nabla_1^4 + \nabla_2^4] + 2\pi[\delta(\mathbf{r}_1) + \delta(\mathbf{r}_2)] + 2\pi\delta(\mathbf{r}_{12}) + \frac{1}{r_{12}}[\nabla_1 \cdot \nabla_2 + \hat{r}_{12} \cdot (\hat{r}_{12} \cdot \nabla_1)\nabla_2] \right\}. \tag{175}$$

This requires a third-order-perturbation theory, with B retained to first order and Z to the second order. Up to ω^4 the expansion corresponding to Eq. (174) gives the following numerical result

$$\Delta\alpha(\omega) = -8.0029 \times 10^{-5} - 8.1516 \times 10^{-6}\omega^2 + 3.006 \times 10^{-7}\omega^4, \tag{176}$$

and the relativistic expression for the frquency-dependend polarizability of helium becomes

$$\alpha_{\rm rel}(\omega) = 1.383160981 + 0.385530216\omega^2 + 0.12753895\omega^4 + 0.04573114\omega^6. \tag{177}$$

The last term Eq. (177) has not been modified from its nonrelativistic value, since the effect of relativity here would be absolutely negligible. In order to write the above expression in terms wavelength, we use

$$\omega = \frac{4\pi a_0}{\alpha(1 - K/2)\lambda} = \frac{911.39198}{\lambda}, \tag{178}$$

where K=2.741 493$\times 10^{-4}$ for ^{4}IIe and the wavelength is in Å units. We obtain the expression for polarizability in terms of wavelength in the form:

$$\alpha_{\rm rel}(\lambda) = 1.383729930 + \frac{3.204546 \times 10^5}{\lambda^2} + \frac{8.822907 \times 10^{10}}{\lambda^4} + \frac{2.624092 \times 10^{16}}{\lambda^6} a_0^3 \tag{179}$$

Optical measurements usually give $n-1$, where n is close to 1 for helium. The higher-order corrections in the relation between the polarizability (a single atom property) and the index of refraction, due to the effects in the medium, are accounted for by the Lorenz-Lorentz equation:

$$\frac{n^2-1}{n^2+2} = \frac{4\pi}{3} N_L a_0^3 = 16.67718 \times 10^{-6} \alpha_{\rm rel}(\lambda) \equiv z \tag{180}$$

where N_L is Loschmid's number. Solving for n to second order in z, we find

$$n - 1 \simeq \frac{3}{2}z + \frac{3z^2}{8} = 34.61527 \times 10^{-6} + \frac{8.016511}{\lambda^2} + \frac{2.207154 \times 10^6}{\lambda^4} + \frac{6.564503 \times 10^{11}}{\lambda^6}. \tag{181}$$

The Verdet constant is given by

$$V = -\frac{e}{2mc^2}\lambda\frac{dn}{d\lambda} = \frac{1.616813 \times 10^7}{\lambda^2}\left[1 + \frac{5.506521 \times 10^5}{\lambda^2} + \frac{2.456618 \times 10^{11}}{\lambda^4}\right] \mu \text{ min/oer cm}, \tag{182}$$

where min refers to rotation. We get from the above equation V=0.661 22±0.00025 at λ=5000Å versus the experimental value 0.637 of Leonard [94], while at λ=8000Å we get V=0.254 816±0.000 015 compared with the experimental value 0.246 (all in units of μ min/oer cm). This shows that there is a significant discrepancy here that is larger than the relativistic effects that we have considered. The experimental results do not appear to be very accurate and new measurements are required of the refractive index n of helium to have a better comparison between our theoretical results and measurements.

Another Way to Calculate Lamb Shift

One of the most difficult parts in two-electron Lamb shift calculations is the Bethe logarithm given by

$$\begin{aligned} \ln(\mathrm{K}) &= \frac{\sum_n < 0|V|n >< n|V|0 > (E_n - E_0)^3 \ln(\mathrm{E_n} - \mathrm{E_0})}{\sum_n < 0|V|n >< n|V|0 > (E_n - E_0)^3} \\ &\equiv \frac{N}{D}, \end{aligned} \tag{183}$$

where $|n>$ are L=1 eigenstates, both bound and continuum, of the Hamiltonian describing the two-electron system. Instead, we use the pseudostate summation method. The interaction V is given by

$$V = z_1 + z_2 = r_1\cos\theta_1 + \mathrm{r_2}\cos\theta_2. \tag{184}$$

Having used pseudostates in the polarizability calculations, it should have been easy to calculate $\ln(K)$ given by the above expression in the length form. But the result obtained using either the length, or velocity, or acceleration form never seemed to approach the known results, no matter how large the psoudostate expansion was in the above expression. The basic reasons are the power of $(E_n - E_0)$ which is 3 instead of -1, as in the polarizability expression, and the presence of $\ln(E_n - E_0)$ in the numerator, which makes matters worse. Combined together, the convergence of the results

becomes extremely slow. Out of frustration, I sought Drachman's help. To solve this problem, he came up with several tricks which I prefer to call good insight. We could then obtain results as accurate as available in the literature. I have used a slightly different notation in this section for the pseudostates in order to conform with our published paper [95].

The Denominator

We transform the denomenator D in Eq. (183) in a form which does not have an intermediate sum $|n>$ by using the commutation relation

$$< n|[H,V]|0 >=< n|V|0 > (E_n - E_0) \tag{185}$$

three times, in order to remove $(E_n - E_0)$:

$$D = \frac{2}{3}(2+K)^2 \{< 0|[H,(\nabla_1+\nabla_2)]\cdot(\nabla_1+\nabla_2)|0 > - < 0|(\nabla_1+\nabla_2)\cdot[H,(\nabla_1+\nabla_2)]|0 >\}. \tag{186}$$

Since the potential term in the Hamiltonian does not commute with $\nabla_1+\nabla_2$, the above expression can be put in the form

$$D_{\rm ex} = \frac{16\pi Z(1+K)}{3} < 0|\delta(\mathbf{r}_1)+\delta(\mathbf{r}_2)|0 >, \tag{187}$$

where closure over the intermediate states $|n>$ has been invoked and Poisson's equation has been used to introduce δ functions. As before, $K = 2/(M+1)$, where M is the mass of the nucleus in units of the electron mass. The terms of the order K^2 have been dropped; within this error the expression is exact. It does depend on the accuracy of the ground state wave function which consists here of 525 terms. Therefore, the error due to the accuracy of the ground state wave function is negligible.

Table XVII. $\ln(K)$ as a function of γ and Pekeris number Ω_p.

Ω_p	γ	D_{acc}	N_{acc}	$\ln(K)$
3	3.644 529	94.114 569	301.053 261	3.198 796
4	4.080 394	101.216 416	346.195 202	3.420 346
5	4.425 096	104.957 668	373.513 205	3.558 703
6	4.849 542	108.413 460	399.676 322	3.686 593
7	5.179 484	110.403 345	416.057 508	3.768 523
8	5.588 226	112.320 411	432.319 315	3.848 983
9	5.888 226	113.508 976	442.840 189	3.901 367
10	6.305 080	114.676 534	453.744 402	3.956 373
11	6.623 156	115.446 146	461.125 678	3.994 293
12	7.004 813	116.207 693	468.586 094	4.032 316
13	7.3	116.735 692	473.876 067	4.059393

Because of the $\ln(E_n - E_0)$ term, it is not possible to reduce N to a similar form. However, we expect the convergence of pseudostates will be similar for N and D. We use the commutation relation [Eq. (185)] twice for each matrix element of Eq. (183) to obtain the acceleration form

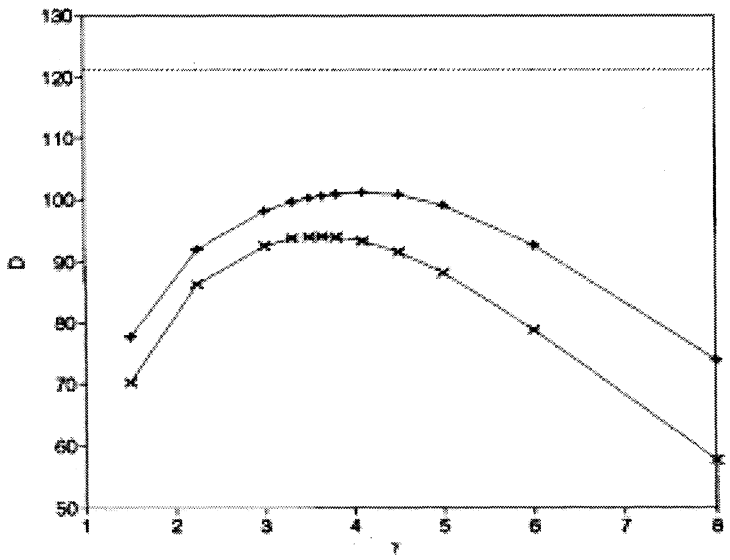

Figure 7: Behavior of D_{acc} for helium as a function of the nonlinear parameter γ. The crosses are for Ω_p=3, and the plus signs are for Ω=4. The dotted line is the "exact" value, obtained from Eq. (187).

$$D_{acc} = -8Z^2(1+K)\sum_n \frac{<0|U|n><n|U|0>}{E_0 - E_n}, \tag{188}$$

where

$$U = \frac{\cos\theta_1}{r_1^2} + \frac{\cos\theta_2}{r_2^2}. \tag{189}$$

This expression for D_{acc} looks like the second-order energy shift induced by the potential U, and it has a variational bound [95]. We can, therefore, choose the nonlinear parameter γ in the pseudostates to maximize D_{acc} in Eq. (188) (cf. Fig. 7).

As the number of $|n>$ is increased the D_{acc} approaches D_{ex} which for He from Eq. (187) is 121.335 143. We calculate N for the same γ and the same number of $|n>$ as for D_{acc}. We give values of $\ln(K)$ as a function of the Pekeris number Ω_p in Table XVII.

Extending The Upper Limit

We assume that the contribution of each term in the pseudostate summation is exact and the remaining error in the total is due to the fact that that the sum does not extend to infinity. We use the method of Dalgarno and Stewart [96] to account for the remainder of the sums beyond the highest pseudoenergy. For high energies they used the following simplified form:

$$\Psi_{n,\mathbf{k}}(\mathbf{r}_1,\mathbf{r}_2) = \frac{1}{2\pi}\left(\frac{k}{2}\right)^{1/2}[u_n(\mathbf{r}_1)e^{i\mathbf{k}\cdot\mathbf{r}_2} + u_n(\mathbf{r}_2)e^{i\mathbf{k}\cdot\mathbf{r}_1}], \tag{190}$$

to represent the singly ionized states in the expression that replaces the discrete one in Eq. (188):

$$F_n(\epsilon) = \frac{16Z^2(1+K)}{3(I_n+\epsilon)} \left| < \Psi_0 | \left[\frac{\mathbf{r}_1}{r_1^3} + \frac{\mathbf{r}_2}{r_2^3} \right] | \Psi_{n,\mathbf{k}} > \right|^2 . \tag{191}$$

Here $\epsilon = k^2$, I_n is the ionization-excitation potential of two-electron systems, and u_n is the wave function of the one-electron system left after single ionization. Without loss of accuracy, we fitted $F_n(\epsilon)$ to the form $[A_n + (B_n/k)\tan^{-1}(\mathrm{C_n/k})]\epsilon^{-3/2}$ and included s states up to n=4. Higher states were included approximately by an exression falling like $1/n^4$. We adjust ϵ_0 so that

$$D_{ex} = D_{acc} + \int_{\epsilon_0}^{\infty} d\epsilon \sum_n F_n(\epsilon). \tag{192}$$

The critical step is now to correct N using the same value of ϵ_0 as for the denominator, modifying the integral by the inclusion of the appropriate logarithmic factor. In Table XVIII, to obtain the exact value of the denominator we give the required value of ϵ_0, the corrected value of the numerator and the improved value of $\ln(K)$; the convergence with Ω_p is significantly improved.

Table XVIII. The ϵ_0, corrected values of N_{corr}, and $\ln(K)$.

Ω_p	ϵ_0	N_{corr}	$\ln(K)$
3	361.0613	520.267 518	4.287 855
4	724.0096	521.248 382	4.295 939
5	1143.441	523.110 217	4.311 284
6	1912.977	524.085 779	4.319 324
7	2734.433	525.086 045	4.327 568
8	4108.808	525.799 439	4.333 447
9	5524.324	526.334 777	4.337 859
10	7729.503	526.911 785	4.342 614
11	9964.945	527.307 234	4.345 874
12	13 253.52	527.650 177	4.348 700
13	16 564.86	527.870 611	4.350 517

Extrapolation and Results

We extrapolate our results by using the deviation ΔD of the denominator from its exact value:

$$\Delta D = D_{ex} - D_{acc} \tag{193}$$

This quantity approaches zero as Ω_p increases. We plot the uncorrected and corrected $\ln(K)$ (cf. Fig. 8).

The slope of the line fitted to the corrected points is 12 times smaller than the uncorrected slope, indicating the improved convergence we expected. The extrapolated result for helium is $\ln(K)$=4.367 58(46).

In Table XIX we show the values of $\ln(K)$, obtained by this method, for a range of atomic numbers Z and compare them with those obtained from the approximate expression of Goldman and Drake [97]. Their approximate expression has been obtained using an expansion in $1/Z$:

$$\ln(\mathrm{K}) = \ln[19.7692669(\mathrm{Z} - 0.00615)^2]. \tag{194}$$

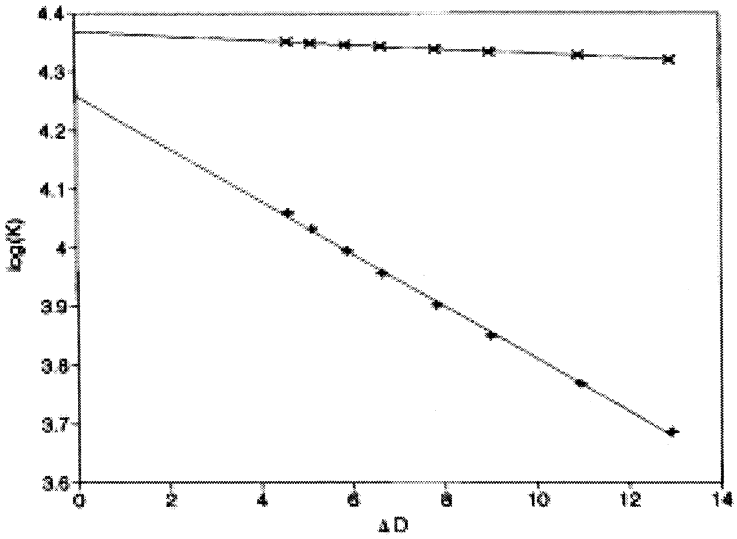

Figure 8: $\ln(K)$ for helium as a function of ΔD. The plus signs show the uncorrected values, using the data from Table XVII, and the crosses are the corrected values from Table XVIII. Linear fits have been made in both cases, and the improved convergence of the corrected values is clear.

Table XIX. Results for a series of two-electron systems.

System	Z	$\ln(K)$	$\ln(K)^a$
He	2	4.367 578	4.364 263
Li^+	3	5.177 763	5.177 249
Be^{+2}	4	5.753 615	5.753 640
Ne^{+8}	10	7.586 072	7.588 068

[a]From Eq. (14) of Ref. [97] which is the same as Eq. (194) given above.

A good fit to our results is the form:

$$\ln(\mathrm{K}) = \ln[19.705541(\mathrm{Z} + 1.35 \times 10^{-5})^2]. \tag{195}$$

The present results may represent the two-electron ground state Bethe logarithm well over the range $2 \leq Z \leq 10$.

$\ln(K)$ for Atomic Hydrogen

It is an obviously interesting question to see how well the above method works for the simpler and better known one-electron (atomic hydrogen) case. Here the ground state wave functtion is known exactly and the pseudostates are of a simple one-electron form:

$$\Psi_0 = \frac{e^{-r}}{\pi^{1/2}}, \qquad \Psi_n = e^{-\gamma r} P_1(\theta) \sum_{j=1}^{\Omega_p} C_j r^n. \tag{196}$$

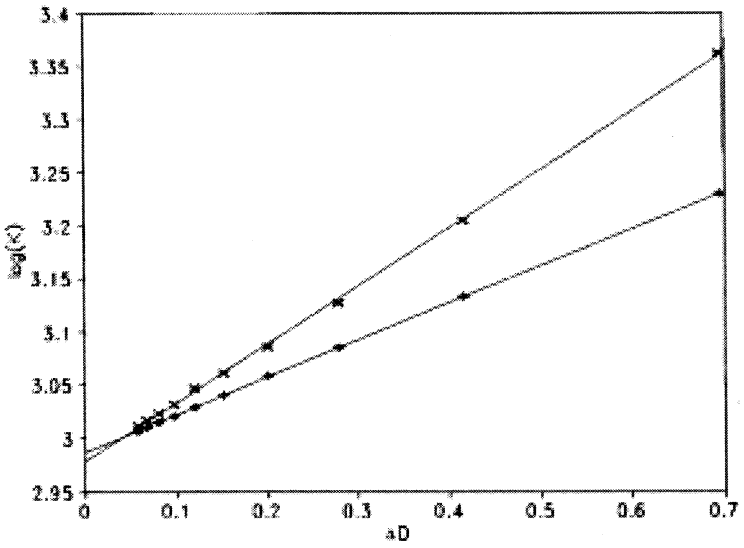

Figure 9: $\ln(K)$ for hydrogen as a function of ΔD. The alternating convergence pattern discussed in the text leads to two distinct lines: crosses are for even values and plus signs are for odd values of Ω_p.

The denominator can be evaluated exactly: D=16/3. All other steps described above can be applied to the one-electron system.

In Fig. 9 we show the unexpected results. In place of the linear relation found for two-electron systems, we obtain an alternating convergence pattern. As Ω_p increases from an odd value to the next even value the numerator increases significantly while the denominator remains unchanged to 7 or 8 significant figures. With the next increase in Ω_p the increase in D resumes. This effect produces two distict lines. We were able to carry the calculations up to Ω_p=22, at which point ΔD=0.057. The extrapolations to ΔD=0 give $\ln(K)$=2.987 125 (from odd values of Ω_p) and $\ln(K)$=2.978 329 (from even values). Combining the two results we can report a "best" value of $\ln(K)$=2.9827 $\pm$0.0044 which should be compared to the accurate value of Haywood and Morgan III [98] $\ln(K)$=2.984 129; our generous error does include this value.

We have not been able to understand this irregular convergence and this remains an interesting unanswered question.

Rydberg States of Li

Traditionally, eigenvalues and eigenfunctions are calculated by the use of the Rayleigh-Ritz variational principle. This procedure has been carried out for states with high quantum numbers, N and L, as well [99]. The disadvantage is eigenvalues of all the states below the state of interest have to be calculated. Drachman realized that when N is large, say 10, the outer electron is so far away [100 a_0 compared to a_0 for the core electrons] from the spherically symmetric core that it does not have much electron-electron correlations, the type taken into account by the Hylleraas functions, with the core electrons. Even the exchange is not important, and most of the of correlations can be taken into account by considering only the long-range interactions. On this basis, he developed

a formalism [100] to calculate energies of states of interest only, using the Feshbach projection operator technique. Since the exchange can be ignored Eq. (71) simplifies to

$$P = P_1 = |\phi_0 >< \phi_0|. \tag{197}$$

The formalism is rather complicated and I give the final result for the effective potential seen by the outer electron at a distance x from the nucleus:

$$\begin{aligned} U(x) &= -\frac{\alpha_1}{x^4} + \frac{6q\beta_1 - \alpha_2}{x^6} + \frac{\delta + 16q^2\gamma_1/5}{x^7} \\ &+ \frac{-\alpha_3 + 15q\beta_2 - \epsilon + \alpha_1\beta_1 - 72q^2\gamma_1[1 + L(L+1)/10]}{x^8} ..... \end{aligned} \tag{198}$$

I alluded to this form in Eq. (155), where I indicated the importance of polarizabilities in the Rydberg states. The core coefficients are described below:

$$S_{k,i} \equiv x^{2i+2} \sum_n \frac{< 0|V_i|n >< n|V_i|0 >}{(E_n - E_0)^k}. \tag{199}$$

Here, as mentioned before, $\alpha_i = S_{1,i}, \beta_i = S_{2,i}$, and $\gamma_i = S_{3,i}$. The third-order polarizability has the form:

$$\delta \equiv x^7 \sum_{n,m} \frac{< 0|V_i|n >< n|V_j|m >< m|V_k|0 >}{(E_n - E_0)(E_m - E_0)}. \tag{200}$$

The values that (ijk) can take are all the permutations of [112]. Finally, the fourth-order hyper-polarizabilty involving the dipole terms has the form:

$$\epsilon \equiv x^8 \sum_{n,m,p} \frac{< 0|V_1|n >< n|V_1|m >< m|V_1|p >< p|V_1|0 >}{(E_n - E_0)(E_m - E_0)(E_p - E_0)}. \tag{201}$$

Drachman [100] developed the formalism for helium atoms and showed that he could obtain the same result as Drake [99] did for the eigenvalues, e.g., N=10 and L=6 his result E=-105.829 80±0.00014 compares very well with -105.829 683 489 MHz of Drake (cf. Table III of Ref. [100]).

Up to now I have not given the interaction potentials V_1, V_2, and V_3. We are now interested in the Rydberg states of Li where the spherical core is He-like and therefore, I give below expressions [101] for three-electron systems:

$$V_1 = \frac{2q^2 w}{x^2} \left[\frac{2 + (Z-1)K}{2+K}\right] P_1(\hat{\mathbf{w}} \cdot \hat{\mathbf{x}}), \tag{202}$$

$$V_2 = \frac{2q^3}{x^3} \left[r_1^2 P_2(\hat{\mathbf{r}}_1 \cdot \hat{\mathbf{x}}) + r_2^2 P_2(\hat{\mathbf{r}}_2 \cdot \hat{\mathbf{x}}) - \frac{4K + ZK^2}{(2+K)^2} w^2 P_2(\hat{\mathbf{w}} \cdot \hat{\mathbf{x}})\right], \tag{203}$$

$$V_3 = \frac{2q^4}{x^4} \left[\frac{2-K}{2+K}[r_1^3 P_3(\hat{\mathbf{r}}_1 \cdot \hat{\mathbf{x}}) + r_2^3 P_3(\hat{\mathbf{r}}_2 \cdot \hat{\mathbf{x}})] - \frac{4K - 2K^2 - ZK^3}{(2+K)^3} w^3 P_3(\hat{\mathbf{w}} \cdot \hat{\mathbf{x}})\right], \tag{204}$$

where $\mathbf{w} = \mathbf{r}_1 + \mathbf{r}_2$ and $q \simeq 1+K^2/2$. In Table XX we give the various quantities for $^7Li^+$ and $^6Li^+$, which have been calculated by using the appropriate Hylleraas type wavefunctions for the ground state and intermediate pseudostates of angular momentum L=1, 2, and 3. Again we use the method of pseudostate summation.

Table XX. Best values of the core parameters used in constructing the effective potential. The upper entry is for ^{6}Li and the lower one is for ^{7}Li.

α_1	β_1	γ_1	α_2
0.192 490 771	0.035 286 879	0.006 806 377	0.113 825 934
0.192 485 410	0.035 286 017	0.006 806 227	0.113 834 685

β_2	γ_2	δ	ϵ
0.016 670 328	0.168 351 237	0.121 337 559	0.027 039 600
0.016 671 511	0.168 362 339	0.121 345 411	0.027 038 073

From the core parameters of Table XX the effective potential of Eq. (198) can be constructed explicitly. Numerically, this potential is

$$U(x) = -\frac{0.19248540}{x^4} + \frac{0.097881}{x^6} + \frac{0.143125}{x^7} - \frac{0.428584 + 0.049005L(L+1)}{x^8} \tag{205}$$

for the case of ^{7}Li. We use the following expression for the energy shift $\Delta(NL)$ away from the unperturbed energy -R/N^2

$$\Delta(NL) = R\left[(U_4 + U_6) + \frac{1}{2}[U_7 + U_8]) \pm \frac{1}{2}[U_7 + U_8]\right], \tag{206}$$

where the reduced Rydberg R=3.289 584 678 $\times 10^9$ MHz for ^{7}Li, and where U_k is the expectation value of that term in $U(x)$ which goes like x^{-k}. Since the unperturbed wavefunction of the outer electron is purely hydrogenic, these expectation values can be evaluated analytically and exactly. Some results are given in Table XXI for N=10 and various values of L (cf. Table II of Ref. [101] for values for other N and L).

Table XXI. Level shifts (in MHz) for ^{7}Li for N=10 due to the effective potential terms U_k. The total and error are obtained as described in Eq. (206).

L	U_4	U_6	$U_7 + U_8$	Total	Error
4	-511.674	2.332	-0.229	-509.457	0.115
5	-177.1181	0.3007	-0.0022	-176.8185	0.0011
6	-72.5341	0.0541	0.0005	-72.4798	0.0003
7	-33.29026	0.01190	0.00014	-33.27829	0.00007
8	-16.554171	0.002929	0.000033	-16.51226	0.000017
9	-8.712722	0.000738	0.000007	-8.711981	0.000004

Since U_8 has been included, α_1/x^4 should also be included to the second order. That is

$$\Delta_2 = \sum_N{}' \frac{< NL|\alpha_1/x^4|N'L >< N'L|\alpha_1/x^4|NL >}{E_N - E_{N'}} \tag{207}$$

Here the intermediate states $N'L$ are the hydrogenic states of the outer electron. This quantity has been calculated for He [100], Δ_2 for ^{7}Li can be obtained by scaling the results for He; Δ_2 being proportional to α_1^2. The results, given in Table XXII, are again shown only for the N=10 and various L. The large relativistic correction due to increase in mass with velocity has been discussed by Bethe and Salpeter [102] and some details are given in [101], as well. We obtained the following expression for the leading relativistic correction:

$$\Delta_{\rm rel} = \frac{\alpha^2 R}{N^3}\left[\frac{3}{4N}[1 - \frac{K}{6}] - \frac{2}{2L+1}\right], \tag{208}$$

which is accurate up to order K^2. Again some results are given in Table XXII.

Table XXII. Second-order corrections, leading realtivistic corrections, and the final total shifts for ^{7}Li in MHz for N=10.

L	Δ_2	$\Delta_{\rm rel}$	Total+Δ_2+$\Delta_{\rm rel}$
4	-0.097	-25.790	-535.343±0.115
5	-0.0090	-18.7122	-195.5397±0.0011
6	-0.0012	-13.8122	-86.2932±0.0003
7	-0.0022	-10.218 88	-43.497 39±0.000 07
8	-0.000 046	-7.471 035	-24.022 31±0.000 02
9	-0.000 011	-5.301 687	-14.013 679±0.000 0004

The fine-structure splitting for the N=10 manifold are shown in Table XXIII, where they are compared with the accurate measurements of Rothery *et al.* [103].

Table XXIII. Fine-structure splitting for the N=10 manifold of ^{7}Li.

Interval	Enegy shift(MHz)	Experiment [103] (MHz)
10G-10H	339.80±0.011	339.7186±0.0031
10H-10I	109.246 6±0.001 1	109.2140±0.0047
10I-10K	42.795 8±0.000 3	
10K-10L	19.475 08±0.000 07	
10L-10M	10.008 63±0.000 02	

Considering the accuracy of the measurements, the agreement between theory and experiment is not very good. Drachman and I [104] extended our work [101] to included corrections to the third order to improve the agreement.

Relativistic Correction to the Polarization Potential

We wish to compute a correction to the energy shift of a Rydberg level due to the Breit-Pauli relativistic Hamiltonian of order α^2. Thus we must carry out a third-order perturbation calculation which has the form

$$V_3(x) = \sum_{n,m} \frac{< 0|h|n >< n|h|m >< m|h|0 >}{(E_0 - E_n)(E_0 - E_m)} - \sum_n \frac{< 0|h|n >< n|h|0 >}{(E_0 - E_n)^2} < 0|h|0 >, \tag{209}$$

where $h=H_{\rm dip}+H_{\rm BP}$. The expression for the Breit-Pauli Hamiltonian $H_{\rm BP}\equiv B$ has been given in Eq. (175) and

$$H_{\rm dip}=\frac{2}{x^2}(\mathbf{r}_1+\mathbf{r}_2)\cdot\hat{\mathbf{x}}. \tag{210}$$

Keeping terms to order α^2 results in the following:

$$\begin{aligned} V_3^{\alpha^2} &= \sum_{n,m}\left[\frac{<0|H_{\rm dip}|n><n|H_{\rm BP}|m><m|H_{\rm dip}|0>}{(E_0-E_n)(E_0-E_m)}+2\frac{<0|H_{\rm dip}|n><n|H_{\rm dip}|m><m|H_{\rm BP}|0>}{(E_0-E_n)(E_0-E_m)}\right] \\ &\quad -\sum_n\frac{<0|H_{\rm dip}|n><n|H_{\rm dip}|0>}{(E_0-E_n)^2}<0|H_{\rm BP}|0> \\ &= -\frac{\Delta\alpha_1}{x^4}, \end{aligned} \tag{211}$$

where we have taken account of the facts that the ground state has angular momentum L=0, the excited states n,m are L=0 or 1, and $H_{\rm BP}$ is rotationally invariant. Our best-converged result, obtained with 161 terms with L=0 and 165 terms with L=1 is $\Delta\alpha_1$ =-4.518×10^{-5}.

Retardation Corrections

As indicated earlier, the Rydberg electron is at a distance from the nucleus much greater compared to the radius of the core. When the distance is greater than $137a_0$, the interaction is no longer purely Coulomb in character. This is because the delay due to the finite light propagation time between the core and the outer electron is comparable to the characteristic time $t=a_0/v$. This retardation (or Casimir effect) brings in a new type of term [105] in the effective potential acting on the Rydberg electron that falls off like x^{-5}. Au, Feinberg, and Sucher [106] have given the following expressions for the modification of the effective potential producing the energy shift in the state $(1s^2NL)$:

$$\Delta_{\rm Ret}^{NL}=\frac{16}{\pi}\sum_n\frac{|<n|z_1+z_2|0>|^2}{(E_n-E_0)^2}I_n, \tag{212}$$

$$\begin{aligned} I_n &= \int_0^\infty\frac{dt}{(t^2+1)}\int_0^\infty\frac{dx}{x^6}R_{NL}^2(x)e^{-2z_nt}[3-5z_n^2+z_n^4+(6z_n-2z_n^3)t] \\ &\quad +\int_0^\infty\frac{dx}{x^6}R_{NL}^2(x)\left[6z_n-\frac{z_n^3}{2}-\frac{3\pi}{2}\right], \end{aligned} \tag{213}$$

where $z_n=\frac{1}{2}\alpha x(E_n-E_0)$. The evaluation of this correction is rather complicated. Nevertheless, we have evaluated the retardation corrections from N=5 to N=21. We give results for the N=10 manifold only in Table XXIV.

Table XXIV. Retardation corrections for lithium in MHz for N=10 manifold.

L=9	L=8	L=7	L=6	L=5	L=4
0.000646286	0.00142682	0.00325464	0.00790948	0.0212477	0.0653658

Lamb-Shift Corrections

Since we are interested in the L-dependent fine-structure splitting of the Rydberg levels only the *change* in the Lamb shift of the two-electron core due its interaction with the outer electron needs to be calculated. The main parts of the Lamb shift (mass renormalization, vacuum polarization, and radiative corrections to the magnetic moment) can be written in terms of $(<\delta(\mathbf{r}_1)>+<\delta(\mathbf{r}_2)>)$, and it is necessary to calculate the dependence of these δ functions on the state of the outer electron. Following Goldman and Drake [107] we can write the expression for the two-electron Lamb shift as

$$\Delta^{NL}_{\rm Lamb} = \frac{8}{3}Z\alpha^2\left[-2\ln\alpha + \frac{19}{30} - \ln K\right](<\delta(\mathbf{r}_1)> + <\delta(\mathbf{r}_2)>). \tag{214}$$

Here the δ functions refer to the two core electrons but are influenced by the outer electron. This correction is proportional to the expectation value of $1/x^4$ and behaves like another correction to the dipole polarizability of the two-electron core. We can write the relativistic corrections as

$$\Delta_{NL} = [1.486\times 10^5 - 3.103\times 10^4]\left\langle\frac{1}{x^4}\right\rangle_{NL} + \Delta^{NL}_{\rm Ret}, \tag{215}$$

where the quantities in the square bracket are the coefficients (in MHz) of the relativistic polarizability and Lamb-shift corrections, respectively. In Table XXV we show the three types of corrections for the experimentally interesting N=10 and their total in MHz.

Table XXV. Relativistic, polarizablity, retardation, Lamb shift corrections and the total uncorrected interval from Table XXII, in MHz, for N=10 manifold.

L	Uncorrected shift	Relativistic polarizability	Retardation	Lamb shift	Total
4	-535.343±0.115	0.1201	0.0654	-0.0252	-535.183±0.115
5	-195.5397±0.0011	0.0416	0.0212	-0.0087	-195.486±0.0011
6	-86.2932±0.0003	0.0170	0.0079	-0.0036	-86.2719±0.0003
7	-43.49739±0.00007	0.0078	0.0033	-0.0016	-43.4879±0.0001
8	-24.02231±0.00002	0.0039	0.0014	-0.0008	-24.0178
9	-14.013679±0.000004	0.0020	0.0006	-0.0004	-14.0115

Finally, in Table XXVI we compare the experimental fine-structure intervals for lithium [103] with the theoretical totals including the uncorrected values and the three small corrections. It is clear that there is better agreement when the small corrections are included. However, higher-order corrections and more measurements seem to be warranted.

Table XXVI. Comparison of level differences for lithium, in MHz, between theory and experiment [103].

Interval	Experiment-Theory	Standard deviation
10G-10H	0.02	0.11
10H-10I	0.0003	0.0048

We [108] have carried out a similar calculation for CIV, O VI, and Ne VIII. But at present there are no measurements accurate enough to compare with our calculations.

Even though there are other interesting topics on which Dr. Drachman and I have worked on together, I stop here. Instead, I mention below two more topics: one with others and one by himself.

Positronium-hydrogen scattering resonances

Drachman once tried to insert the statement "Nobody likes a smooth cross-section" in an article on resonances, but the referee vetoed it. Nevertheless, there is much more interest in scattering resonances than in bland nonresonant behavior. The Ps-H system is rich in interesting physics: There is one particle-stable state called positronium hydride [PsH] with an energy of about 1 eV below the free Ps+H threshold. Using both the stabilization method and the complex rotation method Drachman and Houston [109] found an s-wave resonance in elastic Ps-H scattering at about 4.5 eV.

Since interesting physics usually emerges from the analysis of resonances, it was of interest to understand the mechanism producing this resonance. At first, it was thought that it was due to some threshold process like that producing resonances in electron-hydrogen scattering below the n=2 threshold, but the position obtained was not close enough to a threshold to make this plausible. The best explanation describes it as a Feshbach resonance [110] in which the closed-channel part of the scattering function is the re-arranged system e^+-H^-, corresponding to perturbed hydrogenic bound states. Because of the long-range Coulomb potential between the positron and the negative hydrogen ion one can predict that there should be an infinite series of resonances, of which the one found by Houston and Drachman [109] is just the first. Since the hydrogen ion exists only in the singlet spin state these resonances should not occur in the triplet state. No reliable calculation has found triplet resonances.

There are more subtleties in this system, including some problems with the low-lying resonances expected for $L > 0$ [111] and these have been examined very recently by De Rienzi and Drachman [112,113]. More about this interesting system can be found in the presentation by Dr. H. R. J. Walters in this volume.

Hyperfine Splitting in Muonic Helium

Huang and Hughes [114] calculated the Fermi contact term which yields the hyperfine splitting of the ground state of the muonic helium system ($\alpha^{++}\mu^-e^-$) by using a Hylleraas expansion. They required hundreds of terms in the expansion because of the slow convergence. Drachman [115] noticed that the first term in this expansion gave 99.4% of the contribution, suspecting that a perturbative treatment could be an appropriate way of calculating the Fermi contact term. The large ratio of muonic mass to electron mass suggests an adiabatic Born-Oppenheimer approximation.

The nonrelativistic Hamiltonian of this system is

$$H = -\frac{1}{M}\nabla_x^2 - \frac{1}{m}\nabla_r^2 - \frac{4}{x} - \frac{4}{r} + \frac{2}{|\mathbf{x}-\mathbf{r}|}, \tag{216}$$

$\mathbf{x}$ and $\mathbf{r}$ are the coordinates of the muon and electron, respectively, relative to the nucleus. The reduced masses are M=201.069 and m=0.999863 in units of m_e. The hyperfine splitting is given by

$$\Delta\nu = K \int d\mathbf{x} d\mathbf{r} \Psi^2(\mathbf{x}, \mathbf{r}) \delta(\mathbf{x} - \mathbf{r}), \tag{217}$$

where Ψ is the ground state eigenfunction of H, and K= 14196.11 MHz. In the Born-oppenheimer method, two of the particles are held fixed while we solve for the wave function of the other particle. We hold the muon ($\mathbf{x}$) fixed and solve for $\psi(\mathbf{r})$ of the electron with $\mathbf{x}$ as a parameter

$$\left(-\frac{1}{m}\nabla_r^2 - \frac{2}{r} + V(\mathbf{x}, \mathbf{r}) - E_x\right) \psi_{\mathbf{x}}(\mathbf{r}) = 0, \tag{218}$$

where $V(\mathbf{x}, \mathbf{r}) = -\frac{2}{r} + \frac{2}{|\mathbf{x}-\mathbf{r}|}$. As indicated in Eq. (106), the solution of Eq. (218) can be written as

$$\psi_{\mathbf{x}}(\mathbf{r}) = \psi_0(\mathbf{r})[1 + G(\mathbf{x}, \mathbf{r})], \tag{219}$$

where

$$\psi_0(\mathbf{r}) = \left(\frac{m^3}{\pi}\right)^{1/2} e^{-mr}, \tag{220}$$

satisfies the Coulomb problem and G is due to the adiabatic perturbation $V(\mathbf{x}, \mathbf{r})$. At this point, Drachman expands G in a perturbation series in V and its first order satisfies the equation (108)

$$\frac{1}{m}\nabla_r^2 G_1 - 2\frac{\partial G_1}{\partial r} = V - < V >, \tag{221}$$

where

$$< V >= \int d\mathbf{r} \psi_{\mathbf{x}}(\mathbf{r}) V \psi_{\mathbf{x}}(\mathbf{r}) = 2[1/x - m - e^{-2mx}(1/x + m)] \tag{222}$$

is the expectation value of V. Dalgarno and Lynn [51] have solved an equation similar to Eq. (221) but for an electron in the field of two fixed positive charges. Using their solution with suitable modification, Drachman obtains

$$G_1(\mathbf{x}, \mathbf{x}) = \frac{5}{2} - x - (2/x)E_1(2x) - (1/x+1)\ln(2\gamma x) - e^{-2x}\{\frac{1}{2} + 2x + (1/x+1)[2\ln(2\gamma x) - \mathrm{Ei}(2x)]\}, \tag{223}$$

where E_1 is an exponential integral and Ei is defined in Eq. (114). Now we can solve Eq. (218) for E_x to obtain $E_x = -m + < V > + < VG_1 >$ and determine the muonic wave function by solving the equation

$$[-\frac{1}{M}\nabla_{\mathbf{x}}^2 - \frac{4}{x} - E_x - E]\Phi(\mathbf{x}) = 0. \tag{224}$$

Since muon is close to the nucleus due to its large mass, only small values of x are significant and the Coulomb term dominates. Therefore ignoring the third term, the solution is hydrogenic:

$$\Phi(\mathbf{x}) = (8M^3/\pi)^{1/2} e^{-2Mx}. \tag{225}$$

Finally, letting $\Psi(\mathbf{x},\mathbf{r}) \equiv \Phi(\mathbf{x})\psi_{\mathbf{x}}(\mathbf{r})$, Eq. (217) can be written explicitly as

$$\Delta\nu \approx \frac{32K}{\pi}(Mm)^3 \int_0^\infty dx x^2 e^{-x/a}[1 + 2G_1(m\mathbf{x}, m\mathbf{x})], \tag{226}$$

where $a \equiv [4M + 2m]^{-1} = 1.24 \times 10^{-3}$, and the term quadratic in G_1 has been dropped for consistency, since it is of second order in V.

Expanding G_1 and retaining only the linear term in x, we obtain

$$\begin{aligned} \Delta\nu &\approx (32K/\pi)(mM)^3(2a^2 - 12ma^4) \\ &= (4483.38 - 33.36)\ \text{MHz} \\ &= 4450.02\ \text{MHz}. \end{aligned} \tag{227}$$

The quadratic term in G_1 contributes 0.689 MHz, while the cubic term is -0.005 MHz. Taking half of the quadratic term as an error, the final result is thus $\Delta\nu$=4450.4±0.4 MHz. This agrees with the result of Huang and Hughes [114] and is also close to the result obtained by Lakdawala and Mohr [117].

This is an excellent example of good physics where a rather complicated problem has been reduced by Dr. Drachman to a relatively simple problem by realizing that the muon is so close to the nucleus that it acts as a hydrogenic system and the rest of the problem is amenable to an adiabatic perturbation treatment, where already some available results could be used gainfully to obtain fairly accurate results. Understanding the intricacies of a problem and solving it in a simple way has been the hallmark of Dr. Drachman's research work throughout.

I wish to thank Keith Feggans for retrieving figures, given in this article, from various published papers.

REFERENCES

1. P. M. Morse and W. P. Allis, Phys. Rev. **44**, 269 (1933).
2. A. Temkin, Phys. Rev. **107**, 1004 (1957).
3. A. Temkin, Phys. Rev. **116**, 358 (1959).
4. R. M. Sternheimer, Phys. Rev. **96**, 951 (1954).
5. A. Temkin and J. C. Lamkin, Phys. Rev. **121**, 788 (1961).
6. I. H. Sloan, Proc. Roy. Soc. **281**, 151 (1964).
7. C. Schwartz, Phys. Rev. **124**, 1468 (1961).
8. R. L. Armstead, Phys. Rev. A **171**, 91 (1968).

9. R. J. Drachman and A. Temkin, "Polarized Orbital Approximations," Case studies in atomic collision physics II, ed. by E. W. McDaniel and M. R. C. McDowell, 1972,pp. 401-481.

10. L. Rosenberg, L. Spruch, And T. F. O'Malley, Phys. Rev. **119**, 164 (1960).

11. A. Temkin, Phys. Rev. Lett. **6**, 354 (1961).

12. G. Breit, Phys. Rev. **35**, 569 (1930).

13. E. A. Hylleraas, Z. Physik **48**, 469 (1928); **54**, 347 (1929).

14. A. K. Bhatia and A. Temkin, Rev. Mod. Phys. **36**, 1050 (1964).

15. A. K. Bhatia and A. Temkin, Phys. Rev. **137**, A1335 (1965).

16. H. Feshbach, Ann. Phys. (N.Y.) **19**, 287 (1962).

17. T. F. O'Malley and S. Geltman, Phys. Rev. **137**, A1344 (1965).

18. A. K. Bhatia, A. Temkin, and J. F. Perkins, Phys. Rev. **153**, 177 (1967).

19. A. K. Bhatia and A. Temkin, Phys. Rev. A **64**, 032709 (2001).

20. A. K. Bhatia, Phys. Rev. A **66**, 064702 (2002).

21. Y. Hahn, T. F. O'Malley and L. Spruch, Phys. Rev. **128**, 932 (1962).

22. A. K. Bhatia, Phys. Rev. A **69**, 032714 (2004).

23. A. K. Bhatia, Phys. Rev. A **73**, 012705 (2006).

24. Y. K. Ho, A. K. Bhatia, and A. Temkin, Phys. Rev. A **15**, 1423 (1977).

25. A. K. Bhatia and A. Temkin, Phys. Rev. A **29**, 1859 (1984).

26. R. P. Madden and Codling, Astrophys. J. **141**, 364 (1965).

27. L. Sanche and P. Barrow, Phys. Rev. Lett. **29**, 1639 (1972).

28. H. Morgan and D. Ederer, Phys. Rev. A **29**, 1901 (1984).

29. A. Temkin and A. K. Bhatia, Phys. Rev. A **31**, 1259 (1985).

30. A. Temkin and A. K. Bhatia, "Projection and Quasi-Projection Operators for Electron Impact Resonances on Many-Electron Atomic Targets," Autoinonization: Recent Developments and Applications, ed. by A. Temkin, 1985, pp. 35-70.

31. A. Temkin, A. K. Bhatia, and J. N. Bardsley, Phys. Rev. A **5**, 1663 (1972).

32. G. J. Schulz, Phys. Rev. Lett. **10**, 104 (1963).

33. C. Kuyatt, J. A. Simpson, and S. Mielczarek, Phys. Rev. **138**, A385 (1965).

34. A. Berk, A. K. Bhatia, B. R. Junker, and A. Temkin, Phys. Rev. A **34**, 4591 (1986).

35. G. J. Schulz and R. E. Fox, Phys. Rev. **106**, 1179 (1957).

36. A. K. Bhatia and A. Temkin, Phys. Rev. A **23**, 3361 (1981).

37. K. T. Chung and B. F. Davis, "Hole-Projection Method for Calculating Feshbach Resonances and Inner-Shell Vacancies," Autoinonization: Recent Developments and Applications, ed. by A. Temkin, 1985, pp. 73-102.

38. B. R. Junker, J. Phys. B **15**, 4495 (1982).

39. J. N. H. Brunt, G. C. King, and F. H. Read, J. Phys. B **10**, 433 (1977).

40. A. Temkin, A. K. Bhatia, and Y. S. Kim, J. Phys. B. **19**, L701, 1986).

41. A. K. Bhatia and A. Temkin, Phys. Rev. A **37**, 1415 (1988).

42. A. Temkin and R. J. Drachman, J. Phys. B Lett. **33**, L505 (2000).

43. D. Vrinceanu, A. Z. Msezane, D. Bessis, and A. Temkin, Phys. Rev. Lett. **85**, 3256 (2001).

44. A. Temkin and K. V. Vasavada, Phys. Rev. **160**, 109 (1967).

45. E. S. Chang and A. Temkin, Phys. Rev. Lett. **23**, 399 (1969).

46. D. M. Chase, Phys. Rev. **104**, 838 (1969).

47. A. Temkin and F. H. M. Faisal, Phys. Rev. A **3**, 520 (1971).

48. D. E. Golden, N. F. Lane, A. Temkin, and E. Gerjouy, Rev. Mod. Phys. **43**, 642 (1971).

49. N. Chandra and A. Temkin, Phys. Rev. A**13**, 188 (1976).

50. R. J. Drachman, Phys. Rev. **138**, A1582 (1965).

51. A. Dalgarno and N. Lynn, Proc. Phys. Soc. (London) **A70**, 223 (1957).

52. B. H. Bransden, Proc. Roy. Soc. (London), **A79**, 190 (1962).

53. S. K. Houston and R. J. Drachman, Phys. Rev. A **3**, 1335 (1971).

54. F. E. Harris, Phys. Rev. Letters **19**, 173 (1967).

55. A. K. Bhatia, A. Temkin, R. J. Drachman, and H. Eiserike, Phys. Rev. A **3**, 1328 (1971).

56. A. K. Bhatia, A. Temkin, and H. Eiserike, Phys. Rev. A **9**, 219 (1974).

57. E. L. Chupp, D. J. Forrest, P. R. Higbie, A. N. Suri, and C. Tsai, Nature, **241**, 333 (1973).

58. M. Leventhal, C. J. MacCallum, A. F. Huters, and P.D. Stang, Ap. J. **240**, 338 (1978).

59. R. A. Ferrell, Rev. Mod. Phys. **28**, 308 (1956).

60. A. K. Bhatia, R. J. Drachman, and A. Temkin, Phys. Rev. A **9**, 223 (1974).

61. A. K. Bhatia, R. J. Drachman, and A. Temkin, Phys. Rev. A **16**, 1719 (1977).

62. J. W. Humberston and J. B. G. Wallace, J. Phys. B **5**, 1172 (1972).

63. J. W. Humberston (unpublished).

64. S. K. Houston and R. J. Drachman (unpublished).

65. R. J. Drachman, Phys. Rev. **173**, 190 (1968).

66. A. P. Mills, Jr., Phys. Rev. Lett. **46**, 717 (1981).

67. A. P. Mills, Jr., Phys. Rev. Lett. **50**, 671 (1983).

68. A. K. Bhatia and R. J. Drachman, Phys. Rev. **28**, 2523 (1983).

69. A. Ore and J. L. Powell, Phys. Rev. **75**,1696 (1949).

70. I. Harris and L. M. Brown, Phys. Rev. **105**, 1656 (1957).

71. A. P. Mills, Jr., Phys. Rev. A **24**, 3242 (1981).

72. A. K. Bhatia, Phys. Rev. A **2**, 1667 (1970): G. W. Drake, Phys. Rev. Lett., **24**, 126 (1970).

73. M. Rotenberg and J. Stein, Phys. Rev. **182**, 1 (1969).

74. A. K. Bhatia and R. J. Drachman, Phys. Rev. A **32**, 3745 (1985).

75. S. Chandrasekhar, Astrophys. J. **102**, 223 (1945); S. Chandrasekhar and D. D. Elbert, *ibid* **128**, 633 (1958).

76. H. A. Bethe and R. Peierls, Proc. R. Sco. London, Ser. A **148**, 146 (1935).

77. T. Ohmura and H. Ohmura, Phys. Rev. **118**, 154 (1960).

78. K. L. Bell and A. E. Kingston, Proc. Phys. Soc. (London) **90**, 895 (1967).

79. S. J. Ward, J. W. Humberston, and M. R. C. McDowell, J. Phys. B **18**, L525 (1985).

80. A. K. Bhatia and R. J. Drachman, Phys. Rev. A **30**, 2138 (1984).

81. A. K. Bhatia, R. J. Drachman, and L. Chatterjee, Phys. Rev. A **38**, 494 (1988).

82. A. K. Bhatia and R. J. Drachman, Comments At. Mol. Phys. **22**, 281 (1989).

83. A. K. Bhatia and R. J. Drachman, Phys. Rev. A **45**, 7752 (1992).

84. A. K. Bhatia and R. J. Drachman, J. Phys. B **27**, 1299 (1994).

85. W. G. Sturrs, E. A. Hassels, P. W. Arcunni, and S. R. Lundeen, Phys. Rev. A **38**, 135 (1988); Z. W. Fu, E. A. Hassels, S. R. Lundeen, *ibid.* **46**, R5313 (1992).

86. P. L. Jacobson, D. S. Fisher, C. W. Fehrenbach, W. G. Sturrus, and S. T. Lundeen, Phys. Rev. A **56**, R4361 (1997); **57**, 4065(E) (1998).

87. D. M. Bishop and B. Lam, Mol. Phys. **65**, 679 (1988); J. F. Babb, *ibid.* **81**, 17 (1994).

88. A. K. Bhatia and R. J. Drachman, Phys. Rev. A **59**, 205 (1999).

89. B. Gre'maud, D. Delande, and N. Billy, J. Phys. B **31** 383 (1998); R. E. Moss, Chem. Phys. Lett. **172**, 458 (1990); A. K. Bhatia, Phys. Rev. A **58**, 2787 (1998).

90. J. Shertzer and C.H. Greene, Phys. Rev. A **58**, 1082 (1998).

91. A. K. Bhatia and R. J. Drachman, Phys. Rev. A **61**, 035203 (2000).

92. R. E. Moss, J. Phys. B **32**, L89 (1998).

93. A. K. Bhatia and R. J. Drachman, Phys. Rev. A **58**, 4470 (1998).

94. P. J. Leonard, At. Data Nucl. Data Tables **14**, 22 (1974).

95. A. K. Bhatia and R. J. Drachman, Phys. Rev. A **57**, 4301 (1998).

96. A. Dalgarno and A. L. Stewart, Proce. Phys. Soc. London **76**, 49 (1960).

97. S. P. Goldman and G. W. F. Drake, J. Phys. B **16**, L183 (1983); **17**, L197 (1984).

98. S. E. Haywood and J. D. Morgan III, Phys. Rev. A **32**, 3179 (1985).

99. R. W. F. Drake, in Long-Range Casimir Forces: Theory and Recent Experiments, edited by F. S. Levin and D. A. Micha (Plenum, New York, 1993), p. 107.

100. R. J. Drachman, in Long-Range Casimir Forces: Theory and Recent Experiments, edited by F. S. Levin and D. A. Micha (Plenum, New York, 1993), p. 219 and reference therein.

101. R. J. Drachman and A. K. Bhatia, Phys. Rev. A **51**, 2926 (1995).

102. H. A. Bethe and E. Salpeter, Quantum Mechanicns of One- and Two-Electron Atoms (Springer-Verlag, Berlin, 1957),p 192.

103. N. E. Rothery, C. H. Storry, and E. A. Hassels, Phys. Rev. A **51**, 2919 (1995).

104. A. K. Bhatia and R. J. Drachman, Phys. Rev. A **55**, 1842 (1997).

105. E. J. Kelsey and L. Spruch, Phys. Rev. A **18**, 15 (1978); **18**, 1055 (1978)l J. Bernabeu and R. Tarrach, Ann. Phys. (N.Y.) **102**m 323 (1976).

106. C. K. Au, G. Feinberg, and J. Sucher, Phys. Rev. Lett. **53**, 1145 (1984).

107. S. P. Goldman and G. W. F. Drake, Phys. Rev. Lett. **68**, 1683 (1992).

108. A. K. Bhatia and R. J. Drachman, Phys. rev. A **60**, 2848 (1999).

109. R. J. Drachman and S. K. Houston, Phys. Rev. A **12**, 885 (1975).

110. S. K. Houston and R. J. Drachman, Phys. Rev. A **7**, 819 (1973).

111. Y. K. Ho, Phys. Rev. A **17**, 1675 (1978).

112. J. DiRienzi and R. J. Drachman, Phys. Rev. A **65**, 032721 (2002).

113. J. DiRienzi and R. J. Drachman, Phys. Rev. A **66**, 054702 (2002).

114. K. -N. Huang and V. W. Hughes, Phys. Rev. A**20**,706 (1979); **21**, 1071 (1980).

115. R. J. Drachman, Phys. Rev. A **22**, 1755 (1980).

116. A. Dalgarno and J. T. Lewis, Proc. R. Soc. London Ser. A**233** 70 (1955).

117. S. D. Lakdawala and P. J. Mohr, Phys. Rev. A **22**, 1752 (1980).

CONVERGENT CLOSE-COUPLING APPROACH TO ELECTRON-ATOM COLLISIONS

Igor Bray and Andris Stelbovics
ARC Centre for Antimatter-Matter Studies, Murdoch University, Perth 6150, Australia

The Temkin-Poet model of electron-hydrogen scattering has played a crucial role in the development of many general computational methods for collisions in atomic physics, and in particular the convergent close-coupling (CCC) method. Here we review the CCC method to electron-atom scattering and give the historical perspective of its development utilising the Temkin-Poet model.

I. INTRODUCTION

It was with great pleasure and honour to accept the invitation to make a presentation at the symposium celebrating the life-long work of Aaron Temkin and Richard Drachman. The work of Aaron Temkin was particularly influential on our own during the development of the CCC method for electron-atom collisions. There are a number of key problems that need to be dealt with when developing a general computational approach to such collisions. Traditionally, the electron energy range was subdivided into the low, intermediate, and high energies. At the low energies only a finite number of channels are open and variational or close-coupling techniques could be used to obtain accurate results [1, 2]. At high energies an infinite number of discrete channels and the target continuum are open, but perturbative techniques are able to yield accurate results [3]. However, at the intermediate energies perturbative techniques fail and computational approaches need to be found for treating the infinite number of open channels. In addition, there are also problems associated with the identical nature of electrons and the difficulty of implementing the boundary conditions for ionization processes.

The beauty of the Temkin-Poet model of electron-hydrogen scattering is that it simplifies the full computational problem by neglecting any non-zero orbital angular momenta in the partial-wave expansion, without loosing the complexity associated with the above-mentioned problems [4–9]. The unique nature of the problem allowed for accurate solution leading to benchmark results which could then be used to test the much more general approaches to electron-atom collision problems.

The immense value of the Temkin-Poet model is readily summarised by the fact that the initial papers of Temkin [4] and Poet [7] have been collectively cited around 250 times to date and are still being cited in present times [10, 11]. Many of the citations came from our own work during the course of the development of the CCC method, which we now describe.

II. THE CONVERGENT CLOSE-COUPLING METHOD

At the beginning of the 1990s there were major discrepancies between theory and experiment for the most fundamental electron atom collision systems such as e-H and e-He scattering. For 54.4 eV electron-hydrogen excitation there were two independent measurements of the 2p angular correlation parameters in broad agreement with each other [12, 13], but not with the most sophisticated calculations available at the time [14–17]. For electron-helium scattering, a favourite system for the experimentalists, the discrepancies were even much more widespread over the energy range and variety of excitation parameters. For both targets there was no ab initio description of the total ionization cross sections, measured with an uncertainty of around 5% [18–20]. The CCC method was developed with the view to addressing these problems, starting with the e-H system.

The CCC method is based on the close-coupling method which expands the total e-H wavefunction $\Psi_i^{(+)}(\boldsymbol{r}_1, \boldsymbol{r}_2)$ using a set of known target-space states $\phi_n(\boldsymbol{r}_2)$. The effect of the Temkin-Poet model is to reduce the dimensionality of the problem by reducing the vector nature of the $\boldsymbol{r}$ coordinates to scalars r. In other words, angular dependence of the scattering is neglected. In the original Laguerre-based CCC method [21], the target states $\phi_f^{(\lambda)}(r) = \sum_{n=1}^{N} C_{fn}\xi_n^{(\lambda)}(r)$, where $\xi_n^{(\lambda)}(r)$ is a Laguerre basis with exponential fall-off factor λ, are obtained by diagonalising the hydrogen Hamiltonian

$$\langle\phi_f^{(\lambda)}|H_{\rm T}|\phi_i^{(\lambda)}\rangle = \varepsilon_f^{(\lambda)}\delta_{fi}, \quad i, f = 1, \ldots, N. \tag{1}$$

More recently [22], another way of obtaining the target states is by solving the eigenstate problem in a box

$$H_{\rm T}|\phi_i^{(R_0)}\rangle = \varepsilon_i^{(R_0)}|\phi_i^{(R_0)}\rangle, \quad i = 1, \ldots, N, \tag{2}$$

for $r \leq R_0$, with $\phi_i^{(R_0)}(0) = \phi_i^{(R_0)}(R_0) = 0$. We distinguish between the CCC method using the above two sets of states as CCC-L and CCC-B, respectively.

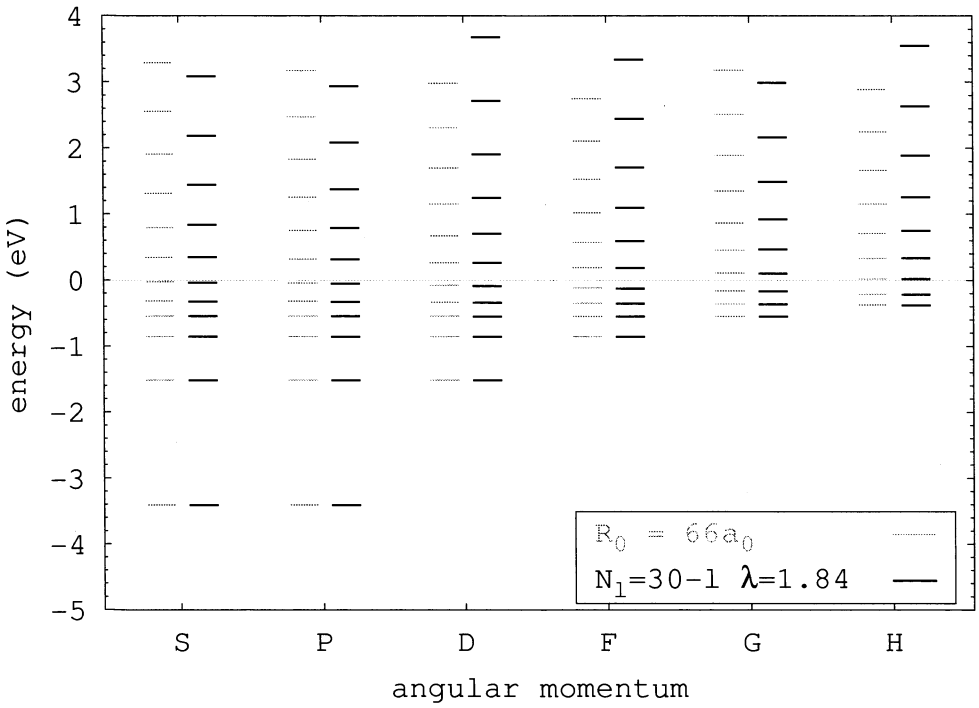

FIG. 1: Hydrogen excited-state energy levels in CCC-B ($R_0 = 66a_0$) and CCC-L ($N_l = 30 - l, \lambda = 1.84$) calculations.

In figure 1 we present the energy levels that can result from Laguerre-based (CCC-L) or box-based (CCC-B) calculations. The parameters specified were chosen in such a way so as to indicate that there is considerable similarity in the two approaches. The negative and low positive-energies are almost identical for all l, with variation occurring only for the higher energies.

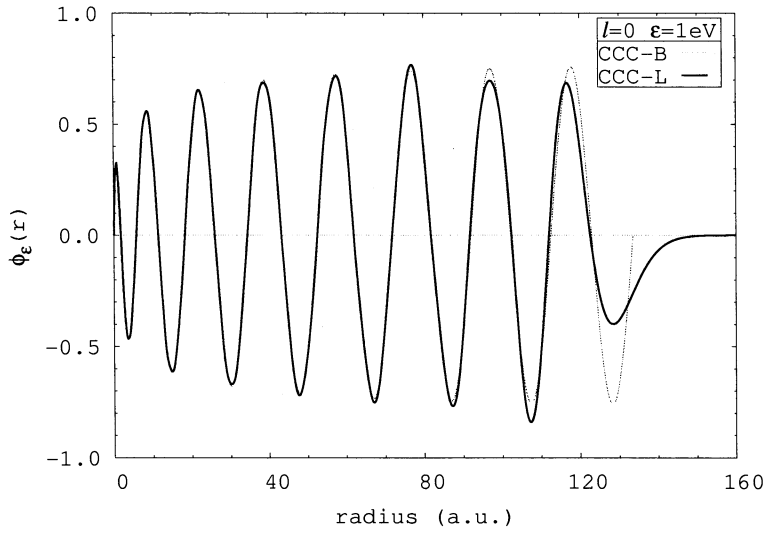

FIG. 2: CCC-B ($N = 70, \lambda = 2$) and CCC-L ($R_0 = 134a_0$) 1 eV suitably normalised wavefunctions for $l = 0$.

Having looked at the energies, in figure 2 we compare the 1 eV wavefunctions for $l = 0$ arising from another set of

calculations. We see that the two functions are almost identical until the larger radial values, with the major variation being where the Laguerre-basis exponential fall-off dominates past 120 a_0.

Once the states $\phi(r)$ are defined, utilising either approach, they are then used to expand the appropriately symmetrised total wavefunction

$$|\Psi_i^{(+)}\rangle = \mathcal{A}|\psi_i^{(+)}\rangle \approx \mathcal{A}\sum_{n=1}^{N}|\phi_n\rangle\langle\phi_n|\psi_i^{(+)}\rangle. \tag{3}$$

In the CCC method we write the resulting close-coupling equations in the form of coupled integral equations for the transition matrix $\langle k_f\phi_f|T|\phi_i k_i\rangle \equiv \langle k_f\phi_f|V|\Psi_i^{(+)}\rangle$, which satisfy

$$\begin{aligned}\langle k_f\phi_f|T|\phi_i k_i\rangle &= \langle k_f\phi_f|V|\phi_i k_i\rangle \\ &\quad + \sum_{n=1}^{N}\int dk \frac{\langle k_f\phi_f|V|\phi_n k\rangle\langle k\phi_n|T|\phi_i k_i\rangle}{E+i0-\varepsilon_n-k^2/2},\end{aligned} \tag{4}$$

where $E = \varepsilon_n + k_n^2/2$ is the total energy, and V is a combination of interaction potentials that depend on the wavefunction symmetry [21]. Note that for the Temkin-Poet model we can write the momenta k as scalars also.

The key feature of the CCC method is that convergence in the results of interest should be observed with increasing number of states N in the expansion of Eq. (3). This has the effect of increasing the number of coupled equations in Eq.(4), whose computational method of solution is specified in Ref. [21].

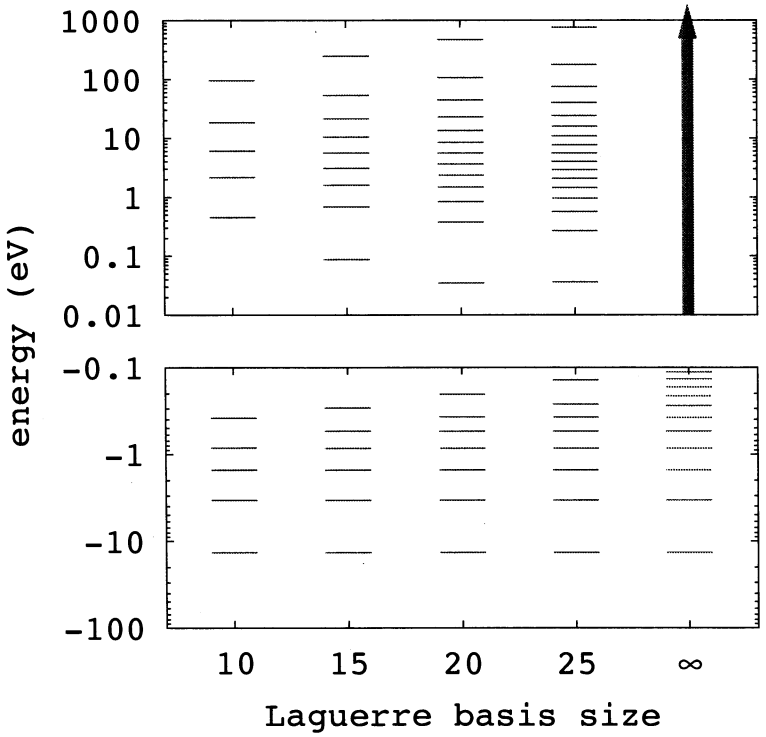

FIG. 3: Hydrogen $l = 0$ energy levels in CCC-L calculations for $\lambda = 1$ and specified basis size.

To check the convergence we shall consider here just the original CCC-L approach. In figure 3 we show what happens to the target-state energies as the Laguerre basis is increased, with both the discrete and the continuous spectra becoming more densely populated.

As discussed earlier, Temkin and Poet [4–9] gave a set of benchmark results for the e-H model problem. In testing the CCC method we need to ensure that convergence is obtained and that it is to the correct values given by Temkin and Poet. In figure 4 we present the results of three CCC calculations, for $N = 5, 10, 30$. We see that for the smallest calculation there can be very large unphysical oscillations in the cross sections, particularly at the lower energies and for the higher transitions. As the size of the calculations increases the cross sections converge to a smooth result that is in good agreement with the benchmark results. The cross sections for the individual transitions are obtained

simply from the magnitudes of the corresponding T-matrix elements obtained from Eq. (4). The total ionization cross section is obtained as a sum of cross sections of all positive-energy states. Note that no comparison of the total ionization cross section was possible [23], but when CCC was applied to the full e-H problem [24] excellent agreement with experiment was obtained.

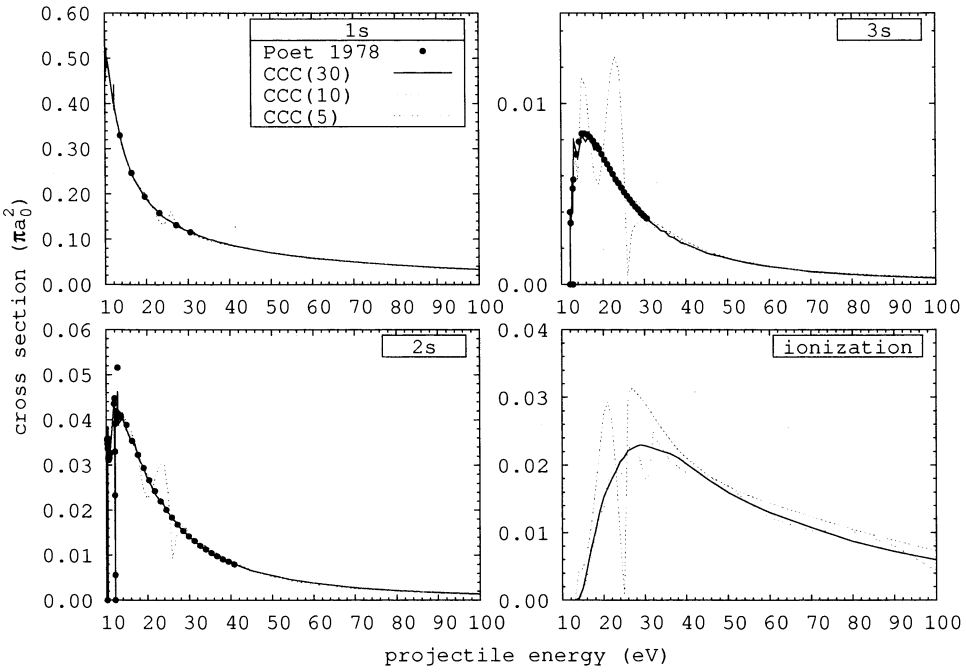

FIG. 4: Temkin-Poet model electron-hydrogen cross sections calculated with the CCC-L method using the specified basis sizes.

Having obtained an overall picture as a function of energy we now look a little closer at a specific incident electron energy of 3 Ry (E=2 Ry). In figure 5 we present a convergence study for all negative-energy states arising in the CCC calculations of specified N. The first thing to note is that the largest cross sections converge first, and that the convergence appears to be from above. The least negative-energy state in each calculation reverse the diminishing cross section trend. These states are not true eigenstates and have the effect of summing the cross sections for all the negative-energy states not explicitly included in the calculations.

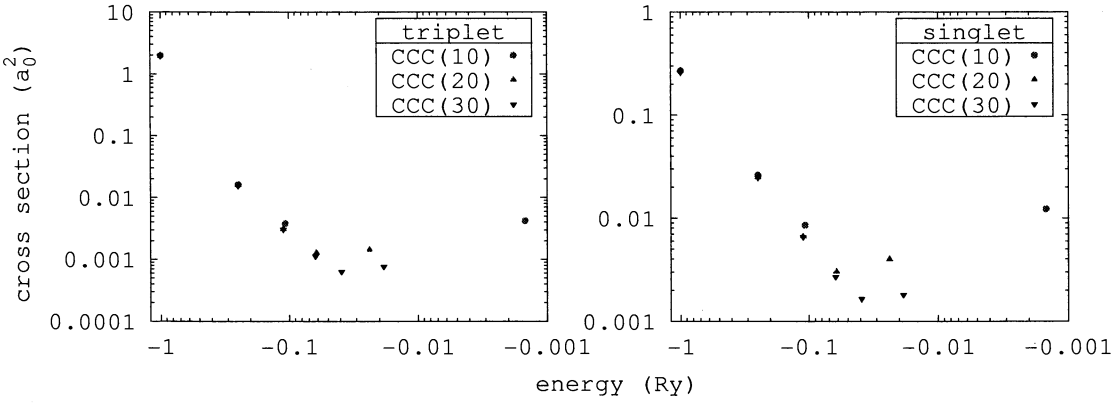

FIG. 5: Temkin-Poet model of 3 Ry e-H scattering. Negative-energy state cross sections calculated with the CCC method of specified basis size.

Successful reproduction of the Temkin-Poet model benchmark results was followed by application to the full e-H 2p excitation problem [21]. However, the CCC results were also unable to reproduce the experiment [12, 13], and were more in agreement with previous calculations [14–17]. Nevertheless, the sound foundations of the CCC method and

its numerous successes elsewhere [25, 26] motivated the experimentalists to revisit the problem [27, 28] yielding much better agreement with the theory.

Having found good agreement with the results of Temkin and Poet for discrete excitation, we realised that the model could be taken further and address some of the fundamental issues in the theory of electron-impact ionization. We have already demonstrated in figure 4 that at any energy above the ionization threshold the total ionization cross section converges with increasing basis size. Now we take a specific incident electron energy and ask the question does the underlying singly differential cross section converge also. In particular, we note from Eq. (4) that when summing over the positive-energy cross sections we sum over all open channels for which $0 \leq \varepsilon_n \leq E$. Since we have two identical electrons in the problem it appears that the identical ionization process with electron energies $e_a = \epsilon_n, e_b = E - \epsilon_n$ and $e_a = E - \epsilon_n, e_b = \epsilon_n$ is being counted twice. Yet the close coupling theory is unitary and does not allow for double-counting.

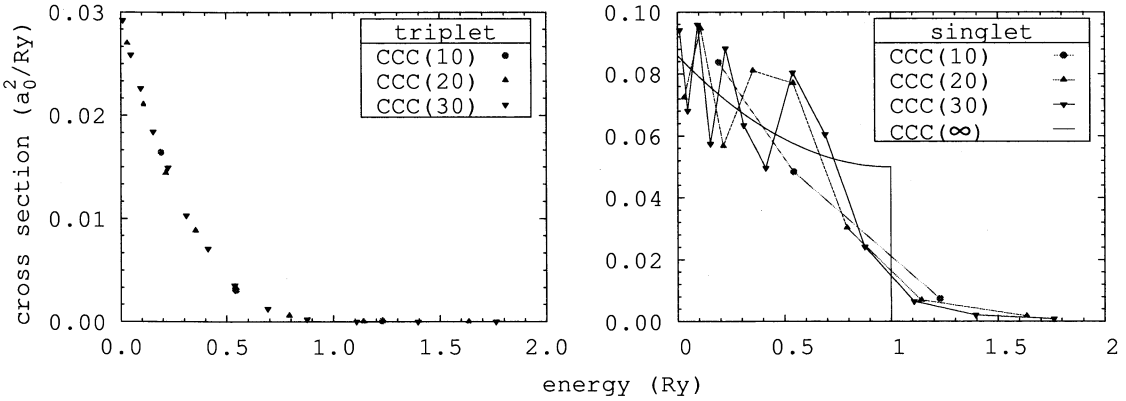

FIG. 6: Temkin-Poet model of 3 Ry e-H scattering. Positive-energy state cross sections calculated with the CCC method of specified basis size. The straight lines connecting the points are there to help guide the eye. The step-function denoted by CCC(∞) is an integral preserving estimate.

In figure 6 we consider the same calculations as presented in figure 5, but this time we look at the positive-energy state cross sections, which have been converted to singly differential cross sections (the integral, rather than the sum, yields the total ionization cross section of figure 4). Looking at the triplet case first, we see convergence to a smooth line which tends to zero at 1 Ry (equal energy-sharing), and remains zero for larger energies. In the singlet case the situation is more complicated. Here we see substantial oscillation and apparently a lack of convergence, particularly at energies below 1 Ry. Observation of this behaviour suggested that the CCC-calculated SDCS is converging to a step function [29], and that solving Eq. (4) is like taking a Fourier expansion of a step function [30]. In this case at the step the underlying amplitudes should converge to half the true amplitude magnitude, and hence the cross section to one quarter of the true cross section. The CCC(∞) estimate given in figure 6 was obtained this way. Subsequently, methods like the exterior complex scaling [31, 32] showed very good agreement with the CCC estimates.

The notion that the CCC methods should yield amplitudes that are zero for $\epsilon_n > E/2$ resolves the apparent problem with double-counting. In effect this reduces the endpoint of the SDCS integration from E to $E/2$, as would be expected in any theory that treats the two electrons identically. Application of these ideas to the full e-H and e-He ionization problems has resulted in excellent agreement with experiment [33, 34].

III. CONCLUSIONS

The Temkin-Poet model has played a crucial role in the development of general electron-atom scattering theories, and continues to do so. It retains the complexity associated with the infinite target discrete and continuous spectrum, as well as electron exchange. The unique nature of the underlying Schrödinger equation allows for an accurate solution leading to benchmark results against which general methods may be tested. It is helpful not only for discrete scattering, but also for ionization problems. The success of the convergent close-coupling method for electron-, photon- and positron- scattering on atoms can all be traced back to the simple model problem first considered by Aaron Temkin

back in 1962.

---

[1] R. K. Nesbet, Phys. Rev. A **20**, 58 (1979).
[2] P. G. Burke and W. D. Robb, Adv. Atom. Mol. Phys. **11**, 143 (1975).
[3] D. H. Madison and W. N. Shelton, Phys. Rev. A **7**, 499 (1973).
[4] A. Temkin, Phys. Rev. **126**, 130 (1962).
[5] A. Temkin and E. Sullivan, Phys. Rev. **129**, 1250 (1963).
[6] H. L. Kyle and A. Temkin, Phys. Rev. **129**, A600 (1964).
[7] R. Poet, J. Phys. B **11**, 3081 (1978).
[8] R. Poet, J. Phys. B **13**, 2995 (1980).
[9] R. Poet, J. Phys. B **14**, 91 (1981).
[10] I. A. Howard and N. H. March, Physics and chemistry of liquids **43**, 559 (2005).
[11] M. J. Mitnik DM, J. Phys. B **38**, 3325 (2005).
[12] E. Weigold, L. Frost, and K. J. Nygaard, Phys. Rev. A **21**, 1950 (1980).
[13] J. F. Williams, J. Phys. B **14**, 1197 (1981).
[14] J. Callaway, Phys. Rev. A **32**, 775 (1985).
[15] W. L. van Wyngaarden and H. R. J. Walters, J. Phys. B **19**, 929 (1986).
[16] D. H. Madison, I. Bray, and I. E. McCarthy, Phys. Rev. Lett. **64**, 2265 (1990).
[17] T. T. Scholz, H. R. J. Walters, P. G. Burke, and M. P. Scott, J. Phys. B **24**, 2097 (1991).
[18] M. B. Shah, D. S. Elliot, and H. B. Gilbody, J. Phys. B **20**, 3501 (1987).
[19] R. G. Montague, M. F. A. Harrison, and A. C. H. Smith, J. Phys. B **17**, 3295 (1984).
[20] M. B. Shah, D. S. Elliot, P. McCallion, and H. B. Gilbody, J. Phys. B **21**, 2751 (1988).
[21] I. Bray and A. T. Stelbovics, Phys. Rev. A **46**, 6995 (1992).
[22] I. Bray, K. Bartschat, and A. T. Stelbovics, Phys. Rev. A **67**, 060704(R) (2003).
[23] I. Bray and A. T. Stelbovics, Phys. Rev. Lett. **69**, 53 (1992).
[24] I. Bray and A. T. Stelbovics, Phys. Rev. Lett. **70**, 746 (1993).
[25] I. Bray, Phys. Rev. A **49**, 1066 (1994).
[26] D. V. Fursa and I. Bray, Phys. Rev. A **52**, 1279 (1995).
[27] H. Yalim, D. Cvejanovic, and A. Crowe, Phys. Rev. Lett. **79**, 2951 (1997).
[28] R. W. O'Neill, P. J. M. van der Burgt, D. Dziczek, P. Bowe, S. Chwirot, and J. A. Slevin, Phys. Rev. Lett. **80**, 1630 (1998).
[29] I. Bray, Phys. Rev. Lett. **78**, 4721 (1997).
[30] A. T. Stelbovics, Phys. Rev. Lett. **83**, 1570 (1999).
[31] M. Baertschy, T. N. Rescigno, W. A. Isaacs, and C. W. McCurdy, Phys. Rev. A **60**, R13 (1999).
[32] P. L. Bartlett and A. T. Stelbovics, Phys. Rev. A **69**, 022703 (2004).
[33] I. Bray, Phys. Rev. Lett. **89**, 273201 (2002).
[34] A. T. Stelbovics, I. Bray, D. V. Fursa, and K. Bartschat, Phys. Rev. A **71**, 052716(13) (2005).

Electron-Molecule Collisions:Quantitative Approaches and the Legacy of Aaron Temkin

B. I. Schneider*
Physics Division, National Science Foundation, Arlington, Virginia 22230 and Electron and Optical Physics Division, National Institute of Standards and Technology, Gaithersburg, MD 20899

I. INTRODUCTION

This article, on electron-molecule collisions, is dedicated to the legacy of my good friend and sometime collaborator, Aaron Temkin on his retirement from the NASA-Goddard Space Flight Center after many years of work at the highest intellectual level in the theoretical treatment of electron-atom and electron-molecule scattering. Aaron's contributions to the manner in which we think about electron-molecule collisions is clear to all of us who have worked in this field. I doubt that the great progress that has occurred in the computational treatment of such complex collision problems could have happened without these contributions. For a brief historical account, see the discussion of Temkin's contribution to electron-molecule scattering in the first article of this volume by Dr. A. K. Bhatia.

In this article, I will concentrate on the application of the so called, non-adiabatic R-matrix theory, to vibrational excitation and dissociative attachment, although I will also present some results applying the Linear Algebraic and Kohn-Variational methods to vibrational excitation. As a starting point for almost all computationally effective approaches to electron-molecule collisions, is the fixed nuclei approximation. That is, one recognizes, just as one does with molecular bound states, that there is a separation of electronic(fast) and nuclear(slow) degrees of freedom. This separation makes it possible to "freeze" the nuclei in space, calculate the collision parameters for the frozen molecule and then, somehow to add back the vibrations and rotations. The manner in which this is done, depends on the details of the collision problem. It is the work of Aaron and a number of other researchers that has provided the guidance necessary to resolve these issues.

II. THE FIXED NUCLEI PROBLEM

A. Geometric Considerations

Let us first consider the relationship between a coordinate system whose origin is centered at the center of mass of a molecule and the laboratory frame of reference. The laboratory frame of reference is illustrated in Figure 1, where the z' axis is defined to lie along the incident electron beam direction and the scattered beam is in the direction (θ', ϕ') relative to this direction. The molecular frame of reference, which is rigidly attached to the molecule, is illustrated

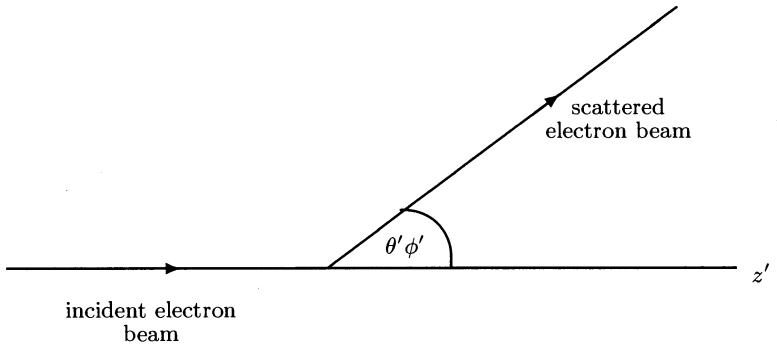

*Electronic address: bschneid@nsf.gov

FIG. 1: Laboratory frame for electron molecule scattering.

in Figure 2 for the case of a diatomic molecule. The center of gravity, G, is chosen as the origin of coordinates, with the z-axis lying along the internuclear axis, R, and the two nuclei labelled as A and B, $R = R_A + R_B$. For a general

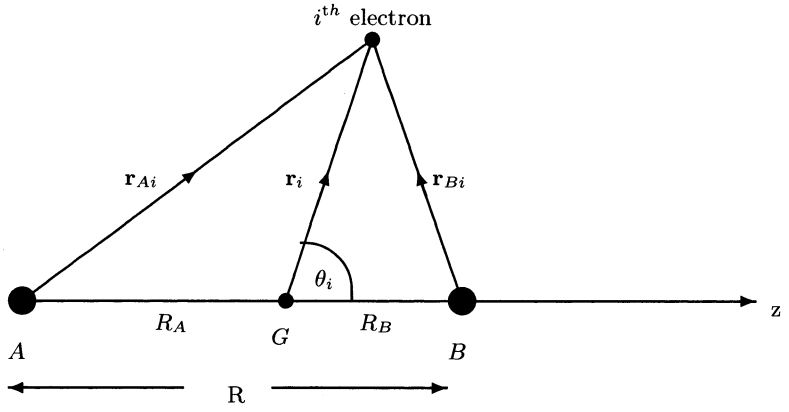

FIG. 2: Molecular frame for electron diatomic molecule collisions.

polyatomic molecule, one would choose the principle axis of inertia to replace the z-axis of the diatomic molecule. The molecular frame is oriented in a direction defined by the Euler angles α, β, γ, discussed, for example, in [33], which takes the laboratory frame of reference into the molecular frame of reference. Almost all electron-molecule scattering calculations are carried out in the molecular reference frame, where it is more natural to treat short-range effects such as exchange and correlation in non-vibrating, non-rotating molecules. Physical quantities, such as scattering amplitudes and cross sections, are extracted from the asymptotic form of the scattering wavefunction, which is typically written in a spherical coordinate system attached to the molecular frame. Consequently, it is necessary to transform the asymtotic form of the scattering wavefunction from the molecular to the laboratory reference frame. All that is required to perform this transormation is,

$$Y_{\ell m}(\theta', \phi') = \sum_{m'} D^{\ell *}_{mm'}(\alpha, \beta, \gamma) Y_{\ell m'}(\theta, \phi), \tag{1}$$

which relates spherical harmonics in the two frames of reference, where $D^{\ell}_{mm'}(\alpha, \beta, \gamma)$ are Wigner rotation matrices, defined in [33] and α, β and γ are Euler angles which transform the laboratory frame of reference into the molecular frame of reference.

B. Dynamics: Fixed Nuclei R-Matrix Treatment

The collision process for an electron scattering from an N electron target molecule, in the fixed nuclei approximation (nuclear kinetic energy= 0), is described by the time-independent Schrödinger equation,

$$H_{N+1}\Psi^{\Gamma} = E(R)\Psi^{\Gamma}, \tag{2}$$

where H_{N+1} is the non-relativistic Hamiltonian defined in atomic units in the molecular frame where Γ designates a given irreducible representation of the molecule. In light, linear molecules, Γ is the projection of the total angular momentum along the internuclear axis. For non-linear molecules, Γ, labels the irreducible representations of the molecular point group. In most of what follows, the presentation will be for linear molecules. This simplifies the algebra but the other cases may also be treated if one admits a more cumbersome notation.

$$H_{N+1} = \sum_{i=1}^{N+1} \left(-\frac{1}{2}\nabla_i^2 - \frac{Z_A}{r_{Ai}} - \frac{Z_B}{r_{Bi}} \right) + \sum_{i>j=1}^{N+1} \frac{1}{r_{ij}} + \frac{Z_A Z_B}{R}. \tag{3}$$

The solutions of this equation depend parametrically on R. There have been a number of successful approaches developed over the past few decades to calculating accurate, ab-initio, wavefunctions to eq(2). Early researchers used

single-center expansions ([1, 2]) and solved the resultant set of coupled, integro-differential equations using Numerov or related numerical integration procedures. Others turned to integral equation formulations. However, the most robust methods were based on multi-center expansions and variational methods to reduce the problem to one of linear algebra. Techniques such as the R-matrix ([7–9]) and Kohn Variational method ([3, 4]) expand the wavefunction in a computationally convenient basis set, substitute the expansion into the Schrödinger equation, and use projection techniques to obtain algebraic equations for the expansion coefficients. In the R-matrix method, which we describe in detail below, the major computational effort is spent solving an eigenvalue problem. In the Kohn Variational method, one is faced with solving a set of real or complex linear algebraic equations. The solution of eq(2) is typically expanded in a set of basis functions designed to explicitly represent channels that are energetically accessible(open channels/P-space) and those that are not (closed channels/Q-space). The P-space components asymptotically contain the scattering information while the Q-space components are needed to describe certain exchange effects, polarization and electron correlation. Often the physical closed states are replaced by pseudostates, which are better adapted to describing these effects using a much smaller set of basis functions. The common characteristic of Q-space basis functions is that they exponentially decay far from the interaction region. It has also become common to include in the expansion pseudostates designed to represent high lying, open channels in the breakup region of the target molecule. These non-physical states are needed to represent, in some fashion, the loss of flux into the continuum. We typically define the P-space basis functions as,

$$\psi^{\Gamma}_{c,i} = \mathcal{A}[\Phi^{\Gamma}_{c}(\mathbf{X}_N;\hat{\mathbf{r}}_{N+1}\sigma_{N+1})u^{0}_{c,i}(r_{N+1})] \tag{4a}$$

$$\Phi^{\Gamma}_{c}(\mathbf{X}_N;\hat{\mathbf{r}}_{N+1}\sigma_{N+1}) = \Phi^{SM_S}_{c}(\mathbf{X}_N;\sigma_{N+1})Y_{\ell_c m_{\ell_c}}(\theta_{N+1},\phi_{N+1}) \tag{4b}$$

$$\Phi^{SM_S}_{c}(\mathbf{X}_N;\sigma_{N+1}) = \sum_{M_{S_c}m_c}\Phi_c(\mathbf{X}_N)\chi_{\frac{1}{2}m_c}(\sigma_{N+1})(S_cM_{S_c}\tfrac{1}{2}m_c|SM_S), \tag{4c}$$

and the Q-space wavefunctions as, $\chi^{\Gamma}_{q}(\mathbf{X}_{N+1})$. Note, that the P-space basis states are constructed as an antisymmetrized product of a set of n physical target states and m one-electron function representing the scattering electron. The channel functions are here taken to be eigenfunctions of total spin S of the $(N+1)$ electron system and its projection, M_S, on the z-axis. The number, M, of Q-space wavefunctions is, in principle, arbitrary, but in practice is restricted to keep the size of the overall expansion manageable. At a minimum, the Q-space states must include enough functions to keep the P and Q space parts of the overall expansion orthogonal. In the R-matrix approach, the one-electron functions may be regular solutions to some model eigenvalue problem, designed to improve convergence of the expansion, but simpler forms may also be employed. The P-space wavefunctions are orthonormal and that requires that certain orthogonality conditions be imposed on the $u^{0}_{c,i}$ one-electron basis. In the Kohn Variational method, the one-electron functions are chosen as unknown linear combinations of asymptotically regular and irregular solutions of either the non-interacting problem or some model problem. Again, there are certain orthogonality conditions that need to be imposed to make the expansion numerically tractable. The linear combination is determined using the Kohn Variational principle. In the R-matrix approach, first developed in [7, 8], the major computational step is the solution of the composite $(N+1)$ electron eigenvalue problem,

$$\left[H_{N+1}+L_{N+1}-E_k(R)\right]\Psi^{\Gamma}_{k}=0 \tag{5a}$$

$$\Psi^{\Gamma}_{k}=\sum_{c=1}^{n}\sum_{i=1}^{m}\psi^{\Gamma}_{c,i}a_{c,i,k}+\sum_{q=1}^{M}\chi^{\Gamma}_{q}b_q \tag{5b}$$

where we have dropped the coordinate labels for notational simplicity. Note, that all the electron coordinates are restricted to lie inside a sphere of radius $r\leq a_0$. Inside the sphere, the composite system is subject to the full dynamical range of effects such as exchange, and short range correlation. Outside the sphere, pure electrostatic effects dominate the interaction of the target and the scattered electron and antisymmetry of target and scattered electron may be ignored. The Bloch operator, L, in eq(5) is defined as,

$$L_{N+1}=\sum_{i=1}^{N+1}\frac{1}{2}\delta(r_i-a)\left(\frac{\partial}{\partial r_i}-b\right), \tag{6}$$

where b is an arbitrary, real constant. One can demonstrate that $H_{N+1}+L_{N+1}$ is Hermitian in a basis of square integrable functions satisfying arbitrary boundary conditions at $r=a_0$. The major computational advantage of the R-matrix approach is its similarity to standard bound state eigenvalue problems. Inside $r=a_0$, the wavefunction may be expanded in a convenient set of basis functions and the problem reduced to the diagonalization of a matrix. The one and two electron integrals are defined inside $r=a_0$ and while most of these matrix elements have a negligible contribution from regions outside $r=a_0$, others must be treated more carefully. For those matrix elements involving

orbitals that have an appreciable contribution from regions $r \geq a_0$, the procedure is to compute the integrals over all of space and subtract the part for $r \geq a_0$. Typically, the subtraction may be done using multipolar expansions and is inexpensive as long as the number of integrals is not too large. In the modern R-matrix codes, all of the orbitals are expanded in a set of multicenter Gaussian type orbitals. The R-matrix orbitals, which must have significant amplitude at $r = a_0$, contain diffuse Gaussians placed at the center of gravity of the molecule for all of the asymptotically important partial waves. For the details see [27, 28]. We now employ the expansion of eq(5b) to solve the scattering problem at energy $E(R)$ in the internal region.

$$\left[H_{N+1} + L_{N+1} - E(R)\right]\Psi^{\Gamma} = L_{N+1}\Psi^{\Gamma} \tag{7a}$$

$$\Psi^{\Gamma} = \sum_k \frac{\Psi_k^{\Gamma}}{[E_k(R) - E(R)]} \langle \Psi_k^{\Gamma} \mid L_{N+1} \mid \Psi^{\Gamma} \rangle \tag{7b}$$

In order to extract the scattering information from this equation, we project Ψ^{Γ} onto the channel functions, $\Phi_c^{\Gamma}(\mathbf{X}_N; \hat{\mathbf{r}}_{N+1}\sigma_{N+1})$ and then set $r_{N+1} = a_0$. This produces the following set of coupled, *algebraic equations.*

$$u_c(a_0) = \sum_{d=1}^{n} \mathcal{R}_{c,d}\left[\frac{\partial u_d(r)}{\partial r} - b u_d(r)\right]|_{r=a_0} \tag{8}$$

In the above equation the radial scattering functions are defined as,

$$u_c(r_{N+1}) = \left(\Phi_c^{\Gamma}(\mathbf{X}_N; \hat{\mathbf{r}}_{N+1}\sigma_{N+1}) \mid \Psi^{\Gamma}(\mathbf{r}_1, \mathbf{r}_2, ...\mathbf{r}_{N+1})\right) \tag{9}$$

and the R-matrix matrix elements as,

$$\begin{aligned} \mathcal{R}_{c,d} &= \frac{1}{2}\sum_k \frac{u_{c,k}(a_0)u_{d,k}(a_0)}{[E_k(R) - E(R)]} \\ u_{c,k}(a_0) &= \sum_i a_{c,i,k} u_{c,i}^0(a_0) \end{aligned} \tag{10}$$

The only remaining task, is to solve these equations and extract the scattering information. To accomplish that requires us to consider the form of the scattering equations in the long-range region. Since the scattered and target electrons are now separated in space, the relevant equations are,

$$\left(\frac{d^2}{dr^2} - \frac{\ell_c(\ell_c+1)}{r^2} + \frac{2(Z_A + Z_B - N)}{r} + k_c^2\right) u_c(r) = 2\sum_{d=1}^{n} V_{c,d}(r) u_d(r) \tag{11}$$

$$k_c^2 = 2(E - E_c)$$

The simplest approach to dealing with these equations is to use the R-matrix method in the external region(s). Consider the region between the two annuli, $r = a_0$ and $r = b_0$. Lets us assume we have already calculated the R-matrix, $\mathbf{R}^I$, from $r = 0$ to $r = a_0$. Using the continuity of the functions and their first derivatives on the interval (a_0, b_0), joining the regions, it is possible to derive an equation for the R-matrix, $\mathbf{R}^{I+1}$, from $r = 0$ to $r = b_0$. This approach, known as the R-matrix propagation method, has a long history in heavy particle collisions [29, 32] and was adapted to electron-atom and electron-molecule scattering by a number of authors [30, 31]. I only quote the fundamental equation,

$$\mathbf{R}^{I+1} = \mathbf{r}_{b_0,b_0}^{I+1} - \mathbf{r}_{b_0,a_0}^{I+1}\left[\mathbf{R}^I + \mathbf{r}_{a_0,a_0}^{I+1}\right]^{-1}\mathbf{r}_{a_0,b_0}^{I+1} \tag{12}$$

where the $\mathbf{r}_{q,q'}^{I+1}$ are the sub-region R-matrices relating the adjacent boundaries, $r = a_0$ and $r = b_0$. Once we have propagated the R-matrix into the far asymptotic region, it can be matched to known analytic forms. At these distances the equations have two linearly independent solutions which may be obtained by a variety of methods; inward numerical integration, inverse power series expansions, analytic techniques or combinations of all of these, depending on the distance. Which linearly independent solutions are used depends on what boundary conditions are imposed on the solution in the far asymptotic region. The easiest ones to deal with impose the conditions that,

$$u_c(r) \underset{r\to\infty}{\sim} k_c^{-\frac{1}{2}}(\delta_{c,d}\sin(\theta_c r) + \cos(\theta_c r)K_{c,d}^{\Gamma}) \tag{13}$$

$$\theta_c = k_c r - \frac{1}{2}\ell_c\pi - \eta_c \ln 2k_c r + \sigma_{\ell_c}$$

Substituting this into eq(8), rearranging terms, leads to an equation for unknown $K_{c,d}$. Other asymptotic forms may easily obtained using the standard relations,

$$\mathbf{S}^{\Gamma} = \left[\mathbf{I} - i\mathbf{K}^{\Gamma}\right]^{-1}\left[\mathbf{I} + i\mathbf{K}^{\Gamma}\right] \tag{14a}$$

$$\mathbf{T}^{\Gamma} = \mathbf{S}^{\Gamma} - \mathbf{I} \tag{14b}$$

In order to obtain the scattering amplitude, it is necessary to express the asymptotic solution as a linear combination of an incident plane wave in channel c plus an outgoing spherical wave in all the open channels, in the laboratory coordinate system.

$$\Psi_c = \Psi_c^{\rm inc} + \Psi_c^{\rm scatt} \tag{15a}$$

$$\Psi_c^{\rm inc} \underset{r'_{N+1}\to\infty}{\sim} \Phi_c(\mathbf{X}_N)\chi_{\frac{1}{2}m_c}(\sigma_{N+1})\exp(ik_c z'_{N+1}) = \tag{15b}$$

$$\frac{i\pi^{1/2}}{k_c r'_{N+1}}\sum_{S\ell_c} i^{\ell_c}(2\ell_c+1)^{\frac{1}{2}}\Phi_c^{SM_S}(\mathbf{X}_N;\sigma_{N+1})(S_c M_{S_c}\tfrac{1}{2}m_c|SM_S)\times(\exp(-i\theta'_c)-\exp(i\theta'_c))Y_{\ell_c 0}(\theta'_{N+1},0),$$

$$\Psi_c^{\rm scatt} \underset{r'_{N+1}\to\infty}{\sim} \sum_d \Phi_d(\mathbf{X}_N)\chi_{\frac{1}{2}m_d}(\sigma_{N+1})f_{dc}(\theta'_{N+1},\phi'_{N+1})\frac{\exp(ik_d r'_{N+1})}{r'_{N+1}}, \tag{15c}$$

The remaining task is to determine the linear combination of molecular frame solutions, needed to reproduce the incoming laboratory frame plane wave of eq(15b). To accomplish this we write,

$$\Psi_c = \sum_{\Gamma} A_c^{\Gamma}\Psi_c^{\Gamma} \tag{16a}$$

$$\Psi_c^{\Gamma} = \sum_d \left[\Phi_d^{\Gamma}(\mathbf{X}_N;\hat{\mathbf{r}}_{N+1}\sigma_{N+1})\Phi_d^{SM_S}(\mathbf{X}_N;\sigma_{N+1})Y_{\ell_d m_{\ell_d}}(\theta_{N+1},\phi_{N+1})u_{dc}(r_{N+1})\right] \tag{16b}$$

$$u_{dc} \underset{r\to\infty}{\sim} \exp(-i\theta_d)\delta_{c,d} - S_{dc}\exp(-i\theta_d) \tag{16c}$$

Inserting eq(16c) into eq(16b) and then substituting the result into eq(16a), results in an asymptotic expression for Ψ_c expressed in the molecular reference frame. By choosing,

$$A_c^{\Gamma} = i\pi^{1/2}k_c^{-1/2}i^{\ell_c}(2\ell_c+1)^{\frac{1}{2}}(S_c i M_{S_c}\tfrac{1}{2}m_c|SM_S)D^{\ell_c *}_{0m_{\ell_c}}(\alpha,\beta,\gamma). \tag{17}$$

and using eq(1) it is possible to demonstrate that we indeed produce the required incident wave in the laboratory reference frame. To my knowledge, this was first demonstrated in a slightly simpler form in the paper of Temkin and Vasavada[5]. The scattering amplitude may immediately be extracted as,

$$f_{dc}(\theta',\phi') = -i\left(\frac{\pi}{k_c k_d}\right)^{1/2}\sum_{\Lambda S\pi}\sum_{\ell_c m_{\ell_c}\ell_d m_{\ell_d} m_{\ell_{d'}}} i^{\ell_c-\ell_d}(2\ell_c+1)^{\frac{1}{2}}(S_c M_{S_c}\tfrac{1}{2}m_c|SM_S)$$
$$\times(S_d M_{S_d}\tfrac{1}{2}m_d|SM_S)T^{\Gamma}_{dc}D^{\ell_c *}_{0m_{\ell_c}}(\alpha,\beta,\gamma)D^{\ell_d}_{m_{\ell_{d'}}m_{\ell_d}}(\alpha,\beta,\gamma)Y_{\ell_d m_{\ell_{d'}}}(\theta',\phi'), \tag{18}$$

In the fixed nuclei approximation, the scattering amplitude depends parametrically on the nuclear coordinates. In keeping with the philosophy of the Born-Oppenheimer approximation, transitions between electronic, vibrational and rotational states of the molecule may be obtained from these amplitudes by simply multiplying by the appropriate ro-vibrational wavefunctions of the target and integrating over the nuclear degrees of freedom. This approach, the so-called adiabatic-nuclei approximation, was first discussed in [34–36], and is valid provided the collision time is short compared with the times for vibration and/or rotation of the neutral molecule. Hence it can be applied in non-resonant regions or at electron collision energies which are not close to threshold. In the case of diatomic molecules in a $^1\Sigma$ state the scattering amplitude for a transition between electronic, vibrational and rotational states defined by the quantum numbers $c\nu_c j_c m_{j_c}$ and $d\nu_d j_d m_{j_d}$ is given by

$$f_{d\nu_d j_d m_{j_d},c\nu_c j_c m_{j_c}}(\mathbf{k}\cdot\hat{\mathbf{r}}) = \langle\chi_{\nu_d}(R)Y_{j_d,m_{j_d}}(\hat{\mathbf{R}})|f_{dc}(\theta',\phi')|\chi_{\nu_c}(R)Y_{j_c m_{j_c}}(\hat{\mathbf{R}})\rangle, \tag{19}$$

where $f_{dc}(\theta',\phi')$ is defined in 18. In this approximation both the rotational and vibrational degress of freedom are assumed to follow the adiabatic-nuclei prescription. In many cases, the prescription is not valid for the vibrational degrees of freedom but is an excellent approximation for the slower rotations. A hybrid theory was developed in [6, 21] to account for such a situation, which occurs frequently in the vibrational excitation of molecules in the presence of electronic resonances. In this approach the electronic and vibrational degrees of freedom are *explicitly* treated using a coupled states expansion. The rotational degrees of freedom are treated as in eq. (19). An alternative approach, the non-adiabatic R-matrix method, which is also applicable to dissociative attachment, is described in the next section.

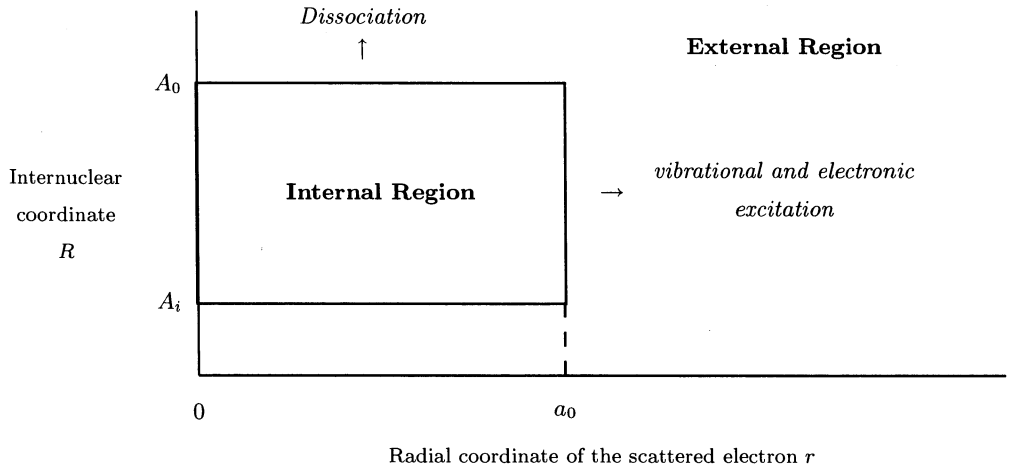

FIG. 3: Partitioning of configuration space in non-adiabatic R-matrix theory.

III. NON-ADIABATIC R-MATRIX THEORY

The adiabatic-nuclei approximation breaks down in the neighbourhood of narrow resonances or close to thresholds. This occurs because the colliding electron spends an appreciable time in the neighbourhood of the molecule allowing it to transfer energy to the nuclear motion with high probability. An interesting debate arose as to whether it was necessary to explicitly couple electronic and nuclear motion, as in a vibrational close coupling method, under these circumstances or whether a simpler conceptual and computational approach would suffice. There were formal theoretical arguments([14–17, 20]) as well as semi-empirical methods ([18]) based on the theoretical arguments that suggested this might indeed be the case, but no fully ab-initio, computational approach existed before 1979-1980. In looking back on these early papers I am quite impressed at the insight and intuition of the Manchester group. Basically, they had the physics under control. It was left to others to develop more quantitative approaches ([37, 38]) and show how first principles calculations verify these early theoretical developments.

We now consider the time-independent Schrödinger equation for a diatomic molecule,

$$(H_{N+1} + T_R)\Psi\mathbf{X}_{N+1}, R) = E\Psi(\mathbf{X}_{N+1}, R), \tag{20}$$

where we explicitly include the nuclear kinetic energy operator,

$$T_R = -\frac{1}{2\mu}\frac{d^2}{dR^2}, \tag{21}$$

and μ is the reduced mass of the two nuclei. We will assume that the molecule does not rotate appreciably during the collision. In Figure 3 we illustrate the partitioning of configuration space adopted in non-adiabatic R-matrix theory. The internal region is taken to be a rectangle defined by $0 \leq r \leq a_0$ and $A_i \leq R \leq A_0$ where a_0 is defined in the same way as in the fixed-nuclei theory given in Section II, A_i is chosen to exclude the nuclear Coulomb repulsion singularity at $R = 0$, where the wave function describing the nuclear motion is negligible, and A_0 is chosen so that the target vibrational states of interest in the calculation have negligible amplitude for $R > A_0$. For $r > a_0$ the molecule separates into an electron plus residual molecule which may be vibrationally and/or electronically excited. For $R > A_0$ the molecule separates into an atom plus an atomic negative ion (dissociative attachment) or into two free atoms plus the electron (three body breakup). In the internal region, Schrödinger equation, takes the form,

$$(H_{N+1} + T_R + L_{N+1} + L_R - E)\Psi^\Gamma(\mathbf{X}_{N+1}, R) = E\Psi^\Gamma(\mathbf{X}_{N+1}, R) \tag{22}$$

where the Bloch operators L_{N+1} and L_R are introduced so that $H_{N+1} + T_R + L_{N+1} + L_R$ is hermitian in the basis of quadratically integrable functions defined over the internal region in Figure 3 and satisfying arbitrary boundary conditions on the boundary of this region. We have already defined L_{N+1} by eq. (6) such that $H_{N+1} + L_{N+1}$ is hermitian for fixed internuclear separation R. The Bloch operator L_R, which is defined by

$$L_R = \frac{1}{2\mu}\left[\delta(R - A_0)\left(\frac{d}{dR} - B_0\right) - \delta(R - A_i)\left(\frac{d}{dR} - B_i\right)\right], \tag{23}$$

where B_0 and B_i are arbitrary constants, is such that $T_R + L_R$ is hermitian over the range $A_i \leq R \leq A_0$. It follows that $H_{N+1} + T_R + L_{N+1} + L_R$ is hermitian as required. We now expand the total wavefunction as,

$$\Psi^\Gamma(\mathbf{X}_{N+1}; R) = \sum_k \Psi_k^\Gamma(\mathbf{X}_{N+1}; R)\Theta_k^\Gamma(R) \tag{24}$$

The Ψ_k^Γ in this equation are the fixed-nuclei R-matrix electronic basis functions defined by eq. (5b) which are solved for a mesh of fixed internuclear values of R spanning the range $A_i \leq R \leq A_0$, and the $\Theta_k^\Gamma(R)$ are functions representing the nuclear motion. Substituting eq.(24) into eq.(22), mutiplying from the left with Ψ_k^Γ, and integrating over all the electronic coordinates, produces the following equation for Θ_k^Γ, *if we ignore the derivative of the R-matrix electronic wavefunction with respect to the internuclear coordinates.*

$$\begin{aligned}
\big[T_R + L_R + E_k(R) - E\big]\Theta_k^\Gamma(R) &= \big(\Psi_k^\Gamma \mid L_{N+1} + L_R \mid \Psi^\Gamma\big) \\
&= \frac{1}{2}\sum_{c\nu_c} u_{c,k}(a_0, R)\chi_{\nu_c}(R)\big[\frac{\partial}{dr} - b\big]u_{c,\nu_c}(r)\mid_{r=a_0} \\
&+ \frac{1}{2\mu}\sum_{[AB]_i} u_{[AB]_i,k}(R)\delta(R - A_0)\big[\frac{\partial}{dR} - B_0\big]u_{[AB]_i}(R)
\end{aligned} \tag{25}$$

The round brackets are used to denote integrations over electronic coordinates only. The two summations are respectively over 1) the electronic/vibrational degrees of freedom of the neutral molecule and 2) the electronically bound/dissociative degress of freedom of the negative ion. Specifically excluded from the sum are the three body states involving a true unbound outgoing electron and two dissociating nuclei, although one could include pseudostates to represent their effect just as is done in electronic breakup. This is the essence of the Born-Oppenheimer approximation and it is here applied to the internal R-matrix states of the compound $(N+1)$ particle system. The physical argument is, in the internal region, even an asymptotically slow moving electron is moving much faster than the nuclei can vibrate or rotate due to the internal electromagnetic forces experienced at small r. Mathematically, we need to examine the adiabatic potential curves for any avoided crossings. If such crossings were present, it would invalidate the argument and non Born-Oppenheimer correction terms would have to be considered to obtain quantitative agreement. The formal solution for Ψ^Γ may be written as,

$$\begin{aligned}
\Psi^\Gamma(\mathbf{X}_{N+1}, R) &= \sum_k \Psi_k^\Gamma(\mathbf{X}_{N+1}, R)\big[T_R + L_R + E_k(R) - E\big]^{-1}\big(\frac{1}{2}\sum_{c\nu_c} u_{c,k}(a_0, R)\chi_{\nu_c}(R)\big[\frac{\partial}{dr} - b\big]u_{c,\nu_c}(r)\mid_{r=a_0} \\
&+ \frac{1}{2\mu}\sum_{[AB]_i} u_{[AB]_i,k}(R)\delta(R - A_0)\big[\frac{\partial}{dR} - B_0\big]u_{[AB]_i}(R)\big)
\end{aligned} \tag{26}$$

The final step is to project this equation onto the asymptotic channel functions,

$$u_{c,\nu_c}(a_0) = \sum_{d\nu_d} \mathcal{R}_{c\nu_c,d\nu_d}\big[\frac{\partial}{dr} - b\big]u_{d,\nu_d}(r)\mid_{r=a_0} + \sum_{[AB]_i} \mathcal{R}_{c\nu_c,i}\big[\frac{\partial}{dR} - B_0\big]u_{[AB]_i}(R)\mid_{R=A_0} \tag{27a}$$

$$u_{[AB]_i}(A) = \sum_{d\nu_d} \mathcal{R}_{i,d\nu_d}\big[\frac{\partial}{dr} - b\big]u_{d,\nu_d}(r)\mid_{r=a_0} + \sum_{[AB]_j} \mathcal{R}_{i,j}\big[\frac{\partial}{dR} - B_0\big]u_{[AB]_j}(R)\mid_{R=A_0} \tag{27b}$$

$$\mathcal{R}_{c\nu_c,d\nu_d} = \frac{1}{2}\sum_k \big\langle \chi_{\nu_c}(R)u_{c,k}(a_0, R) \mid G_k(R \mid R') \mid u_{d,k}(a_0, R')\chi_{\nu_d}(R')\big\rangle \tag{27c}$$

$$\mathcal{R}_{c\nu_c,i} = \frac{1}{2\mu}\sum_k \big\langle \chi_{\nu_c}(R)u_{c,k}(a_0, R) \mid G_k(R \mid A_0)\big\rangle \mid u_{[AB]_i,k}(A_0) \tag{27d}$$

$$\mathcal{R}_{i,c\nu_c} = \frac{1}{2}\sum_k u_{[AB]_i,k}(A_0)\big\langle G_k(A_0 \mid R)\chi_{\nu_c}(R)u_{c,k}(a_0, R)\big\rangle \tag{27e}$$

$$\mathcal{R}_{i,j} = \frac{1}{2\mu}\sum_k u_{[AB]_i,k}(R_0)G_k(A_0 \mid A_0)u_{[AB]_j,k}(A_0) \tag{27f}$$

$$G_k(R \mid R') = \big\langle R \mid \big[T_R + L_R + E_k(R) - E\big]^{-1} \mid R'\big\rangle \tag{27g}$$

The R matrices are defined here as quadratures over the nuclear Green's operator associated with each electronic R-matrix state. In practice, they may be computed as solutions to an inhomogeneous partial differential equation

plus a qudrature or by using the spectral expansion of the Green's operator. The most widely used approach is to project the nuclear Hamiltonian on to a finite basis set of Gaussians or polynomials, diagonalize the resultant matrix and use the approximate eigenvalues and eigenvectors to spectrally resolve the Green's operator. Using a spectral expansion of the Green's operator,

$$G_k(R \mid R') = \sum_q \mid \theta_{k,q}(R)\rangle\big[\epsilon_{k,q} - E\big]^{-1}\langle\theta_{k,q}(R') \mid \tag{28}$$

the R-matrices may be rewitten as,

$$\mathcal{R}_{c\nu_c,d\nu_d} = \frac{1}{2}\sum_{k,q}\big\langle\chi_{\nu_c}(R) \mid u_{c,k}(a_0,R) \mid \theta_{k,q}(R)\big\rangle\big[\epsilon_{k,q} - E\big]^{-1}\big\langle\theta_{k,q}(R') \mid u_{d,k}(a_0,R') \mid \chi_{\nu_d}(R')\big\rangle \tag{29a}$$

$$\mathcal{R}_{c\nu_c,i} = \frac{1}{2\mu}\sum_{k,q}\big\langle\chi_{\nu_c}(R) \mid u_{c,k}(a_0,R) \mid \theta_{k,q}(R)\big\rangle\big\langle\theta_{k,q}(A_0) \mid \big[\epsilon_{k,q} - E\big]^{-1} \mid u_{[AB]_i,k}(A_0) \tag{29b}$$

$$\mathcal{R}_{i,c\nu_c} = \frac{1}{2}\sum_{k} u_{[AB]_i,k}(A_0) \mid \theta_{k,q}(A_0)\big\rangle\big[\epsilon_{k,q} - E\big]^{-1}\big\langle\theta_{k,q}(R) \mid u_{c,k}(a,R) \mid \chi_{\nu_c}(R)\big\rangle \tag{29c}$$

$$\mathcal{R}_{i,j} = \frac{1}{2\mu}\sum_{k} u_{[AB]_i,k}(R_0) \mid \theta_{k,q}(A_0)\big\rangle\big[\epsilon_{k,q} - E\big]^{-1}\big\langle\theta_{k,q}(A_0) \mid u_{[AB]_j,k}(A_0) \tag{29d}$$

Note, that there is a very interesting interpretation of these equations if the variation of the electronic factors are slow and can be removed from the integration. Then, the numerators would involve Franck-Condon factors between vibrational states of the neutral and R-matrix states, while the denominators have zeros at the vibrational R-matrix eigenvalues. Thus, one might expect to see structure in the neighborhood of these zeros with an intensity dependent on the Franck-Condon factors. This is precisely what is seen in the experiments and is fundamental to the success of the Boomerang model.

The additional work required to handle the effects of nuclear motion in this non-adiabatic R-matrix method, are minimal. In particular, there is *no* explicit coupling of the electronic and vibrational degrees of freedom as happens in a vibrational close coupling technique. Perhaps more importantly, the essential readjustment of the nuclei to the environment of a long lived molecular negative ion, is built in to the R-matrix levels. There are other ab-initio approaches ([16, 17]) based on the use of Feshbach projection operator techniques, that share this important feature and also invoke the Born-Oppenheimer approximation, which have also been quite effective in treating vibrational resonances and dissociative attachment.

Once the R-matrices are computed on the surfaces on the internal region, they may be propagated outward to very large distances using a simple generalization of the methods used in the fixed nuclei case. The major difference is the need to include any additional vibrational and/or rotational coupling in the external region. Finally, links between the formal non-adiabatic R-matrix theory and the Boomerang model developed in [18], as well as quantum defect theory, may be found in the references.

IV. RESULTS

There are numerous examples of fixed nuclei electron-molecule, R-matrix theory in the literature. The number of applications of the non-adiabatic theory are much more limited but at the time the theory was developed, it was critical to demonstrate that this ab-initio approach could produce satisfactory agreement in at least one important problem, the vibrational excitation of the N_2 molecule by electrons. The problem was important for a number of reasons. First, although there were a number of vibrational excitation experiments ([10–12]) which were in essential agreement as far as the shapes and peaks in the cross sections, there were disagreements in absolute values. Experiments designed to measure the absolute value of the total cross section also existed ([13]) and those suggested that one of the vibrational excitation experiments was correct. Second, the existing theories had their own limitations. The Hybrid Theory produced qualitative agreement with the observed experimental structure but clearly was either unconverged with respect to the vibrational basis set or lacked in its treatment of the fundamental electron-molecule interaction potential. The semi-empirical Boomerang treatment does a fine job of reproducing the observed structure in the cross section but has to rely on experiment for absolute normalization. Clearly, a fully first principles treatment could and should resolve these issues. In addtion, such an approach should be able to predict as yet unmeasured cross sections such as those between excited vibrational levels. Such a calculation was undertaken while the author was on sabbatical at the Observatoire de Paris in Meudon, France in 1979-80 ([38]). The calculations were done on a CDC6600 computer at the computation center associated with the Université Paris VI. The staff there made it very easy to bring computer

codes from Los Alamos and get them running quite quickly. Almost the entire calculational effort went to computing the R-matrix eigenstates as a function of internuclear distance. The computation of the nuclear Green's operator was done using a variational/spectral approach based on Gaussian type functions. The results are shown in figure 4 to figure 9. Note in figure 4 how the R-matrix curves near the electronic resonance energy are shifted and flatter than the neutral molecule potential. This is a direct effect of the trapping of the electron into what is essentially a π_g antibonding orbital of the molecular negative ion. The results in figure 6 demonstrate the excellent agreement between the calculated and experimental results and point also to the overall normalization of the experimental results of Wong as being correct. Figure 7 comparing the current calculation with the Hybrid Theory shows that both theories have demonstrated that the resonance structure comes from the compound state state vibrational states formed in the collision complex, but the Hybrid Theory calculation has been unable to capture the details. I believe it is a consequence of expanding the scattering wavefunction in the vibrational basis of the neutral molecule. This is slowly convergent in the resonance region and would require a large number of states to reproduce the experimental features. Also shown, are the vibrational cross sections from excited state vibrational levels and the total cross section. The agreement between the R-matrix theory and experiment is gratifying and gives us confidence in the non-adiabatic R-matrix theory.

I will conclude this paper with some examples using the Linear Algebraic (LAM) and Complex Kohn Variational Method (CKVM) to calculate electron-molecule scattering cross section in diatomic and polyatomic systems. The discussion, by necessity, will be brief and the interested reader should consult the references for more details.

A fundamental problem in electron-molecule collisions is to compute reliable cross sections for electronic excitation. The transition from the ground X $^1\Sigma_g^+$ to the b $^3\Sigma_u^+$ of H_2 had been studied experimentally ([39–41] as well as computationally ([42] by a number of researchers . Early theoretical calculations agreed with one of the three experimental results but differed by a factor of two from the other two experiments. Since both the LAM, R-matrix and Schwinger Variational Method had matured enough to perform the calculation with all the relevant electron-molecule terms included, this calculation was undertaken by all three groups ([43–45]. The relevant thoretical and experimental data is shown in figure 10. The three theoretical results were in perfect agreement with one another but disagreed with the earlier theoretical calculation. The calculations also agreed with two of the experimental measurements. This work prompted the third experimental group to re-examine its measurements. It was discovered that these experimental measurements were, in fact, normalized incorrectly. When this was corrected all of the theoretical calculations and all of the experiments agreed. This was very strong evidence of the importance and need of precise calculations where experiments are difficult and uncertainties abound.

Another interesting problem involves the doubly excited $^1\Pi_u$ states of the H_2 molecule. In fig 11 ([46]), we see that there there are two series ($1\sigma_u n\pi_g^+$) and ($1\pi_u^+ n\sigma_g$) which cross as a function of internuclear distance. This must occur if one examines the behavior of the orbitals in the separated and united atom limits. Calculations on the two separate series show very different behavior of the widths of these resonances, one tending to be broad and the other narrow. The question is, if configuration interaction (CI) between the two series is taken into account, do the multiple crossings of these series produce interesting and possibly observable effects. The answer, shown by the calculations, is that CI radically changes the simple picture of two separate resonance series. The widths vary dramatically as a function of R, due to the level crossings. A photoionization experiment was proposed to probe the interesting regions of R using vibrationally excited H_2 but for technical reasons, the experiment could not be performed. It is difficult to prepare vibrationally excited homonuclear molecules experimentally. Nonetheless, this theoretical calculation again demonstrated that powerful computational methods and theory can bring a great deal of insight into electron collisions and photoionization of molecular systems.

Turning to the CKVM, we show in figure 12 the cross section for the elastic scattering of electrons from ethylene [47]. This was one of the earliest calculations performed on a polyatomic molecule and it incorporated a CI based, ab initio optical potential of a few thousand configurations to accurately treat core polarization and electron correlation. While it was expected, on general theoretical grounds, that there would be resonances involving antibonding π orbitals, an unexpected feature appeared in the cross section at very low energies; it nearly vanished. The reason for this was the existence of what is known as a Ramsauer-Townsend minimum in electron atom scattering. In a molecule the situation is not so simple as an atom, where there is spherical symmetry and only s-wave scattering at these energies. However, the higher partial waves do not contribute much to the cross section at these low energies and the situation in this molecule is quite similar to that in the rare gas atoms. Later calculations on a variety of other polyatomic species, some hydrocarbons, some not, revealed that these minima appeared for very low energy collisions in numerous systems. The calculations appear to confirm the results of numerous swarm measurements which have appeared in the literature over many years.

Finally, in figure 13 we show the vibrational excitation of the carbon-oxygen bond in formaldehyde ([48]). Again, a CI based optical potential was employed and the calculation was carried out varying the C-O bond distance in order to treat vibration. This molecule has a low lying shape resonance, very similar to that found in N_2 and other hydrocarbons. This long lived negative ion produces a vibrational pattern similar to that shown in N_2. Coupling to

other vibrational modes in the molecule was ignored in the theoretical calculation and the vibrational motion of the C-O stretch was treated using the simple, one dimensional Boomerang model. In spite of these simplifications, the results were in quite reasonable agreement with available experiment.

V. CONCLUSION

Our ability to calculate accurate cross sections for a wide array of processes involving the collision of electrons with molecules has matured over the past decade and a half. We can now even talk about electron induced chemistry, where it is possible to follow the flow of energy deposited by an incident electron as it migrates between electronic and vibrational modes in small polyatomic molecules. Even larger systems can be treated at lower but still useful levels of approximation. The major goal is to understand how dissociation and/or dissociative attachment proceeds in these systems so that it may be controlled in a variety of important applications from the etching of computer chips to waste management. The early studies discussed in this article paved the way. Aaron Temkin played a very important role in these developments. It would be remiss of me not to mention the pioneering work of other people such as Arvid Herzenberg, Phil Burke, Howard Taylor, Norman Bardsley, and Tom O'Malley who gave us both a conceptual framework to build on as well as some useful computational tools. Aaron, I hope in your "retirement" you will continue to do science with the passion that you have always brought to your work and find even greater time for the other things you enjoy such as family, travelling and music.

---

[1] P. G. Burke and A. L. Sinfailam, J. Phys. B **3** 641 (1970)
[2] P. G. Burke and N. Chandra, J . Phys. B **5** 1696 (1972)
[3] T. N. Rescigno and B. I. Schneider, Phys. Rev. A **37**, 1044 (1988)
[4] B. I. Schneider and T. N. Rescigno, Phys. Rev. A **37**, 3749 (1988)
[5] A. Temkin, and K. V. Vasavada, Phys. Rev. **160**, 109(1960)
[6] N. Chandra and A. Temkin, Phys. Rev. A **13**, 188(1976)
[7] B. I. Schneider, Chem. Phys. Lett. **31** 237(1975)
[8] B. I. Schneider, Phys. Rev. A **11**, 1957(1975)
[9] P. G. Burke, I. Mackey and I. Shimamura, J, Phys. B **10**, 2497(1977)
[10] G. J. Schulz, Phys. Rev. **135**, A988 (1964)
[11] H. Ehrhardt and K. Willman, Z. Phys. **204**, 464 (1967)
[12] S. F. Wong and L. Dube, Phys. Rev. A **17**, 570(1978)
[13] R. E. Kennerley and R. A. Bonham, Phys. Rev. A **17**, 1844 (1978)
[14] A. Herzenberg and F. Mandl, Proc. Phys. Soc. A **270**, 48(1962)
[15] J. N.Bardsley, A. Herzenberg and F. Mandl, Proc. Phys. Soc. **89**, 321(1966)
[16] T. F. O'Malley, Phys. Rev. **150**, 14(1966)
[17] T. F. O'Malley, Phys. Rev. **156**, 230(1967)
[18] D. T. Birtwistle and A. Herzenberg, J. Phys. B **4** 53(1971)
[19] A. U. Hazi, T. N. Rescigno and M. Kurilla, Phys. Rev. A. **23** 1079(1981)
[20] B.I. Schneider, Phys. Rev. A **14**, 1923(1979)
[21] N. Chandra and A. Temkin, Phys. Rev. A **14**, 507(1976)
[22] K. L. Baluja, P.G. Burke and L. A. Morgan, Comput. Phys. Commun. **27**, 299(1982)
[23] C. Bloch, Nucl. Phys. **4**, 503(1957)
[24] P. G. Burke, A. Hibbert and W. D. Robb, J . Phys. B **4**, 153(1971)
[25] K. Pfingst, B. M. Nestmann and S. D. Peyerimhoff, J. Phys. B **27**, 2283(1994)
[26] K. Pfingst, B. M. Nestmann and S. D. Peyerimhoff, *Computational Methods for Electron-Molecule Collisions* Eds. W.M. Huo and F.A. Gianturco (Plenum Press, New York), 293(1995)
[27] L. A. Morgan, J. Tennyson, C. J. Gillan and X. Chen, X., J. Phys. B **30**, 4087(1997)
[28] L. A. Morgan, J. Tennyson, and C. J. Gillan, Comput. Phys. Commun. **114**, 120(1998)
[29] J. C. Light and R. B. Walker, J. Chem. Phys. **65**, 4272(1976)
[30] B. I. Schneider and R. B. Walker, J. Chem. Phys. **70**, 2466 (1979).
[31] B. I. Schneider and H. S. Taylor, J. Chem. Phys. **77**, 379(1982).
[32] J. C. Light, R. B. Walker, E. B. Stechel and T. G. Schmalz, Comput. Phys. Commun. **17**, 89(1979)
[33] M.E. Rose,*Elementary Theory of Angular Momentum* (John Wiley & Sons, New York, London) 1957
[34] D. M. Chase, Phys. Rev. **104**, 838 (1956)
[35] S. I. Drozdov, Sov. Phys. JETP **1**, 591 (1955)
[36] S. I. Drozdov, Sov. Phys. JETP **3**, 759 (1956)
[37] B.I. Schneider, M. LeDourneuf and P. G. Burke, J. Phys. B **12**, 1365(1979)

[38] B.I. Schneider, M. LeDourneuf and Vo Ky Lan, Phys. Rev. Lett. **43**, 1926 (1979)
[39] M. L. Khakoo, S. Trajmar, R. McAdams and W. T. Shyn, Phys. Rev. A **35**, 2832 (1986)
[40] H. Nishimura, J. Phys. Soc. Jpn **55**, 3301 (1986)
[41] R. I. Hall and L. Andric, J. Phys. B **17**, 3815 (1984)
[42] S. Chung and C. C. Lin, Phys. Rev. A **17** 1874 (1978)
[43] B.I. Schneider and L.A. Collins, J. Phys. B **18**, L857 (1985)
[44] M. A. P. Lima , T. L. Gibson , K. Takatsuka and V. McKoy, J. Phys. B **18** L865 (1985)
[45] K. L. Baluja, C. J. Noble and J. Tennyson, J. Phys. B **18** L851 (1985)
[46] L. A. Collins, B.I. Schneider, C.W. McCurdy, S. Yabushita, and C.J. Noble, Phys. Rev. Lett. **57**, 980 (1986)
[47] B. I. Schneider, T. N. Rescigno, B. H. Lengsfield and C. W. McCurdy, Phys. Rev. Lett. **66**, 2728 (1991)
[48] B.I. Schneider, T. N. Rescigno and C.W. McCurdy, Phys. Rev. A **42**, 3132 (1990).

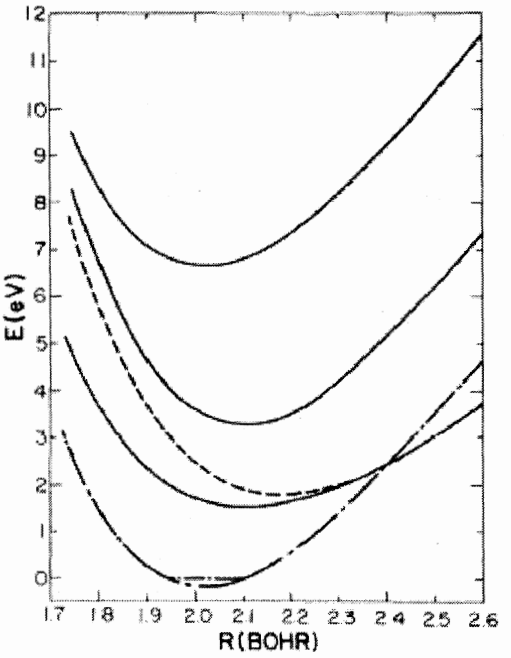

Potential curves for N_2 and N_2^-: Dash-dotted line, ground state of N_2; dotted line, resonant state of N_2^-; and solid line, *R*-matrix states of N_2^-.

Fig. 4: The R-Matrix Potential Curves

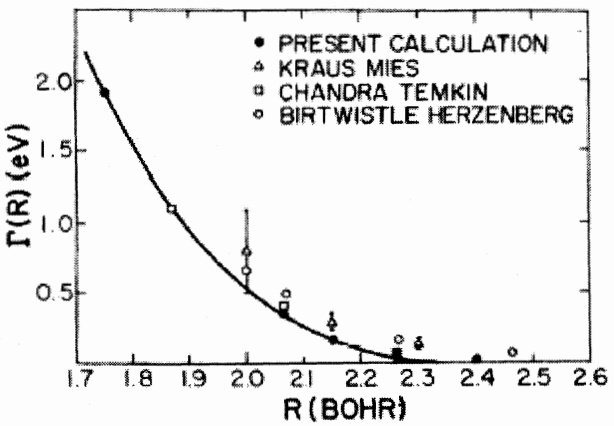

Width resonance as a function of internuclear distance in N_2.

FIG. 5: Resonance Width for e + N_2 Scattering

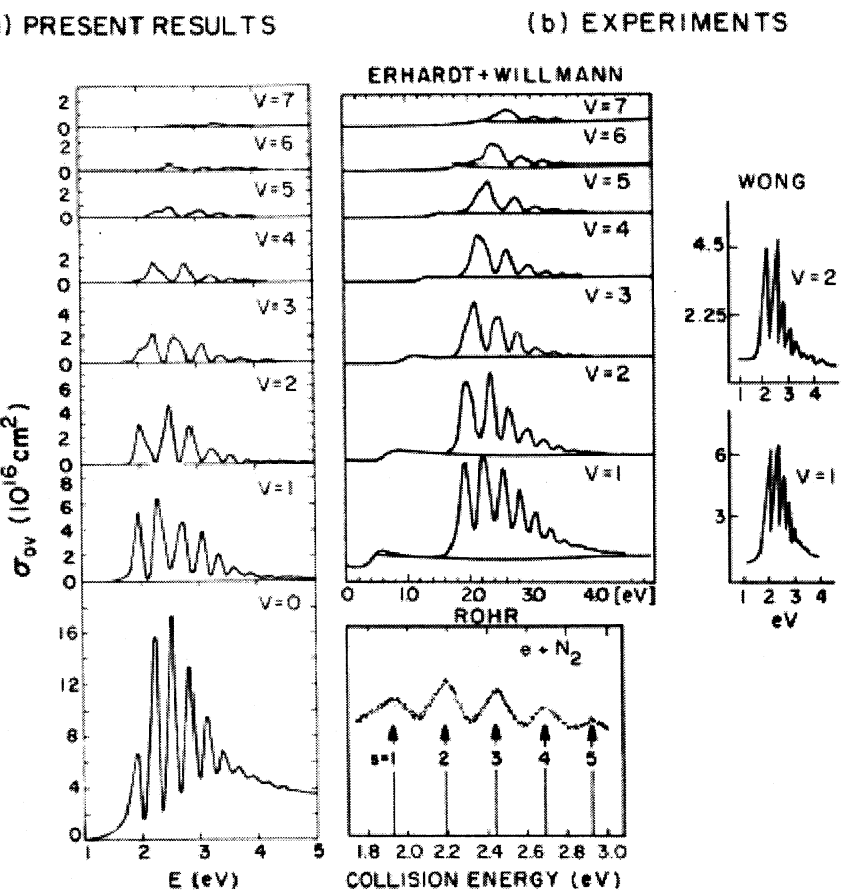

Comparison of calculated and experimental vibrational excitation cross sections for N_2.

FIG. 6: Calculated versus Experimental Vibrational Excitation Cross Section for e + N_2 Scattering

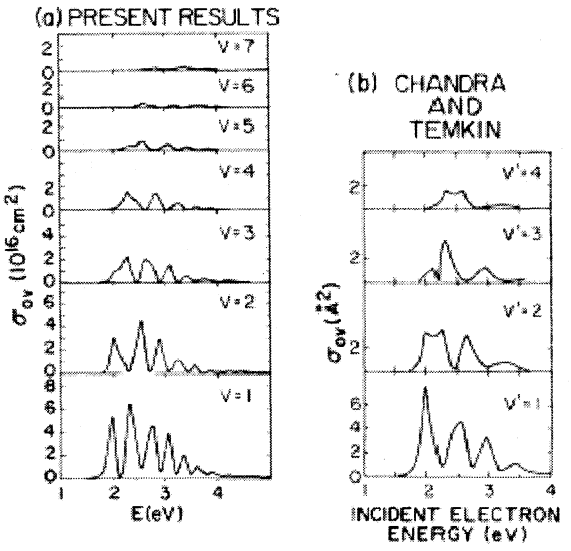

Comparison of calculated cross sections for vibrational excitation in N_2.

FIG. 7: Comparison of R-matrix and Hybrid Theory Vibrational Excitation Cross Section for e + N_2 Scattering

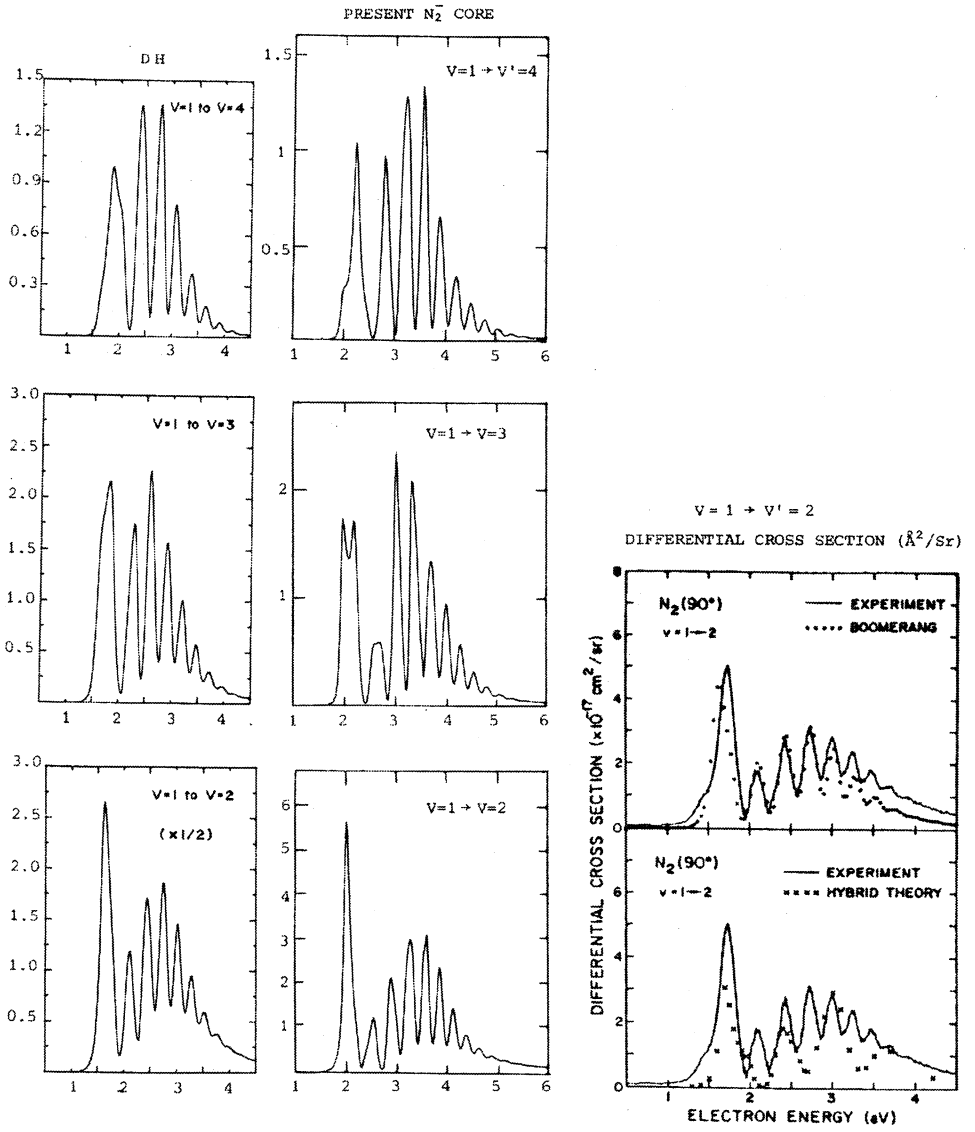

Vibrational excitation cross sections $c_{1\to v}(\text{Å}^2)$
a. Dubé Herzenberg (DH) Boomerang results.
b. N_2^- core approximation present results.
c. Comparison of Wong's experimental results with Dubé–Herzenberg and Chan dra–Temkin theoretical results.

FIG. 8: Calculated and Experimental Excited State Vibrational Excitation Cross Section for e + N_2 Scattering

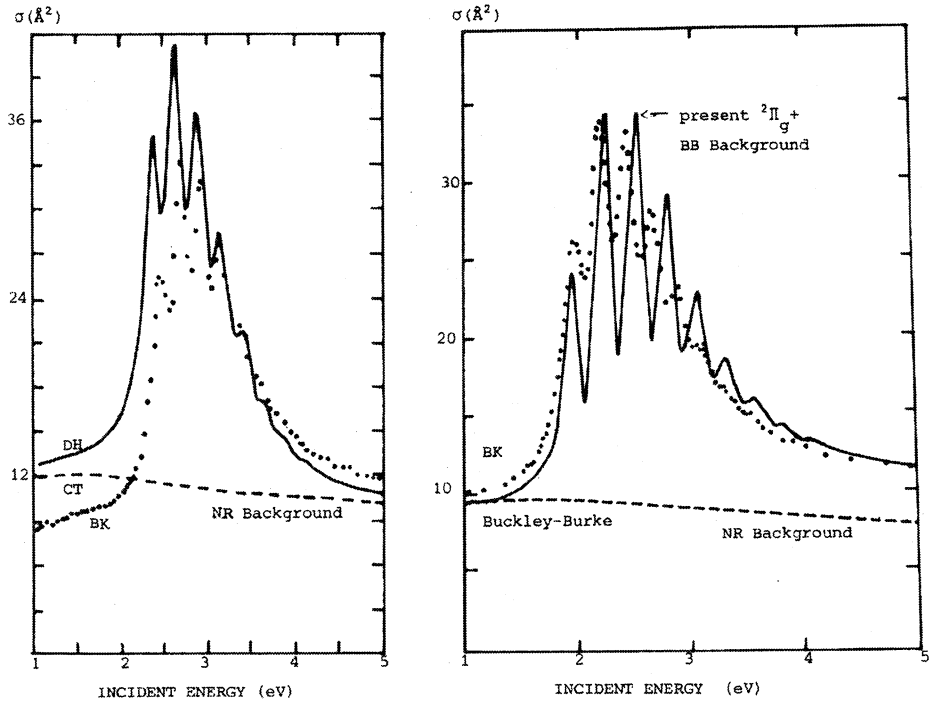

The total scattering cross section ($Å^2$) for e+N_2 (v=0)

a. Bonham and Kennerly (• • •) compared with the theoretical sum (———) of Dubé–Hertzenberg $^2\prod_g$ resonant results and Chandra–Temkin non-resonant background (--------).

b. Bonham and Kennerly experimental results (• • •) compared with the theoretical sum (———) of the present N_2^- core $^2\prod_g$ resonant results and Buckley–Burke non-resonant background (--------).

FIG. 9: The Total Cross Section for e + N_2 Scattering

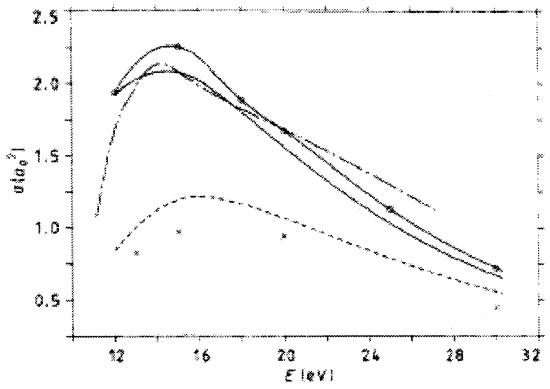

Comparison of theoretical calculations of the X $^1\sum_g$–b $^3\sum_\mu$ total excitation cross sections as a fnction of incident electron energy for e–H_2 scattering. Nomenclature: full curve, present SEC calculations; broken curve, present OSE; chain curve, SEC (Baluja et al. 1985); full curve with circles, SEC (Lima et al. 1985); crosses, OSE (Holley et al. 1981).

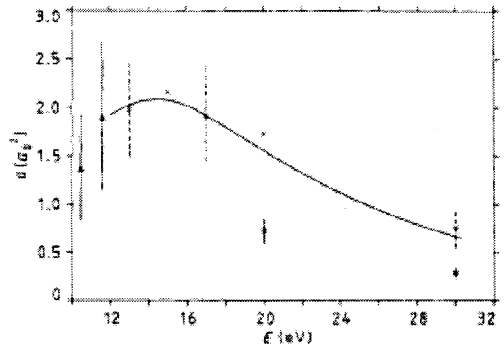

Comparison of theoretical and experimental X $^1\sum_g^+$–b $^3\sum_\mu$ cross sections, Nomenclature: full curve, present SEC calculations; circles, experimental results (Khakoo et al. 1985); crosses, experimental results (Nishimura et al. 1985); triangles, experimental results (Hall and Andrié 1984).

FIG. 10: Electronically Inelastic Scattering from the X $^1\Sigma_g^+$ State to the b $^3\Sigma_u^+$ State of H_2

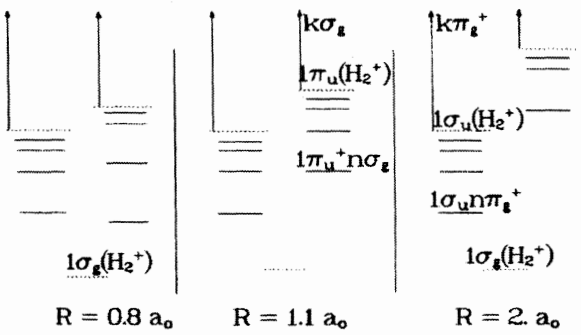

Schematic representation for the $^1\prod_u$ symmetry of the $1\sigma_u n\pi_g^+$ and $1\pi_u^+ n\sigma_g$ Feshbach resonance series of H_2^+ lying below the $1\pi_u$ threshold for $e^- - H_2^+$ scattering as a function of *R*. The resonances are depicted by solid lines, the states of H_2^+ by dashed lines.

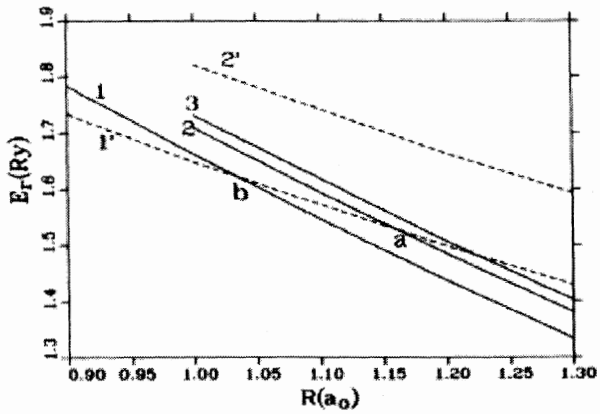

Resonant position E_r as a function of R for the lowest few $^1\prod_u$ resonances in the $1\sigma_u n\pi_g^+$ (solid lines) and $1\pi_u^+ n\sigma_g$ (dashed lines) series in 2CC. The numbers give the order of the resonances within each series.

FIG. 11: Structure of the Double Excited Resonant State of the $^1\Pi_u$ States H_2

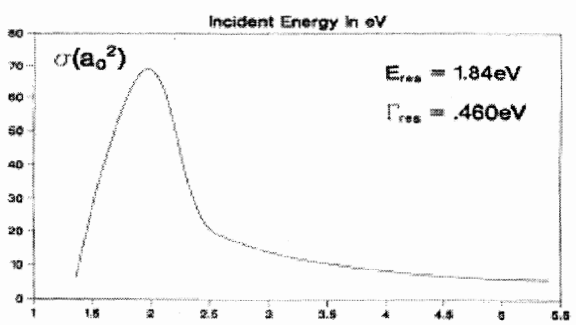

$^2B_{2g}$ partial integrated cross section for $e^- - C_2H_4$ scattering.

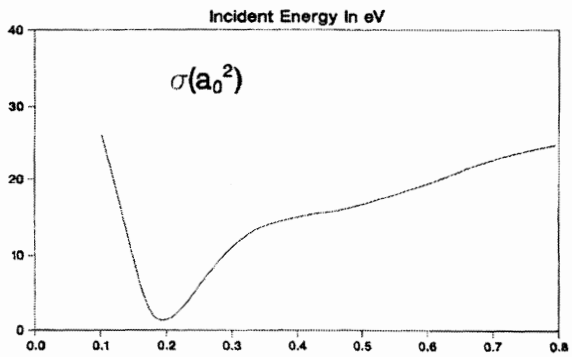

^2A_g partial integrated cross section for $e^- - C_2H_4$ scattering.

FIG. 12: Cross Section for Elastic Electron Scattering from Ethylene

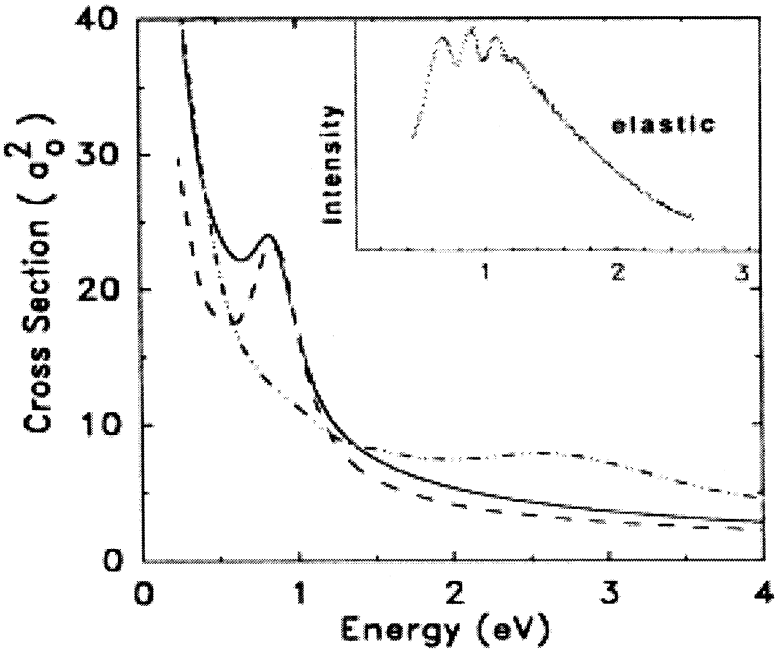

Elastic differential cross section for e^-–CH_2O. Solid Curve: optical-potential results at 90°; dashed curve: optical-potential results at 120°; dash-dotted curve: static-exchange result at 90°. Inset: Experimental results of Benoit and Abouaf (Ref. 8).

FIG. 13: Cross Section for Vibration Excitation in Formaldehyde

DOUBLE PHOTOIONIZATION NEAR THRESHOLD

Ralf Wehlitz
Synchrotron Radiation Center, UW-Madison, Stoughton, WI 53589

ABSTRACT

The threshold region of the double-photoionization cross section is of particular interest because both ejected electrons move slowly in the Coulomb field of the residual ion. Near threshold both electrons have time to interact with each other and with the residual ion. Also, different theoretical models compete to describe the double-photoionization cross section in the threshold region. We have investigated that cross section for lithium and beryllium and have analyzed our data with respect to the latest results in the Coulomb-dipole theory. We find that our data support the idea of a Coulomb-dipole interaction.

INTRODUCTION

The double-photoionization process, where the absorption of a single photon leads to the ejection of two electrons, is an interesting and also challenging subject in physics, because the breakup of a Coulomb system into three particles cannot be described analytically. Especially the threshold region, where both ejected electrons have time to interact with each other, has attracted the interest of theorists and experimentalists trying to find models of this seemingly simple process. Historically, interest has focused on a similar process, namely single ionization by electron impact, where — similar to the double-photoionization process — two free electrons are in the final state, but leaving a *singly* charged ion behind. This interest was stimulated by its relevance for studying the gas discharge process.

In 1948 Wigner made a first attempt to describe the energy dependence of electron-impact ionization near threshold (ref. 1). This attempt lead to a linear law, i.e., the cross section is proportional to the energy above threshold (excess energy). Early experiments by Fox and Hickam *et al.* (refs. 2 and 3) seemed to support this law, even for the case of double ionization by electron impact.

Soon thereafter, Wannier examined the threshold region again and developed his famous threshold law (ref. 4). The idea is that in the asymptotic limit both emitted electrons have the same momentum (traveling on the "Wannier ridge") and are emitted back-to-back because of the Coulomb repulsion. If one electron would be faster than the other, the slower electron would be recaptured by the ion because of the missing shielding of the ion's potential by the fast electron. This leads to a power law for the double-electron escape at threshold, i.e., $\sigma \propto E^{\alpha}$, with α being the Wannier exponent, which depends on the charge of the residual ion. For instance, for a neutral target, α=1.127 for electron-impact ionization and α=1.056 for double photoionization. In the extreme case where the residual ion has an infinite charge and the interaction between the electrons becomes negligible, one obtains again α=1.0, which corresponds to the Wigner law.

Experimental evidence for α>1.0 was obtained by McGowan and Clark for electron impact ionization of atomic hydrogen (ref. 5); they found α=1.13(3) for E<0.4eV. An early photoionization experiment performed by Van der Wiel (ref. 6) produced data that were compatible with the Wannier's power law, but were not accurate enough to prove it. The first photoionization experiment that clearly supported Wannier's exponent was performed by Kossmann *et al.* (ref. 7) who found α=1.05(2) for double photoionization of helium. Samson *et al.* repeated the experiment (ref. 8) but used atomic oxygen instead of helium and found α=1.077(3).

Although the experiments mentioned above (refs. 5, 7, 8) are all in support of Wannier's theory, an alternate description of the electron double escape was developed by Temkin (see, e.g., ref. 9). This theory is based on the notion that, even near threshold, one electron is faster than the other and, thus, one electron has a larger distance from the ion than the other one. Therefore, the slower electron and the residual ion can form a dipole that rotates until the slow electron is "far away" from the ion. The fast electron experiences a field created by this Coulomb dipole and the cross section will exhibit a *modulation*, in contrast to the Wannier theory. The electron-impact cross section σ can be described as follows: $\sigma \propto E\,(\ln E)^{-2}\,[1+C\sin(\alpha \ln(E) + \mu)]$, with E the excess energy and C, α and μ suitable parameters. Note that the electron emission is

not necessarily back-to-back anymore. It is worthwhile to mention that the formula given above can be applied to electron-impact ionization and double photodetachment because, in both cases, the residual ion and slow electron forms a dipole without a net charge. For double photoionization, however, this formula needs to be modified, because the "dipole" formed by the slow electron and residual ion has now a net charge.

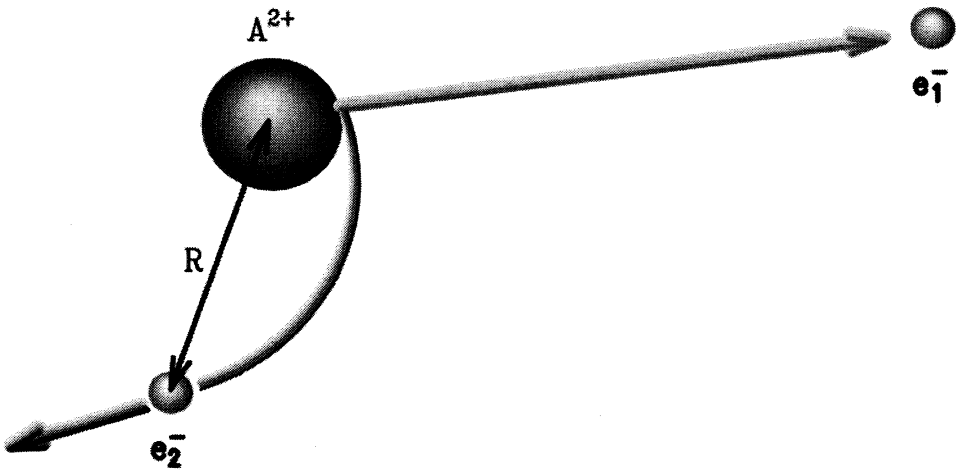

Figure 1 Sketch of the two electrons leaving a doubly charged ion behind after double photoionization.

Figure 1 illustrates the situation described above. While electron "1" is fast and far away, the slow electron "2" forms together with the ion a rotating dipole until it reaches a distance larger than "R" and its path becomes a straight line. Experimental evidence that the Coulomb-dipole theory seems to be a realistic (measurable) model was given by Donahue *et al.* (ref. 10) studying double photodetachment of H^-, and by Bae and Petersen (ref. 11) studying double photodetachment of K^-. Although in both cases the cross section near threshold can be described by Wannier's power law, it is also possible to fit the formula of the Coulomb-dipole theory to their data. While the authors decided not to favor one of the theories, a detailed analysis performed later by Friedman *et al.* (ref. 12) indicates that the Coulomb-dipole theory provides a better modeling of the near threshold behavior of the cross section.

Considering the situation described above, we decided to investigate the double-photoionization cross section of lithium and beryllium near threshold. Up to that point, there was no clear evidence for the Coulomb-dipole theory, and double-photoionization experiments near threshold have been performed only for the elements He and O. Our Li and Be data along with a preliminary fit model have been published recently (refs. 13, 14).

EXPERIMENT

The experiments were performed at the Synchrotron Radiation Center (SRC) in Wisconsin, which has an 800-MeV electron storage ring that provides synchrotron radiation for various beamlines. The Li experiment was performed on the PGM Undulator beamline and the Be experiment was performed on the 4-m NIM beamline. Generally, the monochromatized photon beam enters the experimental chamber through a differential pumping stage. This pumping stage helps maintaining a very good vacuum in the beamline while working with gases in the experimental chamber. It also houses an array of filters that can be used to suppress second-order and stray light. The photon beam intersects an effusive beam of metal vapor that is created in a resistively heated furnace. The furnace can be electrically biased to prevent thermal electrons from reaching the interaction region. While thermal electrons do not have enough energy to ionize our target, the electric pulse applied across the interaction region, in order to extract the ions, is strong enough to accelerate these electrons to a sufficiently high kinetic energy. The ions extracted from the

interaction region are accelerated into a drift tube and detected by a Z-stack of microchannel plates. This time-of-flight method allows us to separate the different charge states of our photoionized target atoms. Further details of the experiments can be found in references 13, 14, and 15.

RESULTS

After measuring the double-photoionization cross section of Li, we applied the Wannier threshold law to our data and found an exponent α=1.054(7), which is close to the predicted value of 1.056. However, the difference between the fit curve and our data points exhibits a non-statistical modulation that reminded us on the modulation in the Coulomb-dipole theory. As mentioned above, a corresponding theory for double photoionization had not been developed at that time. However, Aaron Temkin provided us with a preliminary formula that fits nicely and even better to our data than the Wannier formula over 1.4 eV above threshold (ref. 13). At this point we believed that the applicability of the (modified) Coulomb-dipole theory is due to the strong asymmetry in the Li atom. For double ionization near threshold, one electron is ejected from the 2s shell while the other electron is ejected from the 1s shell. The binding energy of the 2s electron is only 5.4 eV whereas the 1s electron is tightly bound at 64.4 eV. Thus, Li is very different from He where both electron have the same binding energy.

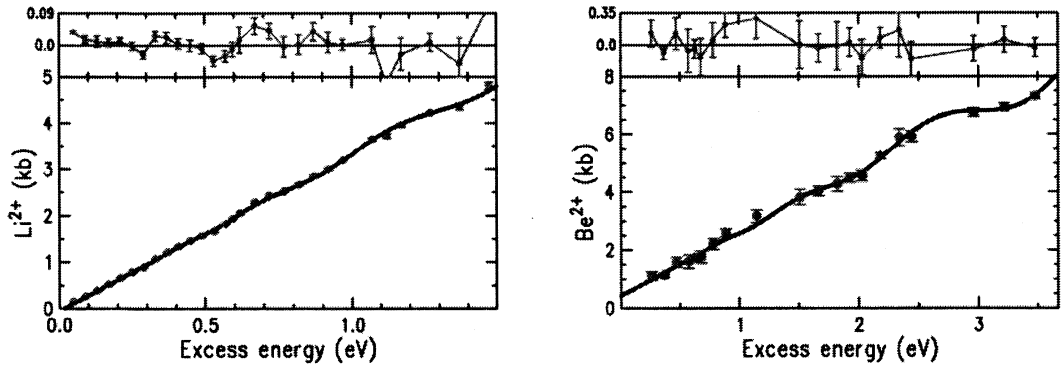

Figure 2 Double-photoionization cross section of Li (left) and Be (right) as a function of excess energy near threshold. The fit curves are according to Equation 1. The top panels show the difference of the fit curve from the data points.

In order to test this hypothesis we decided to measure the double-photoionization cross section of Be that is similar to He in so far as both outer s-electrons are emitted. The Wannier threshold law seemed to fit up to 1.8 eV above threshold but, to our surprise, we found again an oscillatory behavior of the difference between our data points and the fit curve (ref. 14). A preliminary formula, suggested by Temkin, yielded again a better agreement with our data than the Wannier power law.

Only very recently Temkin and Bhatia[1] found a formula that correctly describes the double-photoionization cross section σ near threshold within the framework of the Coulomb-dipole theory, namely:

$$\sigma \propto E + E^2/(\ln E)^2 * M(E), \text{ with } M(E)=B \sin[A \ln(E) + C]. \quad (1)$$

Here, E is the excess energy and A, B, and C are suitable constants. From an experimental point of view the appearance of the new fit curve is only marginally different from the curves that we have used in the past. Unfortunately, the analytical expression is strictly valid only for the first ~10^{-6} eV above threshold, an energy range that will experimentally not be accessible in the near future. Drs. Temkin and Bhatia are in

[1] Private communication (2006)

the process of applying their theory to the numerical evaluation of the cross sections in the experimental energy range, for the three targets He, Li, and Be. This will provide a more stringent test of the theory than the parametric fit based on Eq. (1). Our Li and Be data along with the new fit curves are shown in Figure 2. In either case, the data displayed in the top panels show the difference between the cross section data and the fit curve. The fit curves seem to match the data very well since this difference exhibits just a random scatter of the points. One of the predictions of the Coulomb-dipole theory is the target independence of the parameter A in the equation above. From our fits we obtain values for the A parameter of 12.4(1) for Li and 12.1(10) for Be, which are in excellent agreement with this prediction.

Now the question arises: what about helium? No oscillations have been found in this case, neither experimentally (ref. 7) nor theoretically (ref. 16). Nevertheless, we applied the Coulomb-dipole theory to the He data and found a fit curve that is compatible with the He data. However, the agreement may be fortuitous and more precise data are called for. It will be of interest to see if the numerical calculations of Temkin and Bhatia will find a significant reduction in the magnitude of the oscillation for the He target compared to Li an Be, as is require by the data.

It is worthwhile to note that in his 1982 paper (ref. 9), Temkin gives the approximate range for the A parameter, namely $7 < A < 160$. Our A-parameter values (see above) as well as the values of Donahue *et al.* (ref. 10), A=42, and Bae and Petersen (ref. 11), A=9.4, are within the expected range.

SUMMARY

In order to test the Coulomb-dipole theory, we have determined the double-photoionization cross section of Li and Be near threshold. We have found oscillations in the cross section that are consistent with the recently developed Coulomb-dipole theory for double photoionization. Although this theory is, strictly speaking, only applicable for the first $\sim 10^{-6}$ eV it provides a good description of the energy dependence of the experimental data. The A parameter that describes the "wavelength" of the oscillations is indeed target independent (for Li and Be) as predicted and is of the expected order of magnitude.

While our data are in good agreement with the Coulomb-dipole theory, the rather large error bars do not allow us to make a final decision without some doubt. Although the three-body Coulomb interaction in the double-photoionization process is of fundamental importance, it is experimentally hardly accessible for two reasons. First, the cross section starts at zero at threshold resulting in very low count rates. Second, the "near threshold region" is not well defined and theory suggests that the threshold laws are applicable for only the fist 10^{-6} eV, an energy range that is not accessible by experiment at the moment. Of course, there is always hope that the theory is approximately valid for higher energies in the few-eV region.

I wish to thank Jaques Bluett, Dragan Lukic, and Scott Whitfield for their various contributions to the experiments. In particular, I want to thank Aaron Temkin for many stimulating discussions and for developing, together with Anand Bhatia, the Coulomb-dipole theory for double photoionization. The experiments were performed at the Synchrotron Radiation Center (SRC), which is supported by NSF under Grant No. DMR-0084402.

REFERENCES

1. E. P. Wigner, Phys. Rev. **73**, 1002 (1948).

2. W. M. Hickam, R. E. Fox, and T. Kjeldaas, Jr., Phys. Rev. **96**, 63 (1954).

3. R. E. Fox, W. M. Hickam, T. Kjeldaas, Jr., and D. J. Grove, Phys. Rev. **84**, 859 (1951).

4. G. H. Wannier, Phys. Rev. **90**, 817 (1953).

5. J. W. McGowan and E. M. Clarke, Phys. Rev. **167**, 43 (1968).

6. M. J. Van der Wiel, Phys. Lett. **41A**, 389 (1972).

7. H. Kossmann, V. Schmidt, and T. Andersen, Phys. Rev. Lett. **60**, 1266 (1988).

8. Z. X. He, R. Moberg, and J. A. R. Samson, Phys. Rev. A **52**, 4595 (1995).

9. A. Temkin, Phys. Rev. Lett. **49**, 365 (1982).

10. J. B. Donahue, P. A. M. Gram, M. V. Hynes, R. W. Hamm, C. A. Frost, H. C. Bryant, K. B. Butterfield, D. A. Clark, and W. W. Smith, Phys. Rev. Lett. **48**, 1538 (1982).

11. Y. K. Bae and J. R. Petersen, Phys. Rev. A **37**, 3254 (1988).

12. J. R. Friedman, X. Q. Guo, M. S. Lubell, and M. R. Frankel, Phys. Rev. A **46**, 652 (1992).

13. R. Wehlitz, J. B. Bluett, and S. B. Whitfield, Phys. Rev. Lett. **89,** 093002 (2002).

14. D. Lukic, J. B. Bluett, and R. Wehlitz, Phys. Rev. Lett. **93**, 023003 (2004).

15. R. Wehlitz, D. Lukic, C. Koncz, and I. A. Sellin, Rev. Sci. Instrum. **73**, 1671 (2002).

16. U. Kleimann, T. Topçu, M. S. Pindzola, and F. Robicheaux, J. Phys. B **39**, L61 (2006).

APPLICATION OF THE FINITE ELEMENT METHOD TO ATOMIC AND MOLECULAR PHYSICS

Janine Shertzer
College of the Holy Cross, Worcester MA 01610

ABSTRACT

The finite element method (FEM) is a numerical algorithm for solving second order differential equations. It has been successfully used to solve many problems in atomic and molecular physics, including bound state and scattering calculations. To illustrate the diversity of the method, we present here details of two applications. First, we calculate the non-adiabatic dipole polarizability of H_2^+ by directly solving the first and second order equations of perturbation theory with FEM. In the second application, we calculate the scattering amplitude for e-H scattering (without partial wave analysis) by reducing the Schrödinger equation to set of integro-differential equations, which are then solved with FEM.

I. INTRODUCTION

The finite element method (FEM) is a powerful numerical tool for solving differential equations, including eigenvalue problems [1]. FEM utilizes a piecewise interpolation scheme, in which the unknown function is approximated locally by a simple polynomial. Although the method was originally developed to solve problems in structural mechanics, Frank Levin was one of the first to recognize that FEM could be used to study few-body systems [2]. For bound states, FEM has been used to calculate to high accuracy the energy and structure of three-body Coulomb systems with arbitrary masses [3]. Another important application is the study of atoms and molecules in strong external fields [4]; when the wave function is strongly distorted, the piecewise interpolation approach is often superior to standard hydrogenic or Gaussian basis set expansion. FEM can also be used to study collisions, where the complicated boundary conditions associated with scattering can be treated in a straightforward fashion. Accurate phase shifts and inelastic cross sections have been calculated for e-H collisions for $0 \le L \le 3$ [5]. For the Temkin-Drachman Retirement Symposium, I have selected two FEM examples which reflect the research interests of the honorees.

Richard Drachman has contributed greatly to our understanding of long-range interactions. In his series of papers on the Rydberg states of Helium [6] and Lithium [7], he has provided a rigorous theoretical description for Rydberg atoms based on an effective polarization potential. An important extension of this work has been the formulation of an effective polarization potential for the Rydberg electron of H_2; microwave spectroscopy of high Rydberg states provided a mechanism for determining the multipole moments of the ionic core, including the static dipole polarizability [8].

The measurement of α_s for H_2^+ motivated several groups (including Drachman and Bhatia [9]), to calculate the polarizability of H_2^+ without invoking the Born-Oppenheimer approximation. In section II, we present a description of a FEM calculation of the dipole polarizability of H_2^+.

Aaron Temkin's contributions to scattering theory have had a major and lasting impact on the field. With his method of polarized orbitals [10], he was the first to include the effects of polarization and exchange in the ansatz for the wavefunction. In 1962, he introduced the now famous Temkin-Poet model [11]. For the past eight years, I have had the privilege to collaborate with Aaron, pursuing a new approach to scattering that does not use partial wave analysis. The scattering amplitude is calculated directly by solving a set of coupled integro-differential equations. Section III summaries our progress to date and outlines our plans for the future. Atomic units are used throughout.

II. NONADIABATIC DIPOLE POLARIZABILITY OF H_2^+

In the late 90's, experiments on the Rydberg states of H_2 provided a mechanism for determining the static dipole polarizabiltiy of H_2^+ to high precision [8]. At that time, the only theoretical calculation for α_s employed the Born-Oppenheimer approximation [12]. Given the accuracy of the new results, it was not surprising that there was a discrepancy between the experimental value α_s =3.1681(7) and the theoretical value α_s^{BO}=3.1713 on the order of m_e / m_p. This breakdown of the Born-Oppenheimer approximation motivated several groups to attempt a non-adiabatic calculation of the dipole polarizability.

The static dipole polarizability α_s is defined in terms of the second order correction to the energy due to the presence of an external electric field $\vec{\varepsilon}$:

$$E^{(2)} = -\tfrac{1}{2}\alpha_s \varepsilon^2 = \left\langle \Psi^{(1)}(\vec{r},\vec{R}) \,|\, (1+\delta)\,\vec{\varepsilon}\cdot\vec{r} \,|\, \Psi^{(0)}(\vec{r},\vec{R}) \right\rangle \qquad (1)$$

where $(1+\delta) = \frac{(2m_p+2)}{(2m_p+1)}$. In the variational approach, the first order correction to the wave function is expanded in a basis set that includes nuclear and electronic states. Using FEM, one can solve directly the first and second order equations of perturbation theory [13]. The first step is to carry out the frame transformation that reduces the number of variables in the problem.

Frame transformation

In the space-fixed laboratory frame (x', y', z'), the electric field is aligned with the z'-axis (see Fig. 1). After separating out the center-of mass motion, the (field-free) Hamiltonian for the relative motion is given by

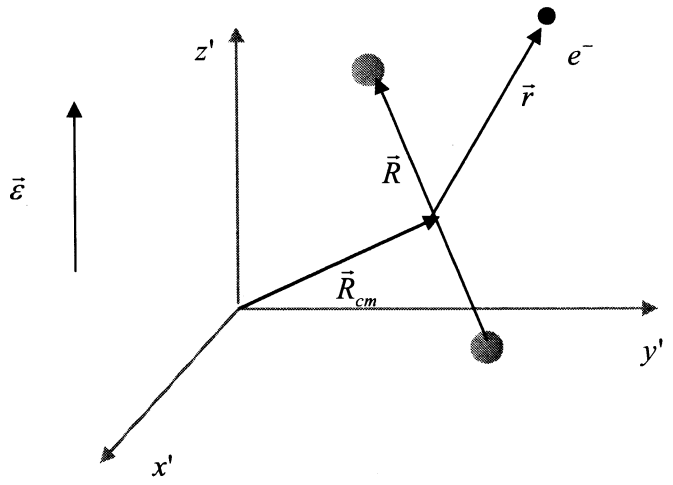

Figure 1. H_2^+ in the space-fixed (laboratory frame). $\vec{\varepsilon}$ indicates the direction of the external electric field.

$$H = -\frac{1}{2\mu}\nabla_R^2 - \left(\frac{1}{2}+\frac{1}{8\mu}\right)\nabla_r^2 + V(\vec{R},\vec{r}) \tag{2}$$

where

$$V(\vec{R},\vec{r}) = \frac{1}{R} - \frac{1}{|\vec{r}+\frac{\vec{R}}{2}|} - \frac{1}{|\vec{r}-\frac{\vec{R}}{2}|} \tag{3}$$

and $\mu = m_p/2$.

The vector $\vec{R}$ lies along the internuclear axis and $\vec{r}$ is the vector from the center of the internuclear axis to the electron. The Hamiltonian commutes with L^2 and L_z, and in general, the non-adiabatic wave function $\Psi(L, M'; \vec{r}, \vec{R})$ depends on all six coordinates.

To simplify the problem, we perform a rotation $\Re(\Phi', \Theta', 0)$ which leaves the internuclear axis aligned with the new z-axis. It appears that we have eliminated two degrees of freedom, since the wave function is now a function of only $\vec{r}$ and R. But there is a price to pay for this frame transformation. The Hamiltonian does not commute with L_z; M is not a good quantum number and the Hamiltonian is not diagonal in the basis spanned by the eigenstates of L^2 and L_z. The electric field, which appears in the matrix element of Eq. (1), is now a function of the Euler angles

$$\vec{\varepsilon} = \varepsilon(-\sin\Theta'\,\hat{x} + \cos\Theta'\,\hat{z}). \tag{4}$$

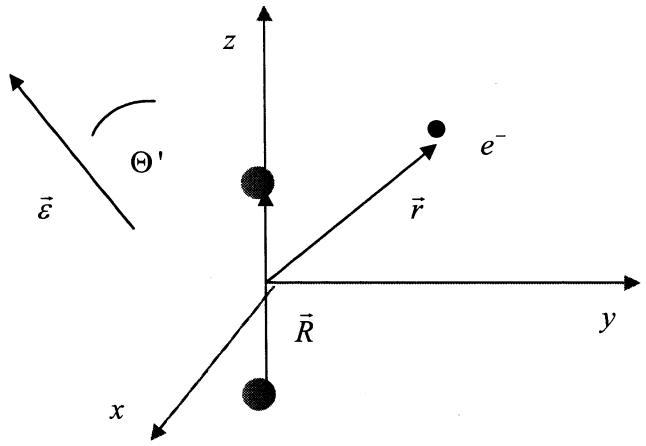

Figure 2. H_2^+ in the body-fixed frame. $\vec{\varepsilon}$ indicates the direction of the external electric field.

Despite these complications, it is still desirable to work in the body-fixed frame. Ultimately, we must reduce the problem to a solution of a set of differential equations in three variables if we are to apply the FEM.

The space-fixed wave function (with 'good' quantum numbers L, M') is a linear combination of the body-fixed wave functions,

$$\Psi_{SF}(L,M';\vec{r},\vec{R}) = \sum_{M=-L}^{L} D^{L}_{MM'}(\Phi',\Theta',0)\Psi_{BF}(L,M;\vec{r},R) \tag{5}$$

where $D^{L}_{MM'}(\Phi',\Theta',0)$ are the coefficients of the irreducible representation associated with the rotation $\Re(\Phi',\Theta',0)$. The Hamiltonian in the body-fixed frame is given by

$$H = \frac{1}{2\mu}\left[p_R^2 + \frac{1}{R^2}\left(L^2 + L_e^2 - 2L_z^2 - L_{e-}L_{+} - L_{e+}L_{-}\right)\right] + \left(\frac{1}{2} + \frac{1}{8\mu}\right)\left[p_r^2 + \frac{1}{r^2}L_e^2\right] + V(\vec{r},R) \tag{6}$$

where

$$L_{\pm}\Psi_{BF}(L,M;\vec{r},R) = \sqrt{L(L+1) - M(M\pm 1)}\,\Psi_{BF}(L,M\pm 1;\vec{r},R). \tag{7}$$

Perturbation Theory

We now return to the evaluation of the matrix element in Eq. (1). It is clear that we must start in the space-fixed frame, where the 'good' quantum numbers associated with the unperturbed ground state are $L = 0$ and $M' = 0$; from the Wigner-Eckart theorem, we know that the first order correction to the wave function must be a state with $L = 1$ and $M' = 0$. Therefore, we re-express Eq. (1) more precisely as

$$E^{(2)} = -\tfrac{1}{2}\alpha_s \varepsilon^2 = \left\langle \Psi_{SF}^{(1)}(1,0;\vec{r},\vec{R}) \,|(1+\delta)\,\vec{\varepsilon}\cdot\vec{r}\,|\, \Psi_{SF}^{(0)}(0,0;\vec{r},\vec{R}) \right\rangle \tag{8}$$

where $\Psi_{SF}^{(0)}$ and $\Psi_{SF}^{(1)}$ are found by solving the zeroth and first order equations of perturbation theory:

$$H\,\Psi_{SF}^{(0)}(0,0;\vec{r},\vec{R}) = E^{(0)}\Psi_{SF}^{(0)}(0,0;\vec{r},\vec{R}) \tag{9a}$$

$$(H - E^{(0)})\Psi_{SF}^{(1)}(1,0;\vec{r},\vec{R}) = -(1+\delta)\,\vec{\varepsilon}\cdot\vec{r}\;\; \Psi_{SF}^{(0)}(1,0;\vec{r},\vec{R}). \tag{9b}$$

For the special case $L = 0$, $M' = 0$, there is a one-to-one correspondence between the space-fixed wave function and the body-fixed wave function

$$\Psi_{SF}^{(0)}(0,0;\vec{r},\vec{R}) = \Psi_{BF}^{(0)}(0,0;\vec{r},R). \tag{10}$$

The body-fixed Hamiltonian is diagonal since $L_{\pm}\Psi_{BF}^{(0)}(0,0;\vec{r},R)=0$. Furthermore, the wave function is independent of the electronic azimuthal angle ϕ, and the resultant differential equation (in three variables)

$$\left\{\frac{1}{2\mu}\left[p_R^2 + \frac{1}{R^2}L_e^2\right] + \left(\frac{1}{2} + \frac{1}{8\mu r^2}\right)\left[p_r^2 + \frac{1}{r^2}L_e^2\right] + V(\vec{r},R) - E^{(0)}\right\}\Psi_{\mathrm{BF}}^{(0)}(0,0;r,\theta,R) = 0 \tag{11}$$

can be solved with FEM for the ground state energy and wave function. We obtained $E^{(0)} = -0.597\,139\,055(8)$.

In order to obtain the first order correction to the wave function, we need to solve Eq. (9b) by transforming it to the body-fixed frame. The zeroth order wave function $\Psi_{SF}^{(0)}$ is given by Eq. (10) and the dipole interaction is given by

$$\vec{\varepsilon}\cdot\vec{r} = \varepsilon\, r(\cos\Theta'\cos\theta - \sin\Theta'\sin\theta\cos\phi). \tag{12}$$

Using Eq. (5), the first order correction to the wave function $\Psi_{SF}^{(1)}$ is re-expressed in the body-fixed frame as

$$\Psi_{SF}^{(1)}(1,0;\vec{r},\vec{R}) = \cos\Theta' \Psi_{BF}^{(1)}(1,0;\vec{r},R) + \tfrac{1}{\sqrt{2}}\sin\Theta' [\Psi_{BF}^{(1)}(1,1;\vec{r},R) - \Psi_{BF}^{(1)}(1,-1;\vec{r},R)]; \qquad (13)$$

the (body-fixed) Hamiltonian is given by Eq. (6).

The resultant coupled equations depend on the five variables Θ', r, θ, ϕ and R. Equating terms that multiply $\cos\Theta'$ and $\sin\Theta'$, we can eliminate the dependence on the Euler angle Θ'. We are left with three coupled differential equations for the body-fixed wave functions $\Psi_{BF}^{(1)}(1, M; \vec{r}, R)$, $M = 0,\pm 1$. The dependence on the electronic azimuthal angle ϕ can be obtained analytically; one can show that the wave functions must be of the form

$$\Psi_{BF}^{(1)}(1,0;\vec{r},R) = \varepsilon f(r,\theta,R) \qquad (14a)$$

$$\Psi_{\mathrm{BF}}^{(1)}(1,\pm 1;\vec{r},R) = \pm\tfrac{1}{\sqrt{2}}\varepsilon\, g(r,\theta,R)\, \mathrm{e}^{\pm i\phi} . \qquad (14b)$$

Thus we have reduced the problem to a set of two coupled equations in three variables:

$$\left[H_{00} - E^{(0)}\right] f(r,\theta,R) + \frac{1}{\mu R^2}\left(\frac{\partial}{\partial\theta} + \cot\theta\right) g(r,\theta,R) = -r\cos\theta\, \Psi_{BF}^{(0)}(r,\theta,R) \qquad (15a)$$

$$\left[H_{11} - E^{(0)} + \left(\frac{1}{2\mu R^2} + \frac{1}{2r^2} + \frac{1}{8\mu r^2}\right)\frac{1}{\sin^2\theta}\right] g(r,\theta,R) + \frac{1}{\mu R^2}\frac{\partial}{\partial\theta} f(r,\theta,R) = r\sin\theta\, \Psi_{BF}^{(0)}(r,\theta,R) \qquad (15b)$$

where

$$H_{MM} = \frac{1}{2\mu}\left[p_R^2 + \frac{1}{R^2}(L_e^2 + 2\delta_{M,0})\right] + \left(\frac{1}{2} + \frac{1}{8\mu}\right)\left[p_r^2 + \frac{1}{r^2}L_e^2\right] + V(\vec{r},R). \qquad (16)$$

Eqs. (15a) and (15b) are solved with FEM. Once we know $f(r,\theta,\phi)$ and $g(r,\theta,\phi)$ we can construct the first order correction to the wave function and evaluate the matrix element of Eq. (8) to determiner α_s.

In Table I, we compare the FEM value of α_s with the experimental value and several variational calculations; also included is the Born-Oppenheimer result. It is interesting to note that there remains a discrepancy between the theoretical and experimental value of α_s, that cannot be accounted for by relativistic corrections.

TABLE I. Experimental and theoretical values for the dipole-polarizability of H_2^+.

Author (year)	Ref.	α_s
Bishop and Lamb (1988) *Born-Oppenheimer*	[12]	3.1713
Jacobson et. al (1997) *Experiment*	[8]	3.168 1(7)
Shertzer and Greene (1998)	[13]	3.168 2(4)
Bhatia and Drachman (1999)	[9]	$3.168\ 0^{+.0018}_{-.0001}$
Taylor *et al.* (1999)	[14]	3.168 725 6(1)
Moss (1999)	[15]	3.168 726
Jacobson *et al.* (2000) *Experiment*	[16]	3.167 96(15)
Korobov (2001)	[17]	3.168 725 76
Hilico *et al.* (2001)	[18]	3.168 725 803(1)
Yan *et al.* (2003)	[19]	3.168 725 802 67(1)

DIRECT CALCULATION OF THE SCATTERING AMPLITUDE

We present here a new approach to scattering which does not use partial wave analysis [20]. The basic idea is to reduce the Schrödinger equation to a set of coupled integro-differential equations that can be solved with FEM for the scattering wave function. The wave function is then used in the integral expression for the scattering amplitude.

e-H Scattering (static approximation with exchange)

Our first application is electron-hydrogen scattering in the static approximation (with exchange). The trial wave function is given by

$$\Psi_k^{\pm}(\vec{r}_1,\vec{r}_2) = \psi_k^{\pm}(\vec{r}_1)\phi_{1s}(r_2) \pm \psi_k^{\pm}(\vec{r}_2)\phi_{1s}(r_1), \tag{17}$$

where $\psi_k^{\pm}(\vec{r})$ is an unknown function. We require that the wave function satisfy the Schrödinger equation for the two-electron system subject to the asymptotic boundary condition

$$\psi_k^{\pm}(\vec{r}) \to e^{ikr\cos\theta} + f_k^{\pm}(\theta)\frac{e^{ikr}}{r} \tag{18}$$

as $r \to \infty$. Projecting the Schrödinger equation onto $\phi_{1s}(r_2)$, we have

$$\left\langle \phi_{1s}(r_2) \middle| \nabla_1^2 + \nabla_2^2 + \frac{2}{r_1} + \frac{2}{r_2} - \frac{2}{r_{12}} + k^2 - 1 \middle| \Psi_k^{\pm}(\vec{r}_1,\vec{r}_2) \right\rangle = 0 \tag{19}$$

Carrying out the integration over the coordinates of the second electron, we are left with a integro-differential equation for the unknown function $\psi_k^{\pm}$:

$$\left[\nabla^2 + V(r) + k^2\right]\psi_k^{\pm}(\vec{r}) \;\pm (k^2+1)\phi_{1s}(r)\left\langle \phi_{1s} \mid \psi_k^{\pm}\right\rangle \pm \phi_{1s}(r)\left\langle \phi_{1s}\left| \tfrac{-2}{|\vec{r}-\vec{r}'|}\right| \psi_k^{\pm}\right\rangle = 0 . \tag{20}$$

where $V(r) = 2e^{-2r}(1+\frac{1}{r})$.

Although FEM can be applied to integro-differential equations, the last term $\left\langle \phi_{1s}\left| \frac{-2}{|\vec{r}-\vec{r}'|}\right| \psi_k^{\pm}\right\rangle$ is problematic because it involves a numerical integration over d^3r' for *each* value of $\vec{r}$. This is computationally prohibitive. To eliminate this problem, we introduce a new function

$$\alpha_k^{\pm}(\vec{r}) = \left\langle \phi_{1s} \mid \tfrac{-2}{|\vec{r}-\vec{r}'|} \mid \psi_k^{\pm}\right\rangle \tag{21}$$

which satisfies

$$\nabla^2 \alpha_k^{\pm}(\vec{r}) = 8\pi\phi_{1s}(r)\psi_k^{\pm}(\vec{r}) \tag{22}$$

subject to the boundary condition

$$\alpha_k^{\pm}(\vec{r}) \to \frac{-2}{r}\left\langle \phi_{1s} \mid \psi_k^{\pm}\right\rangle \tag{23}$$

as $r \to \infty$. Eq. (20) is now replaced by *two* coupled integro-differential equations

$$\begin{aligned} \left[\nabla^2 + V(r) + k^2\right]\psi_k^{\pm}(\vec{r}) \pm \phi_{1s}(r)\alpha_k^{\pm}(\vec{r}) \pm (k^2+1)\,\phi_{1s}(r)\left\langle \phi_{1s} \mid \psi_k^{\pm}\right\rangle &= 0 \\ \nabla^2 \alpha_k^{\pm}(\vec{r}) - 8\pi\phi_{1s}(r)\psi_k^{\pm}(\vec{r}) &= 0 \end{aligned} \tag{24}$$

which are solved with FEM. The solution yields $\psi_k^{\pm}(r,\theta)$, $\alpha_k^{\pm}(r,\theta)$ and $f_k^{\pm}(\theta)$ (where we have assumed azimuthal symmetry).

In general, the scattering amplitude obtained directly from the FEM calculation is not accurate unless the FEM grid is very large ($r_{\max} \to \infty$). The results are sensitive to the accuracy of the wave function on the boundary, where it is highly oscillatory.

Integral formula for the scattering amplitude

In order to reduce the computational effort and improve the accuracy of the scattering amplitude, we employ the integral formula for $f_k^{\pm}(\theta)$ given by

$$f_k^{\pm}(\theta) = -\frac{1}{4\pi}\int e^{-i\vec{k}\cdot\vec{r}_1}\,\phi_{1s}(r_2)\left[-\frac{2}{r_1}+\frac{2}{r_{12}}\right]\Psi_k^{\pm}(\vec{r}_1,\vec{r}_2)\,d^3r_1\,d^3r_2 . \tag{25}$$

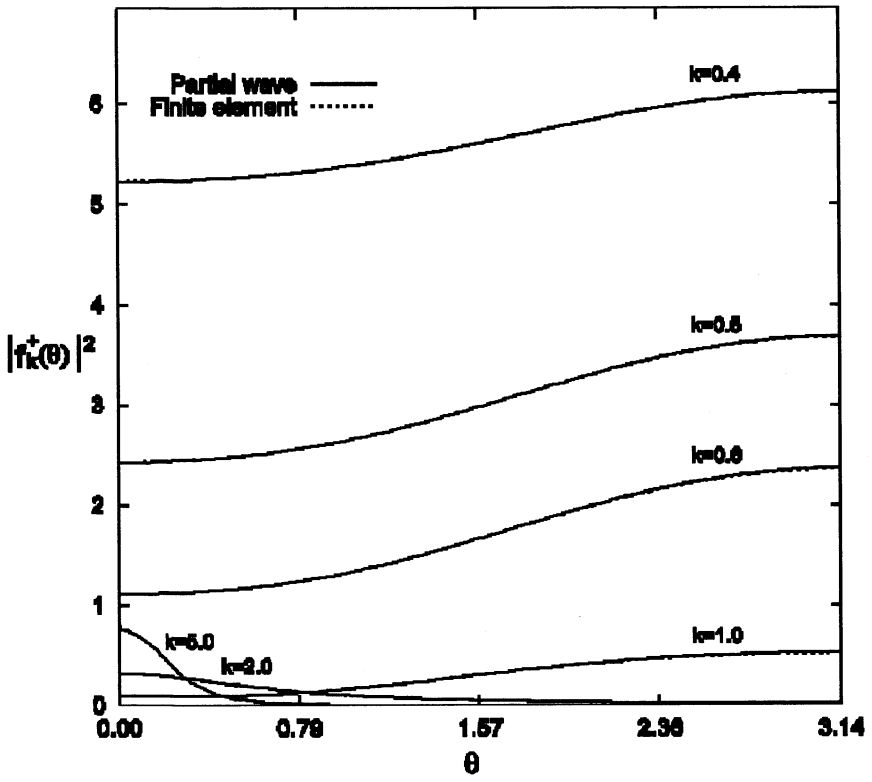

Figure 1. Results for $|f_k^+(\theta)|^2$ obtained with FEM are compared with fully converged partial wave results.

Using the ansatz of Eq. (17), we have

$$f_k^{\pm}(\theta) = -\frac{1}{4\pi}\int e^{-i\vec{k}\cdot\vec{r}_1}\phi_{1s}(r_2)\left[-\frac{2}{r_1}+\frac{2}{r_{12}}\right]\left[\psi_k^{\pm}(r_1,\theta_1)\,\phi_{1s}(r_2)\pm\psi_k^{\pm}(r_2,\theta_2)\,\phi_{1s}(r_1)\right]d^3r_1 d^3r_2 . \quad (26)$$

The accuracy of $f_k^{\pm}(\theta)$ now depends on how well the wave function $\psi_k^{\pm}(r,\theta)$ is represented in the interaction region. In general, the integral expression is not particularly useful because it involves a six dimensional integration. However, using our definition for $\alpha_k^{\pm}(r,\theta)$, we can analytically integrate over four of the six variable to obtain

$$f_k^{\pm}(\theta) = \frac{1}{2}\int J_o(kr'\sin\theta'\sin\theta)\,e^{-ikr'\cos\theta'\cos\theta}\left[V(r')\,\psi_k^{\pm}(r',\theta')\pm\phi_{1s}(r')\,\alpha_k^{\pm}(r',\theta')\right]\sin\theta' r'^2\,dr'd\theta'$$
$$\pm\frac{4}{k^2+1}\int\phi_{1s}(r)\,\psi_k^{\pm}(r',\theta')\sin\theta' r'^2\,dr'd\theta' . \quad (27)$$

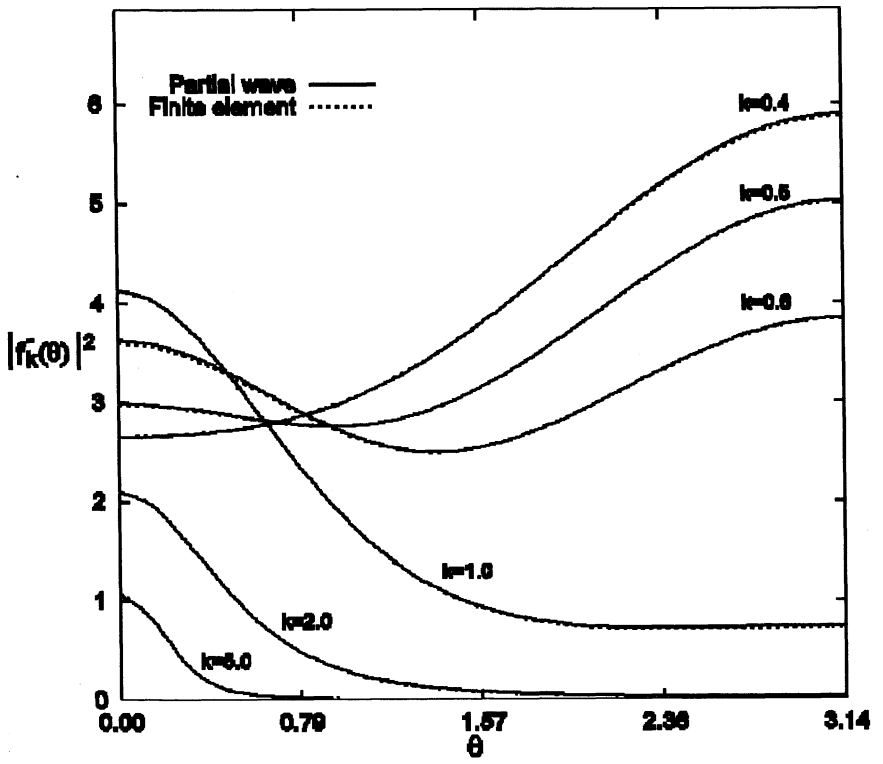

Figure 2. Results for $|f_k^-(\theta)|^2$ obtained with FEM are compared with fully converged partial wave results.

The final integration is done numerically.

Using the integral formula, we can obtain extremely accurate and stable results with relatively little computational effort. Unlike partial wave analysis, the computational effort is independent of energy. In Figs. (1) and (2), we compare our results with a fully converged partial wave calculation [21] for the elastic scattering amplitude for e-H in the static approximation (with exchange).

In order to extend this analysis beyond the static exchange approximation, we need to include correlation in the wave function, via an explicit dependence on $\cos\theta_{12}$. Eventually we plan to include excitation channels in order to obtain the inelastic cross sections.

ACKNOWLEDGMENTS

I am deeply indebted to Aaron, Dick and Anand for all their guidance and encouragement over the past two decades. I never hesitated to ask them questions, and they never hesitated to provide the answers. I have learned atomic physics from the masters.

REFERENCES

[1] K. J. Bathe, *Finite Element Procedures in Engineering Analysis* (Prentice-Hall, Englewood Cliffs, 1982).

[2] W.K. Ford and F.S. Levin, Phys. Rev. A **29**, 43 (1984); F.S. Levin and J. Shertzer, Phys. Rev. A **32**, 3285 (1985); Phys. Rev. Lett. **61**, 1089 (1988); R. Kozack and F.S. Levin, Phys. Rev. C **36**, 883 (1987).

[3] J. Ackermann and J. Shertzer, Phys. Rev. A **54**, 365 (1996); J.F. Babb and Shertzer, Chem. Phys. Letts. **189**, 287 (1992).

[4] J. Shertzer, Phys. Rev. A **39**, 3833 (1989); J. Shertzer, A. Chandler, and M. Gavrila, Phys. Rev. Lett. **73**, 2039 (1994); J. Ackermann, J. Shertzer, and P. Schmelcher, Phys. Rev. Letts. **78**, 199 (1997).

[5] J. Botero and J. Shertzer, Phys. Rev. A **46**, R1155 (1992); J. Shertzer and J. Botero, Phys. Rev. A **49**, 3673 (1994).

[6] R. J. Drachman, Phys. Rev. A **26**, 1228 (1982); **31**, 1253 (1985); **33**, 2780 (1986); **37**, 979 (1988); **47**, 694 (1993).

[7] R. J. Drachman, Phys. Rev. A **46**, 5389 (1992); **51**, 2926 (1995); **55**, 1842 (1997).

[8] W.G. Sturrus, E.A. Hessels, P.W. Arcuni, and S.R. Lundeen, Phys. Rev. **38**, 135 (1988); **44**, 3032 (1991); P.L. Jacobson, D.S. Fisher, C.W. Fehrenback, W.G. Sturrus, and S.R. Lundeen, Phys. Rev. A **56**, R4361 (1997); **57,** 4065(E) (1998).

[9] A.K. Bhatia and R.J. Drachman, Phys. Rev. A **59**, 205 (1999).

[10] A. Temkin, Phys. Rev. **107**, 1004 (1957); A. Temkin and C.J. Lamkin, Phys. Rev. **121,** 788 (1961).

[11] A. Temkin, Phys. Rev. A **126**, 130 (1962); R. Poet, J. Phys. B **11,** 3081 (1978).

[12] D.M. Bishop and B. Lam, Mol. Phys. **65,** 679 (1988).

[13] J. Shertzer and C.H. Greene, Phys. Rev. A **58,** 1082 (1998).

[14] J.M. Taylor, A. Dalgarno, and J.F. Babb, Phys. Rev. A **60,** R2630 (1999).

[15] R.E. Moss, Chem. Phys. Lett. **311**, 231 (1999).

[16] P.L. Jacobson, R.A. Komara, W.G. Sturrus, and S.R. Lundeen, Phys. Rev. A **62**, 012509 (2000).

[17] V.I. Korobov, Phys. Rev. A **63**, 044501 (2001).

[18] L. Hilico, N. Billy, B. Gremaud, and D. Delande, J. Phys. B **34**, 491 (2001).

[19] Z.C. Yan, J.Y. Zhang, and Y. Li, Phys. Rev. A **67,** 062504 (2003).

[20] J. Shertzer and A. Temkin, Phys. Rev. A **63**, 062714-1 (2001); Phys. Rev. A **70**, 042710-1 (2004).

[21] Anand Bhatia, private communication.

GENERAL FORMS OF WAVE FUNCTIONS FOR DIPOSITRONIUM, Ps_2

D. M. Schrader

Marquette University

ABSRACT

The consequences of particle interchange symmetry for the structure of wave functions of the states of dipositronium was recently discussed by the author [1]. In the present work, the methodology is simply explained, and the wave functions are explicitly given.

INTRODUCTION

Dipositronium and higher aggregrates of positronium are the most symmetrical of all molecules. The symmetry operations that commute with the Hamiltonian include electron interchange and positron interchange as required by the Pauli exclusion principal, as well as electron-positron interchange, which is closely related to the concept of charge conjugation. Other commuting operators include those for spatial inversion and for spin and orbital angular momentum. The first complete and correct treatment of the influence of these operators on the structure of the wave functions was recently given by the author [1]. In that work, arguments for the methods used were given extremely succinctly owing to space limitations; here we explain the methods fully and clearly, and we give all the wave functions explicitly.

Charge conjugation means reversal of the charges for all particles. The Hamiltonian and the wave functions are invariant to this operation. For positronium, Ps, charge conjugation is equivalent to interchanging the electron and positron. In terms of the wave function, we affect this by inverting the spatial coordinates and exchanging the spin coordinates. The parities of these operations in terms of angular momentum quantum numbers are l and $s + 1$, respectively. The eigenvalue for electron-positron interchange, which we call "r," is thus $(-1)^{l+s+1}$. Electrons and positrons have opposite intrinsic parities [2], so their interchange gives another factor of (-1). The charge conjugation parity C is thus $-r$ for Ps in all its states.

That $(-1)^{l+s} = C$ for Ps is a geometrical coincidence – the positions of the two particles and their center of mass happen to be collinear. For Ps_2 the situation is quite different: charge conjugation is still equivalent to electron-positron interchange, but the latter is not expressed in the wave function by coordinate inversion. Thus, for Ps_2, we can no longer relate angular momentum quantum numbers to charge conjugation parity. Electron-positron interchange involves the interchange of both the electrons, each with either positron, thus introducing one more factor of (-1); thus we assume that $C = r$ for the states of Ps_2. Since photons have intrinsic charge conjugation parity -1, C can also be written as $(-1)^n$, where n is the number of photons issued in the complete annihilation of the system. This is true for both Ps and Ps_2 in all their states.

GROUP THEORY AND THE SYMMETRY OF WAVE FUNCTIONS OF Ps_2

Kinghorn and Poshusta [3] were first to use abstract group theory to study the structure of Ps_2 wave functions. They realized that the wave functions of Ps_2 must transform as irreducible representations of some group. They observed that the two operators for the like-particle interchange, the two for the antiparticle interchange operators, and their combinations together with the identity operator constitute a group that is isomorphic with the point group D_{2d}. They used this group to guide the construction of spatial factors of the wave functions while ignoring the role of spin in symmetry considerations. Some errors resulted from this procedure.

D_{2d} is a prime group. Since the three interchange operators are mutually independent and commuting, we believe that the group controlling the symmetry of wave functions is the direct product of three subgroups, those for electron interchange, positron interchange, and electron-positron interchange. Therefore the correct group is not prime. This is the idea that underlies the present work.

It should be understood that Ps_2, as Ps, is an atom, and as such it belongs to the full rotation point group as well.

Conventions of Group Theory and Wave Function Nomenclature

To proceed, we need to refine our concepts of points and particles. We consider a 4-dimensional space for each particle: three dimensions for ordinary space and one for spin. Spin space consists of two discrete points, which are variously called "±1/2," "↑" and "↓," or "α" and "β." We consider four points placed arbitrarily in this 4D space, labeled *a, b, c,* and *d.* We label our particles 1, 2, 3, and 4. There are 4! distinct arrangements of our four particles on these four points. One such arrangement is: 1 on *a,* 2 on *b*, 3 on *c*, and 4 on *d*. We call this the "reference configuration."

There are two distinct types of particle interchange operators, those that interchange two specified particles regardless of which points they are on [4], and those that interchange any particles that are on two specified points [5]. Each type gives rise to a group theory of its own "flavor." The two flavors, or conventions, due to Bunker [4] and Wigner [5], respectively, are equally valid and useful, and differ only in bookkeeping details. Usually, one need not even be aware which convention one is working with, but in the present case the distinction is crucial, owing to traditional practices of wave function nomenclature.

3D wave functions are often denoted by Greek letters, sometimes with a subscript to indicate the state involved, for example, φ_{1s}. The particle of interest and the point in space where the function sits the may be indicated by subscripts on the function's argument, which is a vector in 3D space: $\varphi_{1s}(\boldsymbol{r}_{2b})$. In contrast, the symbols α and β, commonly but incorrectly called "spin functions," are in fact not functions but rather the names of points in 1D spin-space, as noted above. The complete 4D wave function for particle 2 in a *1s*-orbital centered on point *b* with spin "up" is: $\varphi_{1s}(\boldsymbol{r}_{2b})\alpha(2)$. It is important to note the mixed usage of the Greek letters: One defines a function in 3D space; the other, a point in 1D spin-space. When performing particle interchange operations in 4D space, one must be aware of this difference, else one will mix the two conventions of group theory, and errors will result.

In essence, we must devise interchange operators of mixed conventions in order to complement the mixed conventions of traditional wave function nomenclature. Properly done, this will give us operators that faithfully represent particle interchanges, and will provide us with a factorable group for the structure of wave functions of Ps_2.

Each of the four particles of Ps_2 can have either of two spins, so the total number of spin functions is $2^4 = 16$. The number of spin states must be the number that have $M = 0$, which is $\binom{4}{2} = 6$. The group we seek has order 8 since it is the direct product of three subgroups each of order 2.

Particle Interchange Operators

We find that the following definitions conform to the distinction between the two conventions of group theory, and yield a factorable group that governs the structure of wave functions for the states of Ps_2: We define interchange operators of the Bunker-type [4] ($\hat{P}_{12}$, $\hat{P}_{13}$, etc.) and of the Wigner-type [5] ($\hat{Q}_{ab}$, $\hat{Q}_{bd}$, etc.), and two operators that accommodate the nomenclature conventions for wave functions. For the interchange of identical particles μ and ν,

$$\hat{R}_{\mu\nu} = \hat{P}^{(3D)}_{\mu\nu}\,\hat{Q}^{(spin)}_{[\mu][\nu]} \tag{1}$$

for the interchange of antiparticles,

$$\hat{S}_{ep} = \hat{Q}^{(3D)}_{[\mu][\eta]}\,\hat{P}^{(spin)}_{\mu\eta} \times \hat{Q}^{(3D)}_{[\lambda][\nu]}\,\hat{P}^{(spin)}_{\lambda\nu} \tag{2}$$

Particle numbers inside square brackets denote the points occupied by the indicated particles in the reference configuration. The desired group is $\{\hat{E},\hat{R}_{\mu\nu}\}\otimes\{\hat{E},\hat{R}_{\lambda\eta}\}\otimes\{\hat{E},\hat{S}_{ep}\}$, which is isomorphous with D_{2h}.

A 4D function of any specified symmetry can be projected from an unsymmetrical function by the application of:

$$\hat{T}_{pqr} = (1 + r\hat{S}_{ep})(1 + q\hat{R}_{\lambda\eta})(1 + p\hat{R}_{\mu\nu}) \tag{3}$$

The symmetry numbers (p,q,r) designate the irreducible representations of D_{2h}. For the states of Ps_2, $p = q = -1$, and $r = C$.

The utility of the group D_{2h} is principally that it requires us to correctly craft the interchange operators. We have done this immediately above, and now we turn to the more pedestrian task of deducing resulting general forms for the wave functions. We can do this with only tangential reference to the underlying group theory.

SPIN DEPENDENCE OF THE WAVE FUNCTIONS

Molecular hydrogen has two pairs of particles, and the non-identical particles are not related by interchange operators. Consequently, wave functions for its states are factorable into 3D and spin-dependent parts. For Ps_2, however, the two types of particles are related by an interchange operator, and factorability of its wave functions may no longer be possible for all states. For states with factorable wave functions, each of the symmetry quantum numbers is likewise factorable: $r = r^{(spin)}r^{(3D)}$, and similarly for p and q. In the interest of clarity, we first seek factorable wave functions as we proceed to the spin coupling problem.

We must first consider two distinct schemes for spin coupling: one that first couples identical particles, then couples electron pairs with positron pairs; and another that first couples electron-positron pairs into Ps-like two-particle functions, then couples these. We denote the first scheme as $(e,e';p,p')$, and the second, $(e,p;e',p')$. We indicate spin functions of the latter scheme with tildes. In both schemes, 1 and 2 denote electrons, and 3 and 4, positrons.

Systems of two particles have four spin functions, a singlet and a set of triplets. In terms of the one-electron spin functions α and β, the triplet functions are:

$$\begin{aligned}\sigma_{11}(1,2) &= \alpha(1)\alpha(2)\\ \sigma_{10}(1,2) &= \tfrac{1}{\sqrt{2}}\big(\alpha(1)\beta(2) + \beta(1)\alpha(2)\big)\\ \sigma_{1-1}(1,2) &= \beta(1)\beta(2)\end{aligned} \tag{4}$$

and the singlet:

$$\sigma_{00}(1,2) = \tfrac{1}{\sqrt{2}}\big(\alpha(1)\beta(2) - \beta(1)\alpha(2)\big) \tag{5}$$

The subscripts are the spin quantum numbers s and m. For positronium-like functions, the singlet function, for example, would be:

$$\tilde{\sigma}_{00}(1,3) = \tfrac{1}{\sqrt{2}}\big(\alpha(1)\beta(3) - \beta(1)\alpha(3)\big) \tag{$\tilde{5}$}$$

Hereafter, we suppress particle labels for simplicity, and rely on tildes or their absence to indicate antiparticle or particle pairs, respectively. Quantum numbers for the two-particle spin functions are given in Table 1.

Spin functions for Ps_2 in the $(e,e';p,p')$-scheme are now given. Functions in the $(e,p;e',p')$-scheme are gotten simply by inserting tildes over all spin functions. For $S = 2$,

$$\begin{aligned}
\Gamma_{22} &= \sigma_{11}\sigma_{11} \\
\Gamma_{21} &= \tfrac{1}{\sqrt{2}}(\sigma_{11}\sigma_{10} + \sigma_{10}\sigma_{11}) \\
\Gamma_{20} &= \tfrac{1}{\sqrt{6}}(\sigma_{11}\sigma_{1-1} + 2\sigma_{10}\sigma_{10} + \sigma_{1-1}\sigma_{11}) \\
\Gamma_{2-1} &= \tfrac{1}{\sqrt{2}}(\sigma_{10}\sigma_{1-1} + \sigma_{1-1}\sigma_{10}) \\
\Gamma_{2-2} &= \sigma_{1-1}\sigma_{1-1}
\end{aligned} \tag{6}$$

Four more wave functions can be expressed in terms of σ_{1m}. For $S = 1$,

$$\begin{aligned}
\Gamma_{11} &= \tfrac{1}{\sqrt{2}}(\sigma_{11}\sigma_{10} - \sigma_{10}\sigma_{11}) \\
\Gamma_{10} &= \tfrac{1}{\sqrt{2}}(\sigma_{11}\sigma_{1-1} - \sigma_{1-1}\sigma_{11}) \\
\Gamma_{1-1} &= \tfrac{1}{\sqrt{2}}(\sigma_{10}\sigma_{1-1} - \sigma_{1-1}\sigma_{10})
\end{aligned} \tag{7}$$

and for $S = 0$,

$$\Gamma_{00} = \tfrac{1}{\sqrt{3}}(\sigma_{11}\sigma_{1-1} - \sigma_{10}\sigma_{10} + \sigma_{1-1}\sigma_{11}) \tag{8}$$

From σ_{1m} and σ_{00} we can write:

$$\begin{aligned}
\Gamma^{g}_{11} &= \tfrac{1}{\sqrt{2}}(\sigma_{11}\sigma_{00} + \sigma_{00}\sigma_{11}) \\
\Gamma^{g}_{10} &= \tfrac{1}{\sqrt{2}}(\sigma_{10}\sigma_{00} + \sigma_{00}\sigma_{10}) \\
\Gamma^{g}_{1-1} &= \tfrac{1}{\sqrt{2}}(\sigma_{1-1}\sigma_{00} + \sigma_{00}\sigma_{1-1})
\end{aligned} \tag{9}$$

and

$$\begin{aligned}
\Gamma^{u}_{11} &= \tfrac{1}{\sqrt{2}}(\sigma_{11}\sigma_{00} - \sigma_{00}\sigma_{11}) \\
\Gamma^{u}_{10} &= \tfrac{1}{\sqrt{2}}(\sigma_{10}\sigma_{00} - \sigma_{00}\sigma_{10}) \\
\Gamma^{u}_{1-1} &= \tfrac{1}{\sqrt{2}}(\sigma_{1-1}\sigma_{00} - \sigma_{00}\sigma_{1-1})
\end{aligned} \tag{10}$$

Finally:

$$\Gamma'_{00} = \sigma_{00}\sigma_{00} \tag{11}$$

Platzman and Mills [6] used the $(e,p;e',p')$-scheme, and denoted their spin functions as $|S,C,P\rangle$, where *"P"* indicates "parity." The relationships between the spin functions as expressed in the two schemes are significant for us, and are displayed in Table 2, from which the quantum numbers for the states of Ps_2 can be easily deduced: From Table 2, the quantum numbers $p^{(\text{spin})}$ and $q^{(\text{spin})}$ are read from the left hand side, and $r^{(\text{spin})}$ from either. $p = p^{(\text{spin})}p^{(3D)} = -1$ gives $p^{(3D)}$ and similarly for q. $r^{(3D)}$ is independent of the other symmetry numbers and apparently can be either ± 1. The relationships $C = r = r^{(\text{spin})}r^{(3D)} = (-1)^n$ yields n, the number of photons required for complete annihilation. Evidently n can be any non-negative integer. Its value determines that of $r^{(3D)}$, or *vice versa.* These quantum numbers are collected in Table 3.

3D DEPENDENCE OF THE WAVE FUNCTIONS

Table 3 shows that, of the six spin functions, four have a complete set of the symmetry numbers (p,q,r), and therefore qualify as the spin functions of factorable wave functions. For these four functions, general forms of the 3D factors can be written down at once. For the remaining two, the problem is more complicated.

Factorable Cases

A suitable 3D factor $\mathcal{F}_{pqr}$ is gotten by projecting from an unsymmetrical function of the four 3D coordinates f with the desired values of the symmetry numbers (see eq. (3)):

$$\mathcal{F}_{pqr}(\vec{r}_1,\vec{r}_2,\vec{r}_3,\vec{r}_4) = \hat{T}_{pqr} f(\vec{r}_1,\vec{r}_2,\vec{r}_3,\vec{r}_4) \tag{12}$$

This is the sum of eight terms, and it can be expressed as the product of the row matrix

$$[1\ p\ q\ pq\ \ r\ pr\ qr\ pqr] \tag{13}$$

and the column matrix

$$[f(1234)\ f(2134)\ f(1243)\ f(2143)\ \ f(3412)\ f(3421)\ f(4312)\ f(4321)]^{\mathrm{T}} \tag{14}$$

For simplicity, we omit all characters in the arguments of f except particle numbers. We further simplify by omitted the column matrix altogether hereafter since it is the same for all states, and designate each wave function by only its row matrix (13). This we can write succinctly by indicating only signs. For example, for the 3D partner of the spin function Γ_{20} (see Table 3), $\mathcal{F}_{--r} \equiv \mathcal{F}_{--C}$, is indicated as:

$$[+--+\ \ r\ -r\ -r\ r] \equiv [+--+\ \ C\ -C\ -C\ C] \tag{15}$$

The four factorable wave functions are:

$$\begin{aligned} \Psi^{(1)}_{\Lambda C} &= \mathcal{F}_{--C}\,\Gamma_{2M} \\ \Psi^{(2)}_{\Lambda C} &= \mathcal{F}_{--C}\,\Gamma_{1M} \\ \Psi^{(3)}_{\Lambda C} &= \mathcal{F}_{--C}\,\Gamma_{00} \\ \Psi^{(4)}_{\Lambda C} &= \mathcal{F}_{++C}\,\Gamma'_{00} \end{aligned} \tag{16}$$

Λ denotes the angular momentum quantum numbers, and superscripts, the states. It is clear that the first three states are degenerate except for small spin-spin and spin-orbit interactions, which is reminiscent of the states of Ps.

Non-factorable Cases

The fourth function in Table 3, $\Gamma^g_{10} \equiv \tilde{\Gamma}_{10}$, and the fifth, $\Gamma^u_{10} \equiv \tilde{\Gamma}^u_{10}$, are clearly not candidates for being parts of factorable wave functions, for the like-particle interchange operators interchange the functions as well as the particles; *e.g.*,

$$\hat{R}_{12}\Gamma^u_{10} = \Gamma^g_{10} \tag{17}$$

We resort to a simple, direct tactic: we project from some unsymmetrical 4D function, say $f(1234)\sigma_{10}\sigma_{00}$, using the operator in eq. (3) with $p = q = -1$ and $r = C$. We arrive at a suitable expression for the wave function:

$$[+-+-\ \ 0000]\sigma_{10}\sigma_{00} + [0000\ \ C(+-+-)]\sigma_{00}\sigma_{10} \tag{18}$$

We could just as well project from $f(1234)\sigma_{00}\sigma_{10}$, giving:

$$[++--\ \ 0000]\sigma_{00}\sigma_{10} + [0000\ \ C(++--)]\sigma_{10}\sigma_{00} \tag{19}$$

These two functions are clearly independent and equally valid. We take a linear combination of them:

$$[a(+-+-)\ \ bC(++--)]\sigma_{10}\sigma_{00} + [b(++--)\ aC(+-+-)]\sigma_{00}\sigma_{10} \tag{20}$$

where a and b are disposable. We subject them to the constraint $|a|^2+|b|^2 = 1$ to preserve normalization. Perhaps these parameters will be determined by energy minimization, or to avoid a contradiction for a given value of C. In any case, we denote the expression (20) as $\Psi^{(5,6)}_{\Lambda C}(a_C, b_C)$, and write the last two wave functions as

$$\Psi^{(5)}_{\Lambda+}(a_+,b_+)$$
$$\Psi^{(6)}_{\Lambda-}(a_-,b_-) \qquad (21)$$

We see that the 3D and spin factors of these wave functions do not conform to any irreducible representation of the D_{2h} group, but that the overall functions do.

CONCLUSION

In this note we give general forms of the wave functions of Ps_2. Still to be considered are: orbital angular momentum, annihilation rates, asymptotic forms, and computational strategies.

REFERENCES

1. D. M. Schrader, Phys. Rev. Lett. **92**, 043401 (2004).
2. P. A. M. Dirac, Proc. Camb. Phil. Soc. **26**, 361 (1930).
3. For example, D. B. Kinghorn and R. D. Poshusta, Phys. Rev. A **47**, 3671 (1993).
4. P. R. Bunker and P. Jensen, *Molecular Symmetry and Spectroscopy* (NRC Research Press, Ottawa, 1998).
5. E. P. Wigner, *Group Theory* (Pure and Applied Physics **5**, Academic Press, New York, 1959).
6. P. M. Platzman and A. P. Mills, Jr., Phys. Rev. B **49**, 454 (1994).

Table 1. Quantum numbers for two-particle spin functions; identical particles on top, antiparticles on the bottom.

Spin functions	$p^{(\mathrm{spin})}$	$p^{(\mathrm{3D})}$	Intrinsic parity	$r^{(\mathrm{spin})}$	$r^{(\mathrm{3D})}$	C
σ_{00}	−1	1	1			
σ_{1m}	1	−1	1			
$\tilde{\sigma}_{00}$			−1	−1	$(-1)^l$	$(-1)^l$
$\tilde{\sigma}_{1m}$			−1	1	$(-1)^l$	$(-1)^{l+1}$

Table 2. Spin functions of the present work (left side) and the corresponding functions of Platzman and Mills [6] (right side, $|SCP\rangle$; these authors give expressions only for the two $|0{+}{+}\rangle$ states). For clarity, only functions with $M = 0$ are shown.

1,2,3,4 = *e,e′,p,p′*	1,2,3,4 = *e,p,e′,p′*
$\Gamma_{20} = \frac{1}{\sqrt{6}}(\sigma_{11}\sigma_{1-1} + 2\sigma_{10}\sigma_{10} + \sigma_{1-1}\sigma_{11})$	$\tilde{\Gamma}_{20} = \lvert 2{+}{+}\rangle = \frac{1}{\sqrt{6}}(\tilde{\sigma}_{11}\tilde{\sigma}_{1-1} + 2\tilde{\sigma}_{10}\tilde{\sigma}_{10} + \tilde{\sigma}_{1-1}\tilde{\sigma}_{11})$
$\Gamma_{10} = \frac{1}{\sqrt{2}}(\sigma_{11}\sigma_{1-1} - \sigma_{1-1}\sigma_{11})$	$\tilde{\Gamma}^{g}_{10} = \lvert 1{-}{-}\rangle = \frac{1}{\sqrt{2}}(\tilde{\sigma}_{10}\tilde{\sigma}_{00} + \tilde{\sigma}_{00}\tilde{\sigma}_{10})$
$\Gamma_{00} = \frac{1}{\sqrt{3}}(\sigma_{11}\sigma_{1-1} - \sigma_{10}\sigma_{10} + \sigma_{1-1}\sigma_{11})$	$-\frac{1}{2}\tilde{\Gamma}_{00} + \frac{\sqrt{3}}{2}\tilde{\Gamma}'_{00} = -\frac{1}{2}\lvert 0{+}{+}\rangle_t + \frac{\sqrt{3}}{2}\lvert 0{+}{+}\rangle_s$ $= -\frac{1}{2\sqrt{3}}(\tilde{\sigma}_{11}\tilde{\sigma}_{1-1} - \tilde{\sigma}_{10}\tilde{\sigma}_{10} + \tilde{\sigma}_{1-1}\tilde{\sigma}_{11} - 3\tilde{\sigma}_{00}\tilde{\sigma}_{00})$
$\Gamma^{g}_{10} = \frac{1}{\sqrt{2}}(\sigma_{10}\sigma_{00} + \sigma_{00}\sigma_{10})$	$\tilde{\Gamma}_{10} = \lvert 1{+}{-}\rangle = \frac{1}{\sqrt{2}}(\tilde{\sigma}_{11}\tilde{\sigma}_{1-1} - \tilde{\sigma}_{1-1}\tilde{\sigma}_{11})$
$\Gamma^{u}_{10} = \frac{1}{\sqrt{2}}(\sigma_{10}\sigma_{00} - \sigma_{00}\sigma_{10})$	$\tilde{\Gamma}^{u}_{10} = \lvert 1{-}{+}\rangle = \frac{1}{\sqrt{2}}(\tilde{\sigma}_{10}\tilde{\sigma}_{00} - \tilde{\sigma}_{00}\tilde{\sigma}_{10})$
$\Gamma'_{00} = \sigma_{00}\sigma_{00}$	$\frac{\sqrt{3}}{2}\tilde{\Gamma}_{00} + \frac{1}{2}\tilde{\Gamma}'_{00} = \frac{\sqrt{3}}{2}\lvert 0{+}{+}\rangle_t + \frac{1}{2}\lvert 0{+}{+}\rangle_s$ $= \frac{1}{2}(\tilde{\sigma}_{11}\tilde{\sigma}_{1-1} - \tilde{\sigma}_{10}\tilde{\sigma}_{10} + \tilde{\sigma}_{1-1}\tilde{\sigma}_{11} + \tilde{\sigma}_{00}\tilde{\sigma}_{00})$
$-\frac{1}{2}\Gamma_{00} + \frac{\sqrt{3}}{2}\Gamma'_{00} = -\frac{1}{2\sqrt{3}}(\sigma_{11}\sigma_{1-1} - \sigma_{10}\sigma_{10} + \sigma_{1-1}\sigma_{11} - 3\sigma_{00}\sigma_{00})$	$\tilde{\Gamma}_{00} = \lvert 0{+}{+}\rangle_t = \frac{1}{\sqrt{3}}(\tilde{\sigma}_{11}\tilde{\sigma}_{1-1} - \tilde{\sigma}_{10}\tilde{\sigma}_{10} + \tilde{\sigma}_{1-1}\tilde{\sigma}_{11})$
$\frac{\sqrt{3}}{2}\Gamma_{00} + \frac{1}{2}\Gamma'_{00} = \frac{1}{2}(\sigma_{11}\sigma_{1-1} - \sigma_{10}\sigma_{10} + \sigma_{1-1}\sigma_{11} + \sigma_{00}\sigma_{00})$	$\tilde{\Gamma}'_{00} = \lvert 0{+}{+}\rangle_s = \tilde{\sigma}_{00}\tilde{\sigma}_{00}$

Table 3. Quantum numbers associated with the spin functions of Ps_2.

Spin functions	$p^{(\mathrm{spin})}$	$q^{(\mathrm{spin})}$	$r^{(\mathrm{spin})}$	$p^{(3D)}$	$q^{(3D)}$	$r^{(3D)}$	Intrinsic parity	C
$\Gamma_{20}, \tilde{\Gamma}_{20}$	1	1	1	−1	−1	±1	1	±1
$\Gamma_{10}, \tilde{\Gamma}'_{10}$	1	1	−1	−1	−1	±1	1	∓1
Γ_{00}	1	1	1	−1	−1	±1	1	±1
$\Gamma^g_{10}, \tilde{\Gamma}_{10}$	$\Gamma^u_{10}, \tilde{\Gamma}^u_{10}$	$-\Gamma^u_{10}, \tilde{\Gamma}^u_{10}$	1			±1	1	±1
$\Gamma^u_{10}, \tilde{\Gamma}^u_{10}$	$\Gamma^g_{10}, \tilde{\Gamma}_{10}$	$-\Gamma^g_{10}, \tilde{\Gamma}_{10}$	−1			±1	1	∓1
Γ'_{00}	−1	−1	1	1	1	±1	1	±1
$\tilde{\Gamma}_{00}$			1			±1	1	±1
$\tilde{\Gamma}'_{00}$			1			±1	1	±1

DOUBLY EXCITED RESONANCES IN THE POSITRONIUM NEGATIVE ION

Y. K. Ho
Institute of Atomic and Molecular Sciences, Academia Sinica, Taiwan, ROC

ABSTRACT

The recent theoretical studies on the doubly excited states of the Ps^- ion are described. The results obtained by using the method of complex coordinate rotation show that the three-lepton system behaves very much like an XYX tri-atomic molecule. Furthermore, the recent investigation on the positronium negative ion embedded in Debye plasma environments is discussed. The problem is modeled by the use of a screened Coulomb potential to represent the interaction between the charge particles.

INTRODUCTION

This paper describes some of the recent research activities on the doubly excited states of the positronium negative ion. The positronium negative ion, Ps^-, is a three-lepton system consists of two electrons and a positron, and interacting with Coulomb potential. Theoretical calculations of the ground state energy of Ps^- have a long history ever since the early work of Wheeler [1]. Activities have been intensified due to, in part, the discovery of such a system by Mills [2], and his measurement of its annihilation rate [3]. The earlier activities on this system have been summarized and discussed in several reviews and papers [4-8]. The present paper reviews the activities starting, for the most part, from the early 1990s. Since that time, precision calculations on the ground state energy of Ps^- have started. Most of the calculations on the non-relativistic ground state energy have achieved accuracy with uncertainty to within 10^{-10} a.u. These include calculations using the Hylleraas basis by Bhatia and Drachman [9] and by Ho [10] with the latter that employed a double sum for the Hylleraas expansions. Other groups have also calculated the ground state energy of Ps^-. These include Ackemann and Shertzer [11] who used a finite-element method, Krivec *et al* [12] used a stochastic variational method, Korobov [13] used a variational method, Frolov and Smith [14] used a variation method with exponential variational expansions, and Drake and co-workers used a variational method with multi-sum Hylleraas basis [15]. Two very recent works --- Drake *et al* used a triple-sum Hylleraas basis [16] and Frolov used an extensive exponential variational expansion [17] --- have obtained accuracy for the non-relativistic ground state energy with uncertainty to within 10^{-20} a. u..

From the experimental side, the Ps^- ion was first observed by Mills [2] in 1981. Very recently, progress has been reported in some new experiments to investigate this system. A group from FRM II in Munich, Germany, has tried to improve the measurement on the annihilation rate of the Ps^- ion [18]. Another group in Aarhus Positron Facility, Denmark, has planned a series of measurements to study such a system [19]. A proposal in their agenda is to determine the binding energy of this ion. Also, a recent experimental development [20] in positron trapping and accumulation technology has opened up the door to study various properties of atomic systems involving positrons and positronium atoms. For a related system that consists of only leptons, the positronium molecule Ps_2 might have been produced in laboratory by Mills and co-workers [21]. All these experimental activities enhance the motivation for theoretical investigations of this pure-lepton system. Another interesting aspect of this system is the calculations of photo-detachment cross sections that have been carried out by several groups

(Bhatia and Drachman [22], Ward, Humberston and McDowell [23], Frolov [24], and Maniadaki, Nikolopoulos, and Lambropoulos [25]). Accurate photo-detachment cross sections would help experimental determination for the binding energy of the Ps^- ion.

The positronium negative ion in many aspects is very similar to its counter-part of hydrogen negative ion. They both have only one bound state, the $1s^2\ ^1S^e$ state, denoted by the usual spectroscopic notation. Many years ago, Drake [26] and Bhatia [27] have calculated the $2p^2\ ^3P^e$ state as a meta-stable state lying below the H (N=2) threshold. A natural question for Ps^- was raised that should there be a similar $2p^2\ ^3P^e$ meta-stable state lying below the Ps (N=2) threshold. Mills [28], and Bhatia and Drachman [29] have addressed such a question and concluded that due to the mass effect, the $2p^2\ ^3P^e$ state could not form binding lying below the Ps (N=2) threshold. Using the hyperspherical coordinates, Botero [30] calculated this state as a shape resonance immediately lying above the Ps (N=2) threshold. Bhatia and Ho [31] using the method of complex-coordinate rotation and employing highly correlated Hylleraas basis have determined the energy and width for the $2p^2\ ^3P^e$ shape resonance of Ps^-. In the following the complex-coordinate rotation method will be briefly described, and the applications of this method in calculations of high-lying doubly excited states of the Ps^- ion with differ angular momentum are discussed.

RESONANCE CALCULATIONS

The first theoretical investigation [32] of the resonances in Ps^- was reported in 1979 in which the $2s^2\ ^1S^e$ and $3s^2\ ^1S^e$ resonances were calculated using the method of complex-coordinate rotation [33]. For illustrative purpose, the work is briefly described here. The Hamiltonian of Ps^- is

$$\hat{H} = \hat{T} + \hat{V}, \tag{1}$$

with

$$\hat{T} = -\frac{1}{m_1}\nabla_1^2 - \frac{1}{m_2}\nabla_2^2 - \frac{1}{m_p}\nabla_p^2 \tag{2}$$

and

$$\hat{V} = -\frac{2}{r_{1p}} - \frac{2}{r_{2p}} - \frac{2}{r_{12}} \tag{3}$$

where 1, 2, and p denote the electrons 1,2, and the positron, respectively. The mass for particle i is m_i; and r_{ij} represents the distance between particles i and j. For $^{1,3}S^e$ states, wave functions of Hylleraas-type were used with the form

$$\Phi = \sum_{k\,\mathrm{ln}} C_{k\,\mathrm{ln}} \exp[-\alpha(r_{1p} + r_{2p})] r_{12}^n (r_{1p}^k r_{2p}^l \pm r_{1p}^l r_{2p}^k), \tag{4}$$

with $k+l+n \leqq \omega$, where ω, k, l, and n are positive integers or zero. In Eq. (4), the upper sign is for the singlet-spin states, and the lower sign for the triplet-spin states. Also, for the $^1S^e$ states, the summation indexes in Eq. (4) are $k \geqq l \geqq 0$ and $n \geqq 0$. For $^3S^e$ states, the indexes are $k > l \geqq 0$ and $n \geqq 0$. In the complex-rotation method [33], the radial coordinates are transformed by

$$r \rightarrow r\, e^{i\Theta} \tag{5}$$

and the transformed Hamiltonian becomes,

$$\hat{H}_\theta = \hat{T}\exp(-2i\theta) + \hat{V}\exp(-i\theta), \tag{6}$$

where $\hat{T}$ and $\hat{V}$ are the kinetic and the Coulomb part of the potential energies, respective, and

$$N_{ij} = \langle \psi_i | \psi_j \rangle \tag{7}$$

are the overlapping matrix elements

and $$H_{ij} = \langle \psi_i | H(\Theta) | \psi_j \rangle . \tag{8}$$

The complex eigenvalues problem can be solved with

$$\sum_i \sum_j C_{ij} \left(H_{ij} - E N_{ij} \right) = 0 \quad . \tag{9}$$

The complex resonance energy is given by

$$E_{res} = E_r - \frac{i\Gamma}{2}, \tag{10}$$

where E_r is related to the resonance energy and Γ the width.

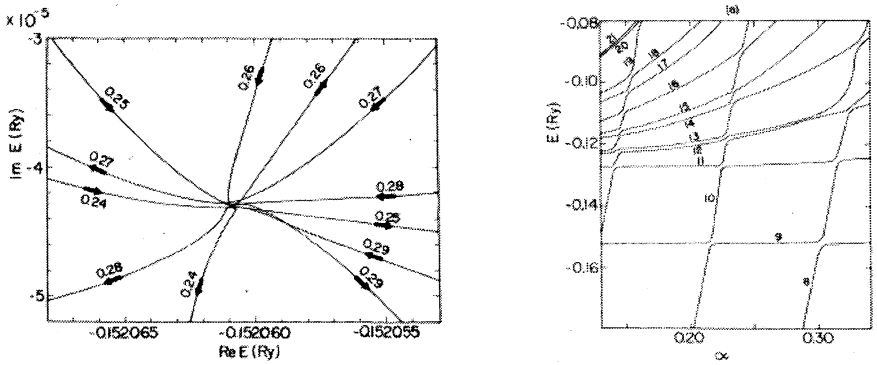

Fig.1. Lowest resonance $2s^2\ ^1S^e$ of Ps^- below the Ps (N=2) threshold (see Ref. [32]).

Fig. 1(a) shows the lowest resonance $2s^2\ ^1S^e$ state of Ps^- below the Ps (N=2) threshold obtained by using the method of complex-coordinate rotation (with 161 terms, ω=10). The arrow indicates the direction of the path coming from different directions for increasing rotational angle θ, as various non-linear parameters from the stabilization plateau (Fig. 1(b)) were used. The paths are nearly stationary for θ=0.2 to 0.35 rad when they come across the resonance position [32]. The recent theoretical calculations of some S-wave resonances in Ps^- included the calculations using the method of complex-coordinate rotation by Ho [34] with Hylleraas-type basis, by Usukura and Suzuki [35] with correlated Gaussians and stochastic variational method, and by Li and Shakeshaft [36] using the Pekeris-type basis wave functions. Several groups have also investigated the resonances in Ps^- from scattering approaches. These include the works by Basu and Ghosh [37] using the close coupling method, by Gilmore *et al* [38] using the pseudo-state close coupling approach, and by Igarashi and Shimamura [39] using the close coupling approximation in hyper-spherical coordinates. A different approach was carried out by Papp *et al* [40] to study the resonances in Ps^- using the Faddeev integral equations with Coulomb-Sturmian basis wave functions.

For angular momentum states with L=1 and L=2, Bhatia and Ho [31, 41] have obtained resonance energies and widths using the complex rotation method and employing correlated Hylleraas basis. For high-angular-momentum doubly excited states ($L \geqq 3$) as the two electrons are further apart, the products of Slater orbitals were used to construct the wave functions [42],

$$\begin{aligned} \Psi(\vec{r}_1, \vec{r}_2) = & \phi_{n_1 l_1}(r_1) \phi_{n_2 l_2}(r_2) Y^{L,M}_{l_1,l_2}(1,2) S(\sigma_1, \sigma_2) \\ & - \phi_{n_1 l_1}(r_2) \phi_{n_2 l_2}(r_1) Y^{L,M}_{l_1,l_2}(2,1) S(\sigma_2, \sigma_1) \end{aligned}, \tag{11}$$

with $$\phi_{nl}(r) = r^n \exp(-\xi_l r) \tag{12}$$

and $$Y^{L,M}_{l_1,l_2}(1,2) = \sum_{m_{l_1} m_{l_2}} C(l_1, l_2, L, m_{l_1}, m_{l_2}, M) Y_{l_1 m_1}(1) Y_{l_2 m_2}(2), \tag{13}$$

where the $Y_{l_2 m_2}$ etc., are the spherical harmonics. Ivanov and Ho [42] have calculated high-angular-momentum resonances with up to L=8 (L-states) and associated with the Ps (N=3, 4, and 5) thresholds. The results were used to construct supermultiplet structures of the doubly excited states of Ps^-.

From the available theoretical results [31, 41, 42], it is apparent that this ($e^- e^+ e^-$) three-body system behaves very much like a tri-atomic XYX molecule, as illustrated in Figs 2-6. Due to the vibrational character of such a molecule, the $^3P^e$ and $^1P^0$ states (see Fig. 2) that have the same "quantum numbers" would be nearly degenerate [43]. This indicates that both the $^3P^e$ and $^1P^o$ states in Ps^- are shape resonances. The rotational character of Ps^- implies that the $^1S^e$, $^3P^0$, and $^1D^e$ states having the same quantum numbers would belong to the same rotor series. In Figs 2-6, each state is classified by a set of quantum numbers *(K, T, N, n, L, S, π)* where *L, S, N, n,* and *π* have the usual spectroscopic meanings. The quantum numbers K and T are "approximately good" quantum numbers, and can be described briefly as follows: K is related to $<-\cos\theta_{12}>$, where θ_{12} represents the angle between the two electron vectors. The more positive the value of K, the closer the value of $<-\cos\theta_{12}>$ is to unity. The two electrons in this situation are located near the opposite sides of the position. The quantum number T describes the orientations between the orbitals of the two electrons. For example, a state with T=0 implies that the two electrons are moving on the same plane. The quantum numbers K and T hence describe the angular correlations between the two doubly excited electrons. States having the same KT quantum numbers, hence belonging to the same rotor series, are grouped together. For a given set of K, T, and N, the allowed L values for the doubly excited states are

$$L = T, T+1, \cdots\cdots, K+N-1. \tag{14}$$

The highest L value for a given [K, T] rotor series is therefore governed by the relationship $L_{(max)} = K + N - 1$. For example, when K=4 and N=5 (the [4, 0] series in Fig. 6) the highest L states is an L =8 state (the $^1L^e$ state). Also in Figs. 2-5, we use the results for the doubly excited intrashell states associated with the positronium N=2, N=3, N=4 and N=5 thresholds, respectively, to construct the I-supermultiplet structures [43]. The quantum number *"I"* is defined as

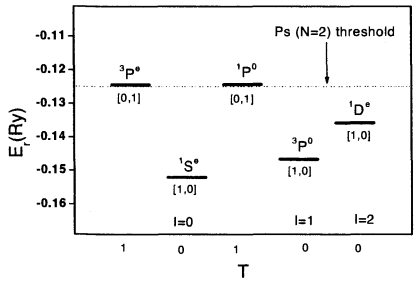

Fig.2. Supermultiplet structures of doubly excited intra-shell states associated with the N=2 Ps threshold. (see Ref. [41, 42]).

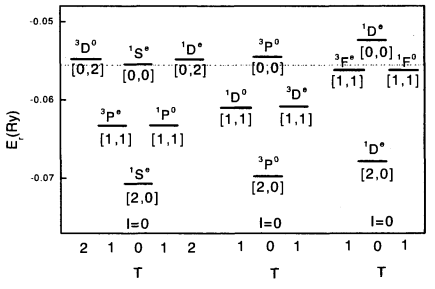

Fig. 3. Supermultiplet structures of doubly excited intra-shell states associated with the N=3 Ps threshold. (see Ref. [41, 42]).

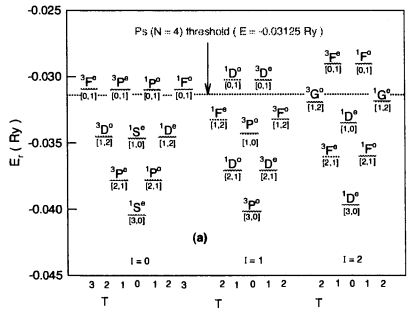

Fig. 4. Vibrational character of the spectra of the doubly excited intrashell states of Ps^- associated with the Ps (N=4) threshold, I values ranging from I=0 to I=2 [41, 42]

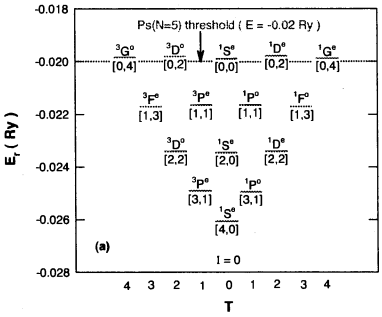

Fig. 5. Vibrational character of the spectra of the doubly excited intrashell states (I=0) of Ps^- associated with the Ps (N=5) threshold (see Ref. [42]).

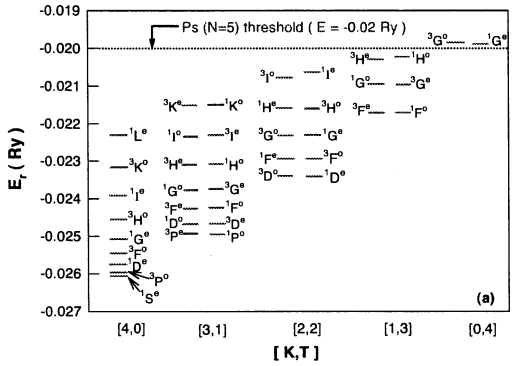

Fig. 6. Rotational character of the spectra of the doubly excited intrashell states of Ps^- associated with the Ps (N=5) threshold. (see Ref. [42]).

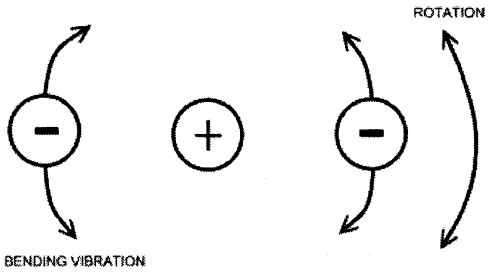

Fig. 7. Doubly excited Ps^- behaves like an XYX tri-atomic molecule.

$$I = L - T, \tag{15}$$

and has the same meaning as the ro-vibrational quantum number R used in molecular physics [43]. For example, states with I=0 are the ground states of various rotor series. From these figures, the vibrational characters of the "molecule" are evident, as shown here in Fig. 7 (Ref.[43, 44]). Other workers have also examined the "molecular" aspects of the positronium negative ion in the literature [45, 46].

In addition to the calculations of the resonance energies and widths for the doubly excited states, the electric-field effects on such states have also been investigated [47]. Fig. 8 shows the Stark effect on the positions of the $^1S^e(2)$ and $^1P^0(1)$ resonances as a function of the external electric field strength. As these two resonance states are nearly degenerate for the field-free case, they will repel each other when the external field is turned on.

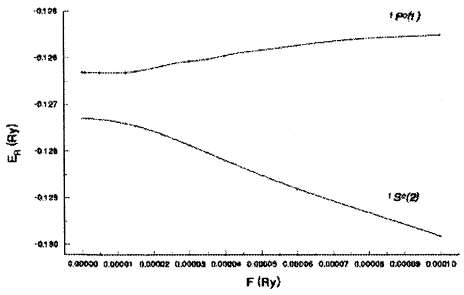

Fig. 8. Positions of the $^1S^e(2)$ and $^1P^0(1)$ resonances as a function of external electric field intensity (see Ref. [47]).

PLASMAS-EMBEDDED POSITRONIUM NEGATIVE IONS

Very recently, the Ps^- embedded in an external environment such as that of plasma has attracted some attention [48]. With the recent developments in laser plasmas produced by laser fusion in laboratories [49], and the continued interest of helium abundances in astrophysics plasmas [50], as well as the recent activities on cold plasmas, it is important to have accurate atomic data available in the literature for helium atoms in various plasma environments [51, 52]. In the Debye-Hückel model for plasmas, the interaction potential between two charge particles is represented by a Yukawa-type potential,

$$\phi(r_a, r_b) = Z_a Z_b \exp(-\mu|r_a - r_b|)/|\vec{r}_a - \vec{r}_b|, \tag{16}$$

where r_a and r_b represent respectively the spatial coordinates of particles A and B, and Z_a and Z_b denote their charges. The screening parameter μ is given as a function of the temperature T and the charge density n by $\mu = \sqrt{e^2 n/\varepsilon_0 k_B T}$ where n is given as the sum of the electron-density N_e and the ion density N_k of k^{th} ion species having the nuclear charge q_k as $n = N_e + \sum_k q_k^2 N_k$. For laser plasma conditions we have $T \sim 1$ keV, $n \sim 10^{22}$ cm^{-3}, and $\mu \sim 0.1$ to 0.2. Such conditions can now be achieved in the laboratories. The model is appropriate for "hot and dense" and "low-density and warm" plasmas [53, 54].

The non-relativistic Hamiltonian describing the three-lepton system (e^+, e^-, e^-) embedded in Debye plasmas characterized by the parameter D is given by

$$H = -\frac{1}{2}\nabla_1^2 - \frac{1}{2}\nabla_2^2 - \frac{1}{2}\nabla_3^2 - \frac{\exp(-r_{31}/D)}{r_{31}} - \frac{\exp(-r_{32}/D)}{r_{32}} + \frac{\exp(-r_{12}/D)}{r_{12}} \tag{17}$$

For the $^1S^e$ states of Ps^- ion, we have employed the wave function [55]

$$\Psi = (1 + P_{12}) \sum_{i=1}^{N} C_i \exp[(-\alpha_i r_{32} - \beta_i r_{31} - \gamma_i r_{21})\omega] \tag{18}$$

where ω is a scaling constant for calculations of resonances, and P_{12} is the permutation operator defined by $P_{12}f(r_{32},r_{31},r_{12}) = f(r_{31},r_{32},r_{12})$. We have used a quasi-random process to choose the non-linear variational parameters α_i, β_i and γ_i (see Ref. [56]). For the $^{1,3}P^o$ states of Ps^-, we have employed the wave functions [57]

$$\Psi = (1 + S_{pn}P_{12})\sum_{i=1}^{N} C_i r_{31}\cos\theta_1 \exp[(-\alpha_i r_{31} - \beta_i r_{32} - \gamma_i r_{21})\omega]. \quad (19)$$

To extract the resonance energy E_r and the resonance width Γ, we have calculated the density of the resonance states using the stabilization method [58]. For a single energy level the following formula has been used,

$$\rho_n(E) = \left|\frac{E_n(\omega_{i+1}) - E_n(\omega_{i-1})}{\omega_{i+1} - \omega_{i-1}}\right|^{-1}_{E_n(\omega_i)=E} \quad (20)$$

where the index i is the i^{th} value for ω and the index n is for the n^{th} resonance. After calculating the density of resonance states $\rho_n(E)$ with the above formula (18), it can be fitted to the following Lorentzian form that yields resonance energy E_r and total width Γ, with

$$\rho_n(E) = y_0 + \frac{A}{\pi}\frac{\Gamma/2}{(E-E_r)^2 + (\Gamma/2)^2}, \quad (21)$$

where y_0 is the baseline offset, A is the total area under the curve from the base line, E_r is the center of the peak and Γ denotes the full width of the peak of the curve at half height. The method has been used and well tested for resonance calculations in other systems [59]. Fig. 9(a) shows a stabilization plot for the $2s^2\,{}^1S^e$ state of the Ps^-, and Fig. 9(b) shows the calculated density of resonance states and a fit to the Lorenztian function with which the resonance energy and width were determined [55, 57]. Fig. 10 shows the $^{1,3}P^o(1)$ resonances energies as functions of the Debye length D and of the screening parameter μ=1/D. Depending on the nature of the autoionization mechanism, the width would decrease for the "+" states and increase for "-" states when the screening effect is increased, as shown here in Fig. 11(a) and (b), respectively. Fig. 12(a) illustrates such autoionization mechanism for the "+" and Fig. 11(b) for the "-" states. A more detail discussion for the screening effect on the autoionization widths can be found in Ref. [57].

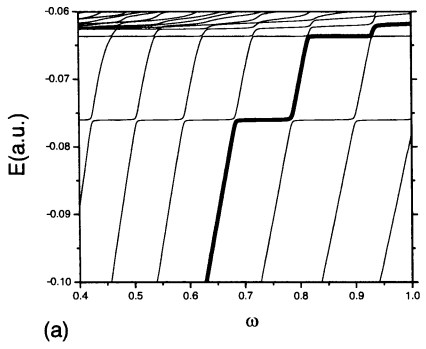

Fig.9a. Stabilization plots of the $2s^2\,{}^1S^e$ state of the Ps^-.

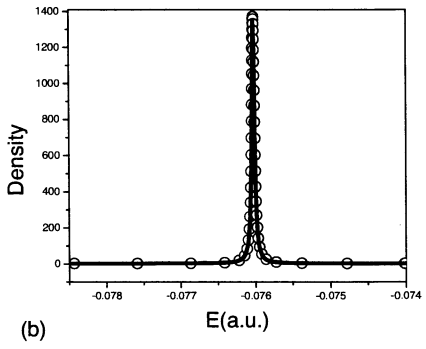

Fig.9b. Calculated density (circles) and in the fitted Lorenztian (solid line) (Ref. [55]).

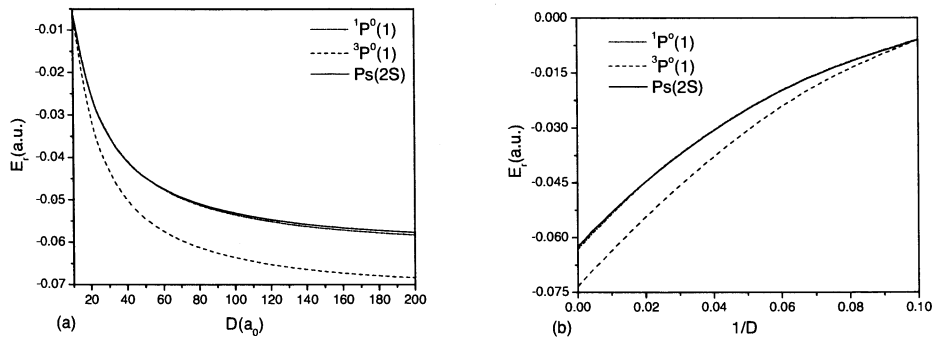

FIG 10. The $^{1,3}P^o$ (1) resonances energies in terms of Debye length D in (a) and in terms of Debye parameter, $1/D$ in (b) along with the *Ps(2s)* threshold energies (solid line) (Ref. [57]).

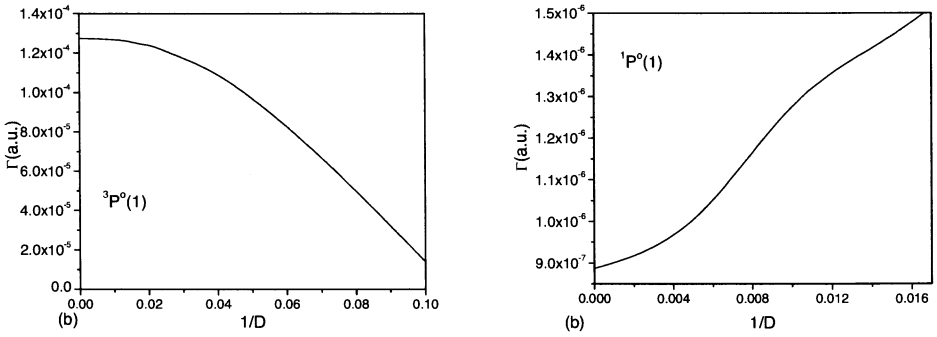

FIG 11. The $^3P^o$ (1) and $^1P^o$ (1) resonances widths as a function of $1/D$ (see Ref. [57]).

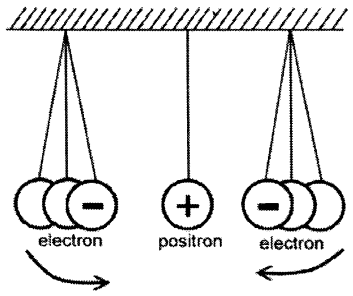

Fig.12 (a) The autoionization mechanism for the "+" states, in which the two electrons are moving toward the positron "in phase."

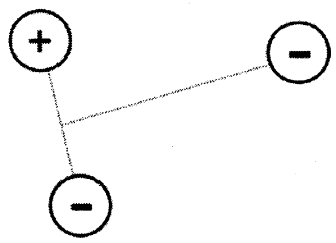

Fig. 12(b) The autoionization mechanism for the "-" states. An electron is bound temporary to the dipole field of the excited positronium atom.

SUMMARY AND DEDICATION

This paper describes the recent theoretical studies on the doubly excited states of the Ps^- ion using the method of complex-coordinate rotation and the stabilization method. Results show that the doubly excited positronium negative ion behaves very much like a XYX tri-atomic molecule. In addition, the recent investigations on the positronium negative ion embedded in the Debye plasmas have been discussed. Our works has been supported by the Nation Science Council of Taiwan, ROC, and I thank Dr. A. K. Bhatia, Dr. I. A. Ivanov, and Dr. S. Kar for their collaborative works on this interesting system. Last, but not the least, I would like to express my sincere gratitude for being invited to the Temkin-Drachman Retirement Symposium. As a postdoctoral research associate spending two years with this wonderful group during the 1975-1977 periods, I am indebted to Dr. Temkin, Dr. Drachman, and Dr. Bhatia for numerous discussions with them. I got interested in the problem of resonances in Ps^- ion [32] after I have worked with Dr. Temkin and Dr. Bhatia on the benchmark calculation in a related problem, the lowest S-wave resonance in electron-hydrogen scattering using the Feshbach projection operator formalism [60]. I was also benefited from being exposed to the method of complex-coordinate rotation, then a state-of-the-art computational tool for resonance calculations, by discussions on many occasions with Dr. Drachman, who was working on the problem of positronium–hydrogen resonance scattering using this method [61]. It is, therefore, most appropriate to dedicate the present paper to Aaron and Dick on this occasion for Temkin-Drachman Retirement celebration. Here, I wish Aaron and Dick happy retirement, and thank them for their great contributions to the areas of atomic physics and positron physics.

REFERENCES

1. E. A. Wheeler, *Ann. NY Acad. Sci.* **48** (1946) 219.
2. A. P. Mills, Jr, *Phys. Rev. Lett.* **46** (1981) 717.
3. A. P. Mills Jr., *Phys. Rev. Lett.* **50** (1983) 671.
4. A. P. Mills, Jr., in *Annihilation in Gases and Galaxies*, edited by R. J. Drachman, NASA Conf. Publ. No. 3058 (NASA, Washington DC, 1990), p. 213.
5. Y. K. Ho, in *Annihilation in Gases and Galaxies* (edited by R. J. Drachman, NASA Conf. Publ. No. 3058 (NASA, Washington DC, 1990), p. 243.
6. J. W. Humberston, *Adv. Atom. Mole. Opt. Phys.* **32** (1994) 205.
7. Y. K. Ho, *Hyperfine Inter.* **73** (1992) 109.
8. Y. K. Ho, *Hyperfine Inter.* **89** (1994) 401.
9. A. K. Bhatia, R. J. Drachman, Nucl. *Instrum. Methods Phys. Res. B* **143** (1998) 195;
10. Y. K. Ho, *Phys. Rev. A* **48** (1993) 4780.
11. J. Ackermann and J. Shertzer, *Phys. Rev. A* **54** (1996) 365.
12. R. Krivec, V. B. Mandelzweig, K. Varga, *Phys. Rev. A* **61** (2000) 062503.
13. V. I. Korobov, *Phys. Rev. A* **61** (2000) 064503.
14. A. M. Frolov, V. H. Smith, Jr., *J. Phys. B* **36** (2003) 4837; A. M. Frolov, *J. Phys.* ***B*****26** (1993) 1031
15. G. W. Drake, Mark M. Cassar, and Razvan A. Nistor, *Phys. Rev. A* **65** (2002) 054501.
16. G. W. F. Drake and M. Grigorescu, *J. Phys. B* **38** (2005) 3377.
17. A. M. Frolov, *Phys. Lett. A* **342** (2005) 430.
18. D. Schwalm, F. Fleischer, M. Lestinsky, K. Degreif, G. Gwinner, V. Liechtenstein, F. Plenge, and H. Scheit, *Nucl. Instrum. Methods B* **221** (2004) 185; F. Fleiser, K. Degreif, G. Gwinner, M. Lestinsky, V. Liechtenstein, F. Plenge, H. Scheit, D. Schwalm, *Can. J. Phys.* **83** (2005) 413.
19. P. Balling, D. Fregenal, T. Ichioka, H. Knudsen, H.-P. E. Kristiansen, J. Merrison and U. Uggerhøj, *Nucl. Instrum. Methods B* **221** (2004) 200.
20. C. M. Surko and R. G. Greaves, *Phys. Plasmas* **11** (2004) 2333.

21. D. B. Cassidy, S. H. M. Deng, R. G. Greaves, T. Maruo, N. Nishiyama, J. B. Snyder, H. K. M. Tanaka, and A. P. Mills, Jr., *Phys. Rev. Lett.* **95** (2005) 195006; S. K Blau, *Physics Today* (January 2006) 23.
22. A. K. Bhatia, R. J. Drachman, *Phys. Rev. A* **32** (1985) 3745.
23. S. J. Ward, J. W. Humberston, and M. R. C. McDowell, *J. Phys. B* **20** (1987) 127.
24. A. M. Frolov, *J. Phys. B* **37** (2004) 853-864
25. K. Maniadaki, L. A. A. Nikolopoulos, and P. Lambropoulos, *Euro. Phys. J. D* **20** (2002) 205.
26. G. W. F. Drake, *Phys. Rev. Lett.* **24** (1970) 126.
27. A. K. Bhatia, *Phys. Rev. A* **2** (1970) 1667.
28. A. P. Mills, Jr., *Phys. Rev. A* **24** (1981) 3242
29. A. K. Bhatia, R. J. Drachman, *Phys. Rev. A* **35** (1987) 4051.
30. J. Botero, Phys. Rev. A **35**, 36 (1987); J. Botero and C. H. Greene, *Phys. Rev. Lett.* **56** (1986) 1366.
31. Y. K. Ho and A. K. Bhatia, *Phys. Rev. A* **45** (1992) 6268.
32. Y. K. Ho, *Phys. Rev. A* **19** (1979) 2347
33. Y. K. Ho, *Phys. Rept.* **99** (1983) 1.
34. Y. K. Ho *Phys. Lett. A* **102** (1984) 348; Y. K. Ho, *Phys. Lett. A* **144** (1990) 237; *Chin. J. Phys.* **35** (1997) 2347.
35. J. Usukura and Y. Suzuki, *Phys. Rev. A* **66** (2002) 010502.
36. T. Li and R. Shakeshaft, *Phys. Rev. A* **71** (2005) 052505.
37. A. Basu and A. S. Ghosh, *Europhys. Lett.* **60** (2002) 46; *Phys. Rev. A* **72** (2005) 062507.
38. S. Gilmore, J. E. Blackwood, and H. R. J. Walters, *NIM B* **221** (2004) 124.
39. A. Igarashi and I. Shimamura, *J. Phys. B* **37** (2004) 4221; A. Igarashi, I. Shimamura and N. Toshima, *New J. Phys.* **2** (2000) 17; *Phys. Rev. A* **58** (1998) 1166
40. Z. Papp, J. Darai, C.-Y. Hu, Z. T. Hlousek, B Konya, and S. L. Yakolev, *Phys. Rev. A* **65** (2003) 032725.
41. A. K. Bhatia and Y. K. Ho, *Phys. Rev. A* **42** (1990) 1119; *Phys. Rev. A* **48** (1993) 264; Y. K. Ho and A. K. Bhatia, *Phys. Rev. A* **44** (1991) 2890; *Phys. Rev. A* **50** (1994) 2155.
42. I. A. Ivanov and Y. K. Ho, *Phys. Rev. A* **60** (1999) 1015; *Phys. Rev. A* **61** (2000) 032501.
43. D. R. Herrick, *Adv. Chem. Phys.* **52** (1983) 1.
44. M. E. Kellman and D. R. Herrick, *Phys. Rev. A* **22** (1980) 1536.
45. J. M. Rost and D. Wingten, *Phys. Rev. Lett.* **69** (1992) 2499.
46. Y. Zhou and C. D. Lin, *Phys. Rev. Lett.* **75** (1995) 2296.
47. I. A. Ivanov and Y. K. Ho, *Phys. Rev. A* **61** (2000) 022510; Y. K. Ho and I. A. Ivanov, *Phys. Rev. A* **63** (2001) 062503.
48. B. Saha, T. K. Mukherjee, P. K. Mukherjee, *Chem. Phys. Lett.* **373** (2003) 218.
49. S. NaKai and K. Mima, *Rep. Prog. Phys.* **67** (2004) 321.
50. D. Leckrone and J. Sugar, *Phys. Scr.* **T4** (1993) 7.
51. H. Okutsu, T. Sako, K. Yamanouchi, G. H. F. Diercksen, *J. Phys. B* **38** (2005) 917.
52. S. Kar and Y. K. Ho, *Int. J. Quan. Chem.* **106** (2006) 814.
53. H. R. Griem in *Principles of Plasma Spectroscopy*, Cambridge Monograph in Plasma Physics (Cambridge University Press 2005).
54. S. Ichimaru in *Plasma Physics,* The Benjamin/Cummings Publishing Company, Inc. (Menlo Park, California 1986) pp5-10.
55. S. Kar and Y. K. Ho, *Phys. Rev. A* **71** (2005) 052503.
56. A. M. Frolov, *Phys. Rev. E* **64** (2001) 036704.
57. S. Kar and Y. K. Ho, *Phys. Rev. A* **73** (2006) 032502.
58. V. A. Mandelshtam , T. R. Ravuri , and H. S. Taylor, *Phys. Rev. Letters* **70** (1993) 1932.
59. S. Kar and Y. K. Ho, *J. Phys. B* **37** (2004) 3177.
60. Y. K. Ho, A. K. Bhaita, and A. Temkin, *Phys. Rev. A* **15** (1977) 1423.
61. R. J. Drachman and S. K. Houston, *Phys. Rev. A* **12** (1975) 885

Symposium in honor of Temkin and Drachman on November 18-19, 2005

Low-energy Scattering of Positronium by Atoms

Hasi Ray
Department of Physics, Indian Institute of Technology Roorkee, Roorkee-247667, Uttaranchal, INDIA
Email: hasi_ray@yahoo.com & rayh1sph@iitr.ernet.in

Abstract

The survey reports theoretical studies involving positronium (Ps) - atom scattering. Investigations carried out in last few decades have been briefly reviewed in this article. A brief description of close-coupling approximation (CCA), the first-Born approximation (FBA) and the Born-Oppenheimer approximation (BOA) for Ps-Atom systems are made. The CCA codes of Ray et al [1-6] are reinvestigated using very fine mesh-points to search for resonances. The article advocates the need for an extended basis set & a systematic study using CCAs.

1 Introduction

The discovery of positronium (Ps), a hydrogen (H) like atom formed by a positron (e^+) and an electron (e^-) in 1953 by Deutsch [7], is an invaluable achievement of the modern science. The atom is itself its anti-atom. Interesting property is that its charge and mass centers coincide. The existence of Ps was first predicted by S. Mohorovicic in 1934 [8] and later on by Ruark in 1945 [9] based on their theoretical investigations which encouraged Deutsch in 1949 [10] to carry out his experimental investigation. The concept of anti-particle was introduced by Dirac in 1928 [11-12] as an anti-electron which was later experimentally observed by Anderson in 1932 [13] and was named as positron.

The collision physics is the most important area of the modern science. The most successful atomic-model by Bohr (1913) and Sommerfeld (1916) was based on the well-known Rutherford scattering (1911) experiment and theory; needless to say that the atomic concept was conceived more than a century ago by Dalton (1808), Gay-Lussac (1808), Avogadro (1811), Maxwell (1811), Mendeleef (1869) and others.

The theoretical studies on Ps and gas atom scattering was initiated by Massey and Mohr [14-15] in 1954 due to its interesting properties. The present progress is due to the continued interests of Fraser [16-18], Fraser & Kraidy [19], Hara & Fraser [20], Martin & Fraser [21], Barker & Bransden [22-23], Bransden [24], Drachman & Houston [25-26], Drachman [27-29], Au & Drachman [30], DiRienzi & Drachman [31-32], Schrader et al [33] and the realization of the fact of all the recent workers doing theories [1-6,34-51] and experiments [52-57] in different countries and different places of the world. The recent news published on 'Universe Today' dated June 8, 2005 has the headline, "The search for Positronium". This could be an important source of many new ideas leading to new physics.

The positrons and Ps are currently employed in the exploration of fundamental effects ranging from condensed matter physics to astrophysics as well as in the diagnostics of living biological systems and of the electronic and structural properties

of industrially important materials. The study of collisions of neutral positronium with other atoms (and molecules) has a number of novel features arising from its light mass and from the coincidence of its centres of charge and mass. Aside from this intrinsic interest, Ps collision data are expected to enhance our understanding of positron slowing down in dense media, Ps diffraction from surfaces, interactions of Ps injected into a plasma, etc. Various industrial applications of positron and positronium beams are discussed by Coleman [58].

Two interacting atoms mutually induce a symmetrical pair of dipoles [59]. The induced polarization potential is the same for electron-atom and positron-atom scattering, in both cases they are attractive [24]. Ps is a highly polarizable atom, its polarizability is eight times higher than that of H. They can exist in two different spin states depending on the spin of positron and electron. The singlet is known as para-Ps with a life time $\sim 10^{-10}s$ and the triplet is known as ortho-Ps having life time $\sim 10^{-7}s$. The electrons are indistinguishable particles. Two electrons can interchange their positions, the phenomenon is known as exchange. The exchange is highly important at low incident energies in presence of more than one electron. The electron spins can be up or down. If both the spins are parallel and total spin is 1, it is known as triplet (-) state; if antiparallel, the total spin is 0 and is known as singlet (+) state.

2 Resonances

In collision physics, the existence of a resonance is an important phenomenon. When a microscopic moving object which is a wave, enters into the scattering chamber near the target, it faces interactions. When it comes out of the scattering zone, the original incident wave gathers a phase shift and the new wave is known as scattered wave. The change in phase which is named as phase shift is the parameter that carries the information of the scattering process. A rapid change in phase shift by π radian in a very narrow energy interval of the incident wave is an indication of the presence of a resonance. It indicates the existence of a bound system if in the s-wave elastic scattering and below threshold of excitation. One can calculate the width of a resonance to get the life time (τ) of the newly formed system.

It is an extremely difficult job to detect a resonance since successful identification needs (i) a very accurate calculation and (ii) sufficient computation facilities. A large number of mesh-points in a very small energy interval, generally $\sim 10^{-2} - 10^{-3}$ eV is required. It necessitates a high-speed computer with a sufficient memory, the knowledge of mathematical computation and programming languages e.g. FORTRAN.

We are interested to discuss the scattering processes at low energies. At high energies the projectile usually ignores all the important delicate interactions with target, so generally it carries no valuable information. At very low energies below excitation threshold, elastic scattering is the only real process. But from just above the threshold different excitation, ionization etc. channels start to open. It is a very difficult task to study the scattering processes at intermediate energies due to presence of many different channels and a very close-coupling among them. The total cross section is the sum of the integrated cross sections of all these channels. Besides these, the partial wave contribution from higher angular momenta start

to dominate above the threshold. Many close peaks may arise in the cross section at the intermediate energies due to opening of different channels and their mixing. These are also named as resonances and have been studied by Higgins & Burke [60-61], Sarkar et al [62-63]. However Zhou et al [64] commented against such resonances. So the subject of above threshold resonances needs more investigation. Above threshold, the phase shift becomes a complex quantity and is known as eigen phase shift.

2.1 Below threshold

The kind of resonances we are interested in, is completely different from the above threshold resonances. This type of a resonance is feasible only below threshold of first excitation when elastic cross section is the total cross section and only s-wave dominates. One needs to investigate both the phase shift and the cross section, but should be careful to use the formulation which derives the cross section directly from amplitude and not from phase shift. If it is a true resonance, this should be reflected both in phase shift and in cross section. It is actually to take a precautionery measure for successful detection since the calculation of phase shift involves a tan-inverse function which may create a numerical error.

The phase shift δ_l can be decomposed as

$\delta_l = \xi_l + \eta_l$.

ξ_l corresponds to the hard sphere scattering or non-resonant part; it does not depend on the shape and depth of the potential. The term η_l depends on the details of the potential. The quantities ξ_l and η_l vary, in general, slowly and smoothly with the incident particle energy. But in certain cases η_l may vary rapidly in a small energy interval of width Γ about a given energy value E_R such that we can write

$$\eta_l = \eta_l^R = tan^{-1}\frac{\Gamma}{2(E_R - E)}$$

In that energy interval the phase shift is therefore given approximately by
$\delta_l \simeq \xi_l + \eta_l^R$.

The physical significance of a narrow resonance can be inferred by examining the amplitude of the radial wave function inside the interaction region. The probability of finding the scattered particle within the potential is much higher near the resonance energy $E = E_R$, so that in that case the particle is nearly bound in the well. Thus the resonance may be considered as a metastable state whose lifetime τ, which is much longer than a typical collision time, can be related to the resonance width Γ by using the uncertainty relation $\Delta t \Delta E \geq \hbar$. Thus, with $\Delta t \simeq \tau$ and $\Delta E \simeq \Gamma$, we have $\tau \simeq \frac{\hbar}{\Gamma}$.

The shape of the cross section curve near a resonance as a function of energy depends on the non-resonant phase shift ξ_l. For the s-wave scattering it is

$$\sigma_l = \frac{sin^2\xi_l(E_R - E)^2 + cos^2\xi_l\Gamma^2 + sin2\xi_l(E_R - E)\Gamma/2}{(E_R - E)^2 + \frac{\Gamma^2}{4}}$$

Two limiting cases for non-resonant phase shift are 0 and $\pi/2$. In the first case the above equation becomes

$$\sigma_l = \frac{\Gamma^2}{(E_R - E)^2 + \frac{\Gamma^2}{4}}$$

which is symmetric and represents a rise in cross section at the resonance energy. In the other case

$$\sigma_l = \frac{(E_R - E)^2}{(E_R - E)^2 + \frac{\Gamma^2}{4}}$$

which is also symmetric but goes down to zero at the resonance energy. If the non-resonant phase shift gets some other value then all sorts of forms of the cross section can occur.

Resonance in the singlet channel in positronium (Ps) and hydrogen (H) scattering was reported by many workers using different approaches [25,35,37-38,65-67]. It was first predicted by Drachman et al [25] using a Feshbach formalism with stabilization and complex rotation methods. Such a resonance using CCA schemes is reported for the first time by Ray [1-2,68-72].

3 Theory

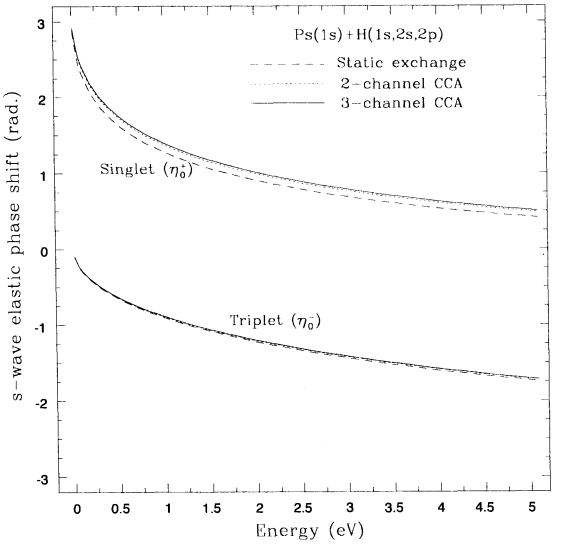

Figure 1: The s-wave elastic phase shifts below inelastic thresholds in Ps-H scattering using target-inelastic CCA theory.

3.1 Close-coupling approximation (CCA) theory

The close-coupling approximation (CCA) is a successful theory to study the low energy scattering phenomenon in atomic physics. The formulation was given by Massey [73]; he is known as the father of atomic physics. Massey applied the

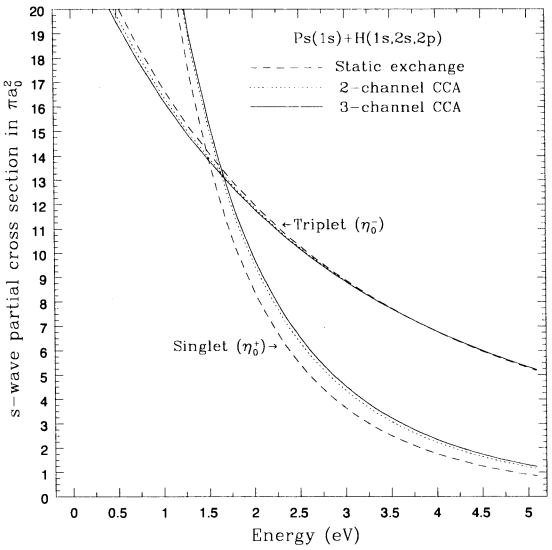

Figure 2: The s-wave elastic cross sections below inelastic thresholds in Ps-H scattering using target-inelastic CCA theory.

theory in e^- - atom scattering. Later Burke et al [74] successfully used this theory for e^+ - atom scattering. Now a days many different groups in the world are using this theory for e^-/e^+ - atom scattering. It was Fraser [16] who used it first for Ps - H scattering. Ray & Ghosh [47-48] merits the credit because they are the first who supplied detailed and converged results. They used a momentum space formalism introduced by Calcutta group [75] whereas Fraser used a coordinate space formalism to write the coupled integral equations. They again add more channels in the CCA basis [1-6,68-72,76-78]. The studies of Fraser [16-18], Fraser et al [19], Hara et al [20] were confined to static-exchange model i.e. considering only the elastic channel in the basis and the H and He targets. Ray [4-6] extended the CCA theory in Ps and lithium (Li) scattering using the static-exchange and a two-channel CCA models.

The theory is based on the very basic principle of quantum mechanics i.e. the eigen state expansion (ESE) methodology in which the total wave function of a quantum mechanical system is expressed as a linear combination of all possible states known as basis set. So one has to use a wide channel space, but practically it is not possible. The number of unknowns exceed the number of equations when non-spherical orbitals like p- and d- states of an atom are considered in channel space. So arose the necessity of an approximation. We should conserve the total angular momentum quantum numbers e.g. 'J' and 'M'. It makes the equations closed i.e. the number of unknowns are equal to the number of equations. This is known as CCA. The accuracy of the method depends on the choice of basis set.

The total wavefunction of Ps-H system $\Psi^{\pm}$ satisfying the Schrödinger equation:

$$H\Psi^{\pm}(\mathbf{r_p}, \mathbf{r_1}, \mathbf{r_2}) = E\Psi^{\pm}(\mathbf{r_p}, \mathbf{r_1}, \mathbf{r_2}) \qquad (1)$$

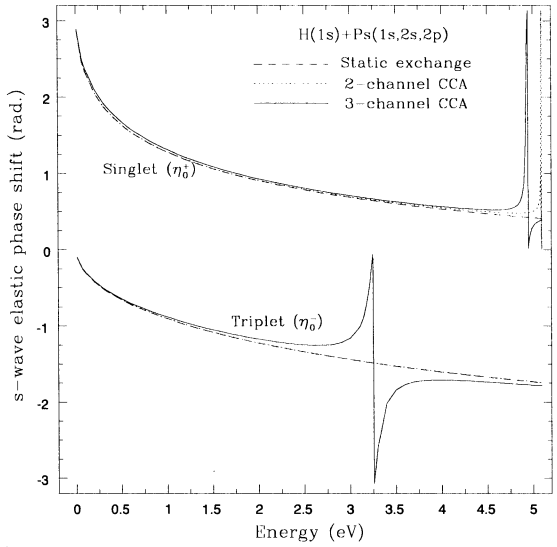

Figure 3: The s-wave elastic phase shifts below inelastic thresholds in Ps-H scattering using projectile-inelastic CCA theory.

is expressed as

$$\Psi^{\pm}(\mathbf{r_p},\mathbf{r_1},\mathbf{r_2}) = \frac{1}{\sqrt{2}}(1\pm P_{12}) \sum_{n_t l_t n_p l_p L J_1 J M} \frac{F_{\Gamma_0 n_t l_t n_p l_p L J_1 J M}(\mathbf{k},\mathbf{k}',R_1)}{R_1} \frac{U_{n_t l_t}(r_2)}{r_2} \frac{V_{n_p l_p}(\rho_1)}{\rho_1}$$

$$\sum_{m_t m_p M_L} \begin{pmatrix} L & l_p & J_1 \\ M & m_p & M_1 \end{pmatrix} \begin{pmatrix} J_1 & l_t & J \\ M_1 & m_t & M \end{pmatrix} Y_{LM_L}(\hat{\mathbf{R}}_1) Y_{l_p m_p}(\hat{\rho_1}) Y_{l_t m_t}(\hat{\mathbf{r}}_2) \quad (2)$$

with

$$H = -\frac{1}{2}\nabla_{\boldsymbol{p}}^2 - \frac{1}{2}\nabla_{\mathbf{1}}^2 - \frac{1}{2}\nabla_{\mathbf{2}}^2 + \frac{1}{|\mathbf{r_p}|} - \frac{1}{|\mathbf{r_1}|} - \frac{1}{|\mathbf{r_2}|} - \frac{1}{|\mathbf{r_p}-\mathbf{r_1}|} - \frac{1}{|\mathbf{r_p}-\mathbf{r_2}|} + \frac{1}{|\mathbf{r_1}-\mathbf{r_2}|} \quad (3)$$

Here P_{12} stands for the exchange operator and $\mathbf{R_i} = \frac{1}{2}(\mathbf{r_p}+\mathbf{r_i})$ and $\boldsymbol{\rho_i} = \mathbf{r_p}-\mathbf{r_i}$; i=1,2; $\mathbf{r_1}$ and $\mathbf{r_2}$ are the position vectors of the electrons belonging to Ps and H respectively and $\mathbf{r_p}$, is that of the positron with respect to the center of mass of the system. $U_{n_t l_t}(\mathbf{r})/r$ and $V_{n_p l_p}(\boldsymbol{\rho})/\rho$ are the radial parts of the wavefunctions of H and Ps respectively and $F_{\Gamma_0\Gamma}(\mathbf{k},\mathbf{k}',R)/R$ is the radial part of the continuum wave function of the moving Ps atom; Γ_0 indicates all the quantities $n_t l_t n_p l_p L J_1 J M$ of Γ at the initial channel.

Projecting the Schrödinger Eqn.(1) just like the Hartree-Fock variational approach and integrating over the desired coordinates, we can get a set of integro-differential equations which can be transformed into the integral equations like Lippmann-Schwinger applying the asymptotic boundary conditions. These coupled integral equations can be formed either in momentum space or in configuration space. We have used momentum space formalism [75]. The set of coupled integral equations obtained for the scattering amplitudes are as follows:

$$f^{\pm}_{n'l',nl}(\mathbf{k}',\mathbf{k}) = B^{\pm}_{n'l',nl}(\mathbf{k}',\mathbf{k}) + \frac{1}{2\pi^2} \sum_{n''l''} \int d\mathbf{k}'' \frac{B^{\pm}_{n'l',n''l''}(\mathbf{k}',\mathbf{k}'') f^{\pm}_{n''l'',nl}(\mathbf{k}'',\mathbf{k})}{k''^2 - k^2_{n''l''} + i\epsilon} \quad (4)$$

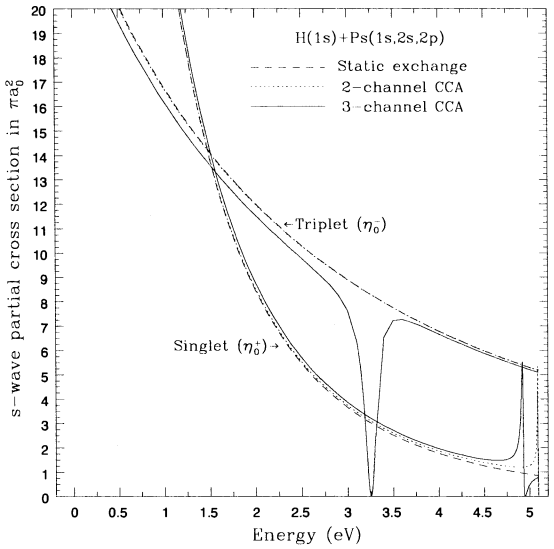

Figure 4: The s-wave elastic cross sections below inelastic thresholds in Ps-H scattering using projectile-inelastic CCA theory.

$B^{\pm}$ indicate the Born-Oppenheimer [79] scattering amplitudes, plus(+) is for the singlet channel and minus(-) for triplet channel. The formulation for the FBA and BOA matrix elements are discussed [80-86] and briefly described here. Similarly $f^{\pm}$ indicate the unknown scattering amplitudes for the singlet and the triplet channels respectively. The summation over $n''l''$ is to include various channels.

These three dimensional coupled integral equations involving $f_{n'l',nl}(\mathbf{k}',\mathbf{k})$ and $B_{n'l',nl}(\mathbf{k}',\mathbf{k})$ can be reduced to the corresponding one dimensional forms through partial wave analysis using the expansion like:

$$\tau^{\pm}_{n'l'm',nlm}(\mathbf{k}',\mathbf{k}) = (kk')^{-1/2} \sum_{J,M} \sum_{L,M_L} \sum_{L',M'_L} \sum_{J_1,M_1} \sum_{J'_1,M'_1} \langle L'l'_p, M'_L m'_p | J'_1 M'_1 \rangle$$

$$\langle Ll_p, M_L m_p | J_1 M_1 \rangle \langle J'_1 l'_t, M'_1 m'_t | JM \rangle \langle J_1 l_t, M_1 m_t | JM \rangle$$

$$Y_{L'M_{L'}}(\hat{\mathbf{k}}') Y_{LM_L}(\hat{\mathbf{k}}) \tau^{J\pm}(k' n'_p n'_t l'_p l'_t, k n_p n_t l_p l_t) \qquad (5)$$

The resulting one dimensional coupled integral equations can be written as a matrix equation like

$$[\mathbf{A}]_{\mathbf{N}\times\mathbf{N}} [\mathbf{X}]_{\mathbf{N}\times\mathbf{1}} = [\mathbf{B}]_{\mathbf{N}\times\mathbf{1}} \qquad (6)$$

which can be solved by matrix inversion method. Here [**A**] is the scattering matrix of $N\times N$ type formed by Born and Born-Oppenheimer scattering amplitudes, [**X**] is the column matrix of $N\times 1$ type formed by unknown CCA scattering amplitudes and [**B**] is again a column matrix of $N \times 1$ type formed by the Born and Born-Oppenheimer [79] scattering amplitudes; the dimension(N) depends on the number of channels included in the expansion basis. We have calculated all the Born and Born-Oppenheimer amplitudes exactly following an analytic approach and then

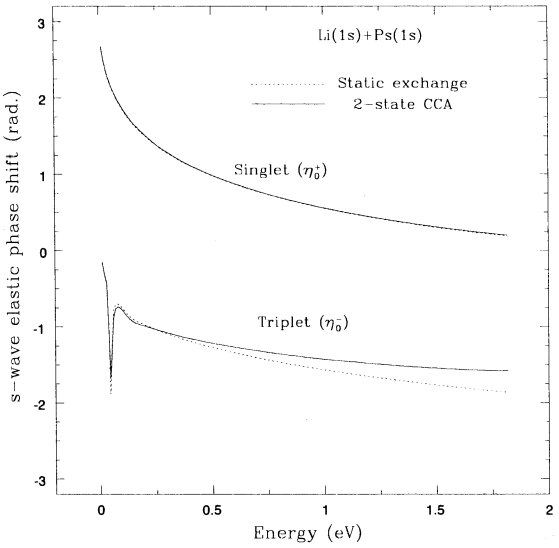

Figure 5: The s-wave elastic phase shifts below inelastic thresholds in Ps-Li scattering using target-inelastic CCA theory.

the remaining part is carried out following numerical approach using computer and FORTRAN programming. The two sets of one dimensional coupled integral equations of scattering amplitudes in momentum space for the singlet(+) and triplet(-) channels respectively, are solved separately for each partial wave(L).

We employ different projectile-elastic and projectile-inelastic CCA-schemes to investigate Ps-H and Ps-Li scattering in the energy region below inelastic threshold. We study s-wave elastic phase shifts and s-wave elastic cross sections using a very fine mesh-points. We perform exact calculations for all the direct and exchange matrix elements considering all the possible Coulomb interactions where the direct first-Born amplitudes vanish if the parity of Ps remains unaltered.

3.2 First-Born approximation (FBA)

The FBA amplitude for the scattering of the Ps by atomic target is expressed as,

$$F_{fi}^{B1} = -\frac{\mu}{2\pi}\int e^{-i\mathbf{k_f}.(\mathbf{x}+\mathbf{r_1}/2)}\eta_f^*(|\mathbf{x}-\mathbf{r_1}|)\phi_f^*(\mathbf{r_2},\mathbf{r_3},..,\mathbf{r_N})[V_{int}]$$
$$\phi_i(\mathbf{r_2},\mathbf{r_3},..,\mathbf{r_N})\eta_i(|\mathbf{x}-\mathbf{r_1}|)e^{i\mathbf{k_i}.(\mathbf{x}+\mathbf{r_1}/2)}d\mathbf{x}d\mathbf{r_1}d\mathbf{r_2}d\mathbf{r_3}..d\mathbf{r_N} \quad (7)$$

where μ is the reduced mass of the system; $\mathbf{x}$, $\mathbf{r_1}$ and $\mathbf{r_i}$ are the position vectors for the positron, the electron in the Ps and the i-th electron in the target atomic system respectively w.r.t. center of mass of the system. N is the number of active electrons present in the system. η_i and η_f are respectively the initial and final state wavefunctions for the positronium atom whereas ϕ_i and ϕ_f are the initial and final state wavefunctions of the atomic target. V_{int} is the interaction potential due to electrostatic Coulomb interaction between the two atomic systems and is

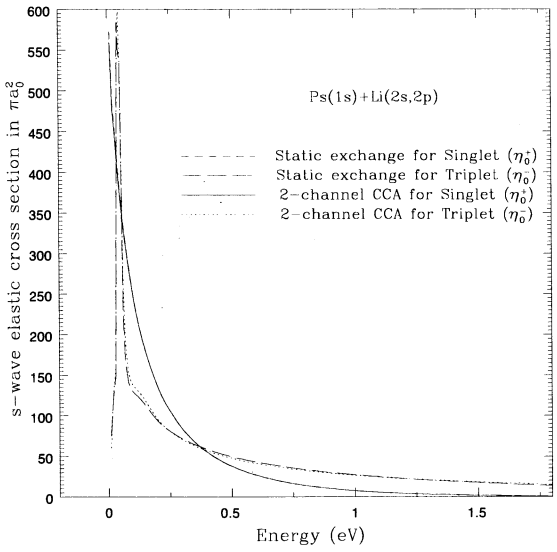

Figure 6: The s-wave elastic cross sections below inelastic thresholds in Ps-Li scattering using target-inelastic CCA theory.

given by

$$V_{int} = \frac{Z}{x} - \frac{Z}{r_1} - \sum_{i=2}^{N} \frac{1}{|\mathbf{x} - \mathbf{r_i}|} + \sum_{i=2}^{N} \frac{1}{|\mathbf{r_1} - \mathbf{r_i}|} \tag{8}$$

Making the substitution $\boldsymbol{\rho} = \mathbf{x} - \mathbf{r_1}$ and $\mathbf{R} = (\mathbf{x} + \mathbf{r_1})/2$ and performing the integrations, the above scattering amplitudes reduce to a general form like :

$$F_{fi}^{B1} = -\frac{4}{q^2}\{I_{Ps}\}\{I_{target}\} \tag{9}$$

Here $\mathbf{q} = \mathbf{k_i} - \mathbf{k_f}$, is the momentum transfer; $\mathbf{k_i}$ and $\mathbf{k_f}$ are the momenta of the projectile in the initial and final states respectively. I_{Ps} and I_{target}, the form factors for Ps and target respectively are given by

$$I_{Ps} = \int \eta_f^*(\boldsymbol{\rho})\{e^{-i\mathbf{q}.\boldsymbol{\rho}/2} - e^{i\mathbf{q}.\boldsymbol{\rho}/2}\}\eta_i(\boldsymbol{\rho})d\boldsymbol{\rho} \tag{10}$$

and

$$I_{target} = \int \phi_f^*(\mathbf{r_2}, \mathbf{r_3}, .., \mathbf{r_N})[Z - \sum_{i=2}^{N} e^{i\mathbf{q}.\mathbf{r_N}}]\phi_i(\mathbf{r_2}, \mathbf{r_3}, .., \mathbf{r_N}) \prod_{i=2}^{N} d\mathbf{r_N} \tag{11}$$

Here Z represent the nuclear charge of target atom.

3.3 Born-Oppenheimer approximation (BOA)

The differential cross section in Ps-H scattering is defined as

$$\frac{d\sigma}{d\hat{\mathbf{k_f}}} = \frac{k_f}{k_i}\{\frac{1}{4} \mid F + G \mid^2 + \frac{3}{4} \mid F - G \mid^2\} \tag{12}$$

if F and G are respectively the direct and exchange matrix elements in space part only.

Accordingly the integrated or the total cross section (σ) can be defined as:

$$\sigma(E_i) = \frac{k_f}{k_i} \int d\hat{\mathbf{k}}_f [\frac{1}{4} \mid F(\hat{\mathbf{k}}_f) + G(\hat{\mathbf{k}}_f) \mid^2 + \frac{3}{4} \mid F(\hat{\mathbf{k}}_f) - G(\hat{\mathbf{k}}_f) \mid^2] \qquad (13)$$

Where

$$F(\hat{\mathbf{k}}_f) = -\frac{1}{\pi} \int e^{-i\mathbf{k_f}.\mathbf{R_1}} \eta_f^*(\boldsymbol{\rho}_1) \Phi_f^*\{\mathbf{r_2}\} [V_{int}^F] e^{i\mathbf{k_i}.\mathbf{R_1}} \eta_i(\boldsymbol{\rho}_1) \Phi_i\{\mathbf{r_2}\} d\mathbf{x} d\mathbf{r_1} d\mathbf{r_2} \qquad (14)$$

$$G(\hat{\mathbf{k}}_f) = -\frac{1}{\pi} \int e^{-i\mathbf{k_f}.\mathbf{R_2}} \eta_f^*(\boldsymbol{\rho}_2) \Phi_f^*\{\mathbf{r_1}\} [V_{int}^G] e^{i\mathbf{k_i}.\mathbf{R_1}} \eta_i(\boldsymbol{\rho}_1) \Phi_i\{\mathbf{r_2}\} d\mathbf{x} d\mathbf{r_1} d\mathbf{r_2} \qquad (15)$$

with $\mathbf{R}_j = \frac{1}{2}(\mathbf{x}+\mathbf{r}_j)$ and $\boldsymbol{\rho}_j = (\mathbf{x}-\mathbf{r}_j)$; j=1,2. Here, $\mathbf{x}$ is the coordinate of positron in Ps, and $\mathbf{r}_j$; j=1,2 are that of electrons in Ps and in H respectively in the incident channel w.r.t. the center of mass of the system. Functions η and Φ indicate the wave functions of Ps and H. Subscript 'i' identifies the incident channel, whereas 'f' represents the final channel. Accordingly $\mathbf{k}_i$ and $\mathbf{k}_f$ are the momenta of the projectile in the initial and final channels respectively.

$$V_{int}^F = \frac{1}{\mid \mathbf{x} \mid} - \frac{1}{\mid \mathbf{r_1} \mid} - \frac{1}{\mid \mathbf{x} - \mathbf{r_2} \mid} + \frac{1}{\mid \mathbf{r_1} - \mathbf{r_2} \mid} \qquad (16)$$

$$V_{int}^G = \frac{1}{\mid \mathbf{x} \mid} - \frac{1}{\mid \mathbf{r_2} \mid} - \frac{1}{\mid \mathbf{x} - \mathbf{r_1} \mid} + \frac{1}{\mid \mathbf{r_1} - \mathbf{r_2} \mid} \qquad (17)$$

Indices F and G indicate the direct and exchange channels respectively.

The computation of Born-exchange matrix element is much more difficult than the direct Born-element. The Fourier transform

$$\frac{e^{-\lambda r}}{r} = \frac{1}{2\pi^2} \int \frac{e^{i\mathbf{p}.\mathbf{r}}}{p^2 + \lambda^2} d\mathbf{p},$$

the Bethe integral

$$\int \frac{e^{i\mathbf{k}.\mathbf{r}}}{r} d\mathbf{r} = \frac{4\pi}{k^2}$$

and the properties of Dirac δ-function are mainly used for analytical evaluation. The numerical integrations are carried out using Gauss-Legendre quadratures.

4 Results & discussion

In the present review article, we discuss the elastic scattering at low energies below the inelastic threshold of excitation in Ps-H and Ps-Li scattering. We use different target-inelastic and projectile-inelastic CCA schemes to study s-wave elastic phase shifts and s-wave elastic cross sections with a very fine mesh points to search for resonances. The incident energies are chosen from 0 to 5.1 eV for Ps-H system. Our results using the static-exchange approximation, target-inelastic 2-channel and 3-channel CCAs are presented in figures 1 & 2 and are giving no trace of resonances. But both the phase shifts and cross sections using projectile-inelastic 2-channel and 3-channel CCAs are showing perfect resonances in singlet channel and are presented in figures 3 & 4. The singlet resonance using projectile-inelastic

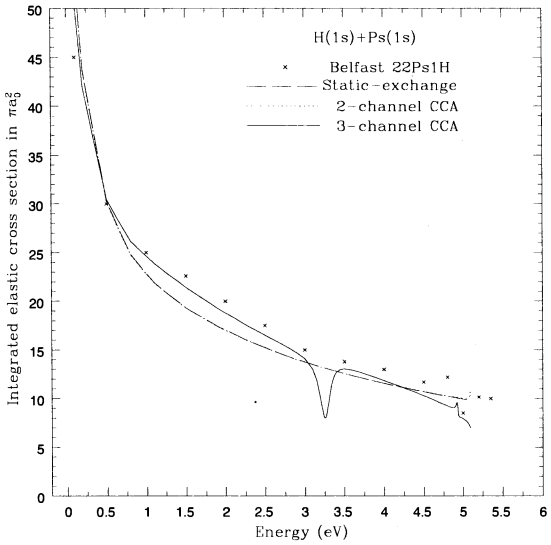

Figure 7: Comparison of total cross sections for Ps-H scattering below inelastic thresholds using projectile-inelastic CCAs, static-exchange approximation and 22Ps1H coupled-pseudostate R-matix theory.

3-channel CCA is shifted to lower energies and broadened in width than 2-channel CCA when it was very close to first excitation threshold. All the corresponding triplet results are also presented in the same figures 1 to 4. No triplet resonance is found except using the projectile-inelastic 3-channel CCA scheme. The triplet resonance is found near the energy 3.25 eV. The corresponding s-wave partial cross section is giving a sharp well. All resonances satisfy the Breit-Wigner formulation of cross section. This kind of perfect resonances were first time observed by Ray [1-2,68-72] using different projectile-inelastic CCA schemes. The singlet resonance was predicted earlier [25,35,46,66-67], but the triplet was new.

We also reinvestigate the s-wave elastic phase shifts and cross sections below inelastic threshold for Ps-Li scattering using static-exchange approximation and 2-channel target-inelastic CCA in a similar fashion. Energy region is chosen from 0 to 1.8 eV i.e. below inelastic threshold of first excitation. Our findings are presented in figures 5 & 6 and are very similar to the earlier results. The triplet channel is more sensitive to long-range forces due to dipole polarizabilty near to threshold. This long range dynamic effect [87-88] is introduced into our calculation through Li(2p) state. In a different way, it is the quantum mechanical effect of strong coupling between the Li(2s) and Li(2p) states. There is no trace of resonances in the singlet channel using both the CCA schemes. But the triplet channel is showing a rapid change in phase shifts $\sim \pi/2$ radian in both the static-exchange and 2-channel CCA at very close to zero energy and the corresponding partial wave cross sections are showing sharp peaks. However these are not resonances. The definition of below-threshold resonances admits a phase shift change of π radian. It is not known to us what it indicates.

In figure 7, we compare the total cross sections. These are again the total elastic cross sections since at the energy region below inelastic/excitation threshold

elastic channel is the only open channel. The projectile-inelastic 2-channel and 3-channel CCA cross sections are presented with static-exchange approximation [47-48] and the 22Ps1H coupled-pseudostate R-matrix data of Blackwood et al [37]. The present results show good agreement. The well in the total cross section curve using projectile-inelastic 3-channel CCA supports the triplet resonance. The small peaks using projectile-inelastic 2-channel and 3-channel CCAs are supporting the singlet resonance.

In addition, the present triplet phase shift data for Ps-H scattering using projectile-inelastic 3-channel CCA fit nicely with non-resonant part as

$$\xi_0 = -1.4053 + 0.1295E - 0.04613E^2$$

and provides the width $\Gamma = 0.15173eV$ and resonance position $E_R = 3.2630eV$.

5 Conclusion

A brief survey on Ps-atom scattering is made. Resonances below excitation threshold are discussed. Thorough reinvestigations are made in Ps-H system with static-exchange, target-inelastic and projectile-inelastic 2-channel and 3-channel CCAs using a very fine mesh points to search for resonances. No resonance is found with static-exchange approximation and target inelastic 2-channel and 3-channel CCAs in Ps-H system. A singlet resonance found in both projectile-inelastic 2-channel and 3-channel CCAs in Ps-H system which for the first time is detected using close-coupling approximation schemes, agree well with earlier predictions. A triplet resonance with 3-channel projectile-inelastic CCA in Ps-H system is a new addition. It needs more investigations using an extended basis set and a systematic study to realize the physical cause of it. In Ps-Li system no resonance is found below inelastic threshold using both the static-exchange and target-inelastic 2-channel CCA. The comparison of total cross section curves below inelastic threshold in Ps-H system supports the existence of both the singlet and triplet resonances.

6 Acknowledgement

Author likes to thank DST, India for Grant No.SR/FTP/PS-80/2001 on 'SERC Fast Track Young Scientists Scheme' for full financial support. I am grateful to R. J. Drachman and A. K. Bhatia for their kind academic support and useful help during the progress.

References

[1] Findings in Ps-H scattering, Phys. Rev. A, in press, (2006).
[2] A new kind of binding, Hasi Ray, ISAMP NEWS LETTER, Vol.I Issue 2 p.6-8 (2005).
[3] H.Ray and A.S.Ghosh, J.Phys. B, **31**, 4427 (1998).
[4] H. Ray, J. Phys. B **32**, 5681 (1999).
[5] H. Ray, J. Phys. B **33**, 4285 (2000).
[6] H. Ray, J. Phys. B **35**, 2625 (2002).

[7] M. Deutsch, Progr. Nucl. Phys., **3**, 131 (1953).
[8] S. Mohorovicic, Astron. Nachr., **253**, 93-108 (1934).
[9] A. E. Ruark, Phys. Rev. Lett., **68**, 278 (1945).
[10] J. W. Shearer and M. Deutsch, Phys. Rev., **78**, 462 (1949).
[11] P. A. M. Dirac, Proc. Roy. Soc. A **117**, 610 (1928).
[12] P. A. M. Dirac, Proc. Roy. Soc. A **118**, 351 (1928).
[13] C. D. Anderson, Phys. Rev., **43**, 491 (1933).
[14] H.S.W.Massey and C.B.O.Mohr, Proc. Phys. Soc. **67**, 695 (1954).
[15] H. S. W. Massey, Positron Annihilation, Proceedings of the Conference held at Wayne State University on July 27-29, 1965 edited by A. T. Stewart and L. O. Roellig, Acedemic Press of New York & London (1967) p. 113-125.
[16] P.A.Fraser, Proc. Phys. Soc., **78**, 329 (1961).
[17] P.A.Fraser, Proc. Phys. Soc., **79**, 721 (1962).
[18] P.A.Fraser, J. Phys. B, **1**, 1006 (1968).
[19] P.A.Fraser and M.Kraidy, Proc. Phys. Soc., **89**, 533 (1966).
[20] S.Hara and P.A.Fraser, J. Phys. B, **8**, L472 (1975).
[21] D.W.Martin and P.A.Fraser, J. Phys. B, **13**, 3383 (1980).
[22] M.I.Barker and B.H.Bransden, J. Phys. B, **1**, 1109 (1968).
[23] M.I.Barker and B.H.Bransden, J. Phys. B, **2**, 730 (1969).
[24] B. H. Bransden, Case Studies ed E. W. McDaniel and M. R. C. McDowell (Amsterdam: North-Holland), **1**, 169-248 (1969).
[25] R.J.Drachman and S.K.Houston, Phys. Rev. A, **12**, 885 (1975).
[26] R.J.Drachman and S.K.Houston, Phys. Rev. A, **14**, 894 (1976).
[27] R.J.Drachman, Phys. Rev. A, **19**, 1900 (1979).
[28] R.J.Drachman, Can. J. Phys., **60**, 494 (1982).
[29] R.J.Drachman, Atomic Physics with positrons, ed. J.W.Humberston and E.A.G.Armour [Plenum, New York] p.203-14 (1987).
[30] C.K.Au and R.J.Drachman, Phys. Rev. Lett., **56**, 324 (1986).
[31] J.DiRienzi and R.J.Drachman, Phys. Rev. A, **65**, 032721 (2002).
[32] J.DiRienzi and R.J.Drachman, J. Phys. B, **36**, 2409 (2003).
[33] D.M.Schrader, F.N.Jacobsen, N.P.Frandsen and U.Mikkelsen, Phys. Rev. Lett., **69**, 57 (1992).
[34] M.T.McAlinden, F.G.R.S.McDonald and H.R.J.Walters, Can J. Phys., **74**, 434 (1996).
[35] C.P.Campbell, M.T.McAlinden, F.G.R.S.McDonald and H.R.J.Walters, Phys. Rev. Lett., **80**, 5097 (1998).
[36] J.E.Blackwood, C.P.Campbell, M.T.McAlinden, F.G.R.S.McDonald and H.R.J.Walters, Phys. Rev. A, **60**, 4454 (1999).
[37] J.E.Blackwood, M.T.McAlinden, and H.R.J.Walters, Phys. Rev. A, **65**, 032517 (2002).
[38] J.E.Blackwood, M.T.McAlinden, and H.R.J.Walters, J. Phys. B, **35**, 2661 (2002).
[39] H.R.J.Walters, A.C.H.Yu, S.Sahoo and Sharon Gilmore, Nucl. Inst. Meth. B, **221**, 149 (2004).
[40] S.J.Ward, J.W.Humberston and M.R.C.McDowell, J. Phys. B, **18**, L525 (1985).
[41] P.V.Reeth and J.W.Humberston, J.Phys.B, **36**, 1923 (2003).
[42] J.W.Humberston and M.Charlton, Positron Physics, printed in UK, University Press (2001).

[43] Y.C.Jean, P.E.Mallon and D.M.Schrader, Principles and applications of positron and positronium chemistry, World Scientific (2003).
[44] S.Chiesa, M.Mella and G.Morosi, Phys. Rev. A, **66**, 042502 (2002).
[45] A.Basu and A.S.Ghosh, Euro. Phys. Lett., **60**, 46 (2002).
[46] Z.C.Yan and Y.K.Ho, J.Phys. B, **36**, 4417 (2003).
[47] H.Ray and A.S.Ghosh, J.Phys. B, **29**, 5505 (1996).
[48] H.Ray and A.S.Ghosh, J.Phys. B, **30**, 3745 (1997).
[49] P.K.Biswas and S.K.Adhikari, Chem. Phys. Lett., **317**, 129 (2000).
[50] A.Ivanov and J.Mitroy, Phys. Rev. A, **65**, 034709 (2002).
[51] G.G.Ryzhikh and J.Mitroy, Phys. Rev. Lett., **79**, 4124 (1997).
[52] N.Zafar, G.Laricchia and M.Charlton, Phys. Rev. Lett., **76**, 1539 (1996).
[53] N.Zafar, G.Laricchia, M.Charlton and A.J.Garner, Phys. Rev. Lett., **76**, 1595 (1996).
[54] A.J.Garner, G.Laricchia and A. Ozen, J. Phys. B, **29**, 5961 (1996).
[55] F.Saito, Y.Nagashima and T.Hyodo, J. Phys. B, **36**, 4191 (2003).
[56] A.P.Mills Jr.,Nucl. Inst. Meth. B, **192**, 107 (2002).
[57] S.Amritage, D.E.Leslie, A.J.Garner and G.Laricchia, Phys. Rev. Lett., **89**, 173402 (2002).
[58] P. G. Coleman, Nucl. Inst. Meth. B **192**, 83 (2002).
[59] John Maddox, Nature, **314**, 315 (1985).
[60] K. Higgins and P. G. Burke, J. Phys. B **24**, L343 (1991).
[61] K. Higgins and P. G. Burke, J. Phys. B **26**, 4269 (1993).
[62] N. K. Sarkar, Madhumita Basu and A. S. Ghosh, J. Phys. B, **26**, L427 (1993).
[63] N. K. Sarkar, Madhumita Basu and A. S. Ghosh, J. Phys. B, **26**, L799 (1993).
[64] Yan Zhou and C. D. Lin, J. Phys. B, **28**, L519 (1995).
[65] B. A. P. Page, J. Phys. B, **9**, 1111 (1976).
[66] Z. C. Yan and Y. K. Ho, Phys. Rev. A, **59**, 2697 (1999).
[67] Z. C. Yan and Y. K. Ho, Phys. Rev. A, **60**, 5098 (1999).
[68] Triplet resonance in Ps and H Scattering, Hasi Ray, Book of abstracts XXIV ICPEAC held at Rosario, Argentina on July 20-26, 2005.
[69] Resonances in Ps and H scattering, Hasi Ray, Book of abstracts XIII International Workshop on Low-energy Positron and Positronium Physics, held at Campinas, SP, Brasil on July 27-30, 2005.
[70] Resonances in Ps-H Scattering, Hasi Ray, Book of abstracts EGAS37, held at Dublin, Ireland on August 3-6, 2005.
[71] New findings in Ps-H scattering, Hasi Ray, Book of abstracts ECAMP8, held at Rennes, France on July 6-10, 2004 p. 3-112.
[72] Resonances on Projectile-inelastic CCA in Ps-H scattering, Hasi Ray, Book of abstracts XXIII ICPEAC, held at Stockholm University, Sweden on July 23-29, 2003 p. Th. 104.
[73] H. S. W. Massey and C. B. O. Mohr, Proc. Roy. Soc., **136**, 289 (1932).
[74] P. G. Burke and K. Smith, Rev. Mod. Phys. **34**, 458 (1962).
[75] A. S. Ghosh, N. C. Sil and P. Mandal, Phys. Rep. **87**, 313 (1982).
[76] A. S. Ghosh, P. K. Sinha and H. Ray, NIMB **143**, 162 (1998).
[77] P. K. Sinha, P. P. Chaudhury and A. S. Ghosh, J. Phys. B **30**, 4644 (1997).
[78] P. K. Biswas and S. K. Adhikari, Phys. Rev. A, **59**, 363 (1999).
[79] N. F. Mott and H. S. W. Massey, The Theory of Atomic Collisions, Third

Edition (Oxford University Press, New York; Reprinted 1987) Vol. II p. 414.
[80] Hasi Ray, Phys. Lett. A, Vol.252, p.316 (1999).
[81] Hasi Ray, Nucl. Inst. Meth. B, Vol.192, p.191 (2002).
[82] Hasi Ray, Phys. Lett. A, Vol.299, p.65 (2002).
[83] Hasi Ray, J. Phys. B, Vol.35, p. 3365 (2002).
[84] Hasi Ray, PRAMANA, Vol.63, p.1063 (2004).
[85] Hasi Ray, PRAMANA, **66**, 415 (2006).
[86] H. Ray, Euro. Phys. Lett., **73**, 21 (2006).
[87] H. R. J. Walters, J.Phys.B **9**, 227 (1976).
[88] R.J.Drachman and A.K.Bhatia, Phys. Rev. A, **51**, 2926 (1995).

THE PHOTODETACHMENT OF Ps^- and LOW-ENERGY e^+-H COLLISIONS

S. J. Ward
Department of Physics, University of North Texas, Denton, Texas 76203, USA

ABSTRACT

Two calculations in the area of positron collisions are presented. The first is the calculation of the photodetachment cross section of the positronium negative ion (Ps^-) using accurate variational wave functions for both the initial bound-state and the final ^1P continuum state. The second is the calculation of partial wave cross sections for Ps($1s$)-formation in e^+-H($1s$) collisions using the hyperspherical hidden crossing method. Since the S-wave Stückelberg phase is close to π, the very small S-wave Ps($1s$) formation cross section can be understood in terms of destructive interference. Other examples in positron collisions are given where it is either known or expected that destructive interference is the cause of the small S-wave Ps($1s$) formation cross section. In addition, examples are presented of processes in atomic physics where the Stückelberg phase is a multiple of $\frac{\pi}{2}$.

I. INTRODUCTION

Dr. Richard Drachman has performed pioneering work in the theory of positron physics. He has been an encouragement and support to me since I was a graduate student. I appreciate Dr. Richard Drachman taking interest in my work and sharing his thoughts. In this paper, I describe some work I have performed with my collaborators on the photodetachment of the positronium negative ion Ps^- (section II) and on low-energy e^+-H($1s$) collisions (section III). These two problems have been of mutual interest to Dr. Richard Drachman and myself. Atomic units will be used in this paper unless explicitly stated.

II. PHOTODETACHMENT of Ps^-

The first interaction I remember with Dr. Richard Drachman was receiving his candid criticism, yet written in an encouraging way, of a preprint that Dr. M. R. C. McDowell (my Ph. D. supervisor) and I had written on e^--Ps when I was a beginning graduate student. As a student, I became interested in Bhatia and Drachman's pioneering calculation on the photodetachment of Ps^-. This calculation was performed shortly after the existence of Ps^- was experimentally verified [2]. Bhatia and Drachman employed the 'loosely' bound approximation which used the asymptotic form of an accurate initial bound-state wave function (220 linear parameters) and a plane-wave for the final-state wave function. They obtained an analytical expression for the photodetachment cross section,

$$a_\lambda(L,V) = (1.32 \times 10^{-18}\mathrm{cm}^2)\,\frac{k^3}{(k^2+\gamma^2)^3}\,, \tag{1}$$

where k is the wave vector of the relative Ps-e^- motion. The term γ is defined in terms of the electron affinity of Ps^-, $\varepsilon_b = 3\gamma^2/4$. Since the initial and final wave functions are the eigenfunctions of the same model Hamiltonian, the length and velocity cross sections are identical. A similar calculation was performed by Ohmura and Ohmura [3] for H^- and has proven to be successful, especially at long wavelengths.

For my Ph.D., I studied e^--Ps scattering and the photodetachment of Ps^- for energies below the Ps($n = 2$) threshold. Humberston, McDowell and I [4] computed the photodetachment of Ps^-. We used an accurate variational wave function for the ground-state and obtained the ^1P continuum wave function for e^--Ps from the Kohn variational method. The ground-state wave function contained 95 linear parameters, whereas the ^1P continuum wave function contained 220 linear parameters. We computed the photodetachment cross section in both the length and velocity formulations.

Figure 1 shows Bhatia and Drachman's cross section with our length and velocity cross sections. The length and velocity cross sections are in excellent agreement with one another. Furthermore, Bhatia and Drachman's cross section agrees well with our cross sections for the overall shape and for the position of the maximum. However, the height of maximum in our cross sections is somewhat lower than in theirs.

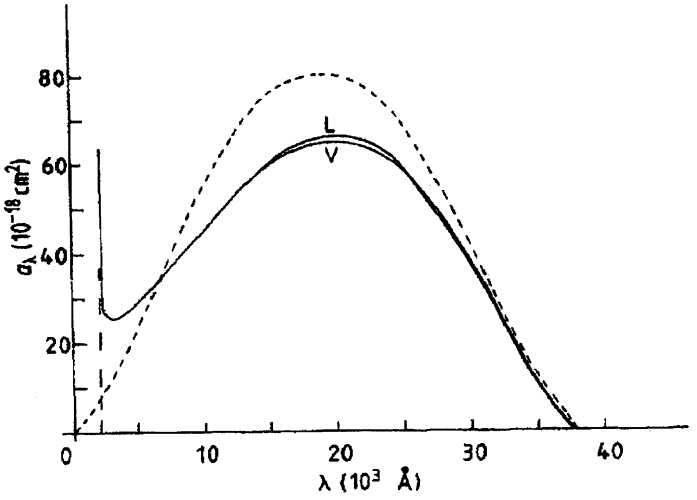

Figure 1. Photodetachment cross section of Ps^-. The L (V) marks the variational length (velocity) cross section. The dashed line (—) denotes Bhatia and Drachman's cross section. The vertical broken line indicates the position of the $n = 2$ threshold.

We followed Bhatia and Drachman in seeing how well the photodetachment cross section satisfies the sum rule

$$S_{-1} = \frac{1}{2\pi^2 \alpha a_0^2} \int_0^{\lambda_0} a_\lambda \frac{d\lambda}{\lambda} \tag{2a}$$

$$= \frac{8}{27} \left\langle \Psi_i \middle| |\mathbf{r}_1 + \mathbf{r}_2|^2 \middle| \Psi_i \right\rangle , \tag{2b}$$

where λ_0 is the threshold wavelength and Ψ_i is the initial-state wave function of Ps^-. In

our variational calculations, we had considered energies only up to the $n = 2$ threshold. In evaluating S_{-1}, we used Bhatia and Drachman's analytical expression for a_λ for energies above the $n = 2$ threshold. The contribution to S_{-1} for these energies is small.

In Table 1 we compare Eq. (2a) with Eq. (2b) evaluated using the length (WHML) and the velocity (WHMV) formulation of the photodetachment cross section. We compare our evaluation of S_{-1} with that evaluated by Bhatia and Drachman, in which they used their 220 linear parameter wave function Ψ_i in Eq. (2b). The velocity results show a discrepancy of less than 2%, the length results show a discrepancy of less than 1%, while Bhatia and Drachman's results show a discrepancy of -6.5%. Thus, by comparing Bhatia and Drachman's photodetachment cross section and the sum rule S_{-1} with the results obtained with the elaborate variational wave functions, it can be seen that the 'loosely' bound approximation works well for Ps^-. This is what Bhatia and Drachman [1] had expected in light of the very small binding energy of Ps^- and the comparison for H^- of the photodetachment cross section computed with the same approximation with an elaborate calculation [8].

Table 1. Values of the sum Rule S_{-1}

Source	(2a)	(2b)
WHML [4]	29.5	29.75
WHMV [4]	29.2	29.75
Bhatia and Drachman [1]	31.7	29.775

To test the accuracy of our 95 linear parameter initial-state wave function of Ps^-, we computed the electron affinity of Ps^- and obtained a value of 0.012004615 [5]. The most accurate prediction of the electron affinity at the time of our calculation was the calculation performed by Bhatia and Drachman [6] using their 220 linear parameter Hylleraas wave function. They obtained the value of 0.012005057 [6]. Using the Kohn variational method, we also computed the singlet and triplet S- and P-wave scattering phase shifts for e^--Ps scattering for energies below the Ps($n = 2$) threshold [4,7]. From S-wave phase shifts we obtained a value of 12.0 ± 0.3 for the singlet S-wave scattering length and a value of 4.6 ± 0.4 for the triplet [4]. From their 220 linear parameter Ps^- bound state wave function, Bhatia and Drachman [9] deduced a value for the singlet S-wave scattering length of 12.233 ± 0.006. The two sets of singlet S-wave scattering lengths agree to within the error bars.

III. e^+-H COLLISIONS

The problem of e^+-H collisions is of interest in astrophysics due to the observation of 511-keV line γ rays from solar flares, the galactic center and above the galactic center [10-12]. Analysis of the width of the 511-keV line using accurate Ps formation cross sections for e^+-H collisions provides information on the ionization state and temperature of the radiating medium. Dr. Richard Drachman studied e^+-H collisions over 30 years ago. For instance, he and his collaborators performed a rigorous bound-state calculation of e^+-H collisions for energies below the Ps formation threshold [13]. They used a generalized Hylleraas function which explicitly included a virtual Ps factor and computed the S-wave phase shifts for e^+-

H($1s$) collisions. In addition to this calculation, Houston and Drachman [14] computed S-wave phase shifts for e^+-H($1s$) collisions below the Ps($1s$) formation threshold using the Harris variational method and scattering lengths using the Kohn variational method. These variational calculations are still considered today as benchmark calculations [15].

Fairly recently, Macek, Ovchinnikov and I applied the hyperspherical hidden crossing method (HHCM) to Ps($1s$) formation in e^+-H($1s$) collisions for energies within the Ore gap [16]. This method had been formulated by Macek and Ovchinnikov to treat the correlated motion of three charged particles of arbitrary mass and charge [17]. The most attractive feature of the HHCM is that it provides insight into the scattering processes. Furthermore, it is ideally suited to treat rearrangement collisions since it treats the rearrangement and excitation on an equal footing.

For the case where there are only two open channels, the S-matrix modulus squared term $|\tilde{S}_{ij}|^2$ for the transition between two levels i and j is given by

$$|\tilde{S}^L_{ij}|^2 = 4P^L_{ij}(1 - P^L_{ij}) \sin^2 \Delta^L_{ij}, \tag{3}$$

where the Stückelberg phase Δ^L_{ij} is

$$\Delta^L_{ij} = \Re \int_C K(R) dR \tag{4}$$

and the one-way transition probability P^L_{ij} is

$$P^L_{ij} = \exp\left(- 2 \Im \int_C K(R) dR \right). \tag{5}$$

The wave vector in the HHCM is defined in terms of the adiabatic energy eigenvalues ε_μ

$$K^2_\mu(R) = 2\left(E - \varepsilon_\mu(R) - \frac{1}{8R^2} \right), \tag{6}$$

where E is the total energy of the three particle system. The contour integral C in Eqs.(4) and (5) starts at the classical turning point R^t_i of $\varepsilon_i(R)$, goes clockwise around the branch point R_b that connects levels i and j, and ends at the classical turning point R^t_j of $\varepsilon_j(R)$.

We computed the S-, P-, and D-wave cross section for Ps($1s$) formation in e^+-H($1s$) collisions in the Ore gap [16]. The P- and D-wave results compared reasonably well with the Kohn variational [18-19] and the Harris-Nesbet [20] results benchmark calculations, respectively. As showed by Humberston [21-22] using the Kohn variational method, the S-wave cross section is very small, except very close to the threshold. The reason for this can be understood from the HHCM [16]. The S-wave Stückelberg phase is close to π, which means that the two amplitudes corresponding to different paths leading to Ps formation destructively interfere. The D-wave contribution to the Ps formation cross section is dominant for about two-thirds of the energy range [16,19,20]. The D-wave Stückelberg phase is close to $\frac{\pi}{2}$, so that there is constructive interference between the two amplitudes that correspond to different paths leading to Ps formation.

Recently, using the HHCM, Shertzer and I [23] computed the S-, P-, D- and F-wave cross section for Ps($1s$) formation in e^+-Li($2s$) collisions in the energy range 0-1.8 eV. In this

energy range, there are only two open channels, elastic scattering and Ps(1s) formation. We confirmed the conclusion of Kohn variational results [24], namely, that away from threshold the S-wave cross section for Ps($1s$) formation in e^+-Li($2s$) collisions is very small. As for e^+-H($1s$), the S-wave Stückelberg phase is close to π, so that there occurs destructive interference between the two amplitudes corresponding to different paths leading to Ps($1s$) formation. At a particular energy, the Stückelberg phase is exactly π which gives a minimum in the Ps($1s$) formation cross section.

Using the Kohn variational method, Van Reeth and Humberston [25] computed the S-, P- and D-wave cross sections for Ps($1s$)-formation in e^+-He collisions in the Ore gap. They found the S-wave Ps($1s$) formation cross section is very small. It may be a universal result that the $L = 0$ Ps($1s$) formation cross section for e^+ collisions with any atom in a S ground-state is small. If so, our HHCM studies of e^+-H($1s$) [16] and e^+-Li($2s$) collisions [23] would suggest that the reason is due to destructive interference and that the Stückelberg phase is close to a multiple of π. Interestingly, McAlinden et. al. [26] recently noted for e^+-H^- collisions at 0.1eV, the S-wave contribution to Ps($1s$) formation cross section is small and the D-wave is dominant. The e^+-H^- collisions problem has been of interest to Dr. Richard Drachman. Straton and Drachman [27] applied orthogonalization corrections to the Coulomb (1^{st} order) Born approximation (CBA) to compute differential and total cross sections for Ps($1s$) formation in e^+-H^- collisions.

The reason why the Stückelberg phase should be close to π for S-wave Ps($1s$) formation in e^+-H($1s$) and e^+-Li($2s$) collisions is not known. There are, however, other examples in the literature of the Stückelberg phase being an integer values of $\frac{\pi}{2}$ which may help shed light on the reason. For instance, Ostrovsky [28] reported for the rearrangement process $d\mu(n_i) + t \rightarrow d + t\mu(n_f)$ for $L = 0$ Stückelberg phases close to integer multiples of $\frac{\pi}{2}$. In particular, for the $1s$-$1s$ transition, the Stückelberg phase is approximately 2π which means that reaction probability is strongly suppressed. This calculation [28] and our HHCM calculations [16,23] suggest that the Stückelberg phase is close to a multiple of π for a rearrangement process for a S ground-state to S ground-state transition. Nielsen and Macek [29] obtained a Stückelberg phase of 3π at a particular energy for the reaction $^4He + {}^4He + {}^4He \rightarrow {}^4He + {}^4He_2$ which gave a minimum in the S-wave transition probability. Miyashita et. al. [30] obtained a minimum in the transition probability for $L = 0$ electron-impact ionization of the collinear $Z = 1/4$ model atom. At the minimum the Stückelberg phase is a multiple of π.

Support from NSF, under grant PHY-0440565, is appreciated. Permission from IOP to reproduce the photodetachment, the sum rule and scattering length results from Ref. [4] is appreciated.

REFERENCES

[1] A. K. Bhatia and Richard J. Drachman, Phys. Rev. A **32**, 3745 (1985).

[2] Allen P. Mills, Jr., Phys. Rev. Lett., **46**, 717 (1981).

[3] Takashi Ohmura and Haruko Ohmura, Phys. Rev. **118**, 154 (1960).

[4] S. J. Ward, J. W. Humberston and M. R. C. McDowell, J. Phys. B **20**, 127 (1987).

[5] S. J. Ward, PhD Thesis, University of London, 1986.

[6] A. K. Bhatia and Richard J. Drachman, Phys. Rev. A **28**, 2523 (1983).

[7] S. J. Ward, J. W. Humberston, and M. R. C. McDowell, J. Phys. B **18**, L525 (1985).

[8] K. L. Bell and A. E. Kingston, Proc. Phys. Soc. (London) **90**, 895 (1967).

[9] A. K. Bhatia and Richard J. Drachman, *Proceedings of the Third International Workshop on Positron (Electron)-Gas Scattering*, edited by Kaupilla, W. E., Stein, T. S., and Wadehra J., (World Scientific, Sinapore, 1986), p. 310.

[10] H. S. W. Massey, Can. J. Phys. **60**, 461 (1982).

[11] M. Leventhal and B. L. Brown, *Proceedings of the Third International Workshop on Positron (Electron)-Gas Scattering*, edited by Kaupilla, W.E., Stein, T.S., and Wadehra J., (World Scientific, Sinapore, 1986), p. 140.

[12] E. Stokstad, Science **276**, 897 (1997).

[13] A. K. Bhatia, A. Temkin, Richard J. Drachman, and H. Eiserike, Phys. Rev. A **3**, 1328 (1971).

[14] S. K. Houston and Richard J. Drachman, Phys. Rev. A **3**, 1335 (1971).

[15] M. W. J. Bromley, and J. Mitroy, Phys. Rev. A **67**, 062709 (2003).

[16] S. J. Ward, J. H. Macek, and S. Yu. Ovchinnikov, Phys. Rev. A **59**, 4418 (1999).

[17] J. H. Macek and S. Yu. Ovchinnikov, Phys. Rev. A **54**, 544 (1996).

[18] C. J. Brown and J. W. Humberston, J. Phys. B **17**, L423 (1984); J. W. Humberston, P. Van Reeth, M. S. T. Watts, and W. E. Meyerhof, J. Phys.B **30**, 2477 (1997).

[19] C. J. Brown and J. W. Humberston, J. Phys.B **18**, L401 (1985).

[20] T. T. Gien, Phys. Rev. A **56**, 1332 (1997).

[21] J. W. Humberston, Can. J. Phys. **60**, 591 (1982).

[22] J. W. Humberston, J. Phys. B **17**, 2353 (1984).

[23] S. J. Ward and J. Shertzer, Phys. Rev. A **68**, 032720 (2003); Nucl. Instrum. Methods Phys. Res. **221**, 206 (2004); Nucl. Instrum. Methods Phys. Res. **241**, 257 (2005).

[24] M. S. T. Watts and J. W. Humberston, J. Phys. B **25**, L491 (1992).

[25] P. Van Reeth and J. W. Humberston, J. Phys. B **28**, L23 (1995); J. Phys. B **30**, L95 (1997); J. Phys. B **31**, L621(1998); J. Phys. B **32**, L103 (1999); J. Phys. B **32**, 3651 (1999).

[26] Mary T. McAlinden, Jennifer E. Blackwood, and H. R. J. Walters, Phys. Rev. A, **65**, 032715 (2002).

[27] Jack C. Straton and Richard J. Drachman, Phys. Rev. A **44**, 7335 (1991).

[28] V. N. Ostrovsky, Phys. Rev. A **61**, 032505 (2000).

[29] Esben Nielsen and J. H. Macek, Phys. Rev. Lett. **83**, 1566 (1999).

[30] Naoyuki Miyashita, Shinichi Watanabe, Michio Matsuzawa and Joseph H. Macek, Phys. Rev. A **61**, 014901 (1999).

ASYMPTOTIC ENERGIES AND QED SHIFTS FOR THE RYDBERG STATES OF HELIUM

G.W.F. Drake
Department of Physics, University of Windsor
Windsor, Ontario, Canada N9B 3P4[1]

ABSTRACT

This paper reviews progress that has been made in obtaining essentially exact solutions to the nonrelativistic three-body problem for helium by a combination of variational and asymptotic expansion methods. The calculation of relativistic and quantum electrodynamic corrections by perturbation theory is discussed, and in particular, methods for the accurate calculation of the Bethe logarithm part of the electron self energy are presented. As an example, the results are applied to the calculation of isotope shifts for the short-lived 'halo' nucleus ^{6}He relative to ^{4}He in order to determine the nuclear charge radius of ^{6}He from high precision spectroscopic measurements carried out at the Argonne National Laboratory. The results demonstrate that the high precision that is now available from atomic theory is creating new opportunities to create novel measurement tools, and helium, along with hydrogen, can be regarded as a fundamental atomic system whose spectrum is well understood for all practical purposes.

INTRODUCTION

The goal of the work presented here is to obtain essentially exact theoretical values for the energy levels for the entire singly excited spectrum of helium and its isotopes, including all terms up to order α^3 Ry, where $\alpha \simeq 1/137.035\,999\,11(46)$ is the fine structure constant. The achievement of this goal requires accurate nonrelativistic eigenvalues, relativistic corrections of order α^2 Ry, and quantum electrodynamic corrections of order α^3 Ry. Recent advances over the past several years now make it possible to obtain solutions to the quantum mechanical three- and four-body problem that are essentially exact for all practical purposes, at least in the nonrelativistic limit. The calculation of the lowest order α^2 Ry relativistic corrections is then straight forward, but the calculation of the QED corections (especially the Bethe logarithm) has remained a long- standing problem in atomic physics. This last problem has also now been solved, as will be described in this paper, thereby opening the way to complete calculations up to order α^3 Ry.

On the experimental side, there is a large body of high precision data available for comparison. The particular significance in relation to the present work is that the theoretical uncertainty in the D-states is now so small that their energies can be taken as absolute points of reference. The measured transition frequencies to the lower-lying S- and P-states can then be used to determine the absolute ionization energies of these states (see Drake and Martin [1]), and from this the QED energy shifts can be determined.

The second goal of this work is to use the comparison between theory and experiment for the isotope shift to determine the nuclear charge radius for various isotopes of helium. There is now considerable interest in using this method to measure the nuclear charge radii of of exotic 'halo' nuclei such as ^{6}He and ^{8}He first discovered by Tanihata [2]. As will be seen, this technique provides a unique measurement tool to perform nuclear size measurements that cannot be done in any other way.

[1]E-mail: GDrake@uwindsor.ca

Table 1: Contributions to the energy and their orders of magnitude in terms of Z, $\mu/M = 1.370\,745\,624 \times 10^{-4}$, and $\alpha^2 = 0.532\,513\,5450 \times 10^{-4}$.

Contribution	Magnitude
Nonrelativistic energy	Z^2
Mass polarization	$Z^2\mu/M$
Second-order mass polarization	$Z^2(\mu/M)^2$
Relativistic corrections	$Z^4\alpha^2$
Relativistic recoil	$Z^4\alpha^2\mu/M$
Anomalous magnetic moment	$Z^4\alpha^3$
Hyperfine structure	$Z^3 g_I \mu_0^2$
Lamb shift	$Z^4\alpha^3 \ln\alpha + \cdots$
Radiative recoil	$Z^4\alpha^3(\ln\alpha)\mu/M$
Finite nuclear size	$Z^4\langle \bar{r}_c/a_0\rangle^2$

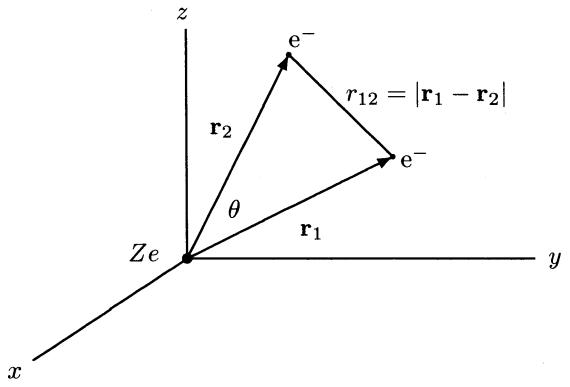

Figure 1: Coordinate system for a helium atom with the nucleus at the origin.

THEORETICAL BACKGROUND

Table 1 summarizes the various contributions to the energy, expressed as a double expansion in powers of $\alpha \simeq 1/137.036$ and the electron reduced mass ratio $\mu/M \simeq 10^{-4}$. Since all the lower-order terms can now be calculated to very high precision, including the QED terms of order α^3 Ry, the dominant source of uncertainty comes from the QED corrections of order α^4 Ry or higher. The comparison between theory and experiment is therefore sensitive to these terms. For the isotope shift, the QED terms independent of μ/M cancel out, and so it is only the radiative recoil terms of order $\alpha^4\mu/M \simeq 10^{-12}$Ry ($\sim$ 10 kHz) that contribute to the uncertainty. Since this is much less than the finite nuclear size correction of about 1 MHz, the comparison between theory and experiment clearly provides a means to determine the nuclear size.

Solution to the Nonrelativistic Schrödinger Equation

The starting point for the calculation is to find accurate solutions to the Schrödinger equation for helium. Considering first the case of infinite nuclear mass, the equation in atomic units is given by

$$\left(-\frac{1}{2}\nabla_1^2 - \frac{1}{2}\nabla_2^2 - \frac{Z}{r_1} - \frac{Z}{r_2} + \frac{1}{r_{12}}\right)\Psi(\mathbf{r}_1,\mathbf{r}_2) = E\Psi(\mathbf{r}_1,\mathbf{r}_2) \tag{1}$$

The usual methods of theoretical atomic physics, such as the Hartree-Fock approximation or configuration interaction methods, are not capable of yielding results of spectroscopic accuracy. For this reason, specialized methods have been developed. As long ago as 1929, Hylleraas suggested expanding the wave function in an explicitly correlated variational basis set of the form

$$\Psi(\mathbf{r}_1,\mathbf{r}_2) = \sum_{i,j,k} a_{ijk}\, r_1^i r_2^j r_{12}^k\, e^{-\alpha r_1 - \beta r_2}\, \mathcal{Y}^M_{l_1 l_2 L}(\hat{\mathbf{r}}_1,\hat{\mathbf{r}}_2) \tag{2}$$

where $r_{12} = |\mathbf{r}_1 - \mathbf{r}_2|$ is the interelectronic separation (see Fig. 1). The coefficients a_{ijk} are linear variational parameters, and α and β are nonlinear variational coefficients that set the distance scale for the wave function. The usual strategy is to include all powers such that $i + j + k \leq \Omega$ (a so-called Pekeris shell), where Ω is an integer. The inclusion of powers of r_{12}, and especially the odd powers, makes the basis set rapidly convergent as Ω increases. The basis set is proveably complete in the limit $\Omega \to \infty$ [3].

For states of higher angular momentum L, the quantity $\mathcal{Y}^M_{l_1 l_2 L}(\hat{\mathbf{r}}_1,\hat{\mathbf{r}}_2)$ denotes a vector-coupled product of spherical harmonics, and the basis set includes a summation over the possible integer values of l_1 and l_2 (with l_2 constrained to be $l_2 = L - l_1$) such that $l_1 \leq L/2$. In addition, the nonlinear parameters α and β are separately optimized for each set of angular momentum terms, and, as discussed in Refs. [4, 5, 6], it is desirable further to 'double' the basis set so that each set of powers $\{i, j, k\}$ is included two (or more [7]) times with different values of α and β. For sufficiently large basis sets, the doubling is very important because it helps to preserve the numerical stability of the wave function, it gives improved accuracy for a given total size of basis set, and it avoids the disasterous loss of accuracy that normally sets in for variational calculations involving the higher-lying Rydberg states [4, 5, 6].

The principal computational steps are first to orthogonalize the χ_{ijk} basis set, and then to diagonalize the Hamiltonian matrix $\mathbf{H}$ in the orthogonalized basis set so as to satisfy the Rayleigh-Schrödinger variational principle

$$\delta \int \Psi\,(H - E)\,\Psi\, d\tau = 0. \tag{3}$$

Finally, a complete optimization is performed with respect to variations in the αs and βs so as to minimize the energy.

For high precision calculations, and especially for the istope shift, it is necessary to include also the motion of the nucleus in the center-of-mass (CM) frame. A transformation to CM plus relative coordinates yields the additional $-(\mu/M)\nabla_1 \cdot \nabla_2$ mass polarization term in the modified Hamiltonian

$$H = -\frac{1}{2}\nabla_1^2 - \frac{1}{2}\nabla_2^2 - \frac{Z}{r_1} - \frac{Z}{r_2} + \frac{1}{r_{12}} - \frac{\mu}{M}\nabla_1 \cdot \nabla_2 \tag{4}$$

in reduced mass atomic units e^2/a_μ, where $a_\mu = (m_e/\mu)a_0$ is the reduced mass Bohr radius, and $\mu = m_e M/(m_e + M)$ is the electron reduced mass, M is the nuclear mass, and $a_0 = \hbar^2/m_e e^2$ is the Bohr radius. The mass polarization term can be treated either by including it as a perturbation (up to second-order),

Table 2: Convergence study for the ground state of helium (infinite nuclear mass case) [7]. N is the number of terms in the 'triple' basis set.

Ω	N	$E(\Omega)$	$R(\Omega)$
8	269	−2.903 724 377 029 560 058 400	
9	347	−2.903 724 377 033 543 320 480	
10	443	−2.903 724 377 034 047 783 838	7.90
11	549	−2.903 724 377 034 104 634 696	8.87
12	676	−2.903 724 377 034 116 928 328	4.62
13	814	−2.903 724 377 034 119 224 401	5.35
14	976	−2.903 724 377 034 119 539 797	7.28
15	1150	−2.903 724 377 034 119 585 888	6.84
16	1351	−2.903 724 377 034 119 596 137	4.50
17	1565	−2.903 724 377 034 119 597 856	5.96
18	1809	−2.903 724 377 034 119 598 206	4.90
19	2067	−2.903 724 377 034 119 598 286	4.44
20	2358	−2.903 724 377 034 119 598 305	4.02
Extrapolation	∞	−2.903 724 377 034 119 598 311(1)	
Korobov [11]	5200	−2.903 724 377 034 119 598 311 158 7	
Korobov extrap.	∞	−2.903 724 377 034 119 598 311 159 4(4)	
Schwartz [12]	10259	−2.903 724 377 034 119 598 311 159 245 194 404 4400	
Schwartz extrap.	∞	−2.903 724 377 034 119 598 311 159 245 194 404 446	
Goldman [13]	8066	−2.903 724 377 034 119 593 82	
Bürgers *et al.* [14]	24 497	−2.903 724 377 034 119 589(5)	
Baker *et al.* [15]	476	−2.903 724 377 034 118 4	

or by including it explicitly in the Hamiltonian. The latter procedure is simpler and more direct, and the coefficient of the second-order term can still be extracted by differencing [4, 6]. A general method for the decomposition of this equation was developed many years ago by Bhatia and Temkin [8], and the effects of mass polarization studied by Bhatia and Drachman [9] for a range of values of μ/M. These authors have also extended the calculation of the second-order mass polarization term for several low-lying states to the He-like ions [10].

As an example, Table 2 shows a convergence study for the very well studied case of the ground state of helium [7]. The quantity R in the last column is the ratio of successive differences between the energies. A constant or slowly changing value of R indicates smooth convergence, and allows a reliable extrapolation to $\Omega \to \infty$. The results clearly indicate that convergence to 20 or more figures can be readily obtained, using conventional quadruple precision (32 decimal digit) arithmetic in FORTRAN. The very large calculation by Schwartz [12], using 104-digit arithmetic, provides a benchmark for comparison.

ASYMPTOTIC EXPANSION METHOD

Richard Drachman is largely responsible for the development of the asymptotic expansion method for helium, based on a core polarization model [16, 17, 18, 19, 20, 21]. It provides a means to give a physical interpretation and meaning to these long strings of significant figures for the nonrelativistic eigenvalues, at least in the limit

Table 3: Variational energies for the $n = 10$ singlet and triplet states of helium.

State	Singlet	Triplet
10 S	−2.005 142 991 747 919(79)	−2.005 310 794 915 611 3(11)
10 P	−2.004 987 983 802 217 9(26)	−2.005 068 805 497 706 7(30)
10 D	−2.005 002 071 654 256 81(75)	−2.005 002 818 080 228 84(53)
10 F	−2.005 000 417 564 668 80(11)	−2.005 000 421 686 604 88(26)
10 G	−2.005 000 112 764 318 746(22)	−2.005 000 112 777 003 317(21)
10 H	−2.005 000 039 214 394 532(17)	−2.005 000 039 214 417 416(17)
10 I	−2.005 000 016 086 516 1947(3)	−2.005 000 016 086 516 2194(3)
10 K	−2.005 000 007 388 375 8769(0)	−2.005 000 007 388 375 8769(0)

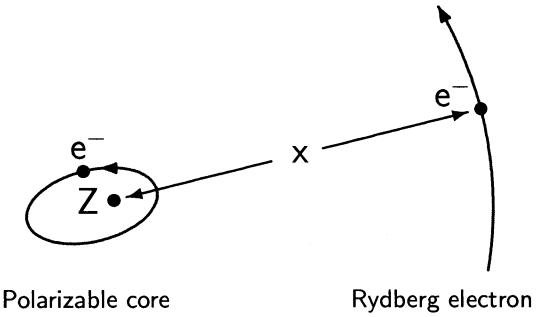

Figure 2: Illustration of the physical basis for the asymptotic expansion method in which the Rydberg electron moves in the field generated by the polarized core.

of large L. As shown in Table 3 for the list of states with $n = 10$, the singlet-triplet splitting goes exponentially to zero with increasing L, so that for $L = 7$ (K-states), the splitting is no longer visible to the 20 figure accuracy of the calculations. This indicates that the Rydberg electron can be treated as a distinguishable particle interacting with a polarizable core consisting of the nucleus and the inner $1s$ electron. The leading figures in the energies correspond to the simple screened hydrogenic energy

$$\begin{aligned} E &= -2 - \frac{1}{2n^2} + \cdots \\ &= -2.005 \cdots \end{aligned} \tag{5}$$

for $n = 10$. Here, the -2 is the energy of the inner $1s$ electron with nuclear charge $Z = 2$, and the $-1/(2n^2)$ is the energy of the outer Rydberg electron for the screened nuclear charge $Z = 1$. For the 10K state, this simple calculation accounts for the leading eight significant figures in the energy, and so all the interesting physics is contained in the figures that come after the eighth.

Our objective now is to see how much of this interesting physics after the eighth figure in the energy (for K-states) can be understood in terms of the asymptotic expansion method. Figure 2 illustrates the physical basis for the core polarization model. Letting x denote the radial coordinate of the Rydberg electron, it moves in the asymptotic potential

$$V(x) = -\frac{Z-1}{x} + \Delta V(x) \tag{6}$$

Table 4: Asymptotic expansion for the energy of the 1s10k state of helium.

Quantity	Value
$-Z^2/2$	–2.000 000 000 000 000 00
$-1/(2n^2)$	–0.005 000 000 000 000 00
$c_4\langle r^{-4}\rangle$	–0.000 000 007 393 341 95
$c_6\langle r^{-6}\rangle$	0.000 000 000 004 980 47
$c_7\langle r^{-7}\rangle$	0.000 000 000 000 278 95
$c_8\langle r^{-8}\rangle$	–0.000 000 000 000 224 33
$c_9\langle r^{-9}\rangle$	–0.000 000 000 000 002 25
$c_{10}\langle r^{-10}\rangle$	0.000 000 000 000 003 73
Second order	–0.000 000 000 000 070 91
Total	–2.005 000 007 388 376 30(74)
Variational	–2.005 000 007 388 375 8769(0)
Difference	–0.000 000 000 000 000 42(74)
	$\simeq$ 3 Hz

where $Z-1$ is the screened nuclear charge, and the polarization potential due to the core is

$$\Delta V(x) = -\frac{c_4}{x^4} - \frac{c_6}{x^6} - \frac{c_7}{x^7} - \frac{c_8}{x^8} - \frac{c_9}{x^9} - \frac{c_{10}}{x^{10}} + \cdots \tag{7}$$

For example, $c_4 = \alpha_1/2$, where α_1 is the dipole polarizability of the core, and the other coefficients are similarly related to the higher multipole moments of the core. Since the core is a one-electron hydrogenic problem, all the c_i coefficients can be calculated exactly as simple rational fractions [6]. For example, $\alpha_1 = 9/(2Z^4)\, a_0^3$.

The screened hydrogenic energy is then given by

$$\Delta E_{nL} = -\frac{(Z-1)^2}{2n^2} + \langle\chi_0 \mid \Delta V(x) \mid \chi_0\rangle + \langle\chi_0 \mid \Delta V(x) \mid \chi_1\rangle \tag{8}$$

where $\mid \chi_1\rangle$ is first-order perturbation correction to $\mid \chi_0\rangle$ due to $\Delta V(x)$; i.e. it satisfies the perturbation equation [22]

$$[h_0(x) - e_0] \mid \chi_1\rangle + \Delta V(x) \mid \chi_0\rangle = \mid \chi_0\rangle\langle\chi_0 \mid \Delta V(x) \mid \chi_0\rangle \tag{9}$$

Continuing with the example of $n = 10$, Table 4 lists the various contributions from the multipole expansion for the case $L = 7$, including the second-order term. The ± 3 Hz accuracy of the asymptotic expansion is more than sufficient for comparisons with experiment. For low L, the asymptotic expansion is much less accurate because the series must be truncated when the terms start increasing. Indeed the expectation values $\langle 1/x^n\rangle$ diverge for $n > 2L+2$. However, the accuracy rapidly improves with increasing L, and there is clearly no need for direct variational calculations for $L > 7$.

Variational Basis Sets for Lithium

The same variational techniques can be applied to lithium and other three-electron atomic systems. In this case, the terms in the Hylleraas correlated basis set have the form

$$r_1^{j_1}\, r_2^{j_2}\, r_3^{j_3}\, r_{12}^{j_{12}}\, r_{23}^{j_{23}}\, r_{31}^{j_{31}}\, e^{-\alpha r_1 - \beta r_2 - \gamma r_3}\, \mathcal{Y}^{LM}_{(\ell_1\ell_2)\ell_{12},\ell_3}(\mathbf{r}_1, \mathbf{r}_2, \mathbf{r}_3)\, \chi_1\,, \tag{10}$$

where $\mathcal{Y}^{LM}_{(\ell_1\ell_2)\ell_{12},\ell_3}$ is again a vector-coupled product of spherical harmonics, and χ_1 is a spin function with spin angular momentum 1/2. As for helium, the usual strategy is to include all terms from (10) such that

$$j_1 + j_2 + j_3 + j_{12} + j_{23} + j_{31} \quad \leq \quad \Omega\,, \tag{11}$$

and study the eigenvalue convergence as Ω is progressively increased. The lithium problem is much more difficult than helium both because the integrals over fully correlated wave functions are more difficult, and because the basis set grows much more rapidly with increasing Ω. Nevertheless, there has been important progress in recent years [23, 24, 25], and results of spectroscopic accuracy can be obtained for the low-lying states.

Bhatia and Drachman have also made important progress in applying the asymptotic expansion methods to the Rydberg states of lithium [26, 27, 28]. The calculations in this case are more difficult because the 'polarizable core' now consists of the nucleus and two $1s$ electrons, and so its multipole moments cannot be calculated analytically.

RELATIVISTIC CORRECTIONS

This section briefly summarizes the lowest-order relativistic corrections of order α^2 Ry, and the relativistic recoil corrections of order $\alpha^2\mu/M$ Ry. The well-known terms in the Breit interaction [29] (including for convenience the anomalous magnetic moment terms of order α^3 Ry) give rise to the first-order perturbation correction

$$\Delta E_{\rm rel} \quad = \quad \langle \Psi_J | H_{\rm rel} | \Psi_J \rangle\,, \tag{12}$$

where Ψ_J is a nonrelativistic wave function for total angular momentum $\mathbf{J} = \mathbf{L} + \mathbf{S}$ and $H_{\rm rel}$ is defined by (in atomic units)

$$\begin{aligned} H_{\rm rel} \quad = \quad & \left(\frac{\mu}{m_{\rm e}}\right)^4 B_1 + \left(\frac{\mu}{m_{\rm e}}\right)^3 \Bigg[B_2 + B_4 + B_{\rm so} + B_{\rm soo} + B_{\rm ss} + \frac{m_{\rm e}}{M}(\tilde{\Delta}_2 + \tilde{\Delta}_{\rm so}) \\ & + \gamma \left(2B_{\rm so} + \frac{4}{3} B_{\rm soo} + \frac{2}{3} B^{(1)}_{3e} + 2B_5 \right) + \gamma \frac{m_{\rm e}}{M} \tilde{\Delta}_{\rm so} \Bigg]\,. \end{aligned} \tag{13}$$

with $\gamma = \alpha/(2\pi)$. The factors of $(\mu/m_{\rm e})^4 = (1 - \mu/M)^4$ and $(\mu/m_{\rm e})^3 = (1 - \mu/M)^3$ arise from the mass scaling of each term in the Breit interaction, while the terms $\tilde{\Delta}_2$ and $\tilde{\Delta}_{\rm so}$ are dynamical corrections arising from the transformation of the Breit interaction to CM plus relative coordinates [30]. These latter terms are often not included in atomic structure calculations, but they make an important contribution to the isotope shift. The explicit expressions for the spin-independent operators are

$$B_1 = \frac{\alpha^2}{8}(p_1^4 + p_2^4) \tag{14}$$

$$B_2 = -\frac{\alpha^2}{2}\left(\frac{1}{r_{12}} \mathbf{p}_1 \cdot \mathbf{p}_2 + \frac{1}{r_{12}^3} \mathbf{r}_{12} \cdot (\mathbf{r}_{12} \cdot \mathbf{p}_1) \mathbf{p}_2 \right) \tag{15}$$

$$B_4 = \alpha^2 \pi \left(\frac{Z}{2} \delta(\mathbf{r}_1) + \frac{Z}{2} \delta(\mathbf{r}_2) - \delta(\mathbf{r}_{12}) \right) \tag{16}$$

and the spin-dependent terms are

$$B_{\rm so} = \frac{Z\alpha^2}{4} \left[\frac{1}{r_1^3} (\mathbf{r}_1 \times \mathbf{p}_1) \cdot \boldsymbol{\sigma}_1 + \frac{1}{r_2^3} (\mathbf{r}_2 \times \mathbf{p}_2) \cdot \boldsymbol{\sigma}_2 \right] \tag{17}$$

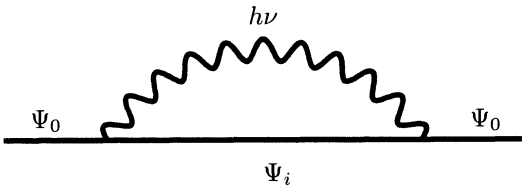

Figure 3: Feynman diagram for the electron self energy.

$$B_{\rm soo} = \frac{\alpha^2}{4}\left[\frac{1}{r_{12}^3}\mathbf{r}_{12}\times\mathbf{p}_2\cdot(2\boldsymbol{\sigma}_1+\boldsymbol{\sigma}_2) - \frac{1}{r_{12}^3}\mathbf{r}_{12}\times\mathbf{p}_1\cdot(2\boldsymbol{\sigma}_2+\boldsymbol{\sigma}_1)\right] \tag{18}$$

$$B_{\rm ss} = \frac{\alpha^2}{4}\left[-\frac{8}{3}\pi\delta(\mathbf{r}_{12}) + \frac{1}{r_{12}^3}\boldsymbol{\sigma}_1\cdot\boldsymbol{\sigma}_2 - \frac{3}{r_{12}^3}(\boldsymbol{\sigma}_1\cdot\mathbf{r}_{12})(\boldsymbol{\sigma}_2\cdot\mathbf{r}_{12})\right] \tag{19}$$

Finally, the relativistic recoil terms are [30]

$$\begin{aligned}\tilde{\Delta}_2 &= -\frac{Z\alpha^2}{2}\left\{\frac{1}{r_1}(\mathbf{p}_1+\mathbf{p}_2)\cdot\mathbf{p}_1 + \frac{1}{r_1^3}br_1\cdot[\mathbf{r}_1\cdot(\mathbf{p}_1+\mathbf{p}_2)]\mathbf{p}_1\right.\\ &\left.+\frac{1}{r_2}(\mathbf{p}_1+\mathbf{p}_2)\cdot\mathbf{p}_2 + \frac{1}{r_2^3}br_2\cdot[\mathbf{r}_2\cdot(\mathbf{p}_1+\mathbf{p}_2)]\mathbf{p}_2\right\}\end{aligned} \tag{20}$$

$$\tilde{\Delta}_{\rm so} = \frac{Z\alpha^2}{2}\left(\frac{1}{r_1^3}\mathbf{r}_1\times\mathbf{p}_2\cdot\boldsymbol{\sigma}_1 + \frac{1}{r_2^3}\mathbf{r}_2\times\mathbf{p}_1\cdot\boldsymbol{\sigma}_2\right) \tag{21}$$

It is then a relatively straight forward matter to calculate accurate expectation values for these operators. Also, asymptotic expansions have been derived for the matrix elements and compared with the direct variational calculations, as discussed in Ref. [6].

QED CORRECTIONS

For a many-electron atom, the total QED shift of order α^3 Ry consists of two parts—an electron-nucleus part $E_{\rm L,1}$ (the Kabir-Salpeter term [31]), and an electron-electron term $E_{\rm L,2}$ originally obtained by Araki [32] and Sucher [33]. The $E_{\rm L,2}$ term is relatively small and stright-forward to calculate. The principal computational challenges come from the $E_{\rm L,1}$ term given by (in atomic units)

$$E_{L,1} = \frac{4}{3}Z\alpha^3\langle\delta(\mathbf{r}_1)+\delta(\mathbf{r}_2)\rangle\left[\ln\alpha^{-2} - \beta(1s n\ell) + \frac{19}{30}\right] \tag{22}$$

where $\beta(1sn\ell)$ is the two-electron Bethe logarithm arising from the emission and re-absorption of a virtual photon (see Fig. 3). It is the logarithmic remainder after mass renormalization, and is defined by

$$\beta(1sn\ell) = \frac{\mathcal{N}}{\mathcal{D}} = \frac{\sum_i |\langle\Psi_0|\mathbf{p}_1+\mathbf{p}_2|i\rangle|^2(E_i-E_0)\ln|E_i-E_0|}{\sum_i |\langle\Psi_0|\mathbf{p}_1+\mathbf{p}_2|i\rangle|^2(E_i-E_0)} \tag{23}$$

The foregoing equations are virtually identical to the corresponding one-electron (hydrogenic) case, except that there the δ-function matrix elements can be replaced by their hydrogenic value

$$\langle\delta(\mathbf{r}_1)+\delta(\mathbf{r}_2)\rangle \to Z^3/(\pi n^3) \tag{24}$$

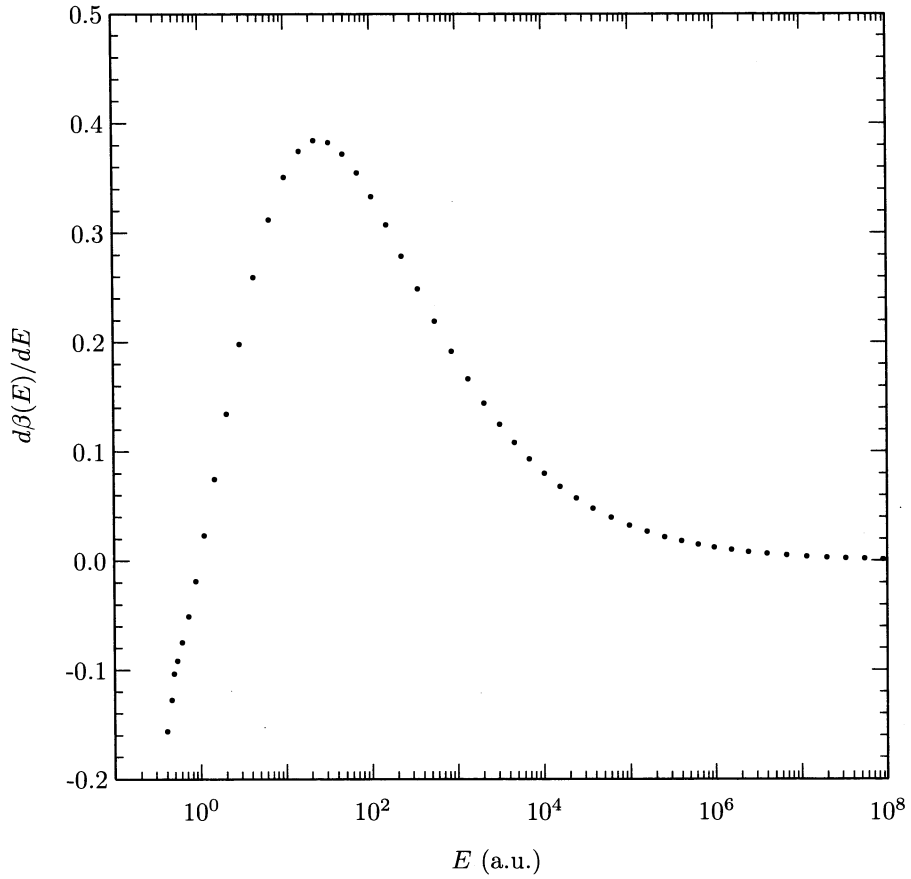

Figure 4: Differential contributions to the Bethe logarithm for the ground state of hydrogen. Each point represents the contribution from one pseudostate.

The sum in the denominator of (23) can be completed by closure with the result

$$\mathcal{D} = \langle\Psi_0|\mathbf{p}(H - E_0)\mathbf{p}|\Psi_0\rangle = 2\pi Z\langle\delta(\mathbf{r}_1) + \delta(\mathbf{r}_2)\rangle \tag{25}$$

where $\mathbf{p} = \mathbf{p}_1 + \mathbf{p}_2$. The numerator is much more difficult to calculate because the sum over intermediate states (including an integration over the continuum) cannot be performed analytically, and a sum over pseudostates nearly diverges at high energies. Schwartz [34] transformed the numerator to read

$$\mathcal{N} = \lim_{K\to\infty}\left(-K\langle\Psi_0|\mathbf{p}\cdot\mathbf{p}|\Psi_0\rangle + \mathcal{D}\ln(K) + \int_0^K k\,dk\langle\Psi_0|\mathbf{p}(H - E_0 + k)^{-1}\mathbf{p}|\Psi_0\rangle\right) \tag{26}$$

However, this is slowly convergent, and expensive in computer time since a matrix diagonalization must be performed at each integration point. Despite this, results of useful accuracy for the lowest-lying S- and P-states have been obtained by this method in Refs. [35], [36], and [37].

An alternative method based on a discrete variational representation of the continuum in terms of pseudostates has been developed by Drake and Goldman [38]. The method is simplest to explain for the case of hydrogen. The key idea is to define a variational basis set containing a huge range of distance scales

Table 5: Convergence of the Bethe logarithm $\beta(1s) = \ln(k_0/\mathrm{R}_\infty)$ for hydrogen. $\mathrm{R}_\infty = 3.289\,841\,960\,360(22) \times 10^9$ MHz is the Rydberg constant.

Ω	N	$\beta(1s)$	Differences	Ratios
2	3	2.73448191727230174149		
3	6	2.94877219077044909822	0.21429027349814735672	
4	10	2.97975301862169611861	0.03098082785124702039	6.917
5	15	2.98361449929795351803	0.00386148067625739942	8.023
6	21	2.98407183714911362800	0.00045733785116010997	8.443
7	28	2.98412247036420809592	0.00005063321509446792	9.032
8	36	2.98412792735460886871	0.00000545699040077279	9.279
9	45	2.98412849201006208099	0.00000056465545321228	9.664
10	55	2.98412854946585020174	0.00000005745578812075	9.828
11	66	2.98412855514977775545	0.00000000568392755370	10.108
12	78	2.98412855570645173753	0.00000000055667398208	10.211
13	91	2.98412855575986426711	0.00000000005341252957	10.422
14	105	2.98412855576496736061	0.00000000000510309350	10.467
15	120	2.98412855576544766988	0.00000000000048030928	10.625
16	136	2.98412855576549294823	0.00000000000004527834	10.608
17	153	2.98412855576549717245	0.00000000000000422422	10.719
18	171	2.98412855576549756974	0.00000000000000039729	10.633
19	190	2.98412855576549760688	0.00000000000000003714	10.697
20	210	2.98412855576549761038	0.00000000000000000351	10.594
Extrap.		2.98412855576549761075		

according to:

$$\chi_{i,j} = r^i \exp(-\alpha_j r)\cos(\theta), \tag{27}$$

with $j = 0, 1, \ldots, \Omega - 1$, $i = 0, 1, \ldots, \Omega - j - 1$, and

$$\alpha_j = \alpha_0 \times g^j, \quad g \simeq 10, \quad \alpha_0 \simeq 1\,. \tag{28}$$

Thus, each increase in Ω introduces another set of terms containing different powers of r, but with a distance scale $1/\alpha_j$ that is approximately a factor of 10 smaller than the previous one (a number close to 10 happens to be the variational optimum). For example, for p-states $\chi_{0,20} \simeq \exp(10^{20} r)\cos\theta$. As shown in Fig. 4, this has the effect of pushing the eigenvalue spectrum up to enormously high energies far above the few tens of atomic units that one would normally expect for a variational basis set. The number of elements is $N = \Omega(\Omega+1)/2$. One then follows the usual procedure of orthogonalizing the basis set, and then diagonalizing the Hamiltonian to generate a set of N pseudostates that can be summed over to calculate the Bethe logarithm.

As an example, for the ground $1s$ state of hydrogen, one would generate a set of pseudostates with p-symmetry, and then calculate the dipole transition integrals in Eq. (23). An additional trick to speed convergence is to include in the basis set terms that behave as r^{l-1} at the origin for pseudostates of angular momentum l. Such terms of course do not contribute to the exact wave functions of angular momentum l, but they do contribute to the effective Green's function that the sum over intermediate states represents (see Ref. [38] for further details). The results in Table 5 demonstrate that the Bethe logarithm calculated in this way converges to the known result for the $1s$ ground state of hydrogen to 20 figure accuracy. Figure 4 shows the differential contributions to the Bethe logarithm from each pseudostate. It is clear that extremely high energies are needed to capture the majority of the Bethe logarithm. The basis set has good numerical stability, and standard quadruple precision (32 decimal digit) arithmetic is sufficient for the example shown.

Table 6: Bethe logarithms $\ln(k_0/Z^2\mathrm{R}_\infty)$ for He-like atoms, from Ref. [38] (see also Ref. [39]).

State	$Z=2$	$Z=3$	$Z=4$	$Z=5$	$Z=6$
$1\ ^1$S	2.983 865 9(1)	2.982 624 558(1)	2.982 503 05(4)	2.982 591 383(7)	2.982 716 949(1)
$2\ ^1$S	2.980 118 275(4)	2.976 363 09(2)	2.973 976 98(4)	2.972 388 16(3)	2.971 266 29(2)
$2\ ^3$S	2.977 742 36(1)	2.973 851 679(2)	2.971 735 560(4)	2.970 424 952(5)	2.969 537 065(5)
$2\ ^1$P	2.983 803 49(3)	2.983 186 10(2)	2.982 698 29(1)	2.982 340 18(7)	2.982 072 79(6)
$2\ ^3$P	2.983 690 84(2)	2.982 958 68(7)	2.982 443 5(1)	2.982 089 5(1)	2.981 835 91(5)
$3\ ^1$S	2.982 870 512(3)	2.981 436 5(3)	2.980 455 81(7)	2.979 778 086(4)	2.979 289 8(9)
$3\ ^3$S	2.982 372 554(8)	2.980 849 595(7)	2.979 904 876(3)	2.979 282 037	2.978 844 34(6)
$3\ ^1$P	2.984 001 37(2)	2.983 768 943(8)	2.983 584 906(6)	2.983 449 763(6)	2.983 348 89(1)
$3\ ^3$P	2.983 939 8(3)	2.983 666 36(4)	2.983 479 30(2)	2.983 350 844(8)	2.983 258 40(4)
$4\ ^1$S	2.983 596 31(1)	2.982 944 6(3)	2.982 486 3(1)	2.982 166 154(3)	2.981 932 94(5)
$4\ ^3$S	2.983 429 12(5)	2.982 740 35(4)	2.982 291 37(7)	2.981 988 21(2)	2.981 772 015(7)
$4\ ^1$P	2.984 068 766(9)	2.983 961 0(2)	2.983 875 8(1)	2.983 813 2(1)	2.983 766 6(2)
$4\ ^3$P	2.984 039 84(5)	2.983 913 45(9)	2.983 828 9(1)	2.983 770 1(2)	2.983 727 5(2)
$5\ ^1$S	2.983 857 4(1)	2.983 513 01(2)	2.983 267 901(6)	2.983 094 85(5)	2.982 968 66(2)
$5\ ^3$S	2.983 784 02(8)	2.983 422 50(2)	2.983 180 677(6)	2.983 015 17(3)	2.982 896 13(2)
$5\ ^1$P	2.984 096 174(9)	2.984 038 03(5)	2.983 992 23(1)	2.983 958 67(5)	2.983 933 65(5)
$5\ ^3$P	2.984 080 3(2)	2.984 014 4(4)	2.983 968 9(4)	2.983 937 2(4)	2.983 914 07(6)

Bethe Logarithms for Helium and Lithium

The basis sets for helium and lithium are more complicated in detail but the principles are the same. In each case the Bethe logarithm comes almost entirely from virtual excitations of the inner $1s$ electron to p-states lying high in the photoionization continuum, and so the basis set must be extended to very short distances for this particle. The outer electrons are to a good approximation just spectators to these virtual excitations.

Results for the low-lying states of helium and the He-like ions are listed in Table 6 (see also Korobov [39]). In order to make the connection with the hydrogenic Bethe logarithm more obvious, the quantity tabulated is $\ln(k_0/Z^2\mathrm{R}_\infty)$. The effect of dividing by a factor of Z^2 is to reduce all the Bethe logarithms to approximately the same number $\beta(1s) = 2.984\,128\,556$ for the ground state of hydrogen. It is convenient to express the results in the form $\beta(1snL) = \beta(1s) + \Delta\beta(nL)/n^3$, where $\Delta\beta(nL)$ is a small number that tends to a constant at the series limit.

Because of the many contributions of Richard Drachman to the core polarization model and the asymptotic expansion method, it is especially appropriate for this volume to discuss the asymptotic expansion for $\Delta\beta(nL)$. Just as for the energy, the Rydberg electron induces corrections to the Bethe logarithm for the $1s$ electron corresponding to the various multipole moments of the core, with the leading term being the dipole term $0.316\,205(6)\langle x^{-4}\rangle/Z^6$ [40, 41]. The complete expression is

$$\beta(1snl) = \beta(1s) + \left(\frac{Z-1}{Z}\right)^4 \frac{\beta(nl)}{n^3} + \frac{0.316\,205(6)}{Z^6}\langle x^{-4}\rangle + \delta_{\mathrm{ho}}\beta(1snl) \tag{29}$$

where the $\beta(nl)$ are hydrogenic Bethe logarithms [42], and $\delta_{\mathrm{ho}}\beta(1snl)$ takes into account contributions from the higher multipole moments. A least squares fit to direct calculations up to $L = 6$ and $n = 6$ for helium yields the results [43]

$$\delta_{\mathrm{ho}}\beta(1snl\ ^1\mathrm{L}) \quad = \quad 95.8(8)\langle r^{-6}\rangle - 845(19)\langle r^{-7}\rangle + 1406(50)\langle r^{-8}\rangle \tag{30}$$

Table 7: Residual two-electron Bethe logs $\Delta_{\rm ho}\beta(1snl)$.

State	$n^3\Delta\beta(1snl)$	Least squares fit	Difference
$3\,^1$D	–0.000 001 08(4)		
$3\,^3$D	0.000 181 74(5)		
$4\,^1$D	–0.000 018 4(3)		
$4\,^3$D	0.000 231 18(7)		
$5\,^1$D	–0.000 026 84(9)		
$5\,^3$D	0.000 249 73(12) [a]		
$4\,^1$F	0.000 006 58(2)	0.000 006 60	–0.000 000 02(2)
$4\,^3$F	0.000 007 63(2)	0.000 007 64	–0.000 000 01(2)
$5\,^1$F	0.000 008 70(3)	0.000 008 69	0.000 000 01(3)
$5\,^3$F	0.000 010 42(3)	0.000 010 41	0.000 000 01(3)
$6\,^1$F	0.000 009 8(1)	0.000 009 83	0.000 000 0(1)
$6\,^3$F	0.000 011 9(3)	0.000 011 98	–0.000 000 1(3)
$5\,^1$G	0.000 000 770(3)	0.000 000 770	0.000 000 000(3)
$5\,^3$G	0.000 000 771(3)	0.000 000 771	0.000 000 000(3)
$6\,^1$G	0.000 001 043(3)	0.000 001 042	0.000 000 001(3)
$6\,^3$G	0.000 001 050(8)	0.000 001 047	0.000 000 003(8)
$6\,^1$H	0.000 000 127(2)	0.000 000 127	0.000 000 000(2)
$6\,^3$H	0.000 000 127(2)	0.000 000 127	0.000 000 000(2)

[a] Corresponds to an energy uncertainty of ±14 Hz.

$$\delta_{\rm ho}\beta(1snl\ ^3{\rm L}) \;=\; 95.1(9)\langle r^{-6}\rangle - 841(23)\langle r^{-7}\rangle + 1584(60)\langle r^{-8}\rangle\,. \tag{31}$$

For example, for the $1s4f\ ^1$F state, $\beta(4\ ^1{\rm F}) = 2.984\,127\,1493(3)$. As can be seen from the comparison in Table 7, for higher L the asymptotic expansions reproduce the direct calculations to within the accuracy of the calculations.

The results as a function of Z can be represented by the $1/Z$ expansion

$$\beta(1sn\ell) = \frac{\beta(1s)+\beta(n\ell)/n^3}{1+\delta_{\ell,0}/n^3} + \frac{1}{n^3}\sum_{i=1}^{\infty}\frac{c_i}{Z^i} \tag{32}$$

The first few c_i coefficients can be estimated from a least-squares fit to the calculated values of $\beta(1sn\ell)$ up to $Z = 18$, resulting in the equations

$$\beta(1\,^1{\rm S}) \;=\; 2.984\,128\,556 - \frac{0.012315(23)}{Z} + \frac{0.02277(30)}{Z^2} + \frac{0.0019(7)}{Z^3}$$

$$\beta(2\,^1{\rm S}) \;=\; 2.964\,978\,525 + \frac{1}{8}\left(\frac{0.32744(66)}{Z} - \frac{0.1460(53)}{Z^2} - \frac{0.0019(7)}{Z^3}\right)$$

$$\beta(2\,^3{\rm S}) \;=\; 2.964\,978\,525 + \frac{1}{8}\left(\frac{0.22193(34)}{Z} - \frac{0.0099(25)}{Z^2} - \frac{0.0510(42)}{Z^3}\right)$$

Table 8: Comparison of Bethe Logarithms for lithium and its ions.

Atom	$Li(1s^2 2s)$	$Li(1s^2 3s)$	$Li^+(1s^2)$	$Li^{++}(1s)$
$\ln(k_0/Z^2 R_\infty)$	2.981 06(1)	2.982 36(6)	2.982 624	2.984 128

$$\beta(2\,^1\mathrm{P}) = 2.980\,376\,467 + \frac{1}{8}\left(\frac{0.0964(3)}{Z} - \frac{0.0940(26)}{Z^2} + \frac{0.022(4)}{Z^3}\right)$$

$$\beta(2\,^3\mathrm{P}) = 2.980\,376\,467 + \frac{1}{8}\left(\frac{0.0771(4)}{Z} - \frac{0.0395(37)}{Z^2} - \frac{0.017(6)}{Z^3}\right)$$

$$\beta(3\,^1\mathrm{S}) = 2.976\,397\,665 + \frac{1}{27}\left(\frac{0.5292(18)}{Z} - \frac{0.367(14)}{Z^2} + \frac{0.016(20)}{Z^3}\right)$$

$$\beta(3\,^3\mathrm{S}) = 2.976\,397\,665 + \frac{1}{27}\left(\frac{0.4296(3)}{Z} - \frac{0.1927(25)}{Z^2} + \frac{0.0425(43)}{Z^3}\right)$$

$$\beta(3\,^1\mathrm{P}) = 2.982\,714\,103 + \frac{1}{27}\left(\frac{0.1216(20)}{Z} - \frac{0.117(13)}{Z^2} + \frac{0.025(19)}{Z^3}\right)$$

$$\beta(3\,^3\mathrm{P}) = 2.982\,714\,103 + \frac{1}{27}\left(\frac{0.0992(11)}{Z} - \frac{0.0661(47)}{Z^2}\right)$$

The leading coefficient on the right-hand-side is just the quantity $(\beta(1s) + \beta(n\ell)/n^3)/(1 + \delta_{\ell,0}/n^3)$ from (32). These equations reproduce the directly calculated values to within the accuracy of the calculations. As a check, the leading c_1 terms inside parentheses for the low-lying states agree with the corresponding coefficients calculated by perturbation theory by Goldman and Drake [44] (see Ref. [38] for further details).

As a final remark, Table 8 compares the Bethe logarithms for the two lowest S-states of lithium with those for the Li-like ions $Li^+(1s^2\ ^1S)$ and $Li^{++}(1s\ ^2S)$. The comparison emphasizes again that the Bethe logarithm is determined almost entirely by the hydrogenic value for the $1s$ electron, and is almost independent of the state of excitation of the outer electrons, or the degree of ionization.

APPLICATIONS TO NUCLEAR SIZE MEASUREMENTS

As stated in the Introduction, one of the goals of this work is to use the comparison between theory and experiment for the isotope shift to determine the nuclear charge radius for various isotopes of helium and other atoms. One of the most interesting and important examples is the charge radius of the 'halo' nucleus ^{6}He. For a light atom such as helium, the energy shift due to the finite nuclear size is given to an excellent approximation by

$$\Delta E_{\mathrm{nuc}} = \frac{2\pi Z e^2}{3}\bar{r}_{\mathrm{c}}^2 \langle \sum_{i=1}^{2} \delta(\mathbf{r}_i) \rangle \tag{33}$$

where $\bar{r}_{\mathrm{c}}$ is the rms nuclear charge radius. If all other contributions to the isotope shift can be calculated to sufficient accuracy (about 100 kHz) and subtracted, then the residual shift due to the change in $\bar{r}_{\mathrm{c}}$ between the two isotopes can be determined from the measured isotope shift. The theory of isotope shifts, including

Table 9: Contributions to the ^{6}He - ^{4}He isotope shift (MHz).

Contribution	$2\,^3S_1$	$3\,^3P_2$	$2\,^3S_1 - 3\,^3P_2$
$\delta E_{\rm nr}$	52 947.324(19)	17 549.785(6)	35 397.539(16)
μ/M	2 248.202(1)	−5 549.112(2)	7 797.314(2)
$(\mu/M)^2$	−3.964	−4.847	0.883
$\alpha^2\mu/M$	1.435	0.724	0.711
$\delta E^{\rm a}_{\rm nuc}$	−1.264	0.110	−1.374
$\alpha^3\mu/M$, $E_{\rm L,1}$	−0.285	−0.037	−0.248
$\alpha^3\mu/M$, $E_{\rm L,2}$	0.005	0.001	0.004
Total	55 191.453(19)	11 996.625(4)	43 194.828(16)
Experiment[b]			43 194.772(56)
Difference			0.046(56)

[a]Assumed nuclear radius is $\bar{r}_{\rm c}(^6{\rm He}) = 2.04$ fm.
[b]Wang et al. [46].

relativistic recoil and radiative recoil contributions, is discussed in detail in Ref. [45], and will not be repeated here. Instead, we show as an example in Table 9 the various calculated contributions to the isotope shift for the $1s2s\ ^3S_1 - 1s3p\ ^3P_2$ transition of ^{6}He relative to ^{4}He. The corresponding experimental value was obtained in a remarkable experiment performed at the Argonne National Laboratory by Z.-T. Lu and collaborators [46], using the techniques of single-atom spectroscopy to trap the short-lived ^{6}He nuclei ($t_{1/2} = 0.8$ s) in the metastable $1s2s\ ^3S_1$ electronic state.

Each term in the table represents the energy difference between ^{6}He and ^{4}He with nuclear masses of 6.018 8880(11) u and 4.002 603 250(1) u respectively. The first entry $\delta E_{\rm nr}$ represents the 'normal' isotope shift due to the common mass scaling of all the nonrelativistic energies in proportion to $\mu/m_{\rm e} = 1 - \mu/M$, and the second entry is the 'specific' isotope shift due to mass polarization, calculated as a first-order perturbation. The remaining entries represent important corrections to these dominant terms. The third entry of order $(\mu/M)^2$ comes from second-order mass polarization, and the next term of order $\alpha^2\mu/M$ Ry is the relativistic recoil term. It contains contributions from the mass scaling of the terms in the Breit interaction, as well as cross-terms with the mass polarization operator, and the mass dependent Stone terms $(m_{\rm e}/M)(\tilde{\Delta}_2 + \tilde{\Delta}_{\rm so})$ in Eq. (13). The term $\delta E_{\rm nuc}$ is the finite nuclear size correction for an assumed nuclear charge radius $\bar{r}_{\rm c} = 2.04$ fm for ^{6}He, relative to the reference value $\bar{r}_{\rm c} = 1.673(1)$ fm for ^{4}He [47], [2] Finally, the two terms of order $\alpha^3\mu/M$ Ry denote the mass-dependent parts of the electron-nucleus ($E_{\rm L,1}$) and electron-electron ($E_{\rm L,2}$) QED shift, including recoil [50] and mass polarization corrections. The key point is that the uncertainty in the much larger mass-independent part of the QED shift (tens of MHz) cancels when the isotope shift is calculated. The residual uncertainty of only 16 kHz shown in Table 9 is then determined primarily by the uncertainty in the nuclear mass of ^{6}He, rather than the atomic physics calculations.

Since the goal of the experiment is to determine the nuclear charge radius for ^{6}He, the final step is to adjust $\bar{r}_{\rm c}$ so as to eliminate the small discrepancy of 0.046(56) MHz shown in Table 9. The various contributions to the isotope shift in Table 9 can be collected together and expressed in the form

$$\mathrm{IS}(2\,^3S - 3\,^3P) = 43\,196.202(16) + 1.008[\bar{r}_{\rm c}^2(^4{\rm He}) - \bar{r}_{\rm c}^2(^6{\rm He})] \qquad (34)$$

[2]This value is based on measurements of the Lamb shift in muonic helium, but attempts to reproduce the measurement have not proved successful, as discussed by Bracci and Zavattini [48]. The consistent, but less accurate value 1.676(8) fm has been obtained from electron scattering [49]. If the electron scattering value is used for ^{4}He, then the size of the error bars for the other helium isotopes increases in proportion, but the results do not otherwise change significantly.

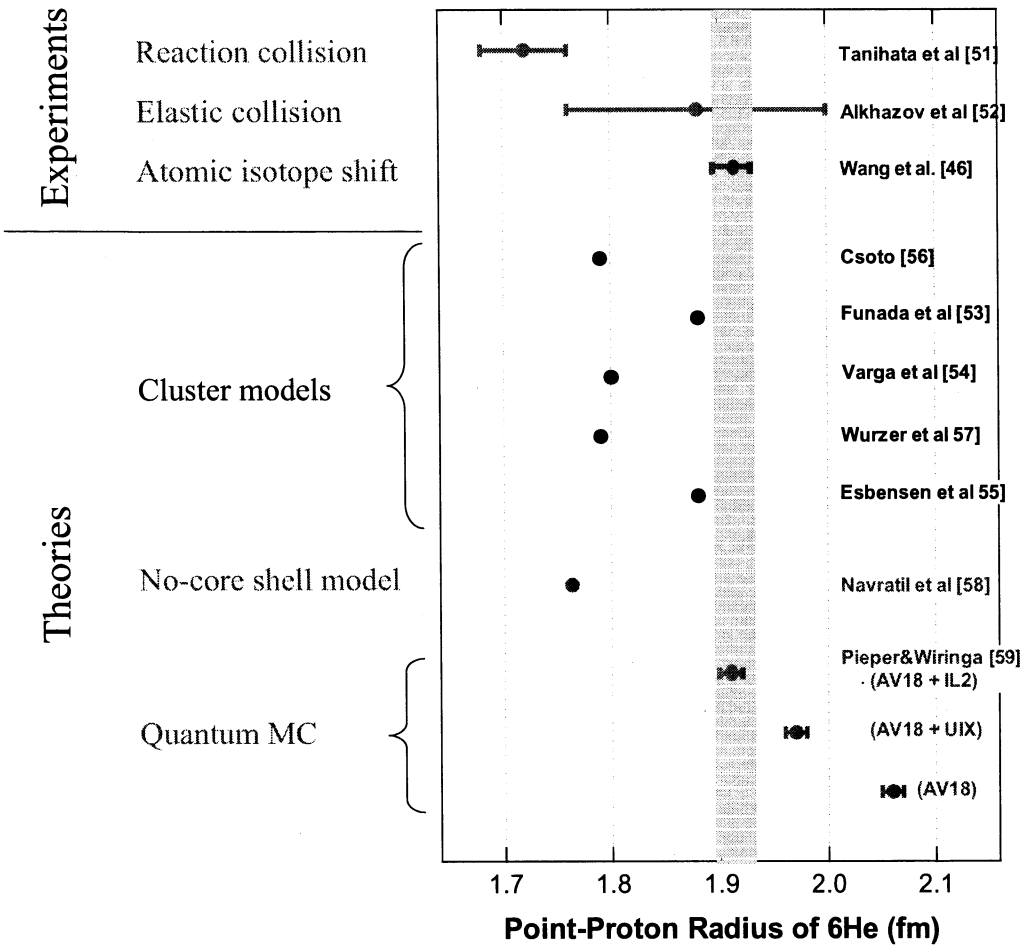

Figure 5: Comparison of the point-proton nuclear charge radius $\bar{r}_{\rm p}$ for ^{6}He with other measurements and theoretical values.

The adjusted nuclear charge radius is then $\bar{r}_{\rm c}(^6{\rm He}) = 2.054(14)$ fm.

The significance of this result in comparison with other measurements and calculations is illustrated in Fig. 5. [3] The first important point is that no other method of measurement is both independent of nuclear structure models, and capable of yielding sufficient accuracy to provide a meaningful test of theory. Ref. [53] was obtained from nuclear reaction cross sections, and Ref. [54] was extracted from elastic scattering from protons (in water). Second, the accuracy is sufficient to rule out all but two of the cluster calculations. Refs. [55, 56, 57] describe ^{6}He in terms of a single $(\alpha + {\rm n} + {\rm n})$ channel, but inclusion of the additional $({\rm t} + {\rm t})$ channel in Refs. [58, 59] produces a substantial disagreement. Also, the *ab initio* calculation based on the

[3]For comparison with theory, it is customary to express the calculated values in terms of an effective rms radius $\bar{r}_{\rm p}$ corresponding to a point-like proton and neutron, which is related to the rms charge radius $\bar{r}_{\rm c}$ by $\bar{r}_{\rm c}^2 = \bar{r}_{\rm p}^2 + \bar{R}_{\rm p}^2 + (N/Z)\bar{R}_{\rm n}^2$, where $\bar{R}_{\rm p} = 0.895(18)$ fm [51] is the rms charge radius of the proton, $\bar{R}_{\rm n}^2 = -0.116(5)$ fm^2 [52] is the mean-square charge radius of the neutron, and N and Z are the neutron and proton numbers.

no-core shell model [60] is in poor agreement. The best agreement is with the *ab initio* quantum Monte Carlo calculations of Pieper and Wiringa [61, 62] based on the AV18 two-body potential and the IL2 three-body potential, while other versions of the model potentials do not agree. The comparison with our value of $\bar{r}_c$ obtained by the isotope shift method is therefore capable of distinguishing amongst the various possible candidates for the effective low-energy nucleon-nucleon interaction potential.

SUMMARY AND CONCLUSIONS

The principle message of this paper is that the helium atom and other quantum mechanical three-body systems can be solved essentially exactly for all practical purposes in the nonrelativistic limit, and there is a systematic procedure for calculating the relativistic and other higher-order QED corrections as perturbations. The solution of the problem of calculating Bethe logarithms means that the theoretical energy levels are complete up to and including terms of order α^3 Ry. Both Aaron Temkin and Richard Drachman have had a profound influence on the field through their study of variational methods and electron scattering phenomena. As shown here, Drachman's asymptotic expansion methods are of key importance in extending the variational results to cover the entire spectrum of singly-excited states. In fact, the accuracy of the asymptotic expansion method increases so rapidly with increasing L that variational calculations become completely unnecessary for $L > 7$.

As a consequence of these advances, helium now joins the ranks of hydrogen and other two-body systems as examples of fundamental atomic systems. The high precision theory that is now available creates new opportunities to develop measurement tools that would otherwise not exist. One such example discussed here is the determination of the nuclear charge radius for the halo nucleus ^{6}He. This opens up a new area of study at the interface between atomic physics and nuclear physics, and it provides important input data for the determination of effective nuclear forces. Other similar experiments have been performed on the lithium isotopes [63], including the halo nucleus ^{11}Li [64], and further work is in progress on ^{8}He at Argonne and ^{11}Be at GSI/TRIUMF.

ACKMOWLEDGMENTS

I would like to express my gratitude to Richard Drachman and Aaron Temkin for many interesting and stimulating discussions over the years, and for the leadership they have provided to the field. In the words of Joe Sucher, the have helped to "slay the dragon of atomic physics." I would also like to thank Wilfried Nörtershäuser at GSI and Z.-T. Lu at the Argonne National Laboratory for their hospitality and inspiration on the experimental side, and Zong-Chao Yan who has contributed tremendously to the calculations, especially for lithium. This work was supported by the Natural Sciences and Engineering Research Council of Canada.

REFERENCES

1. G.W.F. Drake and W.C. Martin, Can. J. Phys. **76**, 597 (1998).
2. I. Tanihata, Nucl. Phys A **522**, C275 (1991).
3. B. Klahn and W.A. Bingel. Theor. Chem. Acta, **44**, 27 (1977); Int. J. Quantum Chem. **11**, 943 (1978).
4. G.W.F. Drake and Z.-C. Yan. Phys. Rev. A, **46**, 2378 (1992).

5. G.W.F. Drake, in *Long-range Casimir forces: Theory and recent experiments on atomic systems*, edited by F.S. Levin and D.A. Micha (Plenum, New York, 1993), pp. 107–217.

6. G.W.F. Drake, Adv. At. Mol. Opt. Phys. **31**, 1 (1993).

7. G.W.F. Drake, M.M. Cassar, and R.A. Nistor, Phys. Rev. A **65**, 054501 (2002).

8. A.K. Bhatia and A. Temkin, Phys. Rev. **137**, 1335 (1965).

9. A.K. Bhatia and R.J. Drachman, Phys. Rev. A **35**, 4051 (1987).

10. A.K. Bhatia and R.J. Drachman, J. Phys. B: At. Mol. Opt. Phys. **36**, 1957 (2003).

11. V.I. Korobov, Phys. Rev. A **66**, 024501 (2002).

12. C. Schwartz, http://xxx.aps.org/abs/physics/0208004.

13. S.P. Goldman, Phys. Rev. A **57**, R677 (1998).

14. A. Bürgers, D. Wintgen, J.-M. Rost, J. Phys. B: At. Mol. Opt. Phys. **28**, 3163 (1995).

15. J.D. Baker, D.E. Freund, R.N. Hill, J.D. Morgan III, Phys. Rev. A **41**, 1247 (1990).

16. R.J. Drachman, Phys. Rev. A **26**, 1228 (1982).

17. R.J. Drachman, Phys. Rev. A **31**, 1253 (1985).

18. R.J. Drachman, Phys. Rev. A **33**, 2780 (1986).

19. R.J. Drachman, Phys. Rev. A **37** 979 (1988).

20. R.J. Drachman, Phys. Rev. A **47**, 694 (1993).

21. R. J. Drachman, in *Long-Range Casimir Forces: Theory and Recent Experiments on Atomic Systems*, edited by F. S. Levin and David Micha (Plenum Press, New York, 1993), pp. 219–272, and earlier references therein.

22. R.A. Swainson and G.W.F. Drake, Can. J. Phys. **70**, 187 (1992).

23. Z.-C. Yan and G.W.F. Drake, Phys. Rev. Lett. **81**, 774 (1998).

24. Z.-C. Yan and G.W.F. Drake, Phys. Rev. A, **66**, 042504 (2002).

25. Z.-C. Yan and G.W.F. Drake, Phys. Rev. Lett., **91**, 113004 (2003).

26. A.K. Bhatia and R.J. Drachman, Phys. Rev. A **45** 7752 (1992).

27. R.J. Drachman and A.K. Bhatia, Phys. Rev. A **51** 2926 (1995).

28. A.K. Bhatia and R.J. Drachman, Phys. Rev. A **55**, 1842 (1997).

29. H.A. Bethe and E.E. Salpeter, *Quantum mechanics of one- and two-electron atoms*, (Springer-Verlag, New York, 1957).

30. A.P. Stone, Proc. Phys. Soc. (London) **77**, 786 (1961); **81**, 868 (1963).

31. P. K. Kabir and E. E. Salpeter, Phys. Rev. **108**, 1256 (1957).

32. H. Araki, Prog. Theor. Phys. **17**, 619 (1957).

33. J. Sucher, Phys. Rev. **109**, 1010 (1958).

34. C. Schwartz, Phys. Rev. **123**, 1700 (1961).

35. J. D. Baker, R. C. Forrey, J. D. Morgan III, R. N. Hill, M. Jeziorska, and J. Schertzer, Bull. Am. Phys. Soc. **38**, 1127 (1993); J. D. Baker, R. C. Forrey, M. Jeziorska, and J. D. Morgan III, private communication.

36. V. I. Korobov and S. V. Korobov, Phys. Rev. A **59**, 3394 (1999).

37. K. Pachucki and J. Sapirstein, J. Phys. B: At. Mol. Opt. Phys. **33**, 455 (2000).

38. G.W.F. Drake and S.P. Goldman, Can. J. Phys. **77**, 835 (1999).

39. V.I. Korobov, Phys. Rev. A **69**, 054501 (2004).

40. S.P. Goldman and G.W.F. Drake, Phys. Rev. Lett. **68**, 1683 (1992).

41. S.P. Goldman, Phys. Rev. A **50**, 3039 (1994).

42. G. W. F. Drake and R. A. Swainson, Phys. Rev. A **41**, 1243 (1990).

43. G.W.F. Drake, Phys. Scr. T95, 22 (2001).

44. S. P. Goldman and G. W. F. Drake, J. Phys. B: At. Mol. Opt. Phys. **17**, L197 (1984).

45. G.W.F. Drake, W. Nörtershäuser, and Z.-C. Yan, Can. J. Phys. 83, 311 (2005).

46. L.-B. Wang, P. Mueller, K. Bailey et al. Phys. Rev. Lett. 93, 142501 (2004).

47. E. Borie and G.A. Rinker, Phys. Rev. A **18**, 324 (1978).

48. L. Bracci and E. Zavattini, Phys. Rev. A **41**, 2352 (1990).

49. I. Sick, Phys. Lett. B 116, 212 (1982).

50. K. Pachucki and J. Sapirstein, J. Phys. B **33**, 455 (2000).

51. I. Sick, Phys. Lett. B **576**, 62 (2003).

52. S. Kopecky, P. Riehs, J.A. Harvey and N.W. Hill, Phys. Rev. Lett. **74**, 2427 (1995); S. Kopecky, J.A. Harvey, N.W. Hill, M. Krenn, M. Pernicka, P. Riehs and S. Steiner, Phys. Rev. C **56**, 2229 (1997).

53. I. Tanihata et al., Phys. Lett. B **289**, 261 (1992).

54. G.D. Alkhazov et al., Phys. Rev. Lett. **78**, 2313 (1997).

55. S. Funada, H. Kameyama and Y. Sakruagi, Nucl. Phys. **A575**, 93 (1994).

56. K. Varga, Y. Suzuki and Y. Ohbayasi, Phys. Rev. C **50**, 189 (1994).

57. H. Esbensen, G.F. Bertsch and K. Hencken, Phys. Rev. C **56**, 3054 (1997).

58. A. Csoto, Phys. Rev. C **48**, 165 (1993).

59. J. Wurzer and H.M. Hofmann, Phys. Rev. C **55**, 688 (1997).

60. P. Navratil, J.P. Vary, W.E. Ormond and B.R. Barrett, Phys. Rev. Lett. **87**, 172502 (2001).

61. S.C. Pieper, V.R. Pandharipande, R.B. Wiringa and J. Carlson, Phys. Rev. C **64**, 014001 (2001).

62. S.C. Pieper and R.B. Wiringa, Ann. Rev. Nucl. Part. Sci. 51, 53 (2001).

63. G. Ewald, W. Nörtershäuser, A. Dax, S. Göte, R. Kirchner, H.-J. Kluge, Th. Kühl, R. Sanchez, A. Wojtaszek, B.A. Bushaw, G.W.F. Drake, Z.-C. Yan, and C. Zimmermann, Phys. Rev. Lett. **93**, 113002 (2004); **94**, 039901 (2005).

64. R. Sanchez, W. Nörtershäuser, G. Ewald, D. Albers, J. Behr, P. Bricault, B.A. Bushaw, A. Dax, J. Dilling, M. Dombsky, G.W.F. Drake, S. Gotte, R. Kirchner, H.J. Kluge, T. Kühl, J. Lassen, C.D.P. Levy, M.R. Pearson, E.J. Prime, V. Ryjkov, A. Wojtaszek, Z.-C. Yan and C. Zimmermann, Phys. Rev. Lett. **96**, 033002 (2006).

THE BUFFER-GAS POSITRON ACCUMULATOR AND RESONANCES IN POSITRON-MOLECULE INTERACTIONS

C. M. Surko
Department of Physics, University of California, San Diego, La Jolla CA 92093

ABSTRACT

This is a personal account of the development of our buffer-gas positron trap and the new generation of cold beams that these traps enabled. Dick Drachman provided much appreciated advice to us from the time we started the project. The physics underlying trap operation is related to resonances (or apparent resonances) in positron-molecule interactions. Amusingly, experiments enabled by the trap allowed us to understand these processes. The positron-resonance "box score" to date is one resounding "yes," namely vibrational Feshbach resonances in positron annihilation on hydrocarbons; a "probably" for positron-impact electronic excitation of CO and N_2; and a "maybe" for vibrational excitation of selected molecules. Two of these processes enabled the efficient operation of the trap, and one almost killed it in infancy. We conclude with a brief overview of further applications of the trapping technology discussed here, such as "massive" positron storage and beams with meV energy resolution.

IT ALL STARTED AT LUNCH WITH MARV

Since this paper is written in conjunction with the symposium marking the retirement of Dick Drachman and Aaron Temkin, I depart from third-person style to relate a personal view of the development of the buffer-gas trap and the physics that has come from it. I came to know Dick near the beginning of the trap project and because of it. I'd like to tell a bit here about the people involved in the development of the trap, including Dick, who helped us achieve important perspective and understanding of key physics issues that have arisen in the past two decades.

The story began in a lunchtime conversation with Marv Leventhal at AT&T Bell Laboratories in Murray Hill, New Jersey in 1983. Marv asked what one could do with positrons in a tokamak plasma. I responded by saying that there were interesting problems for sure, such as study of the turbulent transport of electrons out of the hot plasma. However, I didn't know how to get the positrons into the plasma in the first place (i.e., across the strong magnetic field). Marv said, *"oh, I know how to get them in – that's easy – just convert them to positronium atoms; shoot them in; they'll ionize and you're in business."* That started the whole thing off [1, 2]. Marv had done positron trapping earlier with Ben Brown, and so he was eager to pursue this kind of research. In a very nice experiment, they measured the Doppler linewidth of molecular hydrogen [3], to compare with Marv's balloon measurement of this line coming from the galactic center [4]. Regarding the proposed tokamak application, we did carry it some way forward, but

never actually did the experiment. However, this start enabled us to do many other things that turned out to be quite interesting and have enabled others to do more.

The trap was developed to accumulate positrons and store them efficiently. While the original goal was to provide an intense, pulsed positron source to study turbulence in tokamak fusion plasmas, we quickly realized that it might well have many other applications. By now, the trap has contributed to a wide range of scientific problems, including many aspects of positron interactions with atoms and molecules [5]; study of electron-positron plasmas [6]; commercial-prototype trap-based beams for materials characterization [7]; creation in the laboratory of the first low-energy antihydrogen [8]; and very recent new work to study the positronium (Ps) molecule, Ps_2 [9].

WHAT THE DESIGNERS DESIGNED AND WHO'S DICK DRACHMAN?

The way to make a nearly ideal "antimatter bottle" was known by the mid '80s, albeit not fully realized as such. It was called a Penning-Malmberg trap, adding John Malmberg's name to Penning's [10]. It was Malmberg and colleagues at the University of California, San Diego (UCSD) who developed the Penning trap to efficiently confine large quantities of single component plasma. Thus it was no accident that I later went to UCSD – in large part due to my interests in trapping positrons.

Malmberg and colleagues worked with electrons, but switching to positrons poses no problems from a plasma physics point of view. This nearly ideal "bottle" consists of a uniform magnetic field to confine the particles radially, with electrostatic potentials at the ends to confine their motion along the field. Confinement of plasmas of a single sign of charge in these devices is excellent. A theorem due to Tom O'Neil explains why [11]: the angular momentum of the plasma is dominated by the electromagnetic term, which is proportional to $\Sigma\, r_j^2$, where r_j is the radial position of plasma particle j. If you build a cylindrically symmetric device (i.e., about the magnetic field axis), there are no torques, and hence the plasma can't expand radially.

The trick, however, is getting the positrons into the trap efficiently without unnecessary losses, since positrons are expensive from the scientific point of view. Marv and I thought we might be able to do it using inelastic collisions. Early on, Marv had the idea to use vibrational excitation of molecules, since we wanted to avoid positronium formation that would be present if we used electronic excitation, for example. Good candidates seemed to be H_2 and N_2, since they had relatively large vibrational energies (0.5 and 0.3 eV, respectively). This is where the connection to Dick Drachman began. I had no idea who "Drachman" was, but Marv would say, "*Drachman says*, ..." or "*we should ask Drachman about that.*" This happened so many times that, when Marv said something to this effect standing in the hall outside his office, I made a note to find out who this guy was – he must really be somebody important!

While I had done a bit of atomic physics some 15 years earlier, the trap project provided me with the opportunity to become immersed in the field. I came to know Dick well and consulted him frequently. He provided that calm and reasoned voice to lead us

through many theoretical minefields (vats of snake oil too). He took the time to patiently teach me about theoretical atomic physics and to translate (in language even I could understand) various esoteric papers filled with surprising results (alas, not infrequently wrong). Dick was an enormous help in keeping us on track. He helped make the venture into positron-atomic physics both very productive and most enjoyable. Our first conversations related to vibrational excitation. Baille and Darewych had done a very nice calculation of vibrational excitation of H_2 by positron impact [12], and we wanted to understand what that would mean for us and how we might extrapolate to other targets.

Back at the trap project, we designed what was later to be called a three-stage, buffer-gas, positron accumulator, the principle of which is shown schematically in Fig. 1 [1]. The pressure in stage I is adjusted so that a positron would lose enough energy in one transit through the device to be trapped, then subsequent collisions would further lower the positron energy, so that it would end up trapped and cool in the lowest pressure region in stage III. We realized pretty quickly that, while stage II and III could operate on vibrational excitation, stage I required both a large cross section and a larger energy loss than vibrations could provide. So we planned that the first stage would operate on electronic excitation, even though this would carry with it some loss due to positronium formation.

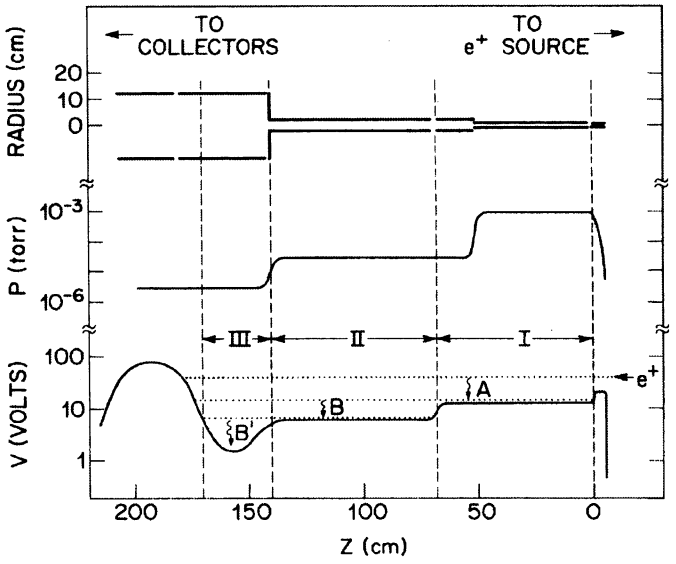

Fig. 1. Schematic diagram of the three stage buffer-gas accumulator *circa* 1988. Top: electrode structure. Middle and bottom: pressure and electrical potential profiles. There is a uniform magnetic field ~ 0.9 kG in the z direction. Stages are labeled I, II and III. The trapping mechanism is inelastic collisions with the N_2 buffer gas, labeled A, B and B′. In 1989, A was electronic excitation, and B and B′ were vibrational excitation of N_2 [13].

By 1985 we had made progress in planning for the trap and the positrons-in-tokamak experiment. It so happened that at that time, Allen Mills and Karl Canter were arranging a 60th birthday celebration at Brandeis for Steve Berko, a giant in the field of

Fig. 2. (a) Photo of the attendees at Steve Berko's 60th birthday symposium at Brandeis in December 1984. It's virtually a who's who in the U. S. world of positron physics including Dick (upper left). Somehow I didn't hear the announcement about the picture. It is one if the few group photos at meetings that I'm sorry to have missed. Reprinted from Ref. [1] with permission from World Scientific Publishing Co. Pte. Ltd, Singapore.

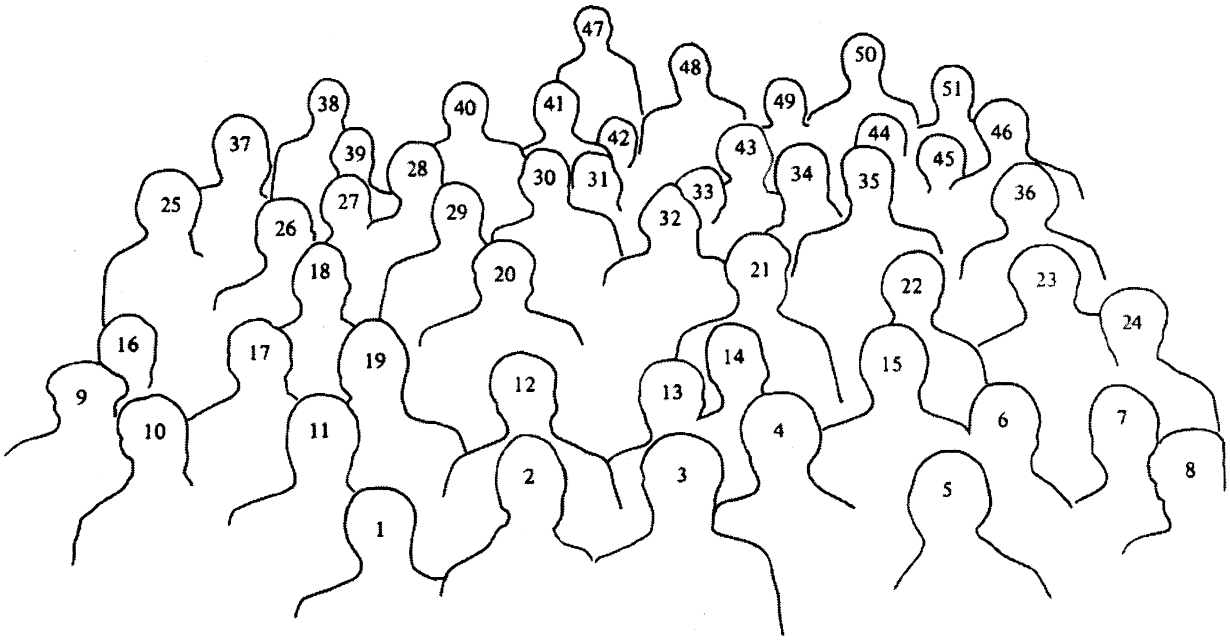

1. J. J. Mader
2. R. M. Nieminen
3. L. O. Roellig
4. P. M. Platzman
5. P. J. Schultz
6. K. G. Lynn
7. Marc Weber
8. D. M. Chen
9. J. T. Weingart
10. Asko Vehanen
11. A. H. Weiss
12. M. A. Shulman
13. Mohammad Haghgooie
14. G. Krithivas
15. R. N. West
16. W. H. E. Rueckner
17. D. C. Schoepf
18. B. L. Brown
19. R. R. Lee
20. Arthur Rich
21. A. T. Stewart
22. Martin Deutsch
23. Stephan Berko
24. A. P. Mills, Jr.
25. P. H. Lippel
26. P. E. Mijnarends
27. S. C. Sharma
28. R. J. Drachman
29. Arun Bansil
30. H. J. Schnitzer
31. W. S. Crane
32. R. M. Langer
33. J. H. Terrell
34. P. H. Carr
35. K. F. Canter
36. Steven Chu
37. Christoph Hohenemser
38. W. F. Huang
39. R. B. Meyer
40. Stephen Cushner
41. Takashi Odagaki
42. Y. J. He
43. Eric Gullikson
44. W. S. Farmer
45. Leigh Sneddon
46. G. M. Beardsley
47. T. N. Horsky
48. Frank Sinclair
49. J. F. C. Wardle
50. Raoul Tawel
51. Piero Sferlazzo

Fig. 2. (b) Roster of names for the Berko symposium picture, December 1984. Reprinted from Ref. [1] with permission from World Scientific Publishing Co. Pte. Ltd, Singapore.

positron studies of solid-state systems, such as the Fermi surfaces in metals. Allen and Karl were planning the proceedings and Allen asked for a paper on our positron-trap project [1]. This first paper on the trap was also the first of only two papers that I've coauthored with Allen. Looking back, the paper was anything but modest in its promises: we "discussed the possibility" of accumulating positron plasmas containing 10^{10} particles and holding them for minutes. The latter turned out to be not too hard, given a few years, but the former has yet to be achieved some 20 years later (but we do hope to do it soon). As shown in Fig. 2, a host of big names attended the Berko symposium, including founders of the field, such as the discoverer of positronium, Martin Deutsch, and the future Nobel Prize winner, Steve Chu. It was really a great time for the positroners! Berko, whom I did not know very well before the meeting, was immensely gracious in accommodating the hoopla made over him. Best of all, I had an opportunity to meet *Drachman*, although I didn't realize at the time his strong connections to Brandeis.

Shortly after the conference, Fred Wysocki came from the Princeton Plasma Lab to Bell Labs as a post doc to spearhead the construction of the trap, and we were off to the "positron accumulator races." Figure 3 shows Marv, Fred, and Al Passner admiring the electrode structure of the first trap (gold plated no less). Al, who was an Associate Member of the Technical Staff at Bell Labs, had worked with me for a number of years before we began the trap project. He made a great contribution to its early success, similar to his contributions to many of our other experiments.

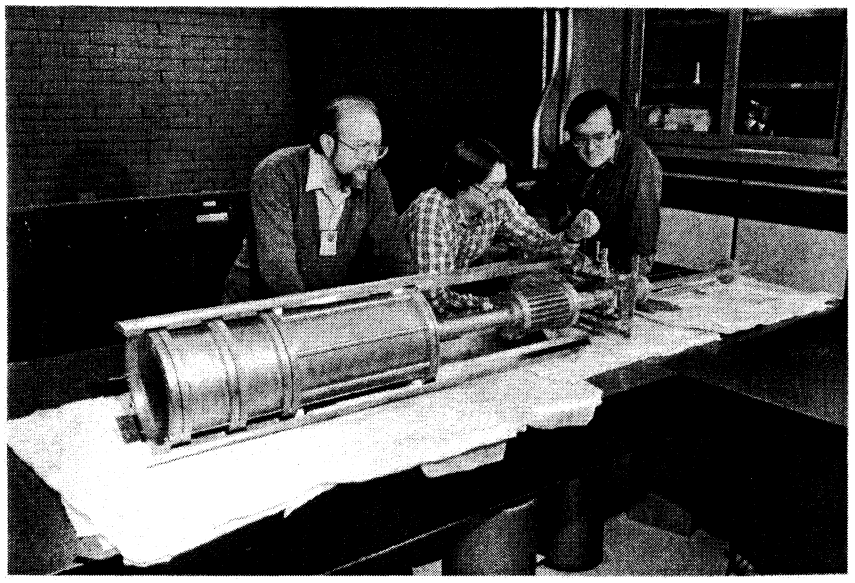

Fig. 3. Gold-plated copper electrode structure of the buffer-gas positron accumulator as assembled in 1986. From left to right, Al Passner, Fred Wysocki, and Marv Leventhal. The electrodes sit on laser tables where equipment for Allen Mills' Ps spectroscopy experiment [14] was to be set up.

MOTHER NATURE HAD OTHER IDEAS, THE THORN IN ALLEN'S SIDE, AND DICK'S SYMPOSIUM

Fred Wysocki designed a very nice device, and so it all looked great. However, when we turned the trap on, the results were terrible. We didn't get anything to speak of with vibrational excitation, but we could trap positrons when we increased the positron energy in the first stage to where we guessed we were exciting the molecules electronically. We tried a large number of molecules, and N_2 seemed to work best for reasons then unknown. Actually, we had wanted to avoid electronic excitation, since for almost all targets, the Ps formation channel is open there too, and the latter is a potent loss process. We had expected 10^6 positrons trapped and minute positron lifetimes, but we got about a factor of 100 less, as shown in Fig. 4. So we had not only an excitation problem, but also a lifetime problem as well. I was nevertheless pretty excited, somehow feeling that, if we weren't making a mistake, there was likely new physics there somewhere. *Lots and lots* of conversations with Dick followed these early results concerning the possible atomic physics processes involved in the trap operation.

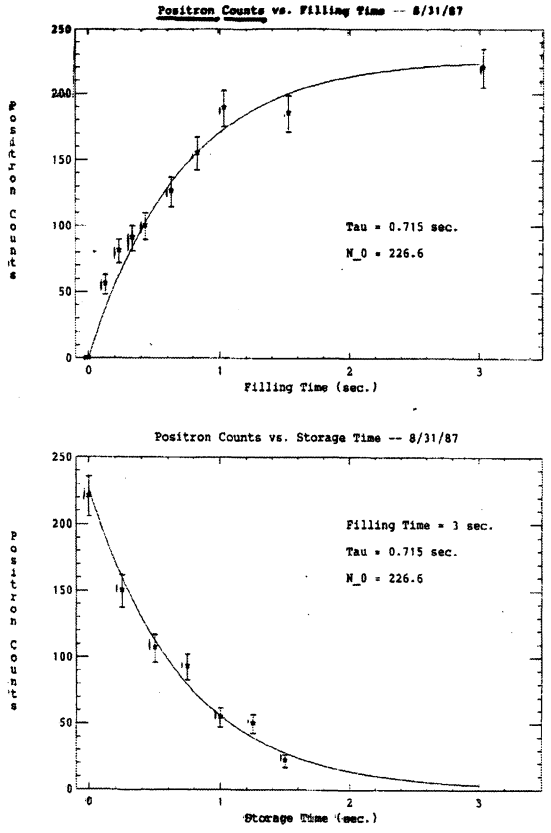

Fig. 4. Data from a trapping experiment in August 1987. Above: number of positrons confined as a function of fill time, maximum number ~ 1 x 10^4. Below: confinement as a function of time after the fill was turned off, indicating a 0.7 s confinement time. The confinement was limited by annihilation on a very low density of large, molecular impurities at pressures < 10^{-9} torr.

Now there was another story unfolding here too. It was often said that, in those days, Bell Labs wasn't dollar limited, but was *space* limited. (Typically the opposite is true in universities.) When we started the trap project, we needed someplace to put it. I had a lab, but it was full of fluid convection apparatus, so no room there. Marv had only a small space, since he did mostly gamma-ray astronomy with groups elsewhere, so we had a problem. Fortunately, Allen (as in A. P. Mills, Jr. – *the* Allen, Allen) just happened to have a big, new-to-him lab in the basement that he hadn't moved into yet. So, we say "*Allen*" (imagine pleasant music in our voices), "*errr, could we borrow your lab for just 18 months; we want to set up a trap and then move it to Princeton to study turbulence in tokamak plasmas?*" "*Well OK*," (says the cooperative Dr. M., Jr.) "*but remember - just 18 months!*" Well, that was in '85, and as I recall, by '87, Allen was unhappy, since (see Fig. 5) there were tons of magnet, etc. sprawled all over his space and no signs of our departure in sight. So Allen began building his new Ps spectroscopy experiment [14] intertwined with ours like spaghetti in a bowl. Then when we first began trapping positrons, Allen was *really* an unhappy camper – well, not really, but he saw the problem coming even before we did. Allen was such a good scientist and believed so much in everybody's science that he couldn't throw us out if we were making progress. If our trap didn't work, we were out on the street (600 Mountain Avenue, Murray Hill NJ, to be precise). But it was working, and "so keep your elbows in," we're going to be very cozy for a while with two "full-bodied" experiments in one underground lab. Great guy, Allen; maybe not overjoyed at that moment, but he really did us a huge favor.

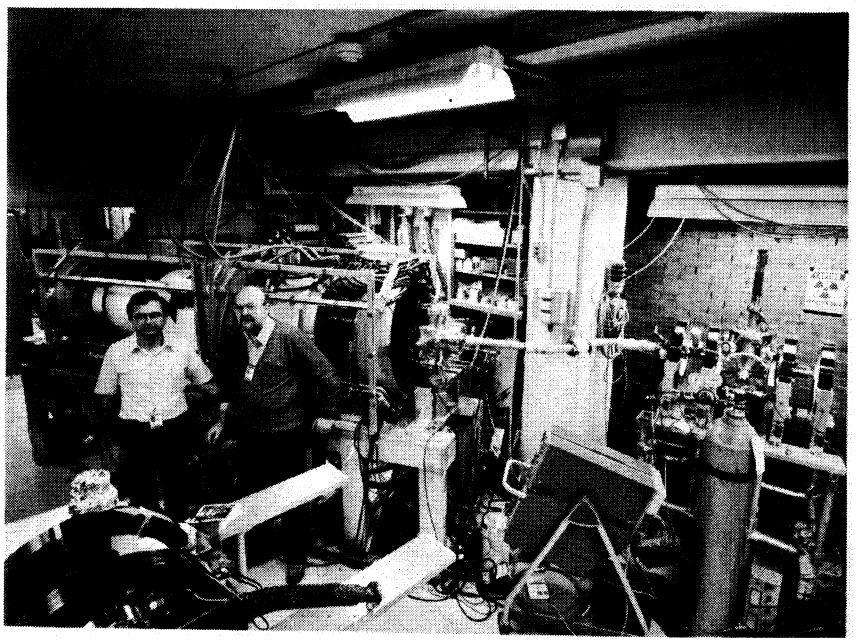

Fig. 5. Al Passner and me standing in front of the first buffer-gas trap in Allen Mills' lab *circa* 1987. The source is on the right behind the gas bottle; and Allen's Ps spectroscopy experiment (Helmholtz coils and rails), which was under construction, is "creeping in" at the lower left.

Back at the trap, we twiddled knobs and got the plasma lifetime to improve a bit at a time somehow. The trap had a continuous feed of tungsten-moderated positrons from a ^{22}Na source, so longer lifetimes meant more particles trapped. But we really didn't know what was going on. The seminal event occurred one afternoon. I came into the lab, and Al Passner was excited. *"Hey Cliff, look at this – I think it's impurities."* He had a small dewar of liquid nitrogen in one hand, and he was looking at the trapped particle signal on an oscilloscope as he poured nitrogen on the trap vacuum chamber. Liquid N_2 on – larger signal; take the LN_2 away – the signal decreased. This was a major turn of events. Sure enough, in the months that followed, we found that the better we made the vacuum, the better the trap worked.

The problem, it turned out, was large hydrocarbon molecules at the $\leq 10^{-9}$ torr level, for reasons no one knew at the time. Basically they had absolutely huge annihilation rates. It was good that Wysocki insisted on building such a good vacuum system in the first place, or the experiment would have never worked. So on the hardware side, we installed an *in situ* liquid nitrogen dewar in the vacuum system next to the final trapping stage to pump impurities, and we began switching out the turbopumps on the system (i.e., which required conventional oil mechanical pumps behind them) in favor of cryopumps that didn't require any backing.

On the physics side, the first major paper was a 1988 Phys. Rev. Letter (PRL) on (no surprise) annihilation on large molecules [15]. As shown in Fig. 6, we found that annihilation rates increased exponentially with molecular size. Plotted here is the conventional normalized annihilation rate, Z_{eff}, which is the measured annihilation rate, Γ, relative to that expected for positrons in a free electron gas of the same density, namely [16],

$$Z_{eff} = \Gamma / \pi r_o^2 c n_m, \qquad (1)$$

In Eq. 1, r_o is the classical electron radius, c is the speed of light, and n_m is the molecular number density. We had the intuition to point out in the PRL that the large Z_{eff} values were likely due to vibrational resonances and invoked the "RRKM" formalism from the chemistry literature to explain it. We were familiar with Heyland's work on small hydrocarbons (see Fig. 6) [17], but we were unaware of the seminal work of Paul and St. Pierre who studied annihilation in dense gases for hydrocarbons as large as butane (C_4H_{10}) [18]. We agreed quantitatively with the previous measurements and extended them to molecules as large as $C_{16}H_{34}$ finding annihilation rates orders of magnitude larger. More significant really was the ability to study positron interactions with molecules in a vacuum environment. There was now no question that the large rates were due to a two body effect, and we could also make independent measurements of the positron temperature [confirmed to be the electrode temperature of 300 K (i.e., 25 meV)].

We were on the road now. The next year we published another PRL announcing the first positron plasma in the laboratory [13]. It contained a modest 3×10^5 e^+, with a Debye screening length, λ_D, which was a similarly modest 1/4 the plasma radius (i.e., a good measure of the plasma regime is the degree to which $\lambda_D << r_p$). Later, John

Malmberg and Hans Dehmelt told me that they were referees for the paper, exceedingly pleasing, because both were giants in the trap field. We realized that the annihilation on molecules might result in a spectrum of ions. At Allen Mills' suggestion, Al Passner looked and sure enough, there was a story to tell there too. We found that annihilation with a 300 K thermal distribution of positrons left a broad spectrum of ions [19]. I'm sorry to say that this is the second of only two papers I coauthored with Allen, during all our time at Bell Labs.

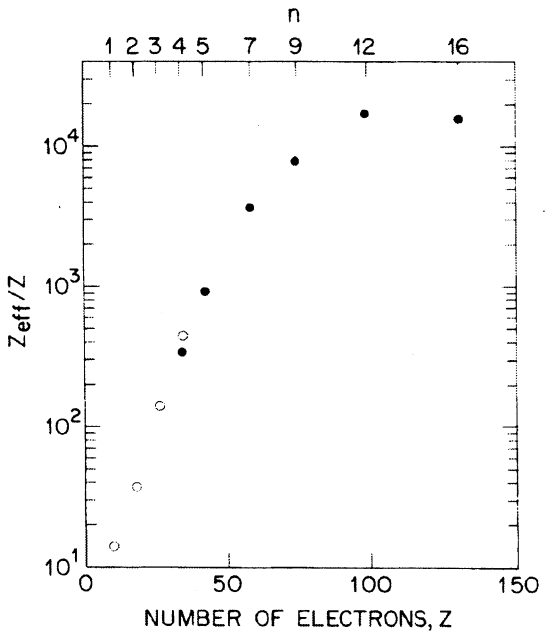

Fig. 6. Normalized annihilation rate Z_{eff}/Z for alkanes (C_nH_{2n+2}) as a function of the number of molecular electrons, Z: Open circles are from an experiment using atmospheric pressure test gas [17], and (•) are data taken with a low-pressure of the test gas in the positron trap. From Ref. [15].

Les Hulett and collaborators at Oak Ridge followed up on this positron-induced ionization effect and produced a series of interesting papers [20, 21]. Initially, there was a disagreement about the significance of our experiment, which resulted (amicably) in a joint publication [22]. Oakley Crawford from the Oak Ridge group wrote a nice theoretical paper that explained the basic phenomenon [23], saying that the incoming positrons annihilate with equal probability on any valence electron, not just the highest-lying molecular orbitals. Later we confirmed this prediction with Doppler broadening measurements [24, 25]; it was only then that I realized the full implications of Crawford's model.

At that point (Fall, '88), I moved from Allen's lab to UCSD in La Jolla, much to his relief. Sadly the collaboration with Marv and interactions with Allen tailed off as the miles separated us and other interests and obligations got in the way. In La Jolla, we continued the studies of annihilation in molecules and continue them still, many generations of experiments later.

Dick's 1989 symposium at Goddard was, from my point of view, something of a coming-of-age party for the trap. We presented a paper on our annihilation results that was well received [26]. I was quite gratified that the trap-based results were embraced by the positron community as "mainstream," something that is frequently not easy coming into a new field with a different technique. The meeting was a great opportunity to meet people who would later play key roles in the science that the trap was to enable.

PHYSICS IN THE TRAP AND MORE CONVERSATIONS WITH DICK

More superb Princeton plasma talent came with Tom Murphy, who joined us at Bell Labs in time to disassemble the trap at Bell and move it to La Jolla. Even while a grad student at Princeton, Tom wrote a great paper on using a Ps beam to study transport in tokamaks [27]. Immediately upon our arrival in La Jolla, Gene Jerzewski joined the effort. His technical expertise and ability to teach students and post docs about hardware were invaluable to our efforts in the years to follow – wonderful contributions on a level with Al Passner's contributions at Bell.

In La Jolla, Tom Murphy focused on understanding *the* problem, namely annihilation in large molecules [28]. He also made great strides in understanding how the three-stage buffer-gas trap actually worked [29]. A key discovery was that the optimum trapping potential difference between stages was ~ 9 – 10 eV per stage for each of the three stages. As described below, this is the energy window in N_2 where the electronic excitation cross section is larger than that for Ps formation due to a resonance in the excitation channel not yet understood. The result is efficient trapping when all stages of the trap are tuned to operate in this regime.

On the annihilation front, Tom cleared up a long-standing ambiguity in the data for annihilation in xenon for a thermal distribution of positrons at 300 K, confirming $Z_{\text{eff}} \approx$ 400 [30], This value would be doubted by theorists for another decade, but is now the accepted number [5]. Tom also made new systematic studies of Z_{eff} for a range of compounds [28]. Along the way, there were innumerable conversations with Dick Drachman about low-energy positron interactions with atomic and molecular targets in our attempt to get some degree of theoretical understanding to match the results provided by our new experimental capabilities. He was kind enough to look over any paper that I sent him, including providing very useful comments and suggestions on our papers when we sent them to him in the draft stage.

In the early 90's, Shengzhang Tang joined us from Ken Roellig's shop, and Rod Greaves came from the plasma community. Koji Iwata did his thesis on annihilation ("*he did <u>all</u> this work for a thesis?*" one member of his doctoral committee asked!), and Mark Tinkle did his thesis on mode diagnostics of positron plasmas. Shenzhang took the last steps that we would take toward a Ps beam fusion diagnostic showing that one could make a pretty good, variable-energy Ps beam by charge exchange on H_2 [31]. We got a very important new tool from Shengzhang, namely our first Doppler broadening measurements [32], an example of which is shown in Fig. 7 [33]. Later this technique allowed us to determine the site of positron annihilation in large molecules [24, 25]; all

valence electrons seem to do the trick, as per Oakley Crawford's prediction a few years earlier. During that period, we also made quantitative studies of inner shell annihilation [34] and studied annihilation in polycyclic aromatic (PAH) molecules, which are important constituents of the interstellar medium [35, 36].

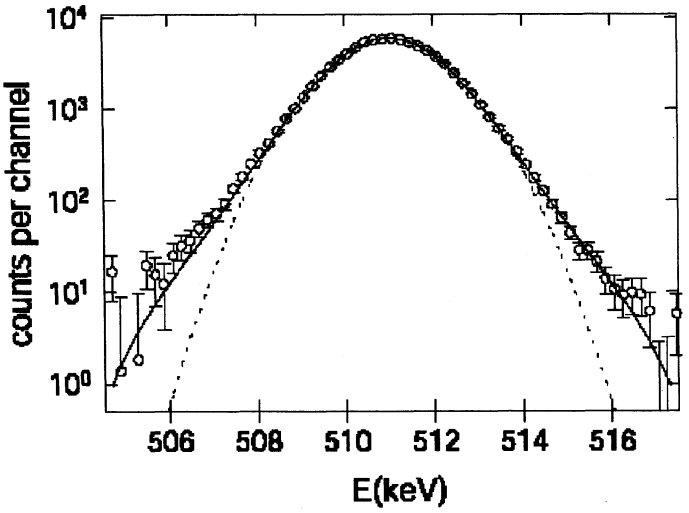

Fig. 7. (open circles) Doppler-broadened gamma-ray spectrum from positron annihilation on helium atoms and comparison with (—) theoretical predictions using a variational wavefunction, and (– –) a Gaussian fit. From Ref. [33].

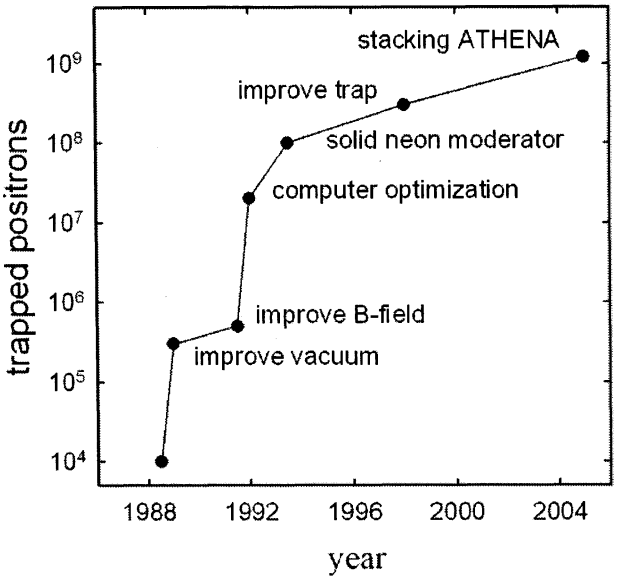

Fig. 8. Progress in trapping positrons with buffer-gas accumulators using ^{22}Na sources with strengths (~ 100 mCi), beginning with the first trap at Bell Labs. All except the last point (ATHENA collaboration [39]) are from the traps at Bell and UCSD.

Around '95, Rod Greaves pushed us to develop further the neon moderator for use with the trap [37]. Invented much earlier by Allen Mills [38], neon was not used as a moderator much, because the energy spread was considerably larger than that of tungsten (i.e., ~ 1.5 eV, FWHM, as compared to ~ 0.5 eV for tungsten), even though neon is more efficient by an order of magnitude. Rod realized that this was not a disadvantage for the trap. The buffer-gas trap has an energy acceptance window ~ 2 eV; and once trapped, the positrons cool to 25 meV, which is far superior to the energy spread of the conventional tungsten-moderated beam. Rod designed a compact system, which is now standard fare for traps and other applications.

In '97, we designed and built a second-generation three-stage positron trap that was somewhat more compact. By then we had improved the overall efficiency of the system by more than a factor of 10^4 as compared with the first results shown in Fig. 4. Figure 8 shows this progress and includes later results from the ATHENA antihydrogen collaboration at CERN. As discussed below, they used a buffer gas accumulator to accumulate positrons, then stacked them in a high-magnetic-field Penning-Malmberg trap.

THE TRAP-BASED BEAM AND THREE POSITRON-ATOMIC PHYSICS QUESTIONS

In '95, Chris Kurz came from MIT to join our group as a post doc, and Steven Gilbert joined to do a thesis and then a short post doc. With Chris, we made the first annihilation measurements as a function of positron temperature, heating them *in situ* in the trap with rf radiation [40]. This was a precursor to Rod Greaves, Chris and Steven realizing that we could make a cold beam by simply dumping the trap slowly [41]. The results, shown in Fig. 9, were spectacular and turned out to be a big advance for us. The

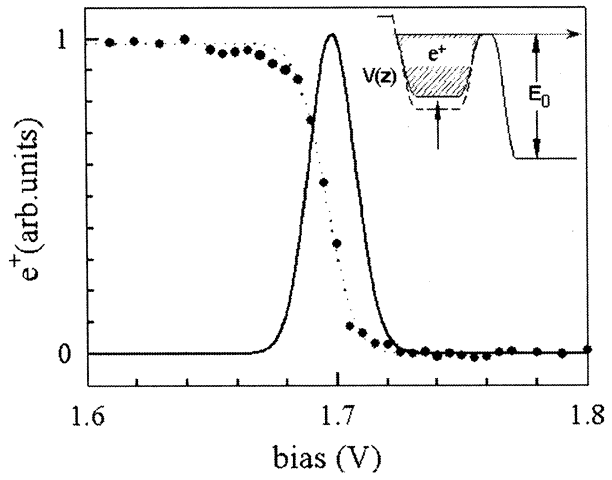

Fig. 9. Retarding potential curve of the cold trap-based positron beam indicating a parallel energy spread of 18 meV, FWHM at 1.7 eV [41]. The inset illustrates the beam-formation technique, whereby the potential of stage III of the positron trap is raised slowly to force the positrons out of the well.

beam was tunable from ~ 100 meV upwards and had a parallel energy spread of 18 meV. It was superior to conventional beams used for atomic physics studies by more than a factor of 10 in energy resolution.

Steven and Rod then decided to try a scattering experiment – vibrational excitation of CF_4. It was supposed to be a preliminary experiment, but turned out so well we sent the results to PRL [42]. What we had done in just two years was to advance the state of the art of positron beams for positron-atomic physics by more than an order of magnitude in energy resolution. We had also developed a new scattering technique that advanced the state of the art, even in electron scattering, particularly for measuring integral inelastic scattering cross sections.

In '98, Rod Greaves moved on to First Point Scientific, Inc., in Agoura Hills CA. There he has developed commercial positron traps and compact neon moderator systems that have aided greatly in allowing people around the world to exploit positron trapping technology [7, 43]. On the science side, he continues to collaborate with our group, and as discussed below, more recently with Allen Mills, who went from Bell Labs to the University of California at Riverside in the late '90s.

Positron cooling is a crucial issue for both plasma and scattering experiments. Rod Greaves had measured gas-cooling times for positrons and found that CF_4 and SF_6 were the best for rapid cooling [44]. This was confirmed by Gilbert's direct measurement of the vibrational cross section for CF_4. Giving the nod to its small annihilation cross section, we subsequently used small amounts of CF_4 in stage III of the trap for rapid cooling. This allowed us to cycle our pulsed positron beam rapidly for scattering and annihilation experiments.

Around that time, the results flowed in. Steven Gilbert made the first energy-resolved measurements of positron annihilation on molecules, discovering huge Feshbach resonances and measuring the first positron-molecule binding energies [45]. Joan Marler did her thesis work under the tutelage of post doc James Sullivan who joined us from the Australian National University in Canberra, thoughtfully bringing his advisor Steve Buckman along for the second year. Steve Buckman and James gave our program an enormous boost, pushing us to measure every conceivable cross section and hunt for every resonance imaginable (at least that's what it seemed like to me) [46-50]. One of their "gifts" was the technique of unfolding electronic excitation cross sections in molecules using the known Franck Condon factors [47] – good physics and great fun.

Turning back to key features of the operation of the positron trap, there are three puzzles.

- Why is N_2 the best trapping gas?
- Why did CF_4 work so well for cooling positrons?
- What's the story with the large annihilation rates in molecules?

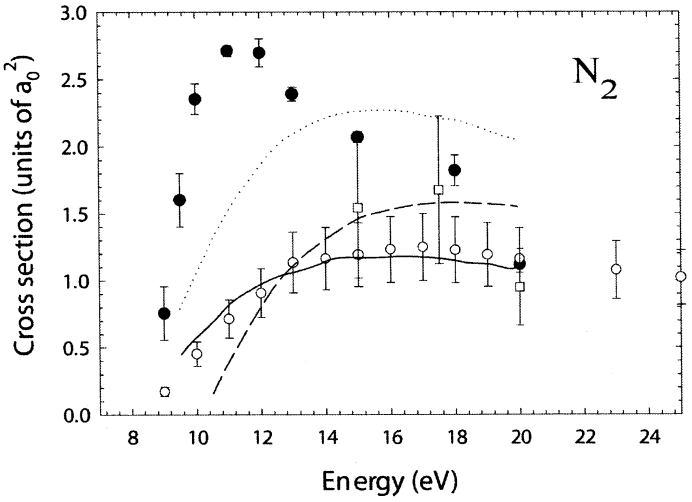

Fig. 10. Positron-impact cross section for the excitation of the $a^1\Pi$ state of N_2 [47, 51]. Shown for comparison (open circles) are electron data for the same cross section [52, 53]. Also shown by the lines are calculations by Marco Lima *et al.*, for the positron-impact process, using three different basis sets for the target. See Ref. [51] for details. The sharp rise at onset and relatively small near-threshold Ps formation cross section make N_2 the molecule of choice for buffer-gas trapping.

The cold beam told it all, more or less – at least all experimentally that is – the theory is about one and a half for three at this point. Shown in Fig. 10 is the positron-impact electronic excitation cross section for N_2 [47]. The unexpected, sharp rise at threshold (some kind of resonance?) opens up faster than the positronium formation cross section, which is a loss process in the positron trap. This resonance is a very efficient way for positrons to lose energy and drop into successive stages in the trap. In CO, there is a similar sharp resonance, but the Ps formation cross section is even larger, so CO is not as good as N_2 for trapping [51]. The case is closed for the experimentalists – the theorists still find this N_2 resonance difficult to explain,[1] as shown by the theory curves in Fig. 10.

The CF_4 vibrational excitation story has a similar ring to it. Gilbert's early measurement of the CF_4 cross section turned out to be inaccurate due to all the machinations we had to go through to measure it, so Joan Marler repeated the measurement, as shown in Fig. 11 [54]. We found a sharp rise at onset there too, and the largest vibrational cross section measured to date. Joan went on to make the same measurement for electron impact – the first *in situ* comparison of state-resolved electron and positron inelastic cross sections [54]. The fact that the cross sections were the same, both in magnitude and shape, provided the needed clue (kindly delivered to us by Gleb Gribakin) to compare the measurements with the predictions of the Born dipole model.

Indeed, the equality of the electron and positron scattering cross sections could be explained quantitatively by long range, electrostatic dipole coupling. Infrared absorption

[1] M. A. P. Lima, private communication, 2005.

measurements provide the strength of the dipole matrix element, and the theory fits quite well with no adjustable parameters. So in this case, the sharp rise in the cross section is not a resonance but arises naturally from the long-range electrostatic coupling. The remaining mystery is that all of the molecules and modes studied to date, except the one homopolar molecule, H_2, have positron-impact vibrational cross sections with a very similar energy dependence, even though the magnitude of the Born dipole coupling is too small by as much as a factor of five for everything except CF_4 [55]. So there's more to be learned here.

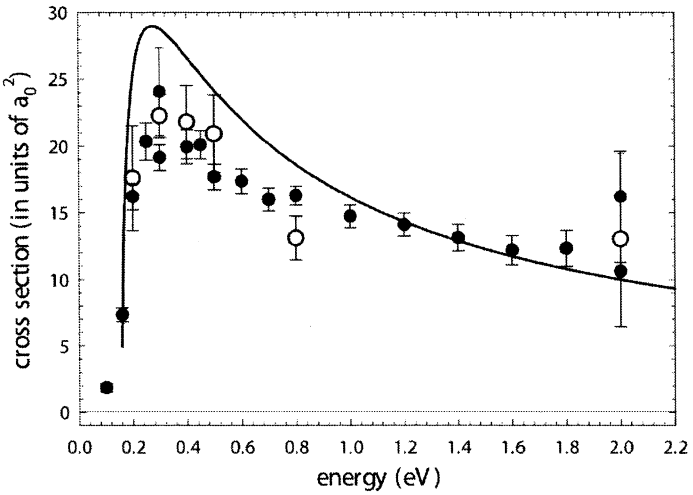

Fig. 11. Positron- and electron-impact cross sections for excitation of the ν_3 asymmetric stretch mode of CF_4. This is the largest positron-impact vibrational cross section measured to date. Also shown for comparison (–) are the predictions of the Born dipole model for this cross section, with no fitted parameters. From Ref. [54].

The final question led to the most spectacular result. As discussed above we, and others before us, had suspected that the large annihilation rates in molecules are due to vibrational resonances [15, 56], but it was hard to nail down experimentally with thermal distributions of positrons. Once we had the cold beam, Steven Gilbert and Levi Barnes (who had just joined the group as a Ph.D. student) took on the very ambitious project of studying annihilation rates in molecules as a function of positron energy. They built a wonderful apparatus such that they could cycle 10^9 positrons with only one background count. This is needed because, while the resonances are quite large, the basic cross section [i.e., the Dirac cross section, c.f., Eq. (1)] is miniscule, and so without a very careful experiment, it is still difficult to distinguish the annihilation from extraneous effects.

The results, as advertised above and illustrated in Fig. 12, were spectacular indeed [45, 57]. Alkane molecules were a favorite target of ours for studying annihilation, because they are conveniently available in a variety of sizes and exhibit huge enhancements in annihilation rates. We found very large enhancements in alkanes with energy spectra that closely mimic the spectra of the molecular vibrational modes, with particularly large resonance associated with the C-H asymmetric stretch mode. The

added bonus was that the annihilation spectra are downshifted from the vibrational spectra. We interpret these data in the context of Gleb Gribakin's vibrational Feshbach resonance model [60] as evidence that positrons bind to alkanes. The downshift is a measure of the positron binding energy, which ranges from ~ 40 meV in butane (C_4H_{10}) to > 200 meV in $C_{12}H_{26}$. Levi Barnes and Jason Young have now carried these experiments further, most recently finding evidence for a second, *positronically excited* bound state in the very large alkanes $C_{12}H_{26}$ and $C_{14}H_{30}$ [57, 58].

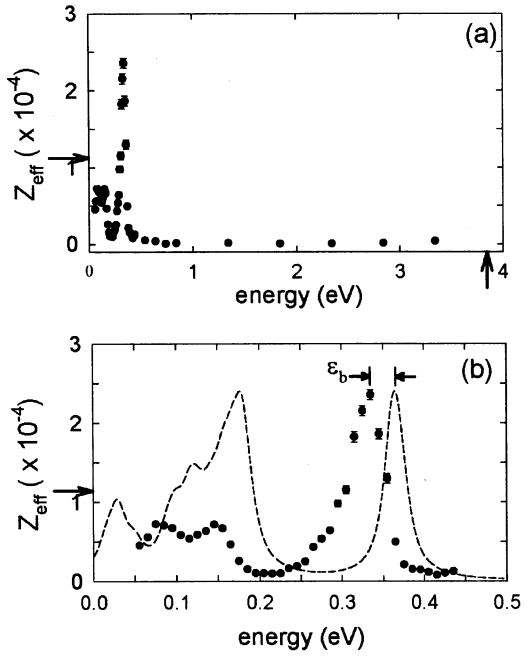

Fig. 12. Z_{eff} for butane (•) as a function of positron energy: (a) 0 to 5 eV, and (b) 0 to 0.5 eV. From Refs. [57] [58]. The arrow on the abscissa in (a) is the threshold for positronium formation. Shown in (b) is the vibrational-mode spectrum of butane (--, arbitrary vertical scale), with each mode broadened by 25 meV [59]. The downshift, ε_b, represents the positron-molecule binding energy which is ~ 40 meV for butane. Arrows on the ordinate indicate values of Z_{eff} for a 300 K Maxwellian distribution of positrons. In (a), Z_{eff} at energies $\geq$ 0.5 eV is ~ 100, comparable to the value of Z = 34 for this molecule, which is expected in the absence of the vibrational resonances.

MORE PHYSICS FROM THE TRAP AND WHAT THE FUTURE MIGHT HAVE IN STORE

I've carried the positron trapping saga and positron-atomic physics story along from the mid 80's to the present. There is a parallel story for positron plasmas that is too lengthy to tell here in any detail [6]. Mark Tinkle did a thesis on the development of mode diagnostics for positron plasmas [61, 62]. Rod Greaves and I did the first electron-positron plasma experiment, studying the instability generated when an electron beam is passed through a positron plasma [63, 64]. Greaves used a rotating electric field to compress positron plasmas radially (the so-called "rotating wall" effect) [44, 65], a tool

recently developed further by James Danielson [66, 67], that has enormous potential for tailoring positron plasmas and beams. James is now continuing this research and developing new methods to trap more positrons (i.e., a "multicell trap" [68]), and to produce much colder (the goal 1 meV, FWHM) positron beams [6].

At First Point Scientific Inc., Rod Greaves developed a commercial prototype buffer gas trap for materials characterization and positron research [43]. The basic buffer-gas trap design was used by the ATHENA collaboration to make the first low-energy antihydrogen [8]. The trap gave them a significant advantage *vis a vis* their competitors in the ATRAP collaboration, who also created low-energy antihydrogen very close to the same time in a set of complementary experiments [8, 69]. James Sullivan and Steve Buckman have now built a trap in Canberra for positron atomic physics research. Mike Charlton has one at Swansea [70], as does Igor Meshkov in Dubna [71], who got the design from Mike and is making a new Ps beam facility for fundamental physics studies.

Very recently, Allen Mills, David Cassidy, Rod Greaves, and collaborators used Rod's version of the buffer gas trap to observe effects they attribute to creation of the first Ps_2 molecules in the laboratory [9]. This line of experiments has enormous promise, and is likely to lead to the creation and study of BEC Ps, which is a long term goal of Allen and Phil Platzman [72, 73].

So it's been a very productive and rewarding time. The Drachman-Temkin symposium is a great place to tell the story. Dick's guidance and counsel was much appreciated by all of us involved in the positron trapping effort. As I finished writing this, one thought occurred to me: What if Marv and I had sat at different lunch tables that day at Bell? I may well have not had the opportunity to work with positrons or meet Dick – it was truly good luck the way it turned out!

I thank Rod Greaves, Marv Leventhal and Allen Mills, Jr., for careful reading of the manuscript.

References

1. Surko, C. M., Leventhal, M., Crane, W. S., *et al.*, The Positron Trap - A New Tool for Plasma Physics, in *Positron Studies of Solids, Surfaces, and Atoms; a Symposium to Celebrate Stephan Berko's 60th Birthday*, edited by J. A. P. Mills, W. S. Crane and K. F. Canter (World Scientific, 1984), p. 222.
2. Surko, C. M., Leventhal, M., Crane, W. S., *et al.*, Use of Positrons to Study Transport in Tokamak Plasmas, *Rev. of Sci. Instrum.* **57**, 1862, 1986.
3. Brown, B. L. and Leventhal, M., Laboratory Simulation of Direct Positron Annihilation in a Neutral-Hydrogen Galactic Environment, *Phys. Rev. Lett.* **57**, 1651, 1986.

4. Leventhal, M., Callum, C. J. M., and Stang, P. D., Detection of 511 Kev Positron-Annihilation Radiation from the Galactic-Center Direction, *Astrophys. J.*, L11, 1978.
5. Surko, C. M., Gribakin, G. F., and Buckman, S. J., Low-Energy Positron Interactions with Atoms and Molecules, *J. Phys. B: At. Mol. Opt. Phys.* **38**, R57 2005.
6. Surko, C. M. and Greaves, R. G., Emerging Science and Technology of Antimatter Plasmas and Trap-Based Beams, *Phys. Plasmas* **11**, 2333, 2004.
7. Greaves, R. G. and Moxom, J. M., Recent Results on Trap-Based Positron Beams, *Mat. Sci. Forum* **445-446**, 419, 2004.
8. Amoretti, M., Amsler, C., Bonomi, G., *et al.*, Production and Detection of Cold Antihydrogen Atoms, *Nature* **419**, 456, 2002.
9. Cassidy, D. B., Deng, S. H. M., Greaves, R. G., *et al.*, Experiments with a High-Density Positronium Gas, *Phys. Rev. Lett.* **95**, 195006, 2005.
10. Malmberg, J. H. and deGrassie, J. S., Properties of Nonneutral Plasma, *Phys. Rev. Lett.* **35**, 577, 1975.
11. O'Neil, T. M., A Confinement Theorem for Nonneutral Plasmas, *Phys. of Fluids* **23**, 2216, 1980.
12. Baille, P. and Darewych, J. W., Collisions Entre Un Positron Et Une Molecule D'hydrogene Avec Excitation De Vibrations, *J. de Phys. Lett.* **35**, 243, 1974.
13. Surko, C. M., Leventhal, M., and Passner, A., Positron Plasma in the Laboratory, *Phys. Rev. Lett.* **62**, 901, 1989.
14. Fee, M. S., Chu, S., A. P. Mills, Jr., *et al.*, Measurement of the Positronium 13S1 - 23S1 Interval by Continuous-Wave Two-Photon Excitation, *Phys. Rev Lett.* **70**, 1397, 1993.
15. Surko, C. M., Passner, A., Leventhal, M., *et al.*, Bound States of Positrons and Large Molecules, *Phys. Rev. Lett.* **61**, 1831, 1988.
16. Fraser, P. A., Positrons and Positronium in Gases, *Adv. in At. and Mol. Phys.* **4**, 63, 1968.
17. Heyland, G. R., Charlton, M., Griffith, T. C., *et al.*, Positron Lifetime Spectra for Gases, *Can. J. Phys.* **60**, 503, 1982.
18. Paul, D. A. L. and Saint-Pierre, L., Rapid Annihilation of Positrons in Polyatomic Gases, *Phys. Rev. Lett.* **11**, 493, 1963.
19. Passner, A., Surko, C. M., Leventhal, M., *et al.*, Ion Production by Positron-Molecule Resonances, *Phys. Rev. A* **39**, 3706, 1989.
20. Hulett, L. D., Donohue, D. L., Xu, J., *et al.*, Mass Spectrometry Studies of the Ionization of Organic Molecules by Low-Energy Positrons, *Chem. Phys. Lett.* **216**, 236, 1993.
21. McLuckey, S. A., Hulett, L. D., Xu, J., *et al.*, Gas-Phase Ionization of Polyatomic Molecules Via Interactions with Positrons, *Rap. Comm. Mass Sp.* **10**, 269, 1996.
22. McLuckey, S. A., Glish, G. L., Donohue, D. L., *et al.*, Positron Ionization Mass Spectrometry: Ionization by Fast Positrons, *Int'l. J. of Mass Spectrometry and Ion Processes* **97**, 237, 1990.
23. Crawford, O. H., Mechanism for Fragmentation of Molecules by Positron Annihilation, *Phys. Rev. A* **49**, R3147, 1994.

24. Iwata, K., Greaves, R. G., and Surko, C. M., Gamma-Ray Spectra from Positron Annihilation on Atoms and Molecules, *Phys. Rev. A* **55**, 3586, 1997.
25. Iwata, K., Gribakin, G. F., Greaves, R. G., *et al.*, Positron Annihilation on Large Molecules, *Phys. Rev. A* **61**, 022719, 2000.
26. Leventhal, M., Passner, A., and Surko, C. M., Positron-molecule Bound States and Positive Ion Production, in *Annihilation in Gases and Galaxies*, edited by R. J. Drachman (National Aeronautics and Space Administration, Washington, DC, 1990), p. 272.
27. Murphy, T. J., Positron Deposition in Plasmas by Positronium Beam Ionization and Transport of Positrons in Tokamak Plasmas, *Plasma Phys. and Controlled Fusion* **29**, 549, 1987.
28. Murphy, T. J. and Surko, C. M., Annihilation of Positrons on Organic Molecules, *Phys. Rev. Lett.* **67**, 2954, 1991.
29. Murphy, T. J. and Surko, C. M., Positron Trapping in an Electrostatic Well by Inelastic Collisions with Nitrogen Molecules, *Phys. Rev. A* **46**, 5696, 1992.
30. Murphy, T. J. and Surko, C. M., Annihilation of Positrons in Xenon Gas, *J. Phys. B: At. Mol. Opt. Phys.* **23**, L727, 1990.
31. Tang, S. and Surko, C. M., Angular Dependence of Positronium Formation in Molecular Hydrogen, *Phys. Rev. A* **47**, 743, 1993.
32. Tang, S., Tinkle, M. D., Greaves, R. G., *et al.*, Annihilation Gamma-Ray Spectra from Positron-Molecule Interactions, *Phys. Rev. Lett.* **68**, 3793, 1992.
33. VanReeth, P., Humberston, J. W., Iwata, K., *et al.*, Annihilation in Low-Energy Positron-Helium Scattering, *J. Phys. B: At. Mol. Opt. Phys.* **29**, L465, 1996.
34. Iwata, K., Gribakin, G., Greaves, R. G., *et al.*, Positron Annihilation with Inner-Shell Electrons in Noble Gas Atoms, *Phys. Rev. Lett.* **79**, 39, 1997.
35. Surko, C. M., Greaves, R. G., and Leventhal, M., Use of Traps to Study Positron Annihilation in Astrophysically Relevant Media, *Hyperfine Interactions* **81**, 239, 1993.
36. Iwata, K., Greaves, R. G., and Surko, C. M., Positron Annihilation in a Simulated Interstellar Medium, *Can. J. Phys.* **51**, 407, 1996.
37. Greaves, R. G. and Surko, C. M., Solid Neon Moderator for Positron Trapping Experiments, *Can. J. Phys.* **51**, 445, 1996.
38. Mills, A. P., Jr. and Gullikson, E. M., Solid Neon Moderator for Producing Slow Positrons, *Appl. Phys. Lett.* **49**, 1121, 1986.
39. Jorgensen, L. V., Amoretti, M., Bonomi, G., *et al.*, New Source of Dense, Cryogenic Positron Plasma, *Phys. Rev. Lett.* **95**, 025002, 2005.
40. Kurz, C., Greaves, R. G., and Surko, C. M., Temperature Dependence of Positron Annihilation Rates in Noble Gases, *Phys. Rev. Lett.* **77**, 2929, 1996.
41. Gilbert, S. J., Kurz, C., Greaves, R. G., *et al.*, Creation of a Monoenergetic Pulsed Positron Beam, *Appl. Phys. Lett.* **70**, 1944, 1997.
42. Gilbert, S. J., Greaves, R. G., and Surko, C. M., Positron Scattering from Atoms and Molecules at Low Energies, *Phys. Rev. Lett.* **82**, 5032, 1999.
43. Greaves, R. G. and Moxom, J., Design and Performance of a Trap-based Positron Beam Source, in *Non-Neutral Plasma Physics V*, edited by M. Schauer, T. Mitchell and R. Nebel (American Institute of Physics, 2003), p. 140.

44. Greaves, R. G. and Surko, C. M., Inward Transport and Compression of a Positron Plasma by a Rotating Electric Field, *Phys. Rev. Lett.* **85**, 1883, 2000.
45. Gilbert, S. J., Barnes, L. D., Sullivan, J. P., *et al.*, Vibrational Resonance Enhancement of Positron Annihilation in Molecules, *Phys. Rev. Lett.* **88**, 0443201, 2002.
46. Sullivan, J., Gilbert, S. J., and Surko, C. M., Excitation of Molecular Vibrations by Positron Impact, *Phys. Rev. Lett.* **86**, 1494, 2001.
47. Sullivan, J. P., Marler, J. P., Gilbert, S. J., *et al.*, Excitation of Electronic States of Ar, H_2, and N_2 by Positron Impact, *Phys. Rev. Lett.* **87**, 073201, 2001.
48. Sullivan, J. P., Gilbert, S. J., Buckman, S. J., *et al.*, Search for Resonances in the Scattering of Low-Energy Positrons from Atoms and Molecules, *J. Phys. B: At. Mol. Opt. Phys.* **34**, L467, 2001.
49. Sullivan, J. P., Gilbert, S. J., Marler, J. P., *et al.*, Positron Scattering from Atoms and Molecules Using a Magnetized Beam, *Phys. Rev. A* **66**, 042708, 2002.
50. Marler, J. P., Sullivan, J. P., and Surko, C. M., Ionization and Positronium Formation in Noble Gases, *Phys. Rev. A* **71**, 022701, 2005.
51. Marler, J. P. and Surko, C. M., Positron-Impact Ionization, Positronium Formation and Electronic Excitation Cross Sections for Diatomic Molecules, *Phys. Rev. A***72**, 062713, 2005.
52. Campbell, L., Brunger, M. J., Nolan, A. M., *et al.*, Integral Cross Sections for Electron Impact Excitation of Electronic State of N_2, *J. Phys. B: At. Mol. Opt. Phys.* **34**, 1185, 2001.
53. Mason, N. J. and Newell, W. R., Electron Impact Total Excitation Cross Section of the $A^1\Pi_g$ State of N_2, *J. Phys. B* **20**, 3913, 1987.
54. Marler, J. P. and Surko, C. M., Systematic Comparison of Positron and Electron Impact Excitation of the N_3 Vibrational Mode of Cf_4, *Phys. Rev. A* **72**, 062702, 2005.
55. Marler, J. P., Gribakin, G., and Surko, C. M., Comparison of Positron-Impact Vibrational Excitation Cross Sections with the Born-Dipole Model, *Nucl. Instrum Methods A*, in press, 2006.
56. Smith, P. M. and Paul, D. A. L., Positron Annihilation in Methane Gas, *Can. J. Phys.* **48**, 2984, 1970.
57. Barnes, L. D., Gilbert, S. J., and Surko, C. M., Energy-Resolved Positron Annihilation for Molecules, *Phys. Rev. A* **67**, 032706, 2003.
58. Barnes, L. D., Young, J. A., and Surko, C. M., Studies of Energy-Resolved Positron Annihilation Rates for Molecules, *Phys. Rev. A*, submitted, 2006.
59. Gribakin, G. F. and Gill, P. M. W., The Role of Vibrational Doorway States in Positron Annihilation with Large Molecules, *Nucl. Instrum. Methods B* **221**, 30, 2004.
60. Gribakin, G. F., Mechanisms of Positron Annihilation on Molecules, *Phys. Rev. A* **61**, 22720, 2000.
61. Tinkle, M. D., Greaves, R. G., Surko, C. M., *et al.*, Low-Order Modes as Diagnostics of Spheroidal Non-Neutral Plasmas, *Phys. Rev. Lett.* **72**, 352, 1994.
62. Tinkle, M. D., Greaves, R. G., and Surko, C. M., Modes of Spheroidal Ion Plasmas at the Brillouin Limit, *AIP Conference Proceedings* **331**, 229, 1995.

63. Greaves, R. G. and Surko, C. M., An Electron-Positron Beam-Plasma Experiment, *Phys. Rev. Lett.* **75**, 3846, 1995.
64. Gilbert, S. J., Dubin, D. H. E., Greaves, R. G., *et al.*, An Electron-Positron Beam-Plasma Instability, *Phys. of Plasmas* **8**, 4982, 2001.
65. Greaves, R. G. and Surko, C. M., Radial Compression and Inward Transport of Positron Plasmas Using a Rotating Electric Field, *Phys. Plasmas* **8**, 1879, 2001.
66. Danielson, J. R. and Surko, C. M., Torque-Balanced High-Density Steady States of Single Component Plasmas, *Phys. Rev. Lett.* **95**, 035001, 2005.
67. Danielson, J. R. and Surko, C. M., Radial Compression and Torque Balanced Steady States of Single-Component Plasmas in Penning-Malmberg Traps, *Phys. Rev. A*, in press, 2006.
68. Surko, C. M. and Greaves, R. G., A Multi-Cell Trap to Confine Large Numbers of Positrons, *Rad. Chem. and Phys.* **68**, 419, 2003.
69. Gabrielse, G., Bowden, N., Oxley, P., *et al.*, Background-Free Observation of Cold Antihydrogen with Field-Ionization Analysis of Its States, *Phys. Rev. Lett.* **89**, 213401, 2002.
70. Clarke, J., vanderWerf, D. P., Charlton, M., *et al.*, Developments in the Trapping and Accumulation of Slow Positrons Using the Buffer Gas Technique, *Nonneutral Plasma Physics V,* edited by M. Schauer, T. Mitchell and R. Nebel (American Institute of Physics, 2003), p. 178.
71. Meshkov, I. N., Lepta Project: Generation and Study of Positronium in Directed Fluxes, *Nucl. Instrum Methods B* **221**, 168 2004.
72. Platzman, P. M. and Mills, A. P., Jr., Possibilities for Bose Condensation of Positronium, *Phys. Rev. B* **49**, 454, 1994.
73. Mills, A. P., Jr., Positronium Molecule Formation, Bose-Einstein Condensation and Stimulated Annihilation, *Nucl. Instrum. Methods B* **192**, 107, 2002.

CALCULATIONS OF POSITRON AND POSITRONIUM SCATTERING

H.R.J. Walters and C. Starrett

Department of Applied Mathematics and Theoretical Physics,
Queen's University, Belfast, BT7 1NN, United Kingdom

ABSTRACT

Progress in the theoretical treatment of positron - atom and positronium - atom scattering within the context of the coupled - pseudostate approximation is described.

INTRODUCTION

Although I (HRJW) was well acquainted with the works of Aaron and Dick, it was some time before I actually met these giants of Atomic Physics in person. My first encounter with Aaron was in 1976. At that time I had already been impressed by the substantive section that had been devoted to his work in the famous text by Mott and Massey on "The Theory of Atomic Collisions" (ref. 1). Here I had read about "Temkin's Method" for treating the total S-wave electron - hydrogen problem (ref. 2) and his polarized orbital technique (refs. 3, 4). The former was later to be exploited by Poet (ref. 5) to create one of the most important benchmarks for electron scattering by atomic hydrogen, the latter became an ubiquitous approximation which is used to the present day. I had also read his edited compendium on "Autoionization" (ref. 6) and, in particular, his own article in that compendium which had done much to clarify my ideas on the topic. The occasion of the meeting was the local UK ATMOP conference which, in 1976, had come to Belfast. It was a very difficult time, for "The Troubles" were then in full swing. Fearful that attendance would be low, Phil Burke had organised a pre - ATMOP workshop that, as it turned out, was attended by a glittering array of international stars, amongst the foremost of whom was Aaron. We at Belfast shall be forever grateful for the support that we received from those who came at that risky time. It is David Thompson that I have to thank for my introduction to Aaron.

It was not until relatively late, 1987, that I met up with Dick. The occasion was the Positron Workshop satellite of ICPEAC which was then held at University College London. Our accommodation was arranged in one of the Halls of Residence of London University. In the mornings we would queue up outside the breakfast hall and, somehow, Dick and I were always first in the queue. It was during these moments that Dick regaled me, in his own inimitable way, with some fascinating anecdotes. It was there that I learnt that Dick's family had passed through London, a loss to British science but a gain to the US. One of the highlights of the London meeting was Dick's talk on "Theoretical aspects of positronium collisions". This can be read in ref. 7, it is a superb and insightful article which I strongly recommend. It was this talk more than anything that persuaded me that Positronic Atomic Physics was really an exciting area worthy of study. Perhaps a better title for the present article would be "The Drachman Programme" for I find that with each step I take I follow in a path already trodden by Dick. So let us begin that Programme.

POSITRON - ATOM SCATTERING

When a positron scatters off an atom, A, the following processes (assuming A contains enough electrons) are possible:

$e^+ + A \longrightarrow$	$e^+ + A$	Elastic Scattering	$(1a)$
	$e^+ + A^*$	Excitation	$(1b)$
	$e^+ + A^{n+} + ne^-$	Ionization	$(1c)$
	$Ps(nlm) + A^+$	Ps Formation	$(1d)$
	$Ps^- + A^{++}$	Ps^- Formation	$(1e)$
	$Ps + A^{(n+1)+} + ne^-$	Transfer Ionization	$(1f)$
	$Ps^- + A^{(n+2)+} + ne^-$	Transfer Ionization with Ps^- Formation	$(1g)$
	$A^+ + \gamma$ rays	Annihilation	$(1h)$

Reactions (1a) to (1c) are also possible using electrons as a projectile. Reactions (1d) to (1h) are unique to the positron. It is these latter reactions which distinguish the positron as a more subtle projectile than the electron. Unlike the electron, the positron competes with the atomic nucleus for the "attention" of the electrons in the system, leading to a more correlated dynamics. Positronium formation is the most obvious manifestation of this competition while the annihilation process gives "pin - point" information on correlation in the system in that it measures the probability that the positron coincides with an electron.

Because of the competition between the positron and the atomic nucleus for electrons, positron - atom scattering is inherently a two - centre process, in contrast to electron - atom scattering where the whole dynamics is essentially centred on the atomic nucleus. It is this two - centre nature which makes the theoretical description of positron - atom scattering so much more difficult than that of electron - atom scattering. Considerable success has been achieved using the coupled - (pseudo)state approach to treat positron scattering by "one - electron" and "two - electron" atoms (refs. 8 - 17). To illustrate what is involved we shall describe the method as applied to positron scattering by atomic hydrogen. [1]

Let $\mathbf{r}_p$ ($\mathbf{r}_e$) be the position vector of the positron (electron) relative to the hydrogen nucleus, ie, the proton. While these coordinates are convenient for describing positron - atom channels, the natural set of coordinates for positronium channels is $\mathbf{R} \equiv (\mathbf{r}_p + \mathbf{r}_e)/2$ and $\mathbf{t} \equiv \mathbf{r}_p - \mathbf{r}_e$ which give the position vector of the positronium centre of mass relative to the proton and the positronium internal coordinate respectively. In the coupled - state approach the wave function for the collision system, Ψ, is expanded as

$$\Psi = \sum_a F_a(\mathbf{r}_p)\psi_a(\mathbf{r}_e) + \sum_b G_b(\mathbf{R})\phi_b(\mathbf{t}) \tag{2}$$

where the first sum is over atomic hydrogen states ψ_a and the second is over positronium states ϕ_b. In the first instance it will be assumed that ψ_a and ϕ_b are eigenstates. The expansion (2) clearly represents both positron - atom (first sum) and positronium - proton (second sum) channels explicitly. Since the states ψ_a and ϕ_b separately form complete sets, the expansion (2) is technically over - complete. However, in practical calculations complete sets of states are never actually used. Substituting (2) into the Schrödinger equation and projecting with $\psi_a(\mathbf{r}_e)$ and $\phi_b(\mathbf{t})$ gives coupled equations for the unknown functions $F_a(\mathbf{r}_p)$ and $G_b(\mathbf{R})$ of the form

$$\begin{aligned} \left(\nabla_p^2 + k_a^2\right) F_a(\mathbf{r}_p) &= 2\textstyle\sum_{a'} V_{aa'}(\mathbf{r}_p)F_{a'}(\mathbf{r}_p) + 2\sum_{b'} \int K_{ab'}(\mathbf{r}_p, \mathbf{R})\, G_{b'}(\mathbf{R})\, d\mathbf{R} \\ \left(\nabla_R^2 + p_b^2\right) G_b(\mathbf{R}) &= 4\textstyle\sum_{b'} U_{bb'}(\mathbf{R})\, G_{b'}(\mathbf{R}) + 4\sum_{a'} \int K^{\star}_{a'b}(\mathbf{r}_p, \mathbf{R})\, F_{a'}(\mathbf{r}_p)\, d\mathbf{r}_p \end{aligned} \tag{3}$$

[1] We use atomic units (au) in which $\hbar = m_e = e = 1$ throughout this article.

where

$$E = \frac{k_a^2}{2} + \epsilon_a = \frac{p_b^2}{4} + E_b \tag{4}$$

E being the total energy and ϵ_a (E_b) being the energy of the state ψ_a (ϕ_b). The symbol $\star$ stands for complex conjugation. In (3) the local potentials $V_{aa'}(\mathbf{r}_p)$ and $U_{bb'}(\mathbf{R})$ come from the direct Coulombic interaction between the positron and the hydrogen atom and between the positronium and the proton respectively. From a computational viewpoint the really difficult objects in (3) are the non - local couplings $K_{ab}(\mathbf{r}_p, \mathbf{R})$ which represent positronium formation. In practice, the coupled equations (3) are reduced to partial wave form and the resulting radial equations are solved using some suitable technique such as the R - matrix method (ref. 18).

The success of the coupled - state approach has in large part been due to the concept of pseudostates. A practical difficulty with using the expansion (2) is how to handle continuum states ψ_a and ϕ_b in the expansion. Such states correspond to the ionization channels of the system. In the pseudostate method the atom and positronium continua are replaced by discrete pseudostates $\overline{\psi}_a$ and $\overline{\phi}_b$ and so (2) becomes an expansion in terms of a finite number of discrete states. Some of these states will be true (discrete) eigenstates ψ_a (ϕ_b), the remainder will be pseudostates $\overline{\psi}_a$ ($\overline{\phi}_b$). The notation ψ_a (ϕ_b) will now be used to mean either an eigenstate or a pseudostate of this finite set. The pseudostates are constructed so that the set of states ψ_a (ϕ_b) diagonalizes the atom (positronium) Hamiltonian H_A (H_{Ps}):

$$\begin{aligned} \langle\psi_a|H_A|\psi_{a'}\rangle &= \epsilon_a\delta_{a,a'} \quad \langle\psi_a|\psi_{a'}\rangle = \delta_{a,a'} \\ \langle\phi_b|H_{Ps}|\phi_{b'}\rangle &= E_b\delta_{b,b'} \quad \langle\phi_b|\phi_{b'}\rangle = \delta_{b,b'} \end{aligned} \tag{5}$$

This means that the coupled equations for $F_a(\mathbf{r}_p)$ and $G_b(\mathbf{R})$ retain the form (3). The diagonalization (5) is normally achieved by using a basis of Slater orbitals (ref. 9) or Laguerre functions (refs. 9, 19, 20). We can think of pseudostates as being "clumps" or "distributions" of eigenstates with the clump being centred upon the energy ϵ_a (E_b). The distribution of a pseudostate over the eigenstate spectrum may be specified in terms of a function

$$f_n(\epsilon) = |\langle\chi_\epsilon \mid \chi_n\rangle|^2 \tag{6}$$

where $\chi_n \equiv \psi_a$ or ϕ_b, as appropriate, and χ_ϵ is an eigenstate of H_A or H_{Ps}, as appropriate, with energy ϵ and the same angular momentum quantum numbers as χ_n. If χ_ϵ is a bound state it is normalized to unity, if a continuum state to a delta function in ϵ, ie,

$$\langle\chi_\epsilon|\chi_{\epsilon'}\rangle = \delta(\epsilon - \epsilon') \tag{7}$$

The quantity $f_n(\epsilon)$ is just the probability that χ_n contains the eigenstate χ_ϵ. Figure 1 illustrates the distribution functions on the continuous part of the spectrum ($\epsilon \geq 0$) for some s - type atomic hydrogen pseudostates used in a 33 - state calculation of e^+ + H(1s) scattering by Kernoghan et al (ref. 14). Figure 2 shows results from the same calculation. The agreement with experiment is very good. Figure 3 demonstrates the power of the method. Here we see how the approximation can give a complete picture of all the main processes. In the coupled pseudostate approach we have a representation of all the main physical processes, ie, excitation of the atom, positronium formation, ionization, in effect a **complete dynamical theory**. How good this representation is, of course, depends upon the choice and number of pseudostates.

In figure 4 we show estimates of the cross sections for e^+ + H(1s) scattering made by Dick for use in an analysis of the annihilation of galactic positrons (ref. 23). These estimates were made in 1978. They are remarkably close to the numbers shown in figure 3 which were calculated 17 years later! But there is more, displayed also in figure 4 are estimates of the cross sections for positron scattering by molecular hydrogen. It will be a long time before such cross sections can be calculated by the sophisticated methods described here, but we would bet that, if they were, they would not be much different from Dick's estimates shown in figure 4, such is our confidence in his judgement.

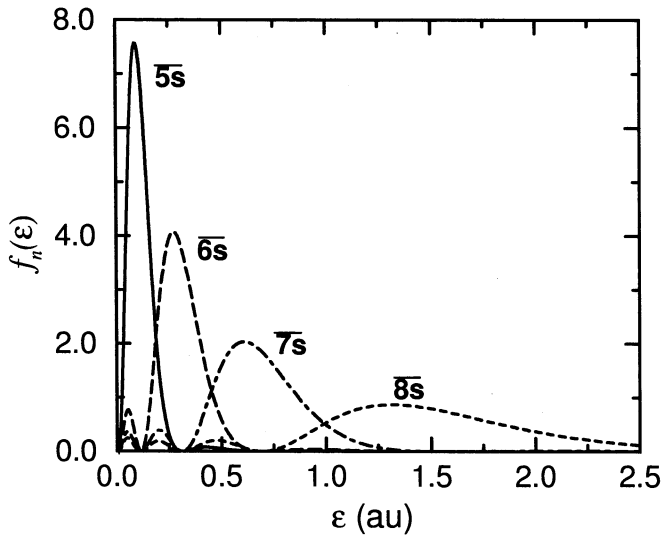

Figure 1: Distribution function f_n for $\overline{5s}$ to $\overline{8s}$ atomic hydrogen pseudostates used in the calculation of ref. 14.

Besides atomic hydrogen, coupled - state calculations have been performed on the alkali metals Li, Na, K, Rb and Cs (refs. 9, 10, 11, 13, 15, 16, 17) which have been treated as "one-electron" systems. An interesting prediction to come out of these calculations is the collapse in ground state positronium formation with a corresponding increase in excited state formation as we ascend the alkali metal series from Li to Cs, this is illustrated in figure 5.

When the atom contains more than one electron (N electrons, say) a new technical feature arises, namely, electron exchange between the formed Ps and the resultant atomic ion. We need now to label not only the states of the atom (a) and the Ps (b) but also the state of the ion (i). the coupled equations then generalise to

$$\begin{aligned}
\left(\nabla_p^2 + k_a^2\right) F_a(\mathbf{r}_p) &= 2\sum_{a'} V_{aa'}(\mathbf{r}_p) F_{a'}(\mathbf{r}_p) \\
&\quad +2N \sum_{i',b'} \int K_{a,i'b'}(\mathbf{r}_p, \mathbf{R}) G_{i'b'}(\mathbf{R}) d\mathbf{R} \\
\left(\nabla_R^2 + p_{ib}^2\right) G_{ib}(\mathbf{R}) &= 4\sum_{i',b'} U_{ib,i'b'}(\mathbf{R})\, G_{i'b'}(\mathbf{R}) \\
&\quad +4\sum_{a'} \int K^{\star}_{a'ib}(\mathbf{r}_p, \mathbf{R})\, F_{a'}(\mathbf{r}_p)\, d\mathbf{r}_p \\
&\quad +4\sum_{i',b'} \int L_{ib,i'b'}(\mathbf{R}, \mathbf{R}')\, G_{i'b'}(\mathbf{R}')\, d\mathbf{R}' \qquad (8)
\end{aligned}$$

The non - local terms $L_{ib,i'b'}(\mathbf{R}, \mathbf{R}')$ describe the conversion of ion and Ps states ($i'b'$) into (ib) through electron exchange. Whereas the positronium formation kernels $K_{a,ib}$ are difficult to handle, the new terms $L_{ib,i'b'}$ are very much more difficult still. It is this new element which makes the generalisation of the "one - electron" case to many electron targets non - trivial. However, the new terms are fundamental to the study of Ps - atom scattering which we discuss in the next section. Missing from (8) is explicit allowance for other new channels that become possible with multi -

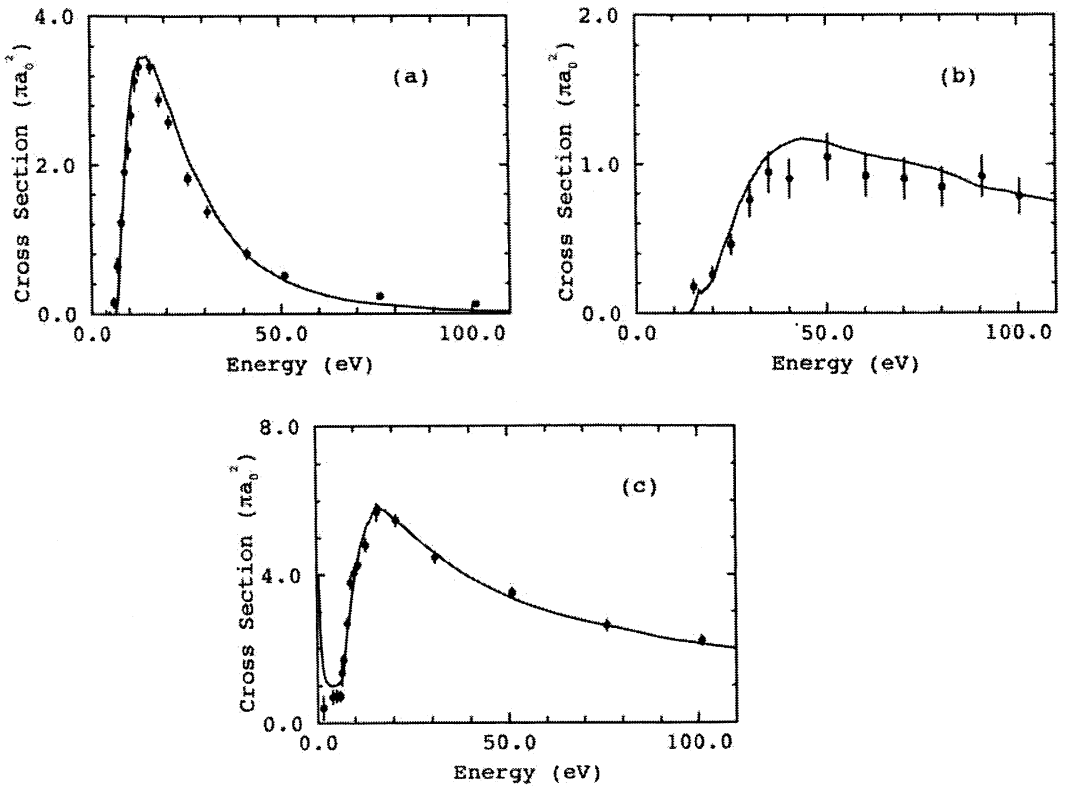

Figure 2: Positron scattering by H(1s): (a) total positronium formation; (b) ionization; (c) total cross section. Solid curve gives the 33-state results from ref. 14. Experimental data are from Zhou et al (ref. 21) and Jones et al (ref. 22).

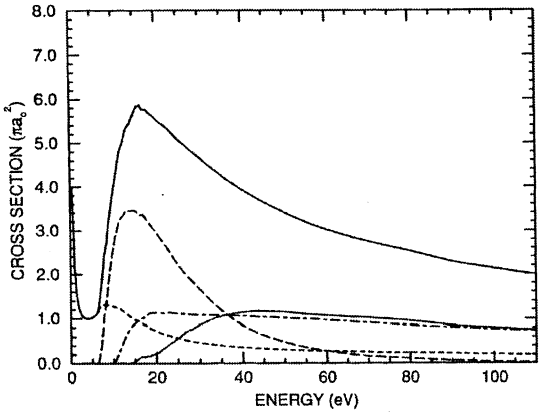

Figure 3: Cross sections in the 33-state approximation of ref. 14 for positron scattering from H(1s): upper solid curve, total cross section; long-dashed curve, total positronium formation; short-dashed curve, elastic scattering; dash-dot curve, H(2p) excitation; lower solid curve, ionization.

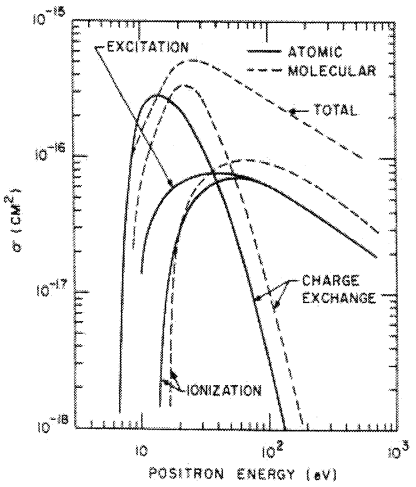

Figure 4: Ps formation (labelled "charge exchange"), ionization, discrete excitation, and total cross sections for e^+ scattering by H(1s) (solid curves) and H_2 (dashed curves), taken from ref. 23.

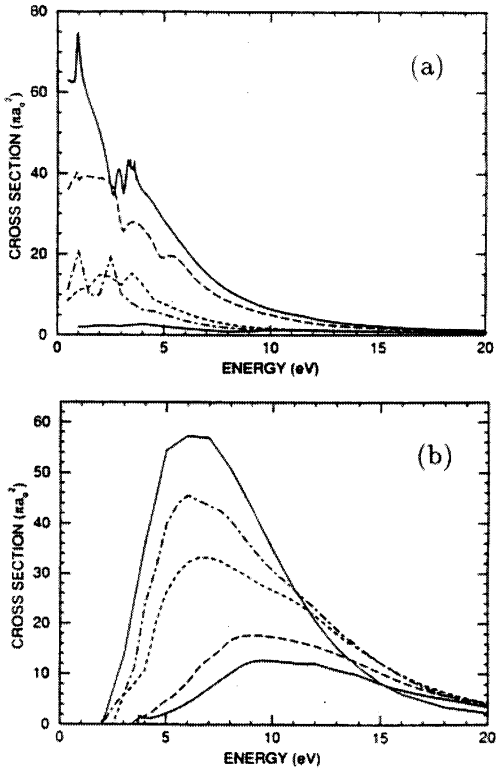

Figure 5: Positronium formation cross sections for Li, Na, K, Rb and Cs: (a) Ps(1s) formation; (b) positronium formation in excited states. Curves: upper solid in (a) and lower solid in (b), Li; long-dashed, Na; short-dashed, K; dash-dot, Rb; lower solid in (a) and upper solid in (b), Cs.

electron atoms, eg, Ps^- formation, see (1). In principle, these could be incorporated into the coupled - state formalism as required. The formalism (8) has been applied to the "two - electron" targets He, Mg, Ca and Zn (refs. 17, 24), again, as for the "one -electron" targets, giving very good agreement with experiment where data exists (ie, He and Mg).

POSITRONIUM - ATOM SCATTERING

The development of monoenergetic Ps beams at University College London (refs. 25 - 28) has led to growing interest in Ps - atom collisions. Ps is the lightest neutral atomic projectile, being like a hydrogen atom but only 1/1000th of its mass, Ps collisions are therefore of considerable fundamental interest. It is important to specify the total spin state of the Ps which can be either singlet or triplet. Ps in the spin singlet state is called "para-positronium" (p-Ps), that in the triplet state "ortho-positronium" (o-Ps). The significance of this classification lies in the different lifetimes of these spin states against the annihilation of the electron and positron into photons. Thus p-Ps(1s) annihilates predominantly into two photons, each of 511 keV, with a lifetime of 0.125ns, while o-Ps(1s) annihilates predominantly into three photons with a much longer lifetime of 142ns. Because Ps has internal degrees of freedom, it is important in a collision experiment to define the electronic state of the beam. In the present state of the art, Ps beams consist essentially of o-Ps(1s) (ref. 27), the corresponding para species, p-Ps(1s), is too short - lived to be transportable as a beam. Experimental capability is at an early stage and measurements have, until recently, mostly been confined to total cross sections. In addition to the beam measurements there are also some cross section data at very low energies deduced from observations of the annihilation rate of o-Ps(1s) in various gases (refs. 25, 29 - 35). Providing that the atomic target is spin unpolarised and that the spins of the particles in the final state are not determined, the collision cross sections for o-Ps and p-Ps are the same (ref. 36). Under these assumptions, we can drop the "ortho" and "para" epithets and talk simply about Ps - atom cross sections.

The fact that Ps has internal degrees of freedom as well as the atom considerably complicates the theoretical description of Ps scattering. That the Ps centre of charge coincides with its centre of mass results in the direct Coulombic interaction between the Ps and the atom being very much weakened compared to the electron exchange interaction between the two particles. We have already met this exchange interaction in positron scattering by multi - electron atoms, see equation (8) where the exchange interaction between the formed Ps and the atomic ion is described by the non - local terms $L_{ib,i'b'}(\mathbf{R},\mathbf{R}')$. The exchange process is very difficult to calculate since it involves electron swapping between two different centres, the Ps and the atom. To illustrate what is involved, let us consider the most fundamental system, Ps scattering by H. For this system the Hamiltonian may be written as

$$\begin{aligned} H &= -\frac{1}{4}\nabla^2_{R_1} + H_{Ps}(\mathbf{t}_1) + H_A(\mathbf{r}_2) + V(\mathbf{R}_1,\mathbf{t}_1,\mathbf{r}_2) \\ &= -\frac{1}{4}\nabla^2_{R_2} + H_{Ps}(\mathbf{t}_2) + H_A(\mathbf{r}_1) + V(\mathbf{R}_2,\mathbf{t}_2,\mathbf{r}_1) \end{aligned} \tag{9}$$

where H_A and H_{Ps} are the atomic and positronium Hamiltonians given by

$$\begin{aligned} H_A(\mathbf{r}_i) &\equiv -\frac{1}{2}\nabla^2_i - \frac{1}{r_i} \\ H_{Ps}(\mathbf{t_i}) &\equiv -\nabla^2_{t_i} - \frac{1}{t_i} \end{aligned} \tag{10}$$

and V is the interaction between the Ps and the H atom,

$$V(\mathbf{R},\mathbf{t},\mathbf{r}) = \left(\frac{1}{|\mathbf{R}+\frac{1}{2}\mathbf{t}|} - \frac{1}{|\mathbf{R}+\frac{1}{2}\mathbf{t}-\mathbf{r}|}\right) - \left(\frac{1}{|\mathbf{R}-\frac{1}{2}\mathbf{t}|} - \frac{1}{|\mathbf{R}-\frac{1}{2}\mathbf{t}-\mathbf{r}|}\right) \tag{11}$$

In the above equations $\mathbf{R}_i \equiv (\mathbf{r}_p + \mathbf{r}_i)/2$ is the position vector of the Ps centre of mass, $\mathbf{t}_i \equiv \mathbf{r}_p - \mathbf{r}_i$ is the Ps internal coordinate and $\mathbf{r}_p(\mathbf{r}_i)$ is the position vector of the positron (ith electron), where all position vectors are referred to the atomic nucleus as origin. Under the Hamiltonian (9) the spin of the positron, s_p, and the total electronic spin, S, of the two electrons are separately conserved. The spatial part of the collision wave function, Ψ^S, for scattering in the electronic spin state S is then expanded as

$$\Psi^S = \sum_{a,b} \left[G^S_{ab}(\mathbf{R}_1)\psi_a(\mathbf{r}_2)\phi_b(\mathbf{t}_1) + (-1)^S G^S_{ab}(\mathbf{R}_2)\psi_a(\mathbf{r}_1)\phi_b(\mathbf{t}_2) \right] \tag{12}$$

where, as before, ψ_a (ϕ_b) is a H (Ps) state satisfying (5), either an eigenstate or a pseudostate. Substituting (12) into the Schrödinger equation and projecting with $\psi_a(\mathbf{r}_2)\phi_b(\mathbf{t}_1)$ leads to coupled equations of the form

$$\left(\nabla^2_R + p^2_{ab}\right) G^S_{ab}(\mathbf{R}) = 4 \sum_{a'b'} \left[V_{ab,a'b'}(\mathbf{R}) G^S_{a'b'}(\mathbf{R}) + (-1)^S \int L_{ab,a'b'}(\mathbf{R},\mathbf{R}') G^S_{ab}(\mathbf{R}') d\mathbf{R}' \right] \tag{13}$$

where the total energy, E, is given by

$$E = \frac{p^2_{ab}}{4} + \epsilon_a + E_b \tag{14}$$

and

$$V_{ab,a'b'}(\mathbf{R}) \equiv \langle \psi_a(\mathbf{r})\phi_b(\mathbf{t}) \left| V(\mathbf{R},\mathbf{t},\mathbf{r}) \right| \psi_{a'}(\mathbf{r})\phi_{b'}(\mathbf{t}) \rangle \tag{15}$$

As before, the non-local couplings $L_{ab,a'b'}(\mathbf{R},\mathbf{R}')$ describe how the state $\psi_{a'}\phi_{b'}$ is converted into the state $\psi_a\phi_b$ by electron exchange between the Ps and the H. It is clear from (11) that

$$V(\mathbf{R},\mathbf{t},\mathbf{r}) = -V(\mathbf{R},-\mathbf{t},\mathbf{r}) \tag{16}$$

From this it follows that the direct potentials $V_{ab,a'b'}$ are zero unless the Ps states ϕ_b and $\phi_{b'}$ have opposite parity. The electron exchange terms do not share this symmetry with the result that exchange is enhanced relative to direct scattering. Indeed, in the simplest coupled - state approximation, static - exchange, where only one atom and one Ps state are retained in (12), the equations (13) reduce to a single equation

$$\left(\nabla^2_R + p^2_{ab}\right) G^S_{ab}(\mathbf{R}) = (-1)^S 4 \int L_{ab,ab}(\mathbf{R},\mathbf{R}') G^S_{ab}(\mathbf{R}') d\mathbf{R}' \tag{17}$$

which contains no direct potential and so is driven solely by the exchange interaction.
It is clear from (12) that the scale of the coupled - state calculation will escalate rapidly as the product of the number of atom states ψ_a times the number of Ps states ϕ_b. For this reason the first calculations adopted a "frozen target" approximation, ie, retained only one atom state in the expansion (12). In figure 6 we show the results of a 22 - state frozen target calculation of Ps(1s) + H(1s) scattering (ref. 37). The 22 states are Ps states and 19 of theses are pseudostates. We see from this figure that, at the higher energies, the main outcome of a collision is ionization of the Ps, hence the importance of including ionization channels (pseudostates) in the coupled - state approximation. Figure 6 shows that elastic scattering "dies" once ionization switches on and that discrete excitation of the Ps(1s) to Ps(n=2) is small at all impact energies, at least in this approximation. Also shown in figure 6 is a first Born estimate (ref. 38) of the contribution to the total cross section coming from collisions in which the H atom is excited or ionized, this suggests that target excitation/ionization is only important above about 20 eV. However, what the first Born approximation cannot tell us is how the solutions to the coupled equations (13) would be changed, for example, for elastic scattering at very low energies, if excited or ionized states of the atom were added to the expansion (12). The inclusion of these states would permit processes in which, for instance, the atom could be "virtually" excited/ionized and then de - excited/de - ionized back to its initial state, the overall result being no change in the observed state of the atom. Such processes, which are really just an interpretation of

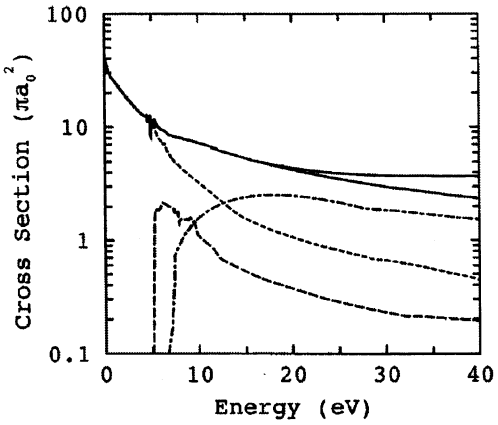

Figure 6: Frozen target total cross section, and its components, for Ps(1s)+H(1s) scattering (ref. 37). Curves: lower solid, total cross section; upper solid, frozen target total cross section with first Born estimate from ref. 38 for H target excitation and ionization added; short-dashed, Ps(1s) elastic scattering; long-dashed, Ps(n=2) excitation; dash-dotted, Ps ionization.

how the coupled equations "work", are referred to as "virtual" excitations[2] and are to be distinguished from real observable excitations which are represented by the first Born approximation in figure 6.

A noticeable feature in figure 6 is the structure near 5eV. A careful analysis of the partial wave contributions to the elastic cross section of figure 6 reveals that this structure corresponds to resonances in the electronic spin singlet partial waves. This is illustrated in figure 7 for the S-, P- and D-waves. However, no resonances appear in the triplet partial waves (see figure 12). What can be the origin of this? We shall return to this point later.

Unfortunately, experimental measurements on an atomic hydrogen target will not be feasible for some time yet. The targets most amenable to experimental study are the noble gases. In figures 8 to 10 we show some experimental results compared with frozen target calculations analogous to that of figure 6 (refs. 39, 40). We begin with figure 8 which compares the frozen target results for He (ref. 39), Ne and Ar (ref. 40) with cross sections deduced from annihilation measurements at very low energies (refs. 29-35). The experimental cross sections correspond to the momentum transfer cross section

$$\sigma_{mom} = \int (1 - \cos\theta) \frac{d\sigma_{el}}{d\Omega} d\Omega \tag{18}$$

where $d\sigma_{el}/d\Omega$ is the elastic differential cross section and θ is the scattering angle of the Ps. At these low energies only elastic scattering is possible. Figure 8 shows two theoretical cross sections, one the total elastic cross section, the other the momentum transfer cross section. We first note the importance of distinguishing between these two cross sections even at such low energies. Secondly, we see that the agreement between theory and experiment on the momentum transfer cross section is not particularly good, especially in the region of the most recent measurements (ref. 33) near 1eV. Figure 9 compares frozen target calculations (refs. 39, 40) with beam measurements of the total cross section for He and Ar (refs. 26, 27, 28) at impact energies of 10eV and above. Except at the lowest energy, the frozen target theory now underestimates the measured cross sections. An exciting new experimental development has been the first measurement of the fragmentation cross section for

[2]Henceforth we shall use the term "excitation" to mean both discrete excitation and ionization.

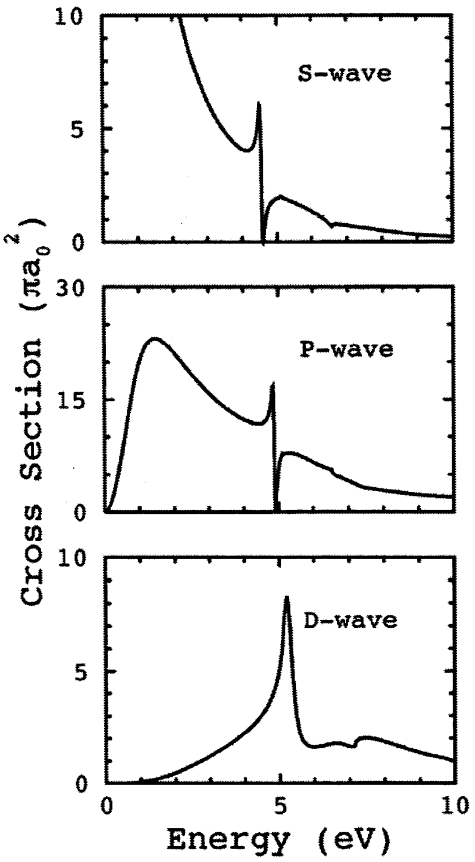

Figure 7: Electronic spin singlet elastic partial wave cross sections in the frozen target 22-state approximation of ref. 37.

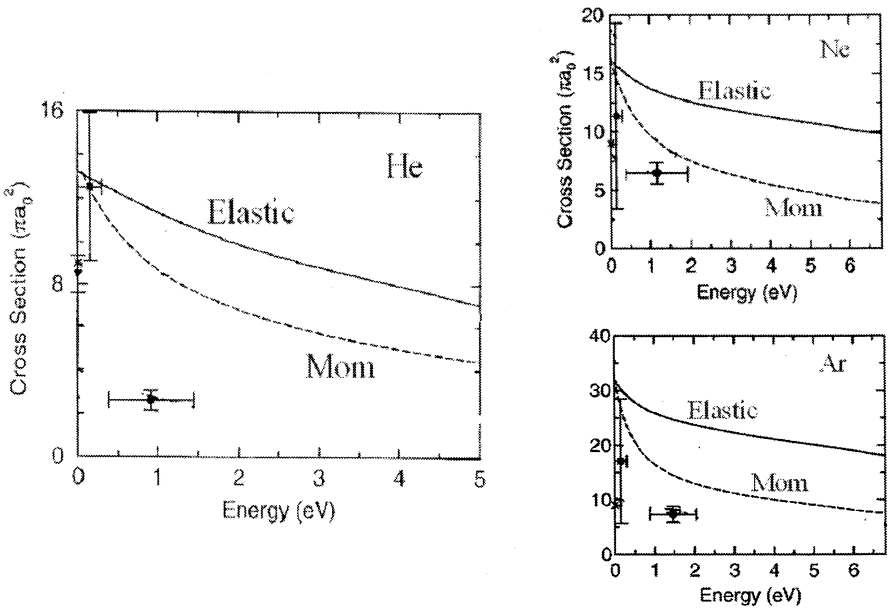

Figure 8: Total elastic and momentum transfer cross sections for Ps(1s) + He, Ne, Ar scattering in the frozen target approximation (refs. 39, 40). Experimental data: triangle, Canter et al (ref. 29); cross, Coleman et al (ref. 31); square, Nagashima et al (refs. 32, 34); circle, Skalsey et al (ref. 33).

Ps (refs. 41, 42) This is shown for a He target in figure 10 where comparison is also made with frozen target results (ref. 39). The agreement between theory and experiment is very satisfactory and contrasts with the difference on the total cross section shown in figure 9. Clearly, there is much still to be understood here. But, even more impressive is the newly acquired experimental capability to measure the Ps fragmentation cross section differential in the longitudinal energy of the ejected positron. The measurements for a He target (refs. 41, 42), which are absolute, are shown in figure 11. It is seen from this figure that, with increasing impact energy E, the differential cross section starts to exhibit a peak near $((E-6.8)/2)$eV. Also shown in figure 11 are theoretical cross sections calculated in a frozen target approximation, not in this case using a coupled pseudostate approximation but an impulse approximation (ref. 43). Overall, the agreement between theory and experiment, both in shape and magnitude, is, all things considered, remarkably good. From the theory it is clear that the development of the peak arises from the desire of the Ps to fragment into the forward direction with roughly equal energies for the ejected electron and positron.

Let us now move on from the frozen target approximation and see what happens when excited target states are included in the expansion (12). Figure 12 shows elastic partial wave cross sections for Ps(1s) + H(1s) scattering calculated in the frozen target approximation and in an approximation in which target excitation is taken into account (ref. 36). In all of the cases shown we see a substantial difference between the two approximations. It is clear that at these energies target excitation, which is virtual in this energy range, is very important for both electronic singlet and triplet scattering. From the singlet cross sections of figure 12 we see that the resonance structure that was observed in the frozen target approximation (figure 7) is preserved but moved down in energy slightly. Figure 13 shows the total cross section in the energy range 0 to 6eV in the two approximations. From this we see that target excitation reduces the very low energy cross section substantially (by about 30%) although giving a slightly higher cross section, in the form of a bump,

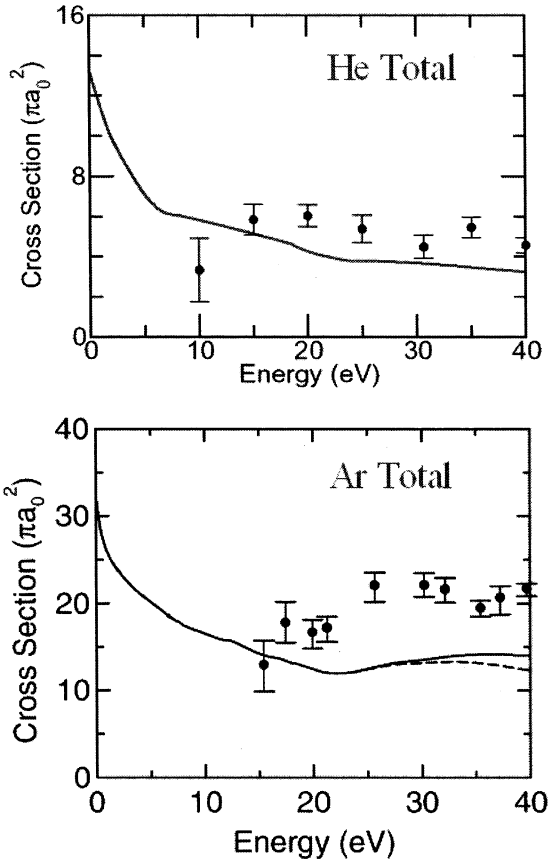

Figure 9: Total cross section for Ps(1s) + He (ref. 39) and Ps(1s) + Ar (ref. 40) scattering in the frozen target approximation: solid curve includes first Born estimate for target excitation (negligible for He in the energy range shown), dashed curve is pure frozen target result. Experimental data are from refs. 26, 27, 28.

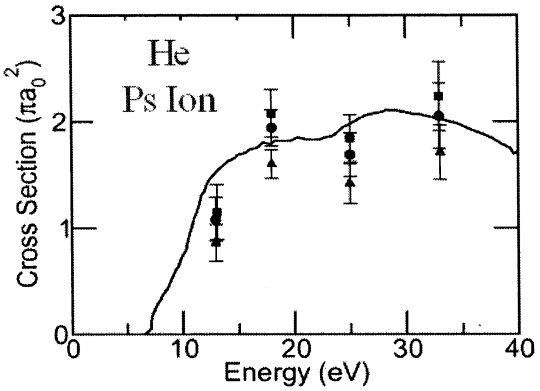

Figure 10: Cross section for fragmentation of Ps in Ps(1s) + He(1^1S) collisions. Curve, frozen target approximation of ref. 39. Experimental data from ref. 42.

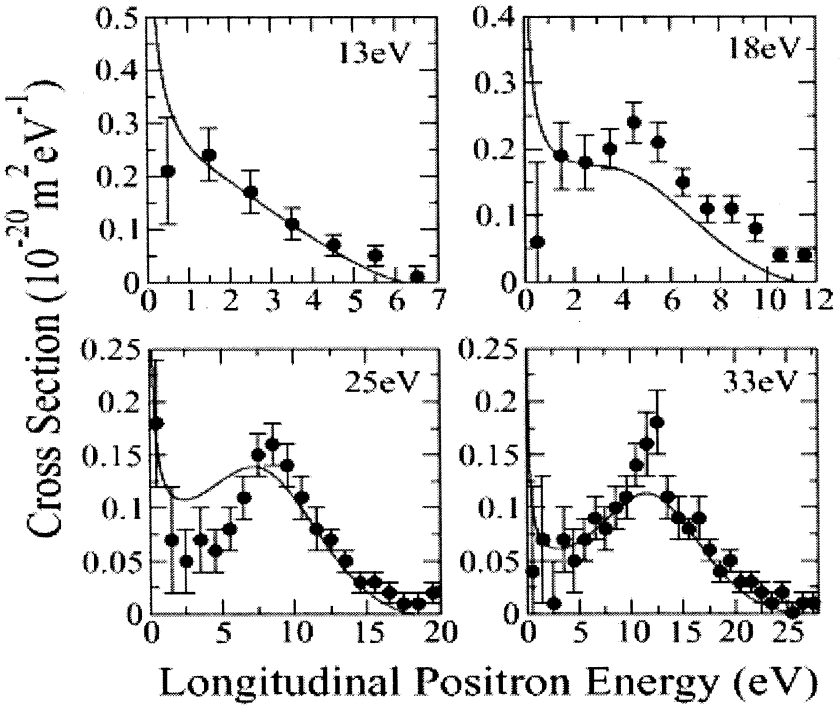

Figure 11: Cross sections differential in the longitudinal energy of the ejected positron for Ps(1s) fragmentation in He(1^1S) at Ps impact energies of 13, 18, 25 and 33eV: curve, impulse approximation calculation of ref. 43; experimental data from refs. 41, 42.

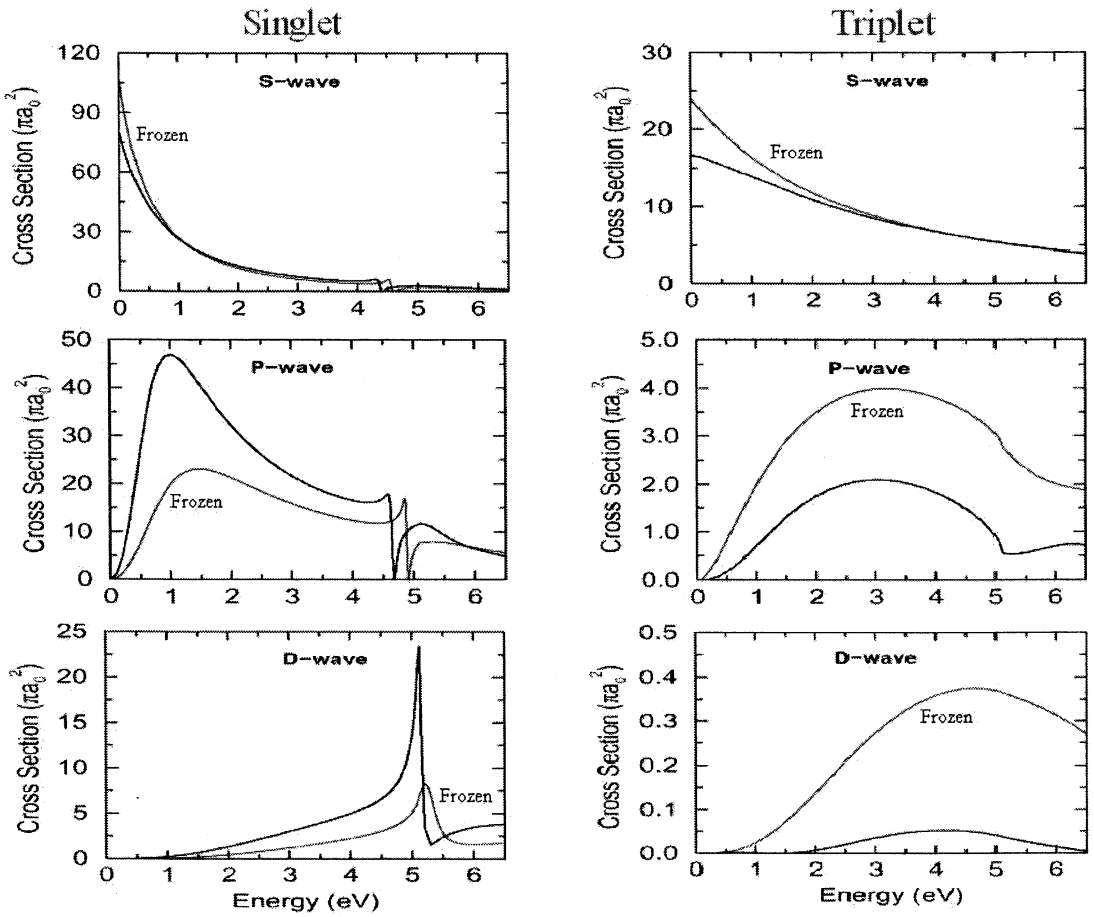

Figure 12: Elastic partial wave cross sections for Ps(1s) + H(1s) scattering in the frozen target approximation (Frozen) and in an approximation including target excitation (ref. 36).

at more elevated energies. Allowing for target excitation also seems to enhance the resonance structure near 5eV somewhat. Could virtual target excitation explain the discrepancies we are seeing between the frozen target theory and experiment in figure 8?

It has been suggested that Ps + He scattering should bear a similarity to Ps + H electronic spin triplet scattering since in both cases the Ps electron is prevented from occupying the same space as an atomic electron by the Exclusion Principle. Figure 14 shows S and P partial waves for Ps(1s) + He(1^1S) elastic scattering both in a frozen target approximation and in an approximation allowing for target excitation (ref. 44). Consistent with the suggestion, we note a clear similarity between figures 14 and 12. However, the differences between the two approximations is smaller for He. This is to be expected since He is less easily excited than H. Figure 15 now shows the consequences for the momentum transfer cross section in He. Allowing for target excitation does move the cross section towards the experiments of Canter et al, Rytsölä et al and Skalsey et al but there is still substantial disagreement. However, as Di Rienzi and Drachman (ref. 45) have most pertinently pointed out, the theoretical situation is obscured by uncertainty about the sensitivity of results to the use of approximate He target wave functions. This issue needs to be resolved.

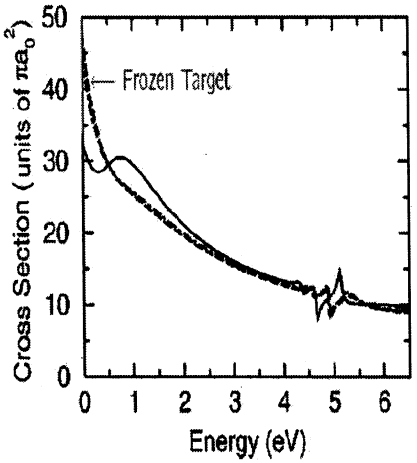

Figure 13: Total cross section for Ps(1s) + H(1s) scattering. Curves: dashed, frozen target results; solid, approximation including target excitation (ref. 36).

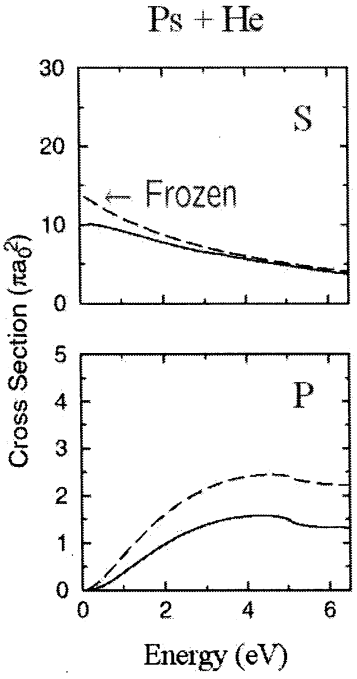

Figure 14: Partial wave cross sections for Ps(1s) + He(1^1S) elastic scattering in the frozen target approximation (dashed curve) and in an approximation allowing for target excitation (from ref. 44).

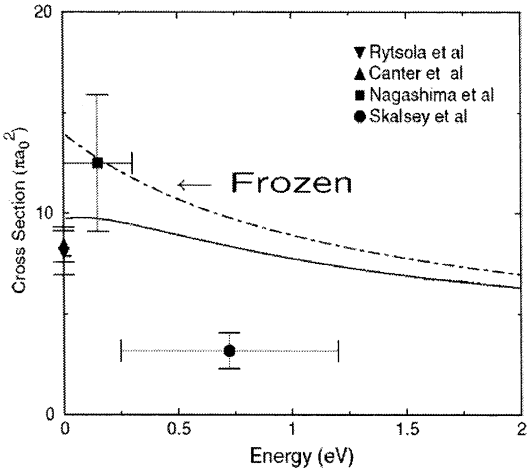

Figure 15: Momentum transfer cross section for Ps(1s) + He(1^1S) scattering. Theory (from ref. 44): dashed curve, frozen target approximation; solid curve, approximation allowing for target excitation. Experiment: square, Nagashima et al (ref. 32); up triangle, Canter et al (ref. 29); down triangle, Rytsölä et al (ref. 30); circle, Skalsey et al (ref. 35).

Let us now return to Ps + H scattering and list the processes that are possible. They are

$$
\begin{aligned}
Ps(1s) + H(1s) &\longrightarrow Ps(nlm) + H(NLM) && (19a)\\
&\longrightarrow e^+ + e^- + H(NLM) && (19b)\\
&\longrightarrow Ps(nlm) + p + e^- && (19c)\\
&\longrightarrow e^+ + e^- + p + e^- && (19d)\\
&\longrightarrow e^+ + H^- && (19e)\\
&\longrightarrow Ps^- + p && (19f)
\end{aligned}
$$

where nlm (NLM) labels any bound state of Ps (H). Using pseudostates, the approximation (12) takes account of (19a) to (19d). In the sense that, in principle, the sets of states ϕ_a and ψ_b could be taken to completeness, (19e) and (19f) are also implicit in (12). However, in practice we need to add (19e) and (19f) explicitly if we want to calculate these processes. The expansion (12) then has to be modified to

$$
\begin{aligned}
\Psi^S = & \sum_{a,b} \left[G^S_{ab}(\mathbf{R}_1)\psi_a(\mathbf{r}_2)\phi_b(\mathbf{t}_1) + (-1)^S G^S_{ab}(\mathbf{R}_2)\psi_a(\mathbf{r}_1)\phi_b(\mathbf{t}_2) \right] \\
& + F(\mathbf{r}_p)\psi^-(\mathbf{r}_1,\mathbf{r}_2)\delta_{S,0} + H\left(\frac{\mathbf{r}_1+\mathbf{r}_2+\mathbf{r}_p}{3}\right)\phi^-(\mathbf{r}_1-\mathbf{r}_p,\mathbf{r}_2-\mathbf{r}_p)\delta_{S,0} \qquad (20)
\end{aligned}
$$

where ψ^- (ϕ^-) is the H^- (Ps^-) wave function. The new terms only contribute to the electronic spin singlet wave function since H^- and Ps^- are electronic singlets. So far, calculations have only been made including the H^- term (refs. 46, 44). The results for the elastic partial waves are shown in figure 16. We see that at the lower energies (below 3.5eV) adding the H^- term does not radically alter the results obtained with inclusion of target excitation, however, in the resonance region between 3.5 and 6.05eV there is a spectacular change in the resonance structure. Whereas the approximation without the H^- term produced only one prominent resonance in each partial wave

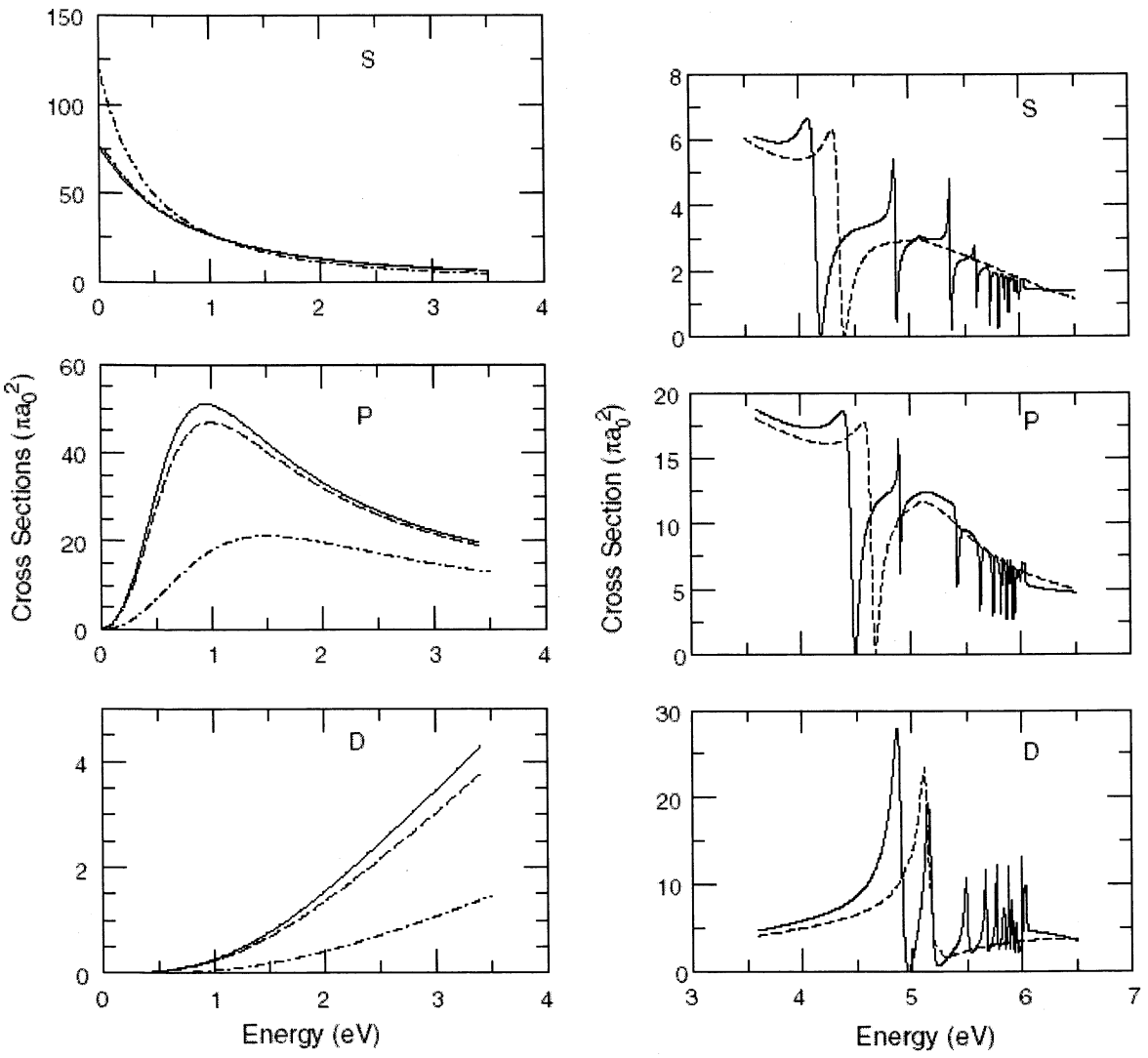

Figure 16: Electronic spin singlet partial wave cross sections for Ps(1s) - H(1s) elastic scattering (ref. 44). Curves: dash - dot, frozen target approximation; dashed, approximation allowing for target excitation; solid, approximation allowing for target excitation and also including the H^- channel.

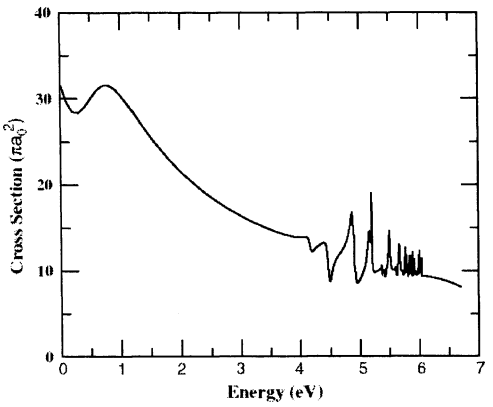

Figure 17: Total cross section for Ps(1s) + H(1s) scattering (from ref. 44).

Table 1: PsH Binding Energy

Approximation	Energy (eV)
Frozen Target	0.634
Target Excitation	0.994
Target Excitation + H^-	1.03
Exact (ref. 50)	1.067

(figures 7 and 12), the addition of the H^- term gives a much richer resonance structure in each partial wave. We now understand the origin of the resonances, they are unstable states of the positron attached to the H^- ion. What we have in each partial wave is an infinite sequence of Rydberg resonances converging on to the H^- formation threshold at 6.05eV. Should this be a surprise? No. As long ago as 1975 Dick and Ken Houston found the first of these resonances in S-wave scattering (ref. 47), and in an insightful paper of 1979 (ref. 48) Dick had already given the correct interpretation. What we see in figure 16 is a visual realisation of his foresight. At this time we do not know the effect of adding the Ps^- channel. That is an interesting new direction for future investigations.

At this point it is useful to summarise where we presently stand with the Ps - H system. In figure 17 we show the latest results (ref. 44) for the total cross section. This calculation allows for target excitation and includes the H^- channel. Also shown in figure 18 is the first realistic calculation of the H^- formation cross section (ref. 46). Note that this cross section is finite at threshold since the final state involves two charged particles, the positron and the H^-. However, everything is not completely settled in the low energy region. The Ps + H system has one true bound state, first predicted by Ore in 1951 (ref. 49). In table 1 we show the energy of this bound state as calculated in the various coupled state approximations. We see that the frozen target approximation can only account for about 60% of the energy. Allowing for target excitation gets us to about 93%. Further addition of the H^- channel brings us to 96.5% which is 3.5% short of very accurate variational results (ref. 50). What is the cause of this discrepancy? Is it the missing Ps^- channel?

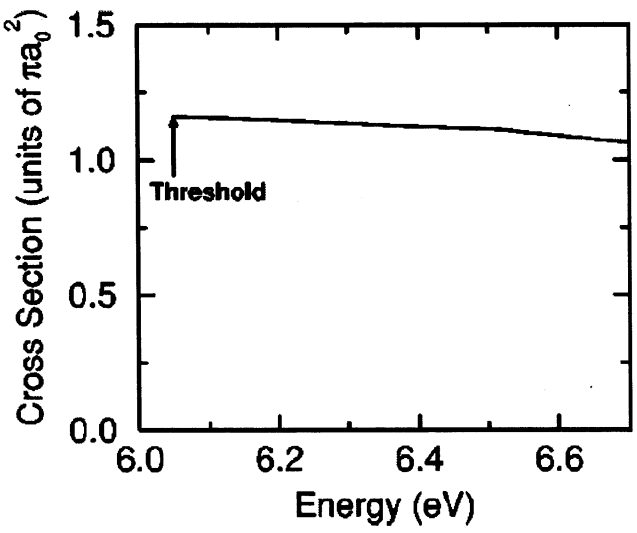

Figure 18: H^- formation cross section for Ps(1s) colliding with H(1s) (from ref. 46).

Finally, It is interesting to compare the early pioneering calculations of Dick and Ken Houston on Ps(1s) + H(1s) scattering (refs. 47, 51) with the most up-to-date results (Van Reeth and Humberston, ref. 52). In table 2 we show the scattering length and effective range for this system. The agreement between the early work and the most recent is remarkably good. Considering how restricted computing facilities were in the 1970s, Dick and Ken had done a really good job.

Table 2: Scattering Lengths and Effective Ranges (in au) for Ps(1s) + H(1s) Scattering

	Van Reeth and Humberston (2003) (ref. 52)	Drachman and Huston (1975, 1976) (refs. 47, 51)
Singlet Scattering Length	4.311	4.5
Triplet Scattering Length	2.126	2.36
Singlet Effective Range	2.27	2.2
Triplet Effective Range	1.39	1.31

POSITRON SCATTERING BY H^-

In 1991 Jack Straton and Dick published an heroic attempt to get a handle on the very difficult problem of positron scattering by H^- (ref. 53). It seems that this process is of Astrophysical importance. They looked at a series of approximations based on the Fock - Tani/Coulomb Born formalism with the purpose of calculating Ps formation. Because $e^+ + H^-$ is such a difficult system, they restricted their calculations to the case where both the Ps and the residual H atom were left in the 1s ground state. Now, $e^+ + H^-$ scattering is just the inverse of the reaction

$$Ps + H \longrightarrow e^+ + H^- \tag{21}$$

and so must be contained within the approximation (20). Inspired by the work of Dick and Jack, McAlinden et al (ref. 54) decided to see what (20) would yield. Like Dick and Jack, they decided to restrict themselves to reactions in which the H atom would be left in the 1s state, ie, they included only the H(1s) state in the sum of (20). Their approximation amounted to a frozen target calculation with the addition of the H^- channel. [3] However, because they used Ps eigenstates and pseudostates in the expansion (20) they were able to take account of Ps formation in excited states, Ps(nlm), and, through the Ps pseudostates, ionization. Some of their results are shown in table 3 where they are compared with Dick and Jack's calculation.

Table 3: Ps Formation Cross Sections (in πa_0^2) for $e^+ + H^-$ Scattering

	Straton and Drachman (ref. 53)	McAlinden et al (ref. 54)		
Energy (eV)	Ps(1s)	Ps(1s)	Ps(2s)	Ps(2p)
0.1	904	567	715	2702
0.5	178	116	134	651
1.0	82.5	57	48	290
5.0		13	4.7	22
10.0		5.0	1.0	3.5

Dick and Jack obtained a range of values for the Ps(1s) formation cross section depending upon the approximation used, the numbers shown in table 3 correspond to their smallest values. Taking account of what a difficult problem this is, it is fair to say that Dick and Jack's results are in the same "ball park". However, the results of McAlinden et al show that, at the lower energies, Ps formation in the $n = 2$ states is much more important than Ps(1s) formation. Ps formation in the $n = 1$ and $n = 2$ states are exothermic processes, the cross sections diverging as $1/E$ as the impact energy, E, tends to zero (ref. 54). It was Dick who brought this to our attention at the Positron Satellite of the Santa Fe ICPEAC in 2001. At the time we were under the impression that the divergence was $1/\sqrt{E}$. In figure 19 we show aggregate Ps formation cross sections from McAlinden et al in the impact energy range 0 to 10eV. Interestingly, we see that Ps($n \geq 3$) formation is comparable to Ps(1s + 2s + 2p) formation at energies above 2eV. However, as figure 20 shows, ionization of the H^- soon starts to dominate with increasing impact energy.

[3] The Ps^- channel was also omitted from (20).

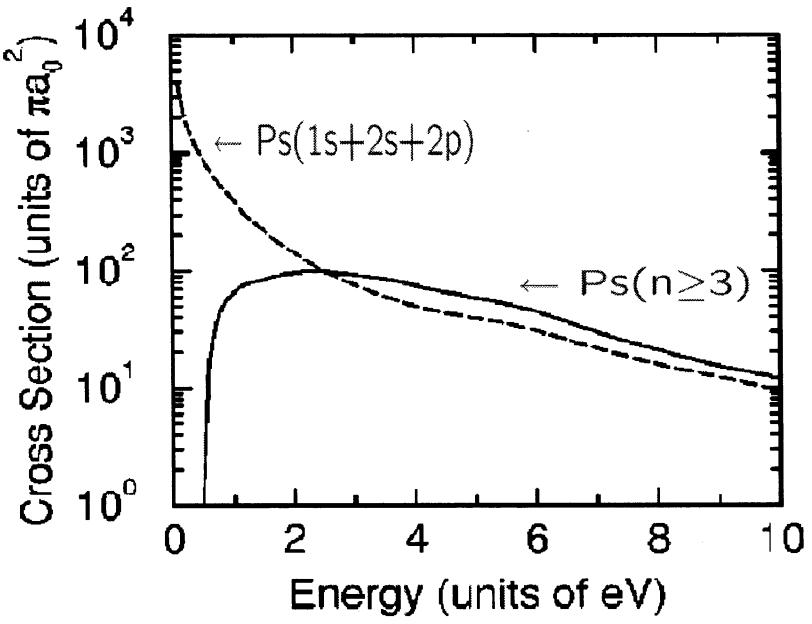

Figure 19: Aggregate Ps formation cross sections from McAlinden et al (ref. 54).

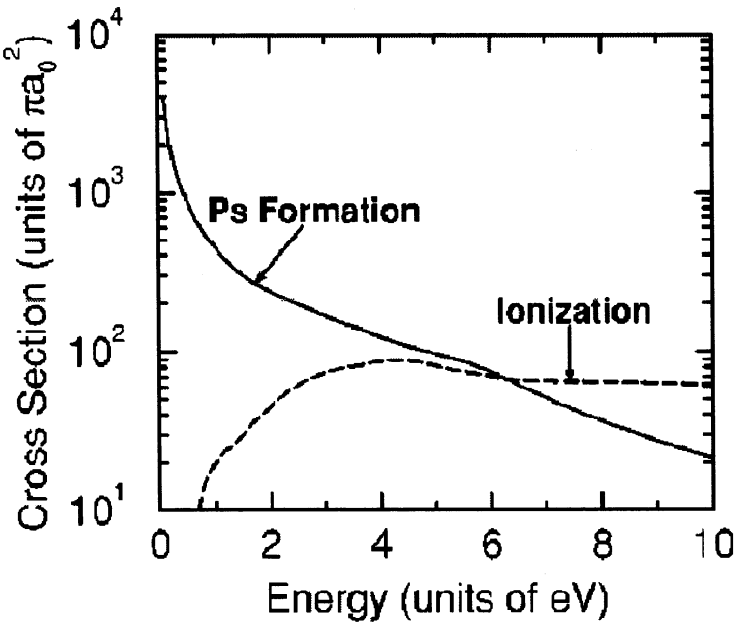

Figure 20: Direct ionization and total Ps formation cross sections from McAlinden et al (ref. 54).

CONCLUDING REMARKS

We are reminded of a remark by Isaac Newton (ref. 55): "If I have seen further it is by standing on ye shoulders of Giants". If we have seen further it is by standing on the shoulders of giants like Dick and Aaron!

REFERENCES

1. N.F. Mott and H.S.W. Massey, *The Theory of Atomic Collisions*, third edition, Oxford University Press, Oxford (1965).
2. A. Temkin, "Nonadiabatic theory of electron - hydrogen scattering", *Phys. Rev.* **126**, 130 (1962).
3. A. Temkin, "Polarisation and exchange effects in the scattering of electrons from atoms with application to oxygen", *Phys. Rev.* **107**, 1004 (1957).
4. A. Temkin, "A note on the scattering of electrons from atomic hydrogen", *Phys. Rev.* **116**, 358 (1959).
5. R. Poet, "The exact solution for a simplified model of electron scattering by hydrogen atoms", J. Phys. B **11**, 3081 (1978).
6. A. Temkin, editor, *Autoionization*, Mono Book Corp., Baltimore (1966).
7. R.J. Drachman, "Theoretical aspects of positronium collisions", in: *Atomic Physics with Positrons*, J.W. Humberston and E.A.G. Armour, eds, Plenum, New York (1987) p203.
8. H.R.J. Walters, A.A. Kernoghan and M.T. McAlinden, "Overview of the present theoretical status of positron - atom collisions", *AIP Conf. Proc.* **360**, 397 (1995).
9. H.R.J. Walters, A.A. Kernoghan, M.T. McAlinden and C.P. Campbell, "Positron collisions with atoms", in: *Photon and Electron Collisions with Atoms and Molecules*, P.G. Burke and C.J. Joachain, eds, Plenum, New York (1997) p313.
10. M.T. McAlinden, A.A. Kernoghan and H.R.J. Walters, "Cross - channel coupling in positron - atom scattering", *Hyperfine Interactions* **89**, 161 (1994).
11. A.A. Kernoghan, M.T. McAlinden and H.R.J. Walters, "Scattering of low energy positrons by lithium", J. Phys. B **27**, L625 (1994).
12. A.A. Kernoghan, M.T. McAlinden and H.R.J. Walters, "An 18 - state calculation of positron - hydrogen scattering", *J. Phys. B* **28**, 1079 (1995).
13. M.T. McAlinden, A.A. Kernoghan and H.R.J. Walters, "Positron scattering by potassium", *J. Phys.B* **29**, 555 (1996).
14. A.A. Kernoghan, D.J.R. Robinson, M.T. McAlinden and H.R.J. Walters, "Positron scattering by atomic hydrogen", *J. Phys.B* **29**, 2089 (1996).
15. A.A. Kernoghan, M.T. McAlinden and H.R.J. Walters, "Positron scattering by rubidium and caesium", *J. Phys.B* **29**, 3971 (1996).
16. M.T. McAlinden, A.A. Kernoghan and H.R.J. Walters, "Positron scattering by lithium", *J. Phys. B* **30**, 1543 (1997).
17. C.P. Campbell, M.T. McAlinden, A.A. Kernoghan and H.R.J. Walters, "Positron collisions with one - and two - electron atoms", *Nuclear Instruments and Methods B* **143**, 41 (1998).

18. P.G. Burke and W.D. Robb, "The R - matrix theory of atomic processes", *Adv. Atom. Mol. Phys.* **11**, 143 (1975).

19. A.T. Stelbovics, "L^2 discretisation of the Coulomb problem in an orthonormal Laguerre function basis", *J. Phys. B* **22**, L159 (1989).

20. I. Bray and A.T. Stelbovics, "Explicit demonstration of the convergence of the close - coupling method for a Coulomb three - body problem", *Phys. Rev. Lett.* **69**, 53 (1992).

21. S. Zhou, H. Li, W.E. Kauppila, C.K. Kwan and T.S. Stein, "Measurements of total and positronium formation cross sections for positrons and electrons scattered by hydrogen atoms and molecules", *Phys. Rev. A* **55**, 361 (1997).

22. G.O. Jones, M. Charlton, J. Slevin, G. Laricchia, Á. Kövér, M.R. Poulsen and S. Nic Chormaic, "Positron impact ionization of atomic hydrogen", *J. Phys. B* **26**, L483 (1993).

23. R.W. Bussard, R. Ramaty and R.J. Drachman, "The annihilation of galactic positrons", *Astrophysical Journal* **228**, 928 (1979).

24. C.P. Campbell, M.T. McAlinden and H.R.J. Walters, "Positron collisions with two - electron atoms: He, Mg, Zn, Ca", *Abstracts of the 6^{th} European Conference on Atomic and Molecular Physics (Siena, Italy, 1998)*, C.Biancalana, P.Bicchi and E.Mariotti, eds, vol 22D p4-33.

25. M. Charlton and G. Laricchia, "Collision phenomena involving positronium", *Comments At. Mol. Phys.* **26**, 253 (1991).

26. A.J. Garner, G. Laricchia and A. Özen, "Ps beam production and scattering from gaseous targets", *J. Phys. B* **29**, 5961 (1996).

27. A.J. Garner, A. Özen and G. Laricchia, "Positronium beam scattering from atoms and molecules", *Nucl. Instrum. Methods Phys. Res. B* **143**, 155 (1998).

28. A.J. Garner, A. Özen and G. Laricchia, "The effect of forward-angle scattering on positronium-gas total cross sections", *J. Phys. B* **33**, 1149 (2000).

29. K.F. Canter, J.D. McNutt and L.O. Roellig, "Positron annihilation in low-temperature rare gases. 1. Helium", *Phys. Rev. A* **12**, 375 (1975).

30. K. Rytsölä, J. Vettenranta, P. Hautojärvi, "An experimental study of positronium bubbles in helium fluids", *J. Phys. B* **17**, 3359 (1984).

31. P.G. Coleman, S. Rayner, F.M. Jacobsen, M. Charlton and R.N. West, "Angular-correlation studies of positron-annihilation in the noble-gases", *J. Phys. B* **27**, 981 (1994).

32. Y. Nagashima, T. Hyodo, F. Fujiwara and I. Ichimura, "Momentum-transfer cross sections for slow positron-He collisions", *J. Phys. B* **31**, 329 (1998).

33. M. Skalsey, J.J. Engbrecht, R.K. Bithell, R.S. Vallery and D.W. Gidley, "Thermalization of positronium in gases", *Phys. Rev. Lett.* **80**, 3727 (1998).

34. Y. Nagashima, F. Saito, N. Shinohara and T. Hyodo, "Positronium - atom/molecule interactions: momentum - transfer cross sections and Z_{eff}", in: *New Directions in Antimatter Chemistry and Physics*, C. M. Surko and F. A. Gianturco, eds, Kluwer, Dordrecht (2001) p291.

35. M. Skalsey, J.J. Engbrecht, C.M. Nakamura, R.S. Vallery and D.W. Gidley, "Doppler - broadening measurements of positronium thermalization in gases", *Phys. Rev. A* **67**, 022504 (2003).

36. J.E. Blackwood, M.T. McAlinden and H.R.J. Walters, "Positronium scattering by atomic hydrogen with inclusion of target excitation channels", *Phys. Rev. A* **65**, 032517 (2002).

37. C.P. Campbell, M.T. McAlinden, F.G.R.S. MacDonald and H.R.J. Walters, "Scattering of positronium by atomic hydrogen", *Phys. Rev. Lett.* **80**, 5097 (1998).

38. M.T. McAlinden, F.G.R.S. MacDonald and H.R.J. Walters, "Positronium - atom scattering", *Can. J. Phys.* **74**, 434 (1996).

39. J.E. Blackwood, C.P. Campbell, M.T. McAlinden and H.R.J. Walters, "Positronium scattering by helium", *Phys. Rev. A* **60**, 4454 (1999).

40. J.E. Blackwood, M.T. McAlinden and H.R.J. Walters, "Positronium scattering by Ne, Ar, Kr, and Xe in the frozen target approximation", *J. Phys. B* **35**, 2661 (2002); **36**, 797 (2003).

41. S. Armitage, D.E. Leslie, A.J. Garner and G. Laricchia, "Fragmentation of positronium in collision with He atoms", *Phys. Rev. Lett.* **89**, 173402 (2002).

42. G. Laricchia, S. Armitage and D.E. Leslie, "Positronium induced collisions", *Nucl. Instrum. Methods Phys. Res. B* **221**, 60 (2004).

43. C. Starrett, M.T. McAlinden and H.R.J. Walters, "Fragmentation of Positronium", *Phys. Rev. A* **72**, 012508 (2005).

44. H.R.J. Walters, A.C.H. Yu, S. Sahoo and S. Gilmore, "Positronium - atom collisions", *Nucl. Instrum. Methods Phys. Res. B* **221**, 149 (2004).

45. J. Di Rienzi and R.J. Drachman, "Approximating the target wave function in positronium - helium scattering", *Phys. Rev. A* **70**, 052706 (2004).

46. J.E. Blackwood, M.T. McAlinden and H.R.J. Walters, "Importance of the H^- channel in Ps - H scattering", *Phys. Rev. A* **65**, 030502 (2002).

47. R.J. Drachman and S.K. Houston, "Positronium - hydrogen elastic scattering", *Phys. Rev. A* **12**, 885 (1975).

48. R.J. Drachman, "Autodissociating Rydberg states of positronium hydride", *Phys. Rev. A* **19**, 1900 (1979).

49. A Ore, "The existence of Wheeler compounds", *Phys. Rev.* **83**, 665 (1951).

50. Z.-C. Yan and Y.K. Ho, "Ground state and S-wave autodissociating resonant states of positronium hydride", *Phys. Rev. A* **59**, 2697 (1999).

51. R.J. Drachman and S.K. Houston, "Positronium - hydrogen elastic scattering: The electronic S=1 state", *Phys. Rev. A* **14**, 894 (1976).

52. P. Van Reeth and J.W. Humberston, "Variational calculations of s-wave positronium - hydrogen scattering", *J. Phys. B* **36**, 1923 (2003).

53. J.C. Straton and R.J. Drachman, "Formation of positronium in $e^+ + H^-$ collisions", *Phys. Rev. A* **44**, 7335 (1991).

54. M.T. McAlinden, J.E. Blackwood and H.R.J. Walters, "Positron scattering by the negative hydrogen ion", *Phys. Rev. A* **65**, 032715 (2002).

55. Letter to Robert Hooke, 5 February 1675 (Julian Calendar).

MUON CATALYZED FUSION

Edward A. G. Armour
School of Mathematical Sciences, University of Nottingham, Nottingham NG7 2RD, UK

ABSTRACT

Muon catalyzed fusion is a process in which a negatively charged muon combines with two nuclei of isotopes of hydrogen, e.g. a proton and a deuteron or a deuteron and a triton, to form a muonic molecular ion in which the binding is so tight that nuclear fusion occurs. The muon is normally released after fusion has taken place and so can catalyze further fusions. As the muon has a mean lifetime of 2.2 microseconds, this is the maximum period over which a muon can participate in this process. This article gives an outline of the history of muon catalyzed fusion from 1947, when it was first realised that such a process might occur, to the present day. It includes a description of the contribution that Drachman has made to the theory of muon catalyzed fusion and the influence this has had on the author's research.

INTRODUCTION

I am very grateful to the organizers for the invitation to speak at this Symposium to mark the retirement of Aaron Temkin and Dick Drachman. It is a very great pleasure to be able to contribute to this occasion in this way.

The particle the muon that is central to muon catalyzed fusion was discovered by Anderson and his first graduate student, Neddermeyer, in 1936 when studying cosmic rays (ref. 1). In accordance with relativistic quantum field theory, there is a negatively charged muon, μ^-, and its positively charged antiparticle, μ^+, each having mass $207m_e$, where m_e is the mass of the electron. Each has a mean lifetime of 2.2 microseconds, before decaying through the weak interaction into an electron or a positron and a neutrino and an antineutrino. See, for example, ref. 2. The muon is a lepton, as it is unaffected by the strong interaction. It follows that it is a fermion with spin $\frac{1}{2}$. In what follows, I will assume that the muon being considered is negatively charged.

If the electron in a hydrogen atom (H) is replaced by a muon, the result is a hydrogen-like atom $p\mu$ called muonium. The reduced mass of this atom is $186m_e$. Thus its bohr radius is $\frac{a_0}{186}$, where a_0 is the bohr radius of H. The binding energy of each of its bound states is $186\times$ (the corresponding value for the H atom). Muonium is thus very compact and strongly bound. The proximity of the positive charge on the proton and the negative charge on the muon make it similar to a neutron.

An electron can bind two protons to form a weakly bound ion, H_2^+, the hydrogen molecular ion. If the electron in this ion is replaced by a muon, the resulting ion in its ground state is very compact and strongly bound like muonium. As is to be expected, these properties remain if either or both protons are replaced by a deuteron (d) or a triton (t).

It has been known since the 1930s that the sun generates its energy by a fusion reaction in which hydrogen is converted into helium (see, for example, Bethe (ref. 3). However, this reaction requires a temperature of several million degrees to overcome the Coulombic repulsion between the protons involved in the reaction. The proton-proton fusion process is very much slower than those involving deuterons or tritons as it involves the weak interaction. Extensive research into using a fusion process of this type as a source of energy here on Earth has been going on for many years. However, even for the most favourable fusion process, $d+t$, very high temperatures are required. See, for example, ref. 4. This has made progress slow.

A natural question to ask is whether any way could be found of bringing about fusion that did not require very high temperatures. In 1947, Frank (ref. 5, 6) suggested that in the presence of protons and deuterons a slow muon might bind to a p to form $p\mu$, which as noted earlier is similar to a neutron. This could come close to a d and form $pd\mu$ which we have seen is tightly bound. Frank thought that it was sufficiently tightly bound that p-d fusion might occur. With luck, this would leave the muon free to catalyze further fusions, i.e. bring about p-d fusion while remaining unchanged at the end of the reaction.

Shortly afterwards Sakharov (ref. 7) discussed the possibility of energy production by such a process and later it was considered further by Zel'dovich (ref. 8). Both concluded pessimistically that a muon was only likely to be able to catalyze one or two fusions.

The first experimental observation of muon catalyzed fusion was made by Alvarez et al. in 1956 (ref. 9). Though unaware of the above theoretical speculations, they correctly interpreted tracks in their bubble chamber at Berkeley as representing p-d fusion catalyzed by a single muon. Bubble chamber tracks representing the path of a muon in a mixture containing hydrogen and a small amount of deuterium that catalyzes two p-d fusions are shown in Figure 1 in ref. 10.

Upon reading about Alvarez's exciting discovery in the New York Times, Jackson (ref. 11) proceeded to make an analysis of energy production. Like Sakharov and Zel'dovich, he came to a pessimistic conclusion: very few fusions could be catalyzed by a single muon.

The scene now shifted, after a pause, to the Soviet Joint Institute for Nuclear Research (JINR) at Dubna, north of Moscow. Interest in muon catalyzed fusion revived when experiments on d-d fusion catalyzed by a muon carried out by Dzhelepov et al. (ref. 12) at Dubna in 1966 revealed a strong and unexpected temperature dependence in the rate of formation of $dd\mu$. This was a very exciting discovery. It strongly suggested that a resonant process was involved and held out the possibility of a large increase in the fusion rate under suitable conditions.

It was not long before a form was suggested for this resonant process. In 1967, Vesman (ref. 13) proposed that the formation of $dd\mu$ could occur by the reaction

$$d\mu + \mathrm{D}_2 \rightarrow [(dd\mu)^* dee] \qquad (1)$$

where the species on the right-hand side is a muonic molecular complex in which $dd\mu$, in a weakly bound excited state, forms one of the nuclei. The energy lost by the system through the formation of the weakly bound state goes into exciting the vibrational and rotational states of the muonic molecular complex. Due to the quantised structure of these states, this will be a resonant process and the formation rate will be very sensitive to the kinetic energy of the $d\mu$. This accounted qualitatively for the temperature dependence observed by Dzhelepov et al.

Such a mechanism depends crucially on the existence of a weakly bound state with binding energy less than the 4.5 eV dissociation energy of D_2. The problem was taken up by two Russian physicists, Gershtein and Ponomarev. Gershtein had earlier been involved in work on muon catalyzed fusion with Zel'dovich (ref. 14). Ponomarev was his graduate student.

After ten years' work, Gershtein and Ponomarev and their group (refs. 15,16) were indeed able to confirm the existence of a weakly bound state of $dd\mu$. They showed that it had rotational and 'vibrational' quantum numbers $(J, v) = (1, 1)$ and binding energy $\sim$2 eV.

The Born–Oppenheimer approximation does not work well for $dd\mu$ as the ratio of the masses of the muon and the deuteron is too large. The method Ponomarev and his group used to remove this difficulty was the adiabatic representation method (ref. 17) in which the energy and wave function of the state were calculated using a large basis set of the form $\left\{\Psi_i(\boldsymbol{r})\frac{1}{R}\chi_i(\boldsymbol{R})\right\}$ where $\boldsymbol{r}$ is the position vector of the muon with respect to the geometric center of the nuclei as origin, $\boldsymbol{R}$ is the internuclear vector, $\Psi_i(\boldsymbol{r})$ is a Born–Oppenheimer wave function for the muon and

$\chi_i(R)/R$ is a nuclear wave function. The $\{\chi_i(R)\}$ were determined by solving close-coupling type integro-differential equations.

Gershtein and Ponomarev were also able to show by this method that a corresponding weakly bound state of $dt\mu$ exists with binding energy $\sim$1 eV. In addition, they were able to show that rapid formation of $dt\mu$ by the Vesman mechanism would enable a muon to catalyze $\sim$100 d-t fusions (ref. 15). The rapid formation rate of $dt\mu$ was confirmed experimentally by Bystritsky et al. (ref. 18) in 1980.

GROWTH OF INTEREST IN MUON CATALYZED FUSION

Initially at Dubna and later at the Kurchatov Institute in Moscow, Ponomarev built up an extensive group of very able Russian physicists working on the problem of muon catalyzed fusion. The very promising advances described above took place at a time when the Cold War made direct contacts with Russian scientists difficult. However, the results were available in the literature, as can be seen from the list of references. They appeared in English after a slight delay, but greater intimacy could be achieved by a reader with a knowledge of Russian.

In 1979 the accelerator at Dubna that had been used in the experiments was shut down for refurbishment. The experimental lead was taken up by collaborations at Los Alamos, led by Jones, at the Paul Scherrer Institute (PSI) in Switzerland led by Petitjean and at the University of Tokyo and KEK in Japan led by Nagamine.

On the theoretical side, the work of Gershtein and Ponomarev became widely known. Outside the Soviet Union, expertise had accumulated for many years on calculations on few-body Coulombic systems using the Rayleigh–Ritz variational method. It was possible that this method might give more accurate results for the binding energies of states of $dd\mu$ and $dt\mu$ than the adiabatic representation method (ref. 17).

The first such calculation in the West was carried out by Bhatia and Drachman (ref. 19). I consider that it was very much in character for Drachman to be the first in this way. I can think of a number of reasons why muon catalyzed fusion appealed to him. The Vesman mechanism (ref. 13), as substantiated by Gershtein and Ponomarev, was a very interesting and exciting process involving an unusual particle, a muon, and the formation of a muonic molecular complex associated with resonant behaviour. Muon catalyzed fusion was a novel topic to an extent that few topics are. It transcended more than national boundaries in the best spirit of science. Drachman's knowledge of Russian made it possible for him to get up-to-date earlier on new developments in Soviet journals and go further and read items such as untranslated reports written by Ponomarev's group. Finally, muon catalyzed fusion just might be a viable way of bringing about fusion at room temperature that could be used as a commercial source of energy.

Bhatia and Drachman (ref. 19) carried out calculations of binding energies of all states of the muonic molecular ions $pp\mu$, $pd\mu$, $pt\mu$, $dd\mu$, $dt\mu$ and $tt\mu$, except the states of $dd\mu$, $dt\mu$ and $tt\mu$ that have $J > 1$. They used the Rayleigh–Ritz variational method with up to 440 basis functions $\{\psi_i\}$ containing Hylleraas-type functions, i.e. functions that are linear in one or more interparticle distances.

For $J = 0$,

$$\psi_i = \mathrm{e}^{-(\gamma r_1 + \delta r_2)} r_1^l r_2^m r_{12}^n \mathrm{D}_0^{0+} \quad (l, m, n \geq 0),$$

where

r_1, r_2 = distances of the muon from the nucleons,

r_{12} = distance between the nucleons,

and D_0^{0+} is a rotational harmonic (ref. 20).

For $J = 1$, the rotational harmonics D_1^{1+} and D_1^{1-} and functions of the angle between the directions of r_1 and r_2 were used to include the unit of angular momentum.

In some cases, the calculated binding energy proved to be rapidly convergent and lower energies were obtained than in any previous calculations. For the key weakly bound states, however, they obtained binding energies consistent with previous results, but significantly smaller in magnitude.

Bhatia and Drachman pointed out that similar results were obtained by Frolov and Efros (ref. 21) at the Kurchatov Institute in Moscow using up to 375 basis functions $\{\chi_i\}$ of the form

$$\chi_i = \exp[-\alpha_{1i}r_1 - \alpha_{2i}r_2 - \alpha_{12i}r_{12}]\Omega_i^J(r_1, r_2),$$

where $\Omega_i^J(r_1, r_2)$ is a function of r_1 and r_2 appropriate to the angular momentum J of the state under consideration. (This work was later published in ref. 22.)

The calculations were followed by many subsequent calculations by the Rayleigh–Ritz variational method using various types of basis set.

For example, Hu (ref. 23) and Szalewicz et al. (ref. 24) used Hylleraas-type basis functions similar to Bhatia and Drachman (ref. 19). Aissing and Monkhorst (ref. 25) relied on exponential basis functions similar to Frolov and Efros (refs 21,22) with many non-linear parameters. Kamimura (ref. 26) showed the effectiveness of using basis functions similar to Frolov and Efros but with exponentials in the form of Gaussians. Vinitsky et al. (ref. 27) and Hara and Ishihara (ref. 28) used Hylleraas-type basis functions with the muon part of the functions expressed in terms of prolate spheroidal coordinates. These calculations gave highly accurate results.

THE RESONANT REACTION THAT LEADS TO FUSION

The most favourable muonic molecular ion for muon catalyzed fusion is $dt\mu$. For example, the d-t fusion rate for this ion is more than 1000 times larger than for any other ion. Also, it produces nearly the highest energy per fusion (17.6 MeV). See, for example, ref. 29.

In the resonant reaction

$$t\mu + D_2 \rightarrow [(dt\mu)_{11}dee] \tag{2}$$

$dt\mu$ is formed in its $J = 1$, $v = 1$ state. However, rapid fusion only takes place if $dt\mu$ is in a state with $J = 0$. It is thus important to know the binding energies and wave functions of the various states of $dt\mu$ below the very weakly bound $(1, 1)$ state. These binding energies are shown in Figure 1 which is taken from a revue article on muon catalyzed fusion by Bhatia and Drachman (ref. 30).

The binding energies in this figure are calculated including only the Coulombic interaction. The resonant formation rate of the complex in reaction (2) is very sensitive to the energy of the $(1, 1)$ state of $dt\mu$. Small corrections due to relativistic, QED, hyperfine and other effects have been calculated. See, for example, refs. 29, 2 and 31.

Reaction (2) is incomplete without an indication of what results from the formation of the $[(dt\mu)_{11}dee]$ complex. With inclusion of the most important decay products, it becomes

$$t\mu + D_2 \underset{\text{back decay}}{\rightleftarrows} [(dt\mu)_{11}dee] \xrightarrow[\text{decay}]{\text{Auger}} [(dt\mu)_{Jv}de]^+ + e, \tag{3}$$

where $(J, v) = (0, 1)$, $(2, 0)$, $(1, 0)$ or $(0, 0)$. If the total angular momentum of the $t\mu + D_2$ is taken to be zero for simplicity, the cross section $\sigma_r(E)$ for this resonant process is determined by the Breit–Wigner formula (ref. 32).

$$\sigma_r(E) = \frac{\pi}{k^2} \frac{\Gamma_e \Gamma_a}{(E - E_r)^2 + \frac{1}{4}(\Gamma_e + \Gamma_a)^2}, \tag{4}$$

where

E = the energy of the system,
E_r = the energy of the resonant state,
k = wave number of the relative motion of $t\mu$ and D_2,
Γ_e = partial width for back decay,
Γ_a = partial width for Auger decay.

It follows from this that the deexcitation rate of $[(dt\mu_{11})dee] = \frac{\Gamma_a}{\hbar}$. It is very important that this is sufficiently fast that the $[(dt\mu)_{11}dee]$ does not simply decay back into $t\mu + D_2$ (ref. 33).

Bhatia et al. (ref. 34) carried out a calculation of the deexcitation rate of the $(1,1)$ state of $dt\mu$ in $[(dt\mu)_{11}dee]$ into all states of lower energy. In $[(dt\mu)_{11}dee]$, the d, t and μ are close together. To a good approximation, they can be looked upon as forming a nucleus of charge $+1$ in a molecular complex, similar to D_2, but with one d nucleus replaced by a fictitious particle with mass equal to that of $dt\mu$.

To be able to carry out their calculations, Bhatia et al. simplified this to a $dt\mu$ in its $(1,1)$ state acting as the nucleus for a hydrogen-like atom in its ground state. They took the initial and final wave functions ψ_i and ψ_f, to be of the form

$$\psi_i = \psi_i(\boldsymbol{r}_1, \boldsymbol{r}_2)\psi_{1s}(\boldsymbol{r}),$$
$$\psi_f = \psi_f(\boldsymbol{r}_1, \boldsymbol{r}_2)F_k(\boldsymbol{r}),$$

where $\boldsymbol{r}_1$ and $\boldsymbol{r}_2$ are the position vectors of the d and μ, respectively, with respect to the t as origin and

$\boldsymbol{r}$ = position vector of the electron with respect to the center of mass of $dt\mu$ as origin.

$\psi_i(\boldsymbol{r}_1, \boldsymbol{r}_2)$ and $\psi_f(\boldsymbol{r}_1, \boldsymbol{r}_2)$ are the initial and final state wave functions for the $dt\mu$. They were calculated using Hylleraas-type basis functions in a similar way to the calculation described in ref. 19.

$\psi_{1s}(\boldsymbol{r})$ is the $1s$ initial state of the electron and $F_k(\boldsymbol{r})$ is its final continuum state.

The Auger decay of the $dt\mu$ in its $(1,1)$ state is brought about by the finite size of the $dt\mu$. If the d, t and μ were all at the same point, the system would indeed be equivalent to a hydrogen atom in its ground state. However, this is only approximately the case; a finite size correction must be included. This is of the form of a multipole expansion

$$V = \frac{e^2\hat{\boldsymbol{r}}}{r^2} \cdot [(m_1 - 1)\boldsymbol{r}_1 + (m_2 + 1)\boldsymbol{r}_2] + \ldots \tag{5}$$

where e is the charge on the proton,

$$m_1 = \frac{m_d}{M}, \quad m_2 = \frac{m_\mu}{M} \quad (M = m_d + m_t + m_\mu)$$

and m_d, for example, is the mass of the deuteron.

The V can be treated as a perturbation using Fermi's Golden Rule. See, for example, ref. 35. The results Bhatia et al. obtained by including the first, dipole term in (5) are given in Table 1. Note that the deexcitation rate to the $(0,1)$ state with zero angular momentum is much larger than the other deexcitation rates.

The results obtained in some other calculations for the key $(1,1) \rightarrow (0,1)$ deexcitation rate are given in Table 2. The calculation in which I was involved (ref. 38) differs from the others in

that it allows for the molecular structure of the $[(dt\mu)_{11}dee]$ complex. It can be seen that allowing for this does not significantly affect the deexcitation rate.

The circumstances that led to this calculation are of interest. In December 1987, I visited the atomic physics group at Goddard Space Flight Center to give a seminar on calculations I was carrying out on positron-hydrogen-molecule scattering. Drachman talked to me about the calculations that he was carrying out with Bhatia and Chatterjee (ref. 34) on the deexcitation rate of the $[(dt\mu)_{11}dee]$ complex. Knowing that I had come into positron physics from theoretical chemistry, he encouraged me to see if I could take the molecular nature of the complex into account when calculating the deexcitation rate. As I pointed out earlier, this was not allowed for in ref. 34. He gave me a translation that he had made of a report by two members of Ponomarev's group, Men'shikov and Faifman, on the treatment of $[(dt\mu)_{11}dee]$ as a molecular complex.

I was sufficiently interested to put my graduate student, Lewis, onto the problem of how to take into account the molecular nature of $[(dt\mu)_{11}dee]$ when calculating the deexcitation rate. It was not long before I came to appreciate the special features of muon catalyzed fusion that had attracted Drachman to it.

Lewis and I collaborated with Hara at RIKEN in Japan to allow for the fact that $[(dt\mu)dee]$ and $[(dt\mu)de]^+$ in reaction (3) should be treated as D_2-like and D_2^+-like molecules, respectively, with one nucleus replaced by a particle of mass equal to that of $dt\mu$ (ref. 38).

Quite soon I was in contact with Ponomarev. I visited him and his group at the Kurchatov Institute in Moscow in 1990 and gave a seminar on my work. The Cold War had ended and contacts with Russian scientists were multiplying to make up for the long period of separation.

With my postdoc, Harston, I went on to collaborate with Faifman and Strizh on the calculation of the rate of the reaction (3) that leads to the formation of $dt\mu$ in a state with zero angular momentum. Men'shikov and Faifman (ref. 32) considered that the inequalities $\Gamma_e \ll \Gamma_a \ll \epsilon$, where ϵ is the kinetic energy of the relative motion of $t\mu$ and D_2, held for Γ_a and Γ_e in equation (4). Under these conditions, $\sigma_r(E)$ is effectively the cross section for the formation of the complex (ref. 39). Also,

$$\sigma_r \approx \frac{2\pi^2}{k^2}\Gamma_e \delta(E - E_r). \tag{6}$$

Γ_e is determined by the matrix element $\langle \chi_f | \bar{V} | \chi_i \rangle$, where χ_i and χ_f are the initial state $t\mu + D_2$ wave function and the wave function for the $[(dt\mu)_{11}dee]$ complex, respectively. $\bar{V}$ is the potential that brings about the formation of the complex, i.e. the interaction between the $t\mu$ and D_2. Men'shikov and Faifman showed that it could more conveniently be taken to be the analogue of V in equation (5), allowing for the molecular structure of the complex.

By skillful use of mathematics (ref. 40), Faifman et al. (ref. 41) were able to evaluate $\langle \chi_f | \bar{V} | \chi_i \rangle$, with $\bar{V}$ the leading dipole term in its multipole expansion. During visits to Nottingham by Faifman and Strizh, this was extended to include the next term which is the quadrupole term (ref. 42). It was found that including the quadrupole term reduced the magnitude of the peak reaction rates by between 20% and 30%.

In fact, this treatment does not allow fully for the molecular nature of the resonant process in which $dt\mu$ is formed in a state with $J = 0$ in which fusion can take place rapidly. Cohen at Los Alamos, who has made many contributions to the theory of muon catalyzed fusion over the years, encouraged me to apply the methods of quantum reactive scattering to reaction (3). This reaction has some similarities with the chemical reaction

$$H + D_2 \rightarrow H + D_2 \text{ or } HD + D. \tag{7}$$

This and other chemical reactions have been extensively studied by these methods. See, for example, ref. 43.

However, comparison of reactions (3) and (7) shows that (3) has a special feature not present in (7), namely the Auger decay process which leads to the loss of the electron. Reaction (7) corresponds quite closely to the much slower side reaction

$$t\mu + \mathrm{D}_2 \leftrightarrows [(dt\mu)_{11}ee] \rightarrow [(dt\mu)_{Jv}e] + \mathrm{D} \tag{8}$$

where $(J, v) = (0,1)$, $(2,0)$, $(1,0)$ or $(0,0)$.

This reaction proceeds through the *same* resonances as reaction (3). In this case, the resonant complex decays forward into the muonic molecule $[(dt\mu)_{Jv}e]$ and a D atom or backward into $t\mu + \mathrm{D}_2$.

One of the methods that has been applied to reaction (7) is the method of Pack and Parker (ref. 44). They use adiabatically adjusting, principal axes hyperspherical coordinates (APH) in their calculations. These are elegant coordinates that transform smoothly between different channels such as $\mathrm{H} + \mathrm{D}_2$ and $\mathrm{HD} + \mathrm{D}$. Together with Pack, my postdoc Zeman and I applied this method to reaction (8) (refs. 45–47).

Unfortunately, there was no easy way of including the Auger decay channel directly in our treatment. However, as pointed out by Men'shikov and Faifman (ref. 32), the coupling between the resonant channels is small as the lifetime of the resonant complex is much longer than the time the complex takes to complete a vibration. Thus the various decay processes operate essentially independently. This made it possible for us to obtain what we expect to be accurate values for Γ_e and Γ_n, the partial widths for back decay and for the decay of the complex into $[(dt\mu)_{Jv}e] + \mathrm{D}$, by analysing our results for the cross section for the resonant reaction (8) using the Breit–Wigner formula.

Owing to the complexity of the calculation, we were only able to consider scattering states with zero total angular momentum. As the $dt\mu$ is in its $(1,1)$ state in the complex, this meant that the fictitious diatomic molecule in the complex, with one nucleus $dt\mu$, had to be in a state with angular momentum equal to 1. Care had to be taken to make sure that all important corrections to the Born–Oppenheimer potential were included in calculating the potential energy surface for the reaction.

An interesting picture of the surface function eigenvalues of the hyperradius ρ is given in Figures 3 and 4 in ref. 46. In Figure 3, the bottom four curves correspond asymptotically to the open channel $(0,1)$, $(2,0)$, $(1,0)$ and $(0,0)$ states of $[(dt\mu)_{Jv}e]$. Figure 4 highlights the curve that corresponds to the closed channel $(1,1)$ state asymptotically among curves that correspond in this region to the various D_2 states.

It was found, as expected, that the reaction proceeded only through the resonances. The resonant states were found to be the vibrational states of the complex with vibrational quantum number $v_c = 3$ and 4. The center of the $v_c = 2$ resonance was calculated to be just slightly below threshold.

Somewhat to our surprise, we found that our calculated value of the back decay rate (ref. 47) was much larger than the value obtained for it by Lane (ref. 33) and comparable with the calculated values of the Auger decay rate in Table 2. Further work is necessary to resolve this discrepancy.

It was a great pleasure for me to be able to give Drachman a copy of this treatment of the resonant process that leads to fusion (ref. 46). It showed what had resulted from his encouragement to me to consider the molecular nature of the complex in reaction (3).

MUON CATALYZED FUSION AS A SOURCE OF ENERGY

I have not said anything so far about muon catalyzed fusion as a possible source of energy. To consider this, we must look at the full muon catalyzed fusion cycle. This begins with the projection of a muon into a mixture of deuterium and tritium at room temperature. The sequence of events is then as shown in Figure 2.

What I have not considered up until now is how the cycle continues after fusion takes place. The muon is a lepton and is thus unaffected by the strong interaction that brings about the d-t fusion

$$d + t \rightarrow \alpha + n. \tag{9}$$

However, the muon is negatively charged and may combine with the α particle to form a bound state. This process is referred to as 'sticking'. If the muon remains bound in this way, it is lost to the cycle.

However, the $\alpha\mu$ is emitted with a kinetic energy of 3.5 MeV (ref. 30). As it slows down in the medium, it undergoes many collisions which may result in the stripping of the muon from the α particle. In addition, the muon can become available through transfer reactions that result in $t\mu$ or $d\mu$ and a free α particle.

We can define an effective sticking probability, w_s, by

$$w_s = w_s^0(1 - R), \tag{10}$$

where w_s^0 is the initial sticking probability and R is the muon reactivation coefficient that measures the extent to which stripping occurs. w_s^0 has been calculated by several methods: variational (refs. 49–51), adiabatic (ref. 52), adiabatic hyperspherical (ref. 53) and Monte Carlo (ref. 54). Detailed calculations have been carried out of R by Cohen (ref. 55), Markushin (ref. 56) and Rafelski et al. (ref. 57).

If we consider the rate values given in Figure 2, the muonic atom formation rate λ_a is much larger than either λ_{dt}, the rate of transfer of a muon from $d\mu$ in its ground $1s$ state to $t\mu$ or $\lambda_{dt\mu}$, the resonant formation rate of $dt\mu$. Consequently, the rate of the muon catalysis cycle λ_c is practically independent of λ_a. For the same reason, it is practically independent of the $dt\mu$ deexcitation rate (see Table 1) and the fusion rate.

λ_c is then given by

$$\frac{1}{\lambda_c} \approx \frac{c_d q_{1s}}{\lambda_{dt} c_t} + \frac{1}{\lambda_{dt\mu} c_d}, \tag{11}$$

where c_d and c_t are the concentrations of deuterium and tritium, respectively, in the mixture ($c_d + c_t = 1$). See refs. 29, 48 and 58. q_{1s} is the probability that the $d\mu$ reaches its ground state. The rate of transfer of the muon from d to t is much slower for $d\mu$ in this state. The first term on the right-hand side of equation (11) is the time the muon spends as $d\mu$ waiting to transfer to t and the second term is the time it spends as $t\mu$ waiting to form the $dt\mu$ molecule.

If sticking did not occur the average number X_c of cycles catalyzed by one muon would be λ_c/λ_0, where $\frac{1}{\lambda_0} = 2.2 \times 10^{-6}$ sec is the mean lifetime of the muon. Sticking modifies it to

$$X_c = \frac{1}{\frac{\lambda_0}{\lambda_c} + w_s}. \tag{12}$$

Theory and experiment indicate that $w_s \approx 0.5\%$ (refs. 48, 58, 59). If $w_s = 0.43\%$, as in Figure 2, it follows from equation (12) that X_c cannot be larger than 232.

With the *estimated* cost of ~ 8 GeV to produce a muon (ref. 60) and a maximum energy release of 17.6 MeV per cycle, break even would be achieved if $X_c \approx 450$. A considerably higher X_c value, at least 900, would be required for muon catalyzed fusion to be a commercially viable source of energy. $X_c = 150$ is currently attainable. Possible ways of making X_c as high as 900 by increasing the density of the deuterium and tritium mixture and decreasing w_s by increasing R are outlined in ref. 61. See equation (10).

14.1 MeV of the 17.6 MeV generated by the *d-t* fusion reaction (9) is carried away by the neutron. The present maximum X_c value of ~ 150 would be adequate for the production of energy by using neutrons obtained in this way to convert ^{238}U into plutonium fuel for conventional fission reactors (refs. 29, 60, 30, 62). Unfortunately, this method of energy production would not be as 'clean' as using the muon catalyzed fusion cycle directly.

The greatly expanded interest in muon catalyzed fusion in the 1980s was followed by a gradual decline in interest with the realisation that it was unlikely to be a viable source of energy. At the beginning of the 90s, the Advanced Energy Projects (AEP) Division of the US Department of Energy withdrew funding from experiments on muon catalyzed fusion at Los Alamos. The AEP Division considered that the research had been successful as it had shown that muon catalyzed fusion was not a viable source of energy.[1]

Experimental work continued at the Paul Scherrer Institute (PSI) in Switzerland (ref. 63, 64) and at Dubna and elsewhere in Russia (ref. 65). In the late 90s and early 2000s, a considerable impetus was given to experimental work on muon catalyzed fusion by Nagamine and his Japanese group from RIKEN who carried out experiments using the pulsed muon beam at the Rutherford Appleton Laboratory (RAL) in the UK (refs. 59, 61, 66) and also by the international collaboration based on Marshall's group at TRIUMF in Canada (refs. 67, 68). This essentially brings us to the present day.

The reader who wishes to obtain an overall view of muon catalyzed fusion should choose from the review articles in refs. 2, 10, 29, 30, 48, 58, 63, 69 and 70. The most recent, detailed overview is given in the Proceedings of the International RIKEN Conference on Muon Catalyzed Fusion and Related Atoms (MuCF01) at Shimoda in Japan in April, 2001 (ref. 71).

CONCLUSION

Today with the maximum number of fusions attained per cycle still only about 150, it is difficult to argue that muon catalyzed fusion should be considered seriously as a possible energy source. However, if Nagamine (ref. 61) or anyone else were able to increase this number to ~ 900, the situation would change, but this seems unlikely.

This is unfortunate but over the years the study of muon catalyzed fusion has given many physicists, not least Dick Drachman and myself, many moments of real pleasure. Nobody knows why physical phenomena can be described using mathematics (ref. 72) but to apply it successfully to an elegant physical problem is an experience to be savoured.

I am very grateful to Dick Drachman for introducing me to muon catalyzed fusion and for many valuable discussions with him over the years about it, positron physics and other subjects. It has always been a great pleasure for me to visit Goddard Space Flight Center and discuss my work with him, Aaron Temkin and Anand Bhatia. I wish Dick and Aaron all the best in their retirement.

[1] James Cohen, private communication, 2005.

Table 1 Calculated values for the deexcitation rates (ref. 34)

Transition	Energy difference ΔE (eV)	Deexcitation rate ($sec^{-}1$)
$11 \rightarrow 01$	34.1745	6.44×10^{11}
$10 \rightarrow 00$	86.6682	3.31×10^{10}
$11 \rightarrow 20$	101.88	8.56×10^{10}
$20 \rightarrow 10$	129.93	5.12×10^{10}
$01 \rightarrow 10$	197.6370	3.32×10^{10}
$11 \rightarrow 00$	318.4797	1.57×10^{9}

Table 2 Other calculations of the $(1,1) \rightarrow (0,1)$ deexcitation rate

Calculation	Deexcitation rate $11 \rightarrow 01$ (sec^{-1})
Vinitsky, Ponomarev and Faifman (ref. 36)	11.4×10^{11}
Scrinzi and Szalewicz (ref. 37)	10.20×10^{11}
Armour, Lewis and Hara (ref. 38)	8.63×10^{11}
Bhatia, Drachman and Chatterjee (ref. 34)	6.44×10^{11}

Figure 1 Energy level diagram and dipole Auger (or internal conversion) transitions f
$dt\mu$ molecular ion (ref. 30). Binding energies for $J = 0$ and $J = 1$ are from ref. 25 and for
ref. 26. Units are eV.

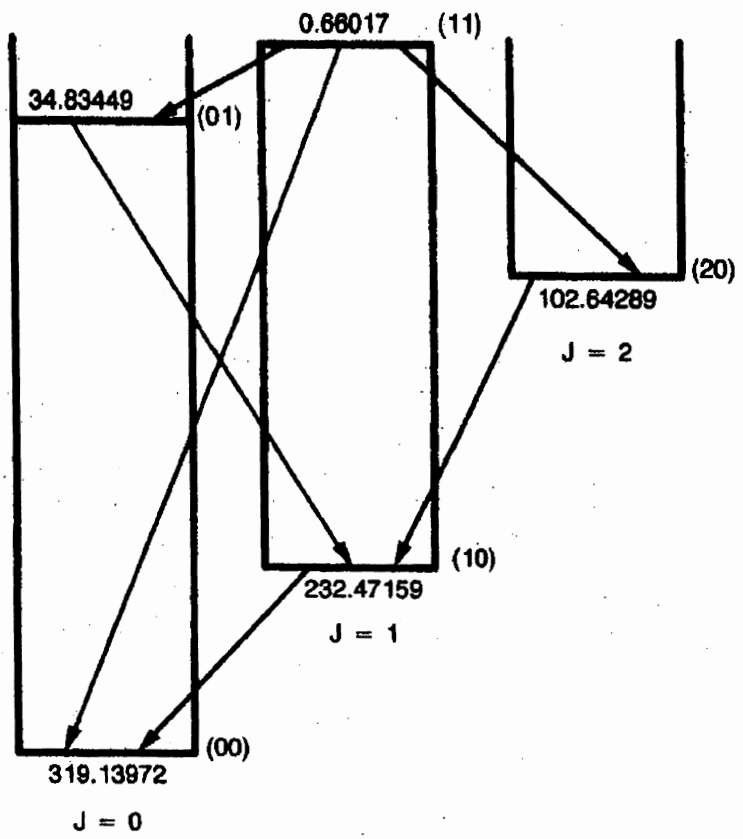

Figure 2 The principal muon catalysis fusion cycle in a deuterium and tritium mixture (ref. 29). Side chains involving d-d and t-t fusion are not shown. λ_a = muonic atom formation rate $\approx 4 \times 10^{12}\, s^{-1}$; λ_{dt} = muon transfer rate from $(d\mu)_{1s}$ to $(t\mu)_{1s} \approx 3 \times 10^{8}\, s^{-1}$; $\lambda_{dt\mu}$ = resonant formation rate of $dt\mu \approx 4 \times 10^{8}\, \mathrm{sec}^{-1}$; ω_s = effective sticking probability $\approx 0.43\%$; λ_c = cycle rate. Values (ref. 48) are for $T = 300\mathrm{K}$ and liquid hydrogen density (4.25×10^{28} atoms m^{-3}).

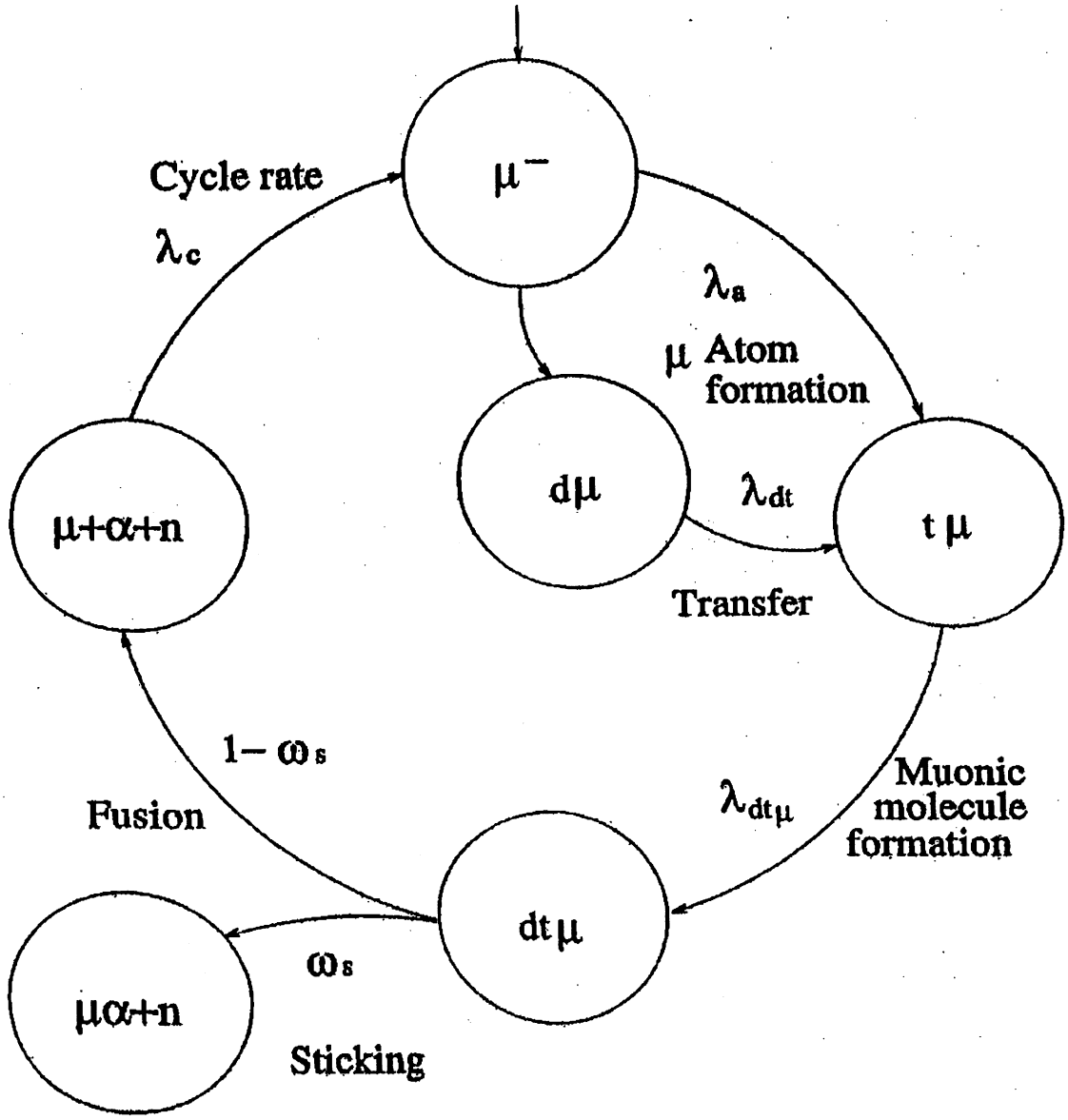

REFERENCES

1. Neddermeyer, S.H. and Anderson, C.D., Phys. Rev. **51**, 884 (1937).

2. Froelich, P., Advances in Physics **41**, 405 (1992).

3. Bethe, H.A., Phys. Rev. **55**, 434 (1939).

4. Annual Report of the EURATOM/UKAEA Fusion Programme 2004/5.

5. Frank, F.C., Nature **160**, 525 (1947).

6. Frank, F.C., Proceedings of an International Symposium on Muon Catalyzed Fusion μCF-89, ed. Davies, J.D. (Rutherford Appleton Laboratory Report RAL-90-022, 1990), p1.

7. Sakharov, A.D., Report of the Physics Institute, Academy of Sciences, USSR (1948).

8. Zel'dovich, Ya. B., Dokl. Akad. Nauk. SSR **95**, 493 (1954).

9. Alvarez, L.W. et al., Phys. Rev. **105**, 1127 (1957).

10. Bracci, L. and Fiorentini, G., Phys. Reports **86**, 169 (1982).

11. Jackson, J.D., Phys. Rev. **106**, 330 (1957); Hyperfine Interactions **82**, 3 (1993).

12. Dzhelepov, V.P., Ermolov, P., Moscalev, V.I. and Filchenkov, V.V., Sov. Phys. JETP **23**, 820 (1966).

13. Vesman, E.A., Sov. Phys. JETP Lett. **5**, 91 (1967).

14. Zel'dovich, Ya. B. and Gershtein, S.S., Soviet Physics Usp. **3**, 593 (1961).

15. Gershtein, S.S. and Ponomarev, L.I., Phys. Lett. **72 B**, 80 (1977).

16. Vinitsky, S.I., Ponomarev, L.I., Puzynin, I.V., Puzynina, T.P., Somov, L.N. and Faifman, M.P., Sov. Phys. JETP **47**, 444 (1978).

17. Vinitsky, S.I. and Ponomarev. L.I., Sov. J. Part. Nucl. **13**, 557 (1982).

18. Bystritsky, V.M. et al., Sov. Phys. JETP **53**, 877 (1981).

19. Bhatia, A.K. and Drachman, R.J., Phys. Rev. A **30**, 2138 (1984).

20. Bhatia, A.K. and Temkin, A., Rev. Mod. Phys. **36**, 1050 (1964); Phys. Rev. **137**, A1335 (1965).

21. Frolov, A.M. and Efros, V.D., Zh. Eksp. Teor. Fiz. Pis. **39**, 449 (1984).

22. Frolov, A.M. and Efros, V.D., J. Phys. B **18**, L265 (1985).

23. Hu, C.Y., Phys. Rev. A **34**, 2536 (1986); **36**, 4135 (1987).

24. Szalewicz, K., Kołos, W., Monkhorst, H.J. and Scrinzi, A., Phys. Rev. A **36**, 5494 (1987).

25. Alexander, S.A. and Monkhorst, H.J., Phys. Rev. A **38**, 26 (1988).

26. Kamimura, M., Phys. Rev. A **38**, 621 (1988).

27. Vinitsky, S.I., Korobov, V.I. and Pozynin, I.V., Sov. Phys. JETP **64**, 417 (1986).

28. Hara, S. and Ishihara, T., Phys. Rev. A **40**, 4232 (1989).

29. Ponomarev, L.I., Contemporary Physics **31**, 219 (1990).

30. Bhatia, A.K. and Drachman, R.J., Comments At. Mol. Phys. **22**, 281 (1989).

31. Bakalov, D. and Korobov, V.I., Hyperfine Interactions **138**, 265 (2001).

32. Men'shikov, L.I. and Faifman, M.P., Sov. J. Nucl. Phys. **43**, 414 (1986).

33. Lane, A.M., Phys. Lett. **98A**, 337 (1983).

34. Bhatia, A.K., Drachman, R.J. and Chatterjee, L., Phys. Rev. A **38**, 3400 (1988).

35. *Physics of Atoms and Molecules*, Bransden, B.H. and Joachain, C.J., First Edition, Longman, London and New York 1983, p116.

36. Vinitsky, S.I., Ponomarv, L.I. and Faifman, M.P., Sov. Phys. JETP **55**, 578 (1982).

37. Scrinzi, A. and Szalewicz, K., Phys. Rev. A **39**, 2855 (1989).

38. Armour, E.A.G., Lewis, D.M. and Hara S., Phys. Rev. A **46**, 6888 (1992).

39. *The Theory of Atomic Collisions*, Mott, N.F. and Massey, H.S.W., Third Edition, Oxford University Press, 1965, p409.

40. Men'shikov, L.I., Sov. J. Nucl. Phys. **42**, 750 (1985).

41. Faifman, M.P., Men'shikov, L.I. and Strizh, T.A., Muon. Cat. Fusion **4**, 1 (1988).

42. Faifman, M.P., Strizh, T.A., Armour, E.A.G. and Harston, M.R., Hyperfine Interactions **101/102**, 179 (1996).

43. Manolopoulos, D.E. and Clary, D.C., Ann. Rep. Prog. Chem. Sec. C: Phys. Chem. **86**, 95 (1989).

44. Pack, R.T. and Parker, G.A., J. Chem. Phys. **87**, 3888 (1987); **90**, 3511 (1989).

45. Armour, E.A.G., J. Chem. Soc., Faraday Trans. **93**, 1011 (1997).

46. Zeman, V., Armour, E.A.G. and Pack, R.T., Phys. Rev. A **61**, 052713 (2000).

47. Zeman, V. and Armour, E.A.G., Hyperfine Interactions **138**, 255 (2001).

48. Breunlich, W.H., Kammel, P., Cohen, J.S. and Leon, M., Annu. Rev. Nucl. Part. Sci. **39**, 311 (1989).

49. Hu, C.Y., Phys. Rev. A **34**, 2536 (1986); **36**, 4135 (1987).

50. Kamimura, M., *Muon Catalyzed Fusion*, eds. Jones, S.E., Rafelski, J. and Monkhorst, H.J., AIP Conference Proceedings No. **181**, American Institute of Physics, New York, 1989, p330.

51. Haywood, S.E., Monkhorst, H.J. and Szalewicz, K., Phys. Rev. **37**, 3393 (1988); **39**, 1634 (1989).

52. Bogdanova, L.N. et al., Nucl. Phys. **454**, 653 (1986).

53. Gusev, V.V., Muon Catal. Fusion **4**, 146 (1989).

54. Cepperley, D. and Alder, B.J., Phys. Rev. A **31**, 1999 (1985).

55. Cohen, J.S., Phys. Rev. Lett. **58**, 1407 (1987); Muon Catal. Fusion **1**, 179 (1987).

56. Markushin, V.E., Muon Catal. Fusion **3**, 395 (1988).

57. Rafelski, H.E., Müller, B., Rafelski, J., Trautmann, D. and Viollier, R.D., Progr. Part. and Nucl. Phys. **22** 279 (1989).

58. Cohen, J.S., *Review of Fundamental Processes and Applications of Atoms and Ions*, ed. Lin, C.D. (World Scientific Singapore, 1993) Chap. 2.

59. Ishida, K., Nagamine, K., Matsuzaki, T. and Kawamura, N., J. Phys. G: Nucl. Part. Phys. **29**, 2043 (2003).

60. Petrov, Yu. V., Nature **285**, 466 (1980); Muon Catal. Fusion **3**, 525 (1988).

61. Nagamine, K., Hyperfine Interactions **138**, 5 (2001).

62. Vecchi, M., Karmanov, F.I., Slovodtchouk, V.I., Konobeyev, A. Yu., Anisimov, V.V., Latysheva, L.N., Pshenichnov, I.A. and Ponomarev, L.I., Hyperfine Interactions **138**, 355 (2001).

63. Petitjean, C., Nucl. Phys. A **543**, 79c (1992).

64. Petitjean, C., Hyperfine Interactions **138**, 191 (2001).

65. Perevozchikov, V.V. et al., Hyperfine Interactions **138**, 417 (2001).

66. Ishida, K. et al., Hyperfine Interactions **138**, 225 (2001).

67. Fujiwara, M.C. et al., Phys. Rev. Lett. **85**, 1642 (2000).

68. Marshall, G.M. et al., Hyperfine Interactions **138**, 203 (2001).

69. Gershtein, S.S., Petrov, Yu. V. and Ponomarev, L.I., Sov. Phys. Usp. **33**, 59 (1990).

70. Armour, E.A.G., Harston, M.R. and Faifman, M.P., *The Physics of Electronic and Atomic Collisions*: XVII International Conference, eds. Andersen, T., Fastrup, B., Folkmann, F., Knudson, F. and Andersen, A., AIP Conf. Proc. No. **295**, American Institute of Physics, New York, 1993, p478.

71. Hyperfine Interactions **38**, Nos. 1–4 (2001).

72. *Disturbing the Universe*, Dyson, F.J., Harper and Row, New York, 1979, p50.

Comments by Dr. Aaron Temkin

I am very flattered to have had the symposium in honor of Dick Drachman and myself at the time of my retirement from the government.

Let me first say a few nice words about my co-honoree. Dick Drackman (and the late Isodore Harris) were the first colleagues I met when I came to Washington DC in 1957 to start my NRC-NAS Resident Research associateship at the Naval Research Laboratory. They knew that I was coming but since I had just returned from Germany (they apparently didn't know that I had completed a Fulbright fellowship) they assumed I was a German. Well after one or two sentences with my New Jersey/New York accent they quickly realized that that was not the case.

After I had moved to NASA/Goddard in 1960 from NBS Dick joined me as a colleague in 1963. By that time Dick had gotten interested in positrons, and he began applying some of our polarized orbital ideas to positron scattering. As is by now well known the dipole part of the static interaction (which is essence of polarized orbital method) is not sufficient to account for e^+-atom scattering. Even including the monopole part of the static interaction is not sufficient for the higher partial waves. I recall, at the time that we came up with the facetious approximation that we called MAFIA (monopole amplification by finagling inappropriate approximations) to enhance the monopole term to get agreement with what by that time had been gotten by elaborate variational calculations.

On a more substantive note, one of the things that Dick did - aside from the many things which have been mentioned in this symposium - is to have encouraged one of the earliest experiments to measure directly low energy positron scattering from He. In those days we were able to finacially support an experiment, this one at General Atomic (San Diago) by D. Herring and J. W. McGowan and coworkers using its linear accelerator to produce high energy positrons and then slow them down and scatter them from Helium [D. G. Costello, D. E. Groce, D. F. Herring, J. W. McGowan, Can J. Phys. **50**, 72 (1972)].

The other thing I would like to say about Dick Drachman is that since he knew both MACSYMA and knows its successor program (MATHEMATICA) for doing both analytical as well as numerical analysis, Dick has done innumerable calculations for me for the purpose of testing various ideas I have had in the course of my own research. In addition, although we have not published too many joint papers, we have been talking physics to each other for over forty years. I don't know how many crazy ideas he has talked me out of. (But I will admit that he has been wrong about a couple of my good ideas.)

Now let me add a couple of words about my own work - in particular about a model which has been talked about at this symposium, known as Temkin-Poet model. Introduced by me in the scattering problem in 1962 as the zeroth order problem of convergent series of approximations for S-wave electron-hydrogen scattering, it was reintroduced by Poet in 1976 who along with it developed some very powerful numerical techniques (which are still being used) to obtain very accurate (model) results particularly in the inelastic domain. Although Poet referred to our paper, he seemed to be unaware of the fact that we had also done calculations in the inelastic domain [H. L. Kyle and A. Temkin, Phys. Rev. **134**, A600 (1964)] and that I even made attempts to apply it to the ionization (threshold) problem [A. Temkin, "A Preface to the Nonadiabatic Theory of Electron-Hydrogen Ionization" GSFC X-641-66-311, July, 1966 (unpublished)].

In conclusion, My thanks to the contributors and attendees at the Symposium. I am honored by their presence. I would like, finally, to thank my closest research colleague, Dr. Anand Bhatia. We

have been together for over 40 years and, at last count, we have collaborated on over 40 papers. This symposium, which was entirely his idea, has entailed a huge amount of effort on his part (which, I should add, was done at a very stressful time in his life, having lost his wife of over 40 years). I can only say that I consider myself (and I am sure Dick feels the same way) very lucky to have had him as a colleague and coworker.

Aaron Temkin

Goddard Space Flight Center

After Dinner Remarks

Prof. J. Sucher
Department of Physics, University of Maryland, College Park, MD 20740

Pioneers and Musketeers

I am happy for the opportunity to close this symposium in honor of the retirement of Dick Drachman and Aaron Temkin, by saying a few words about them.

Before describing my qualifications for this job, let me say that in the late nineties I noticed that some people, Bill Clinton for example, were making more money after retirement than before, giving banquet speeches and getting big bucks for it: So I thought I would go the same route and retire. It hasn't worked out the way I planned. On the contrary: it's costing me.. We're lucky this symposium was held on a Friday. On other days, NASA charges an entrance fee as well as for parking - all in an effort to build up financial resources for the manned trip to Mars. As you all know, the heroes of the evening are both theoretical physicists. But despite that, they are both extremely nice people. I am reminded of a recent New Yorker cartoon: At a party, a woman is introducing her companion to the hostess: "Mary." she says, "I'd like you to meet my friend Edward. He's an economist but he's really very nice." This applies to some physicists also, especially Dick and Aaron.

In case you are not a member of this clan -- and I see there are quite a few normal people here -- there is no need to worry. There will be very few references to physics. When Steven Hawking was advised that for every equation in his book *A Brief History of Time* the sales would be reduced by half, he took out one the two equations he had in the book. Since I hope to make a killing on reprints of this talk there will be no equations at all.

I met Dick Drachman some time after I got to Columbia University as a graduate student in 1952 and Aaron Temkin a few years later, at a party in Manhattan. I came to the University of Maryland in 1957 where I met Anand Bhatia, the stalwart organizer of today's symposium, and took him on as my first graduate student. The total number of man-years involved is exactly 150, so that this is a sort of sesquicentennial anniversary for me. Well, not exactly 150 –I rounded off the numbers a bit because I've always wanted to use the word 'sesquicentennial' in public. There are not many six-syllable words which flow so trippingly off the tongue. Sesquicentennial-- what a thrill.

During a sabbatical year here in 1978, I shared an office with Anand and found the atmosphere was consistently warm and welcoming: lunch at the excellent cafeteria, followed by schmoozing with coffee (more about this later) in one or the other of the three contiguous offices which Aaron, Dick and Anand have, and I hope will continue to have for many years to come.

I think of them as the Three Musketeers of Atomic Physics. They have written hundreds of papers together, in various combinations in their more than 40 years together here, many of these papers are of a pioneering character, as the attendees at the physics part of this symposium learned today. Our subject is very much the richer for it. They are the pioneers and musketeers of the title of my talk.

Aaron, Dick and Anand have survived at NASA, despite all the cost-cutting, under the radar as it were. This was to my good fortune for when I retired in '98. I found a second home here. My office at the University was cluttered with 41 years of detritus and I was somewhat in

the doldrums as far as research was concerned. My wife Dorothy suggested (translation: you have to do this) that I see whether my friends could get me an office here. So I did and they did:(Quote from a former president of Israel: "When your wife says you have to, you have to.".)

Although building 21 was very pressed for space, they quickly found me an office. It had no computer, no telephone and no windows. I was reminded of a scene in a movie in which two characters, who have seen better days, are sitting in a shabby restaurant in Berlin, just after the WWII. The broken windows have been replaced by boards. One of them asks; "Why do you come to this godforsaken place?' The other says, "Well, here I can turn my back on the future, shut out the present and face the past with hope and confidence."

In other words, the office was PERFECT! There was nothing to do but think. I became aware of a paper Aaron was working on, dealing with dispersion relations for electron-hydrogen scattering, a subject pioneered by Ed Gerjuoy, who is right here at this table, in 1960. Alarmed by certain features of the relevant equations which were a surprise to a particle physicist, I was quickly able to write, with Aaron's encouragement, a paper of interest to both particle and atomic physics. In the course of this I learned that Aaron was not only a gentleman but also a scholar of the old school: He patiently read a sequence of drafts and -- get this! and wrote comments and suggested changes in longhand for my edification. They don't make them like that anymore.

The paper was originally titled *Triple Poles in QED*: *Who Ordered That?* and submitted to the Physical Review, the premier journal for physics research in the USA. It may interest the non-physicists among you to learn that often the hardest part of getting a paper published in this journal is not acceptance by the referees but by the copy editors, who are apparently sworn to uphold traditions, some old, some new, in an effort to maintain the decorum and rectitude appropriate for a journal of record. My experience with this paper may also amuse the physicists, who I'm sure have tales of their own in this category. I heard from the editors at once: " The Physical Review does not accept papers with titles containing a question." This was news to me, since I had previously done just that, but I clearly had no choice with a new policy so, much to my dismay, I changed the title to something less snappy. After the paper was accepted, the real fun began.

I had compared two approaches to the problem at hand and shown that while one of these, the particle physics approach, gave one aspect of the answer immediately, unlike the more prosaic atomic physics approach, it did not get some details correctly. So I wrote "There is no free lunch." The copy editor removed this sentence in the galley proof and asked: " Could I substitute a more scientific phrase, such as 'There is no simple explanation?""

Further, while making reference to an incorrect term in a paper of J. Robert Oppenheimer, I had written "This term first appears in a 1927 paper of Oppenheimer . . The copy editor removed the adjective 'first' and wrote: "The Physical Review prefers not to publish claims of novelty or priority."

In cases like this one can either fight or retreat. I decided to do battle and wrote: "I have thought hard about finding a substitute for "There is no free lunch" but found none as concise and telling. The copy editor's suggestion is worse than nothing. On the use of the adjective 'first' I understand and appreciate your policy with regard to claims of priority, but in this case it seems to be misplaced. The Oppenheimer paper was published more than 75 years ago, No one will rise from the dead to claim priority for this term, which moreover is incorrect..." Sometimes you have to be tough! Of course I wouldn't be telling you all this had I not won the battle.

Artilochus famously said: "The fox knows many things while the hedgehog knows one great thing." Like the fox, Dick Drachman knows many, many things, not only in physics but about almost any subject that comes up. Whenever he makes a statement of what the Answer Man of yesteryear's radio

would call an 'ethical fact', I believe him completely. You may not know that Dick is a gardener. For example, he knows all about the ripening of tomatoes. He once told me that beyond a certain point the time it takes for a green tomato to ripen and turn red is the same, whether you pick it from the vine or not. I once told this to my wife. Dorothy, also a gardener, and she said simply: "I don't believe it." I was shocked but kept my peace. Nevertheless, the subject of when to pick came up every year when frost was threatening in Vermont, where we spend the summers, and for a number of years I repeated, like a mantra: "Dick Drachman says it doesn't matter when you pick it". Finally Dorothy had enough: " That's it!" she said. "This is the last time you are going to tell me the Drachman theory of tomato ripening."

If Dick is a fox, Aaron has some of the qualities of a hedgehog. This may best be illustrated by the episode of the coffee machine in the basement of Building 21. When los tres caballeros moved into this building they brought a coffee machine with them. Eventually it was decided that the machine would be communal and people would pay a dime for a cup, except that because they were contributing the machine, the coffee would be free for them, and so it was for many years. However, a new coffee broom swept in at some point, who stated that they had had their money's worth and the three should now pay like everyone else. While Dick and Anand went along, Aaron demurred. He had been grandfathered in and was not about to be deprived of his rights. When I came here in '78, I became aware of this situation. Aaron said I should consider myself as his guest and not pay anything. But I considered myself as a guest of Dick and Anand also and they were paying. What to do? Rounding off two-thirds of ten to the nearest integer, I briefly considered contributing seven cents per cup, but it was too hard to stay with it. At some point Aaron got fed up with the continuing tension involved and bought his own coffee machine, with his own Starbucks coffee, which he has to this day. Of course his highly principled hedgehog stand has a price: I estimate it's costing him about a dollar a cup now.

On behalf of all of us I should like to thank Betty Drachman and Gladys Temkin for hosting this wonderful banquet and Anand Bhatia for the great organization. I conclude with a brief toast in verse:

To Dick and Aaron

On this August, nay, grand occasion,
I eschew the long equation.
There'll be nothing of that sort,
I'm gonna keep it very short.

I ask you trust my calculation:
These guys have earned a celebration.
Let all of us this toast be sharin':
Hip, hip, hurrah for Dick and Aaron!

Many happy years of retirement fun with and without physics!

Joe Sucher
11/18/06

MODELS AND MODELLING, LIFE AND LIVING - MUSINGS OF A MATH TEACHER IN A LETTER TO OLD FRIENDS

S. Kenneth Houston
School of Computing and Mathematics, University of Ulster, Northern Ireland

Dear Dick and Aaron,

It is now thirty-six years since my year at Goddard - almost the entire span of the working life of a UK academic. It is good to see that you found the energy and enthusiasm to work on well past the normal UK retirement age of sixty-five, but then there is no "ageism" in the USA. Mind you, Prime Minister Blair is talking about raising this to seventy! Scientifically, 1969/70 was an exciting and productive year for me, and was a valuable addition to my CV when I came to look for a new job in my homeland a few years later. But the most valuable things to come from that time are friendships that have endured. However my relationship with atomic physics came to an end more or less in 1980. So what have I been up to for the last twenty-five years or so?

Dick, you undoubtedly remember our 1970 paper on a "Simplified Model for Positronium-Helium Scattering" [1], because you mentioned in your talk on *Few-body Positron Theory and the Three H's* at John Humberston's retirement in 2003 that we had been "caught out" [2] at last and that a better result had been obtained. But what I want to draw attention to now is not the physics, but the word "model". This was the first time I had used the word in my scientific work, it was almost the first time I had seen it used in a scientific context, and it was to play a very big part in my subsequent thinking and teaching. In 1970 we used a "model" potential because we could not solve the problem with the "real" potential from the full Hamiltonian for the system.

It was quite some time before I began to realise that even the full Hamiltonian was itself a model, that Quantum Mechanics was a model, that Newton's Laws of Motion were a model. And that we come to an understanding of the universe through a sequence of increasingly complex models, which, we believe, brings us increasingly nearer to "the truth". For me this was a profound thought, and it led me eventually to the philosophy that "mathematical modelling is a way of life". In my professorial inaugural public lecture in 1996, I put forward the thesis that mathematical modelling is a way of life for everyone, because everyone uses mathematics to describe or predict the behaviour of some phenomenon. A child uses a simple linear model to work out the cost of five apples, given the cost of one apple. (Later she will build in the concept of discount for bulk purchase.) The economist builds models to predict the movement of stocks. The meteorologist builds models to predict the behaviour of the weather. (I have expanded on these ideas in [3] and [4] and various other places). Of course these ideas of models and modelling are fairly commonplace today, but that was not the case in the 1970's.

Bravely, but in the company of like minded souls, we started to convert our applied math courses into math modelling courses wherein our students studied and explored the models created by others, and engaged in mathematical modelling, creating their own

models, giving a rationale for the simplifying assumptions made, reflecting on the results of the calculations and seeking to evaluate and validate their work. And herein we, the teachers, had moved from simply teaching mathematics to our students to inducting them into the profession of mathematician. We were admitting them to the community of practice that they had previously only gazed at uncomprendingly. This was a significant development in undergraduate education.

Having taken this step change in attitude we next had to work out good ways of making this happen, and corresponding innovative ways of grading students' work. When I reflected on the way we all went about our business at Goddard, it became clear that we needed, somehow, to mimic in the classroom the ways in which professionals worked. Perhaps the most important aspect of this was the fact that we took our coffee and lunch breaks together. We dined occasionally in each other's houses, and, on a memorable occasion, we de-camped to North Carolina to see the March 1970 total eclipse of the sun. Yes, at coffee we always talked about this and that, but work we also did! We asked questions of one another and discussed with one another the great ideas we had. Then we retreated to solitude, perhaps to the library to read and study, perhaps to our desk to think and write, perhaps to our computer to code our mathematics. Our doors were nearly always open and we visited each other from time to time when new ideas came to us. In summary we were sociable, we read deeply and critically, we reflected, we discussed, we taught one another new things, we made the computer do calculations, we pored over the printouts and eventually we wrote papers and gave presentations in seminars and at conferences. It is also my observation that mathematicians who earn their daily bread in the market place (in distinction to ivory towers or the civil service), usually in the guise of engineers or statisticians or many other occupations, have a working life not too dissimilar from ours - working together, working alone, reading, calculating, reasoning, writing, learning from one another and teaching one another [3].

This way of life is a million miles away from the typical undergraduate education that I, and probably you as well, experienced. Ours was a daily round of lectures, tutorials, problem sheets and lab classes. There were no opportunities to work together on open ended problems, no seminars to give, no essays to write (at least not in mathematics, perhaps physics past my freshman course was different). Yes, we met in the students' cafeteria or bar, but the conversation there was always just about this and that.

That old cynic, Koheleth, said, "There is nothing new under the sun." [5], but what we were attempting to do certainly was new. Lady Wisdom gave the right message, "Wisdom is but one, yet she can do all things; herself unchanging, she makes all things new." [6]. I think we were wise to embark on this innovative venture. At Ulster we introduced a course whose unifying theme was mathematical modelling. Whenever it was appropriate, we used the concepts of models and modelling to teach an approach to a topic. The freshman module I developed over a number of years eventually embedded all the desirable qualities of the way of life of the professional discussed above.

It was a module on methods, models and modelling. Basically it was an introductory course on ordinary differential equations and their applications, and the teaching and

learning of methods for solving these was done more or less in the traditional way. When we came to look at a diversity of situations wherein ODEs were used as models, then my students did the work. With some guidance from me, "the guide on the side" - no longer "the sage on the stage", students, working in small groups, studied various textbooks and papers to research a phenomenon such as, for example, population growth, or projectile motion. The purposes of this study were twofold. They themselves were to learn about the construction of their model and how it was used to describe and predict the behaviour of their chosen phenomenon. But they were also to share this learning with the rest of the class. They were to write up an account of their work in such a way that their peers in the class could study it and thus learn all about that phenomenon. Furthermore they were also to present their work in a forty minute class seminar, again with the objective of helping their peers to learn.

Another task this module demanded of students was to investigate an open ended problem, such as may now be found in the various mathematical modelling competitions such as the ones organised by COMAP [7]. They were to write up their work in a technical report and to present a summary at a poster session. I believe we now had a course that embodied all of the essential features of the way of life of an applied mathematician.

Ulster was not alone in developing such courses. Most of the UK polytechnics were doing something similar. (In 1992, the polytechnics were re-badged as universities and are now commonly referred to as the new or post 1992 universities.) And this whole endeavour was a fruitful field for pedagogical research. I have, for example, published quite a useful review of assessment [8], which is also on the MAA website [9].

I attended my last ICPEAC in 1973, although I have a memory of meeting you, Aaron, at a subsequent conference in Belfast. I am glad to say that I was not left conference-less. The mathematical modelling movement in the UK started the biennial series of International Conferences on the Teaching of Mathematical Modelling and Applications (ICTMA) in 1983 and I have attended all of them. We visited you, Dick, after the 1993 conference in Delaware. I had the honour of serving as President of ICTMA from 1999 to 2003. New work and new friends, and still exciting work!

Well, old friends, I have come to the end of my musings. In conclusion may I wish you both good health and lots of joy in your retirement!

With all good wishes,

Ken

REFERENCES

1. Drachman, R.J. and Houston, S.K., "Simplified Model for Positronium-Helium Scattering", *J Phys. B: Atom. Molec. Phys*, 1970, **3**, pp 1657-1662.
2. "To catch out" is a British expression meaning "to detect a mistake", Oxford Reference Dictionary, 9th edition, 1995, OUP
3. Houston, S.K., "M's and R's in Post-16 Mathematics", *Teaching Mathematics and its Applications,* 1997, **16**, pp192-195
4. Houston, S.K., Rodgers, P. and Simpson, A., "Teaching Mathematics as a Way of Life", in C. Rust, editor, *Improving Student Learning through the Disciplines*, OCSLD, Oxford, 2000, 135-145.
5. Ecclesiastes 1:9
6. The Wisdom of Solomon 7:27
7. COMAP - "The Mathematical Contest in Modeling" - http://www.comap.com/undergraduate/contests/mcm/
8. Houston, K., 2001, "Assessing Undergraduate Mathematics Students" in Holton, D., Editor, The teaching and learning of Mathematics at university level, Kluwer, pp 407-421.
9. Mathematical Association of America, http://www.maa.org/saum/headlines/Houston_fin1.12.html

Hi Dick, Aaron, and Anand,

It was great to see you all this weekend. It is truly the measure of what you have meant to folks that we/they came from so far to wish you well.

Having not attended a positron conference for 10 years, I was very much struck by the unusual bonds of friendship within this community (in particular that people reveled in others' approaches rather thandisparaged them), and the breadth of people's interests within and beyondphysics. I guess I'll have to get cracking on some positron physics again as my dues for renewing my membership.

In listening to the stories of the other graduates of your "school," I had a flash of brilliant hindsight, that I probably should have set aside the method I had proposed for working on the e+H- project and dived more often into working on where you all were headed at the time. (My sense of responsibility to follow through on my promises got in the way of good sense.) As it was, I was rapidly directed onto other pathways by Jim the next year and a big chunck of the accumulated wisdom I learned from you three has just been percolating (and somewhat fading) in my backbrain since then. Indeed, the most productive ideas I applied to Jim's problems derived not from the Fock-Tani technique but from what I learned from you about psuedostates, computer algebra, and the references you gave me that got me going on finding solutions to general-state-to-state integrals. Having spent most of my spare time for the past few years researching and publishing [1] on how to teach whites kids about racism, and optical lens design (designing light weight view camera lenses for my own use), I'm feeling the itch to get back into a good atomic theory problem.

Dick, having blocked you once from doing the the e+H- problem using a likely more reliable method than the Fock-Tani approach, I don't want to block you again by promising to work with you on a, say, kohn approach, and then find myself too swamped from teaching to get it done in a timely fashion. But if this, or another problem of interest, is likely to stay at #13 on your list of projects due to your own lack of time, perhaps I should give something like it a try.

Please pass on to Gladys and Betty my thanks for solving my sugar-in-food issues so deliciously.

Warm Regards,
Jack

[1] Communicating in a group, Jack C. Straton, The Journal of Student Centered Learning (in press, Winter 2005).

Senior Inquiry: A university/high school collaboration, Barbara Traver, Jack C. Straton, Jan Whittlesey, Dave Erhenkranz, Tom Wells, Pat McCreery, Maarja Paris, Candyce Reynolds, and Judy Patton, Academic Exchange Quarterly 7(3), 52-6 (Fall 2003).

Beyond guilt: How to deal with societal racism, Lauren N. Nile and Jack C. Straton, in Multicultural Education 10(4), 2-6 (2003).

White-Bashing: Teaching hot-button issues via indirection, Jack C. Straton, Democracy & Education 13 (4), 69 (Fall, 2000).
Jack C. Straton

List of Participants at the Symposium held on November 18, 2005

1. Dr. E.A.G. Armour
   Mathematics Department
   University of Nottingham
   Nottingham NG7 2RD, UK

2. Dr. K. R. Bartschat
   Physics Department
   Drake University
   Des Moines, IA 50311, USA

3. Dr. A. K. Bhatia
   Laboratory for Solar and Space Physics
   NASA/Goddard Space Flight Center
   Greenbelt, MD 20771, USA

4. Dr. I. Bray
   ARC Centre for Antimatter-Matter Studies
   Murdoch University
   Perth 6150, Australia

5. Dr. M. Charlton
   Department of Physics and Astronomy
   University College London
   London WC1E 6BT, England

6. Dr. L. Chatterjee
   IOP Science and Editorial Office
   1200 G Street, Suite 800
   Washington DC 20005, USA

7. Dr. C.W. Clark
   B102 Radiation Physics Bldg., NIST
   Quince Orchard Rd.
   Gaithersburg, MD 20899, USA

8. Dr. J.W. Cooper
   IPST, University of Maryland
   College Park, MD 20742, USA

9. Dr. M. A. Copland
   IPST, University of Maryland
   College Park, MD 20742, USA

10. Prof. A. Dalgarno
    Harvard-Smithsonian CFA
    60 Garden St.
    Cambridge, MA 02138, USA

11. Dr. A. Dasgupta
    Code 6723
    Plasma Physics Division
    Naval Research Lab
    Washington DC 20375, USA

12. Dr. J. DiRienzi
    College of Notre Dame of Maryland
    Baltimore, MD 21210, USA

13. DR. R. J. Drachman
    Laboratory for Solar and Space Physics
    NASA/Goddard Space Flight Center
    Greenbelt, MD 20771, USA

14. Dr. G.W.F. Drake
    Department of Physics
    University of Windsor
    Windsor Ontario, Canada N9B 3P4

15. Dr. James E. Felten
    NASA/Goddard Space Flight Center
    Greenbelt, MD 20771, USA

16. Dr. E. Gerjuoy
    Department of Physics
    University of Pittsburgh
    Pittsburgh, PA 15260, USA

17. Dr. V. L. Jacobs
    Code 6693
    Navel Research Lab
    4555 Overlook Avenue SW
    Washington DC 20375-5345, USA

18. Dr. Y.K. Ho
    Institute of Atomic and Molecular Sciences
    Academia Sinica
    PO Box 23-166
    Taipei, Taiwan
    Republic of China

19. Dr. C.Y. Hu
    Department of Physics
    CSU-Long Beach
    Long Beach, CA 90840, USA

20. Dr. J. W. Humberston
Department of Physics and Astronomy
University College London
London WC1E 6BT, England

21. Dr. S.R. Lundeen
Department of Physics
Colorado State University
Fort Collins, CO 80523, USA

22. Dr. D. L. Morgan Jr.
728 Polaris Way
Livermore, CA 94550, USA

23. Dr. G. Peach
Department of Physics and Astronomy
University College London
London WC1E 6BT, England

24. Dr. L. O. Roellig
4520 Sioux Drive
Boulder, CO 80303, USA

25. Dr. D. Rosenbaum
South Methodist University
Dallas, TX 75275, USA

26. Dr. J. L. R. Saba
Lockheed Martin Solar and Astrophysical Laboratory
Goddard Space Flight Center
Greenbelt, MD 20771, USA

27. Dr. B.I. Schneider
Physics Department
National Science Foundation
4201 Wilson Blvd.
Arlington, VA 22230, USA

28. Dr. David M. Schrader
Department of Chemistry
Marquette University
PO Box 1881
Milwaukee, WI 53201, USA

29. Dr. J. Shertzer
Department of Physics
College of Holy Cross
Worcester, MA 01610, USA

30. Dr. A.D. Stauffer
Department of Physics and Astronomy
York University
4700 Keele St.
Downsview Ontario, Canada M3J 1P3

31. Dr. J.C. Straton
06 SE 72nd Avenue
Portland OR 97215-2214, USA

32. Prof. J. Sucher
Department of Physics
University of Maryland
College Park, MD 20742 USA

33. Dr. C.M. Surko
Physics Department 0319
University of California SD
9500 Gillmore Drive
La Jolla, CA 92093-0319, USA

34. Dr. A. Temkin
Laboratory for Solar and Space Physics
NASA/Goddard Space Flight Center
Greenbelt, MD 20771, USA

35. Dr. V. L. Teplitz
NASA/Goddard Space Flight Center
Greenbelt, MD 20771, USA

36. Dr. H.R.J. Walters
Department of Applied Mathematics
The Queen's University
Belfast, BT7 1NN, U.K.

37. Dr. R. Wehlitz
Synchrotron Radiation Center
UW-Madison
Stoughton, Wisconsin 53589, USA

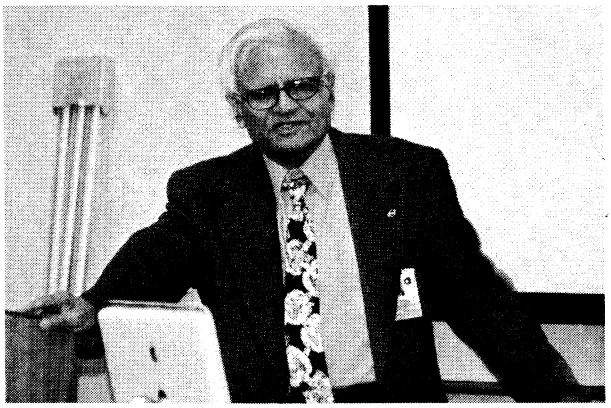

Anand Bhatia

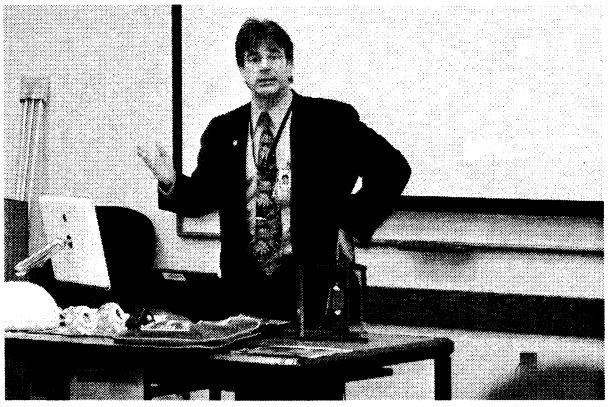

James Garvin

James Garvin

Aaron Temkin

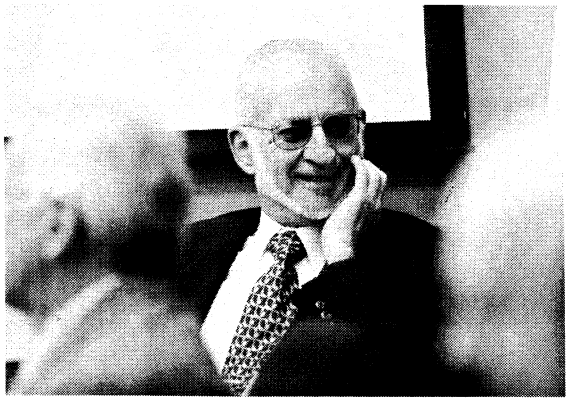

Richard Drachman

Anand Bhatia and
James Garvin (standing)

James Slavin

Aaron Temkin, James Garvin and
James Slavin

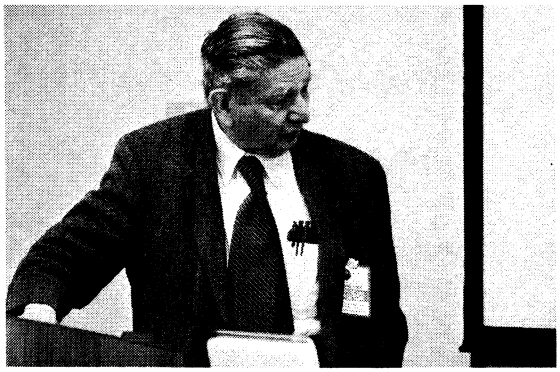

Edward Gerjuoy

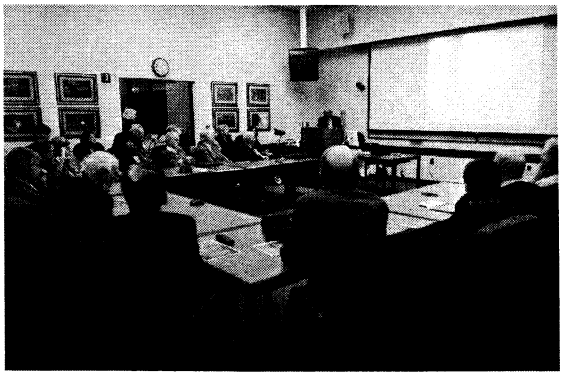

Anand Bhatia and the Audience

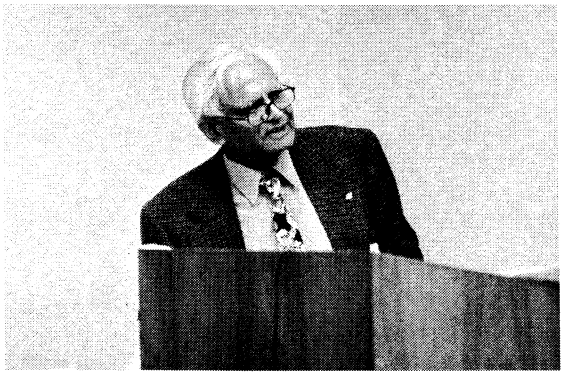

Anand Bhatia

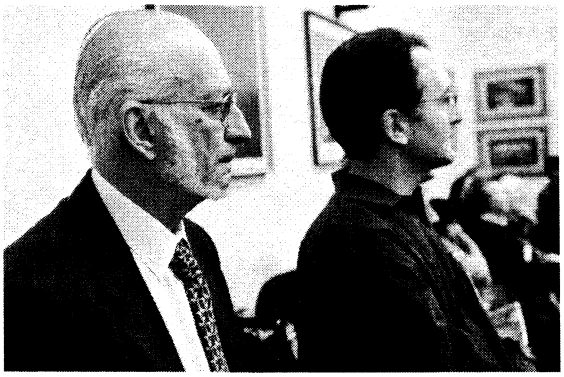

Richard Drachman and
Benjamin Slade

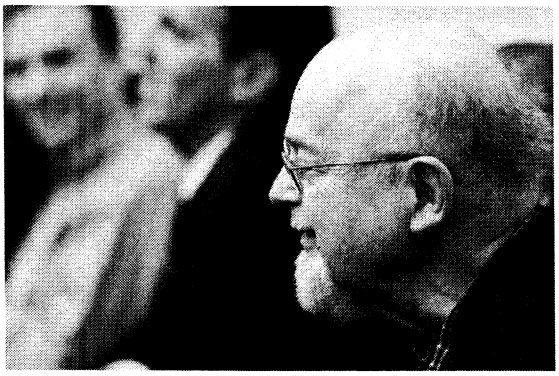

Joseph Sucher

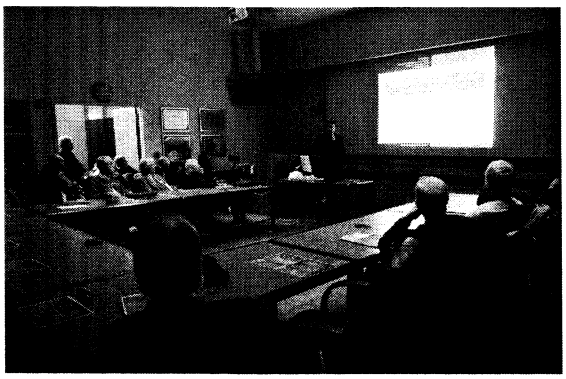

Igor Bray

Igor Bray

Edward Gerjuoy and Igor Bray

Jean and Aaron Temkin

Aaron Temkin, Edward Gerjuoy and Igor Bray

Julie Saba

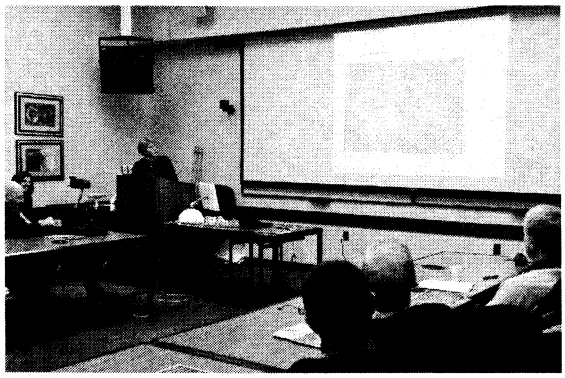

Julie Saba and Others

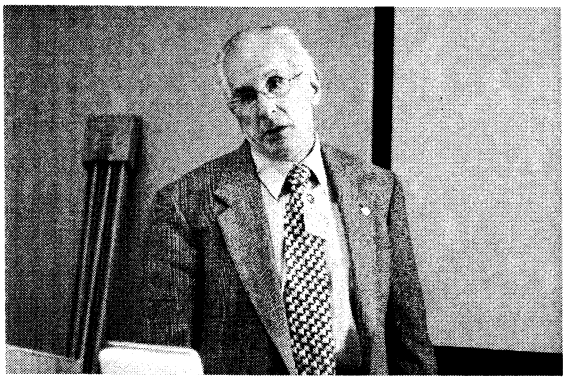

Barry Schneider

Coffee Break

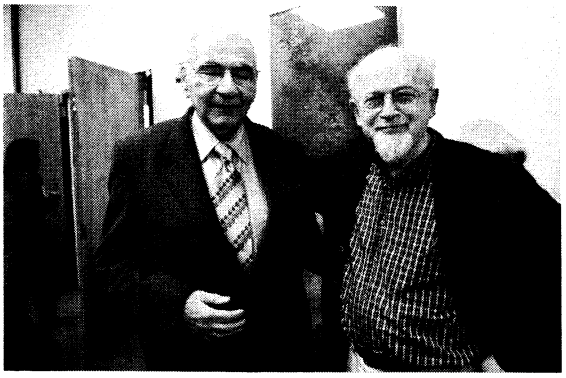

Aaron Temkin and Joseph Sucher

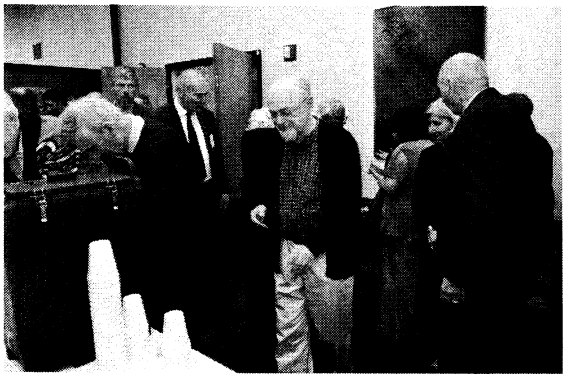

Coffee Break

Gladys and Aaron Temkin and Benjamin Slade

Aaron Temkin and Others

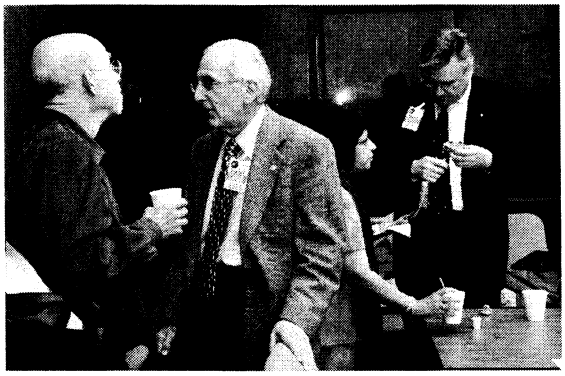

Michael Copland and Barry Schneider

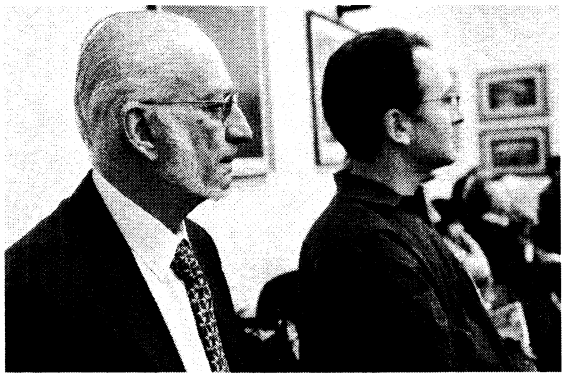

Richard Drachman and Leonard Roellig

Gillian Peach, Aaron, Jean and Phillip Temkin

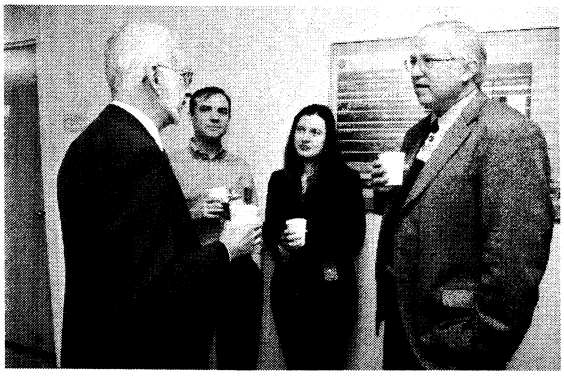

Richard and Jordan Drachman, Efrat Zalishnick and Stephen Lundeen

Joseph Sucher, Aaron and Phillip Temkin, Jonahan Boardman and Deanna Temkin

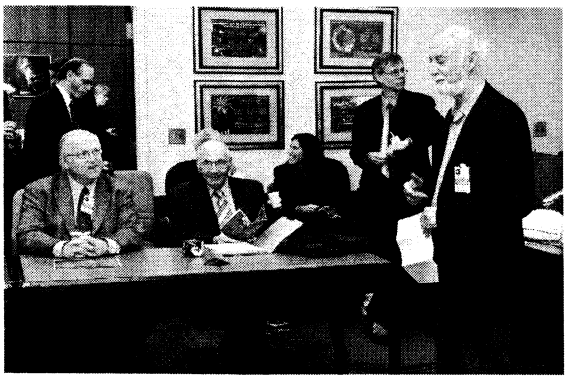

Stephen Lundeen, Aaron Temkin, Ralph Wehlitz, Alex Dalgarno and Others

Richard Drachman, John Cooper, James Walters, Sue Hu, and Leonard Roelling

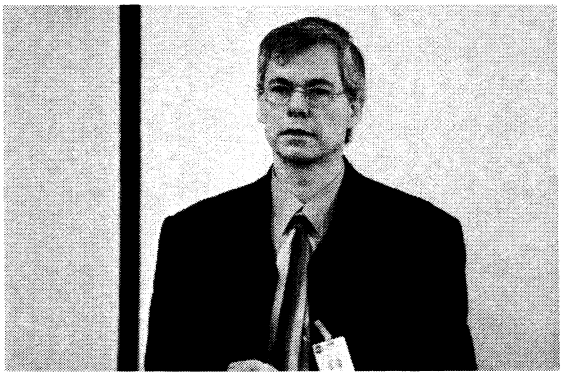

Ralf Wehlitz

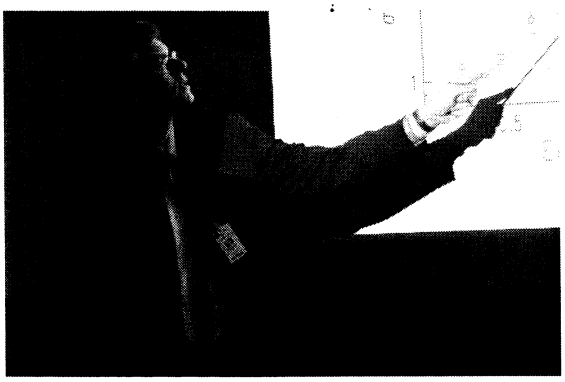

Ralf Wehlitz

Edward Gerjuoy and Joseph Sucher

John Cooper and Lali Chatterjee

Klaus Bartschat and
John Humberston

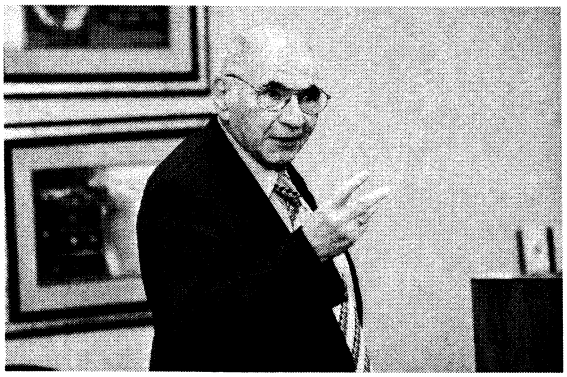

Aaron Temkin

Barry Schneider and Edward Gerjuoy

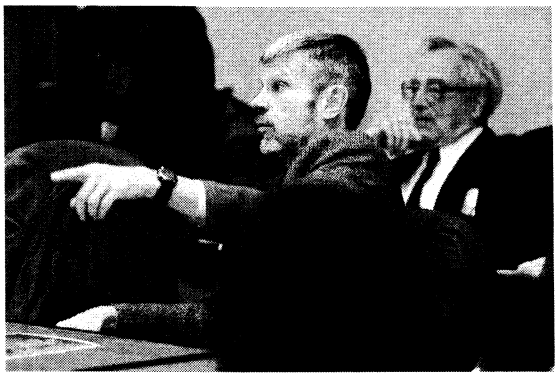

Klaus Bartschat and John Cooper

Janine Shertzer

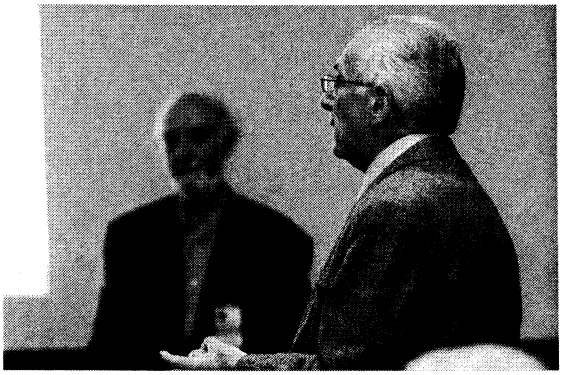

Alex Dalgarno and Barry Schneider

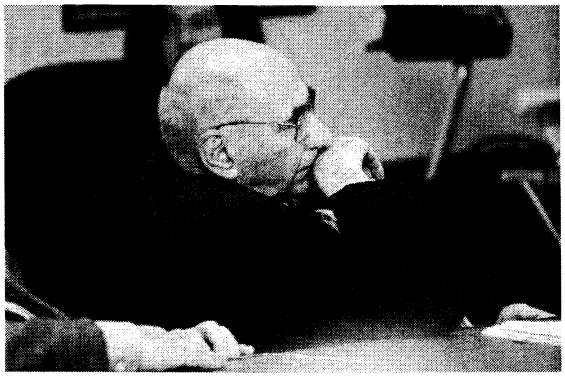

Aaron Temkin

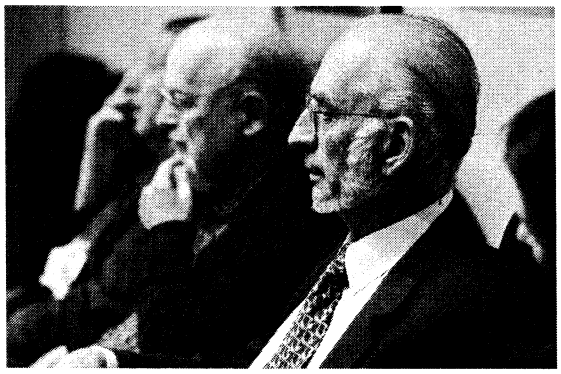

Joseph Sucher and Richard Drachman

Richard Drachman and
Edward Armour

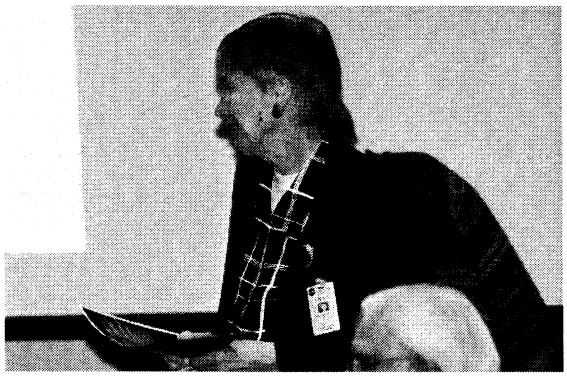

Gillian Peach

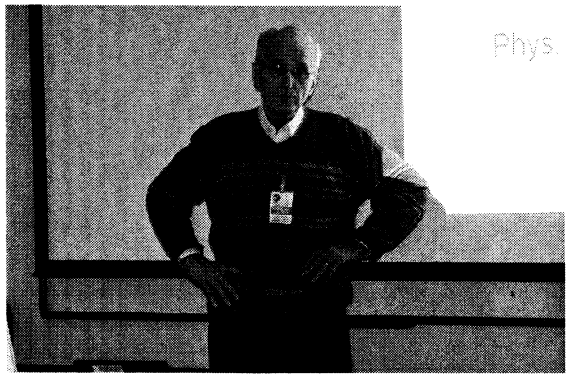

David Shrader

Charles Clark

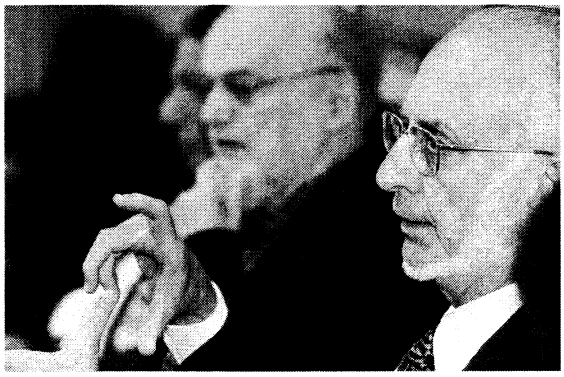

Joseph Sucher and Richard Drachman

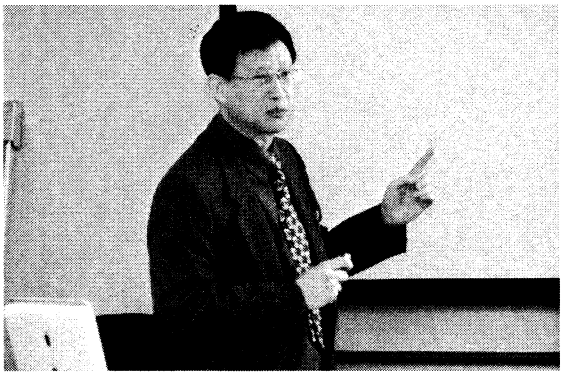

Eugene Ho

Eugene Ho, Gillian Peach
and Audience

Edward Gerjuoy, Joseph Sucher, Jack Straton, Edward Armour

Coffee Break with Two Cakes Brought by Barbara Thompson

Jordan and Richard Drachman, Gladys and Aaron Temkin

Eugene Ho, Richard Drachman and Anand Bhatia

Group Photograph

REPORT DOCUMENTATION PAGE

Form Approved
OMB No. 0704-0188

1. REPORT DATE *(DD-MM-YYYY)*	2. REPORT TYPE	3. DATES COVERED *(From - To)*
27-12-2007	Conference Publication	

4. TITLE AND SUBTITLE

NASA GSFC Science Symposium on Atomic and Molecular Physics

5a. CONTRACT NUMBER

5b. GRANT NUMBER

5c. PROGRAM ELEMENT NUMBER

6. AUTHOR(S)

Anand K. Bhatia, Editor

5d. PROJECT NUMBER

5e. TASK NUMBER

5f. WORK UNIT NUMBER

7. PERFORMING ORGANIZATION NAME(S) AND ADDRESS(ES)

Goddard Space Flight Center
Greenbelt, MD 20771

8. PERFORMING ORGANIZATION REPORT NUMBER

2007-00168-0

9. SPONSORING/MONITORING AGENCY NAME(S) AND ADDRESS(ES)

National Aeronautics and Space Administration
Washington, DC 20546-0001

10. SPONSORING/MONITOR'S ACRONYM(S)

11. SPONSORING/MONITORING REPORT NUMBER

CP-2006-214146

12. DISTRIBUTION/AVAILABILITY STATEMENT

Unclassified-Unlimited, Subject Category: 72
Report available from the NASA Center for Aerospace Information, 7115 Standard Drive, Hanover, MD 21076. (301)621-0390

13. SUPPLEMENTARY NOTES

14. ABSTRACT

This document is the proceedings of a conference on atomic and molecular physics in honor of the retirements of Dr. Aaron Temkin and Dr. Richard Drachman. The conference contained discussions on electron, positron, atomic, and positronium physics, as well as a discussion on muon catalyzed fusion. This proceedings document also contains photographs taken at the symposium, as well as speeches and a short biography made in tribute to the retirees.

15. SUBJECT TERMS

Atomic, Positronium, Electron, Positron, Muon Catalyzed Fusion, Aaron Temkin, Richard Drachman

16. SECURITY CLASSIFICATION OF:			17. LIMITATION OF ABSTRACT	18. NUMBER OF PAGES	19b. NAME OF RESPONSIBLE PERSON
a. REPORT	b. ABSTRACT	c. THIS PAGE			Anand K. Bhatia
Unclassified	Unclassified	Unclassified	Unclassified	267	19b. TELEPHONE NUMBER *(Include area code)* (301) 286-8812